UNIVERSITY OF CALIFORNIA, SAN DIEGO

SAN DIEGO STATE UNIVERSITY

Study of Bifunctional Imidazolylphosphine Ligands on Pd and Pt

A dissertation submitted in partial satisfaction of the requirements for the degree

Doctor of Philosophy

in

Chemistry

by

Yi Gong

Committee in charge:

University of California, San Diego

Professor Joseph M. O'Connor
Professor Clifford Kubiak
Professor Joseph Adams

San Diego State University

Professor Douglas B. Grotjahn, Chair
Professor Tom Cole
Professor Terry Frey

2007

The dissertation of Yi Gong is approved,

and it is acceptable in quality and form for publication

on microfilm

_____

_____

_____

_____

_____

_____
Chair

University of California, San Diego

San Diego State University

2007

DEDICATION

To my parents, my husband, Heng Zhu, my sister and brother who have been the source of my strength.

TABLE OF CONTENTS

LIST OF FIGURES

LIST OF TABLES

ACKNOWLEDGEMENTS

I would like to thank my research advisor, Professor Douglas B. Grotjahn for his generous support and endless guidance. He has always been there for us when we had questions and needed help.

I would also like to thank my doctoral committee members for their time and help they provided through my thesis preparation. I would like to thank Dr. LeRoy Lafferty for helping me with the NMR instruments and Dr. Arnold Rheingold and his group for X-ray structure analysis.

I would like to thank all the people I have worked with in our research group, I had a good time working around them and have learned a lot from each of them. I would especially thank Dr. Sang Van and Dr. Dan Lev for their help when I first joined the group, I would like to thank Dan, Phil, Xi, Jeff for the preparation of the ligands, I would like to thank Dr. Valentin Miranda and Dr. Justin Hoeter for teaching me to use several computer programs. It has been always joyful to work in this lab and it is Professor Grotjahn who made this possible, I would like to express my appreciation again. THANK YOU, Dr. Grotjahn.

Finally, I would like to thank San Diego State University and University of California, San Diego for the opportunity to persue my dream.

VITA

1995	B. S., Shandong University Jinan, Shandong, China
2004	M. A., San Diego State University San Diego, CA
2007	Ph. D., University of California, San Diego San Diego State University San Diego, CA

PUBLICATIONS

1. Douglas B. Grotjahn, Yi Gong, Lev Zakharov, Arnold L. Rheingold. "Changes in Coordination of Sterically Demanding Hybrid Immidazolylphosphine Ligands on Pd(0) and Pd(II)." *J. Am. Chem. Soc.* 2006, 128, 438-453.

2. Douglas B. Grotjahn, Yi Gong, Antonio G. DiPasquale, Lev. N. Zakharov, Arnold L. Rheingold. "Bifunctional Imidazolylphosphine Ligands as Hydrogen Bond Donors Promote N-H Activation and O-H Activation on Platinum" *Organometallics* 2006, *25*, 5693-5695.

3. Douglas B. Grotjahn, Yi Gong, Antonio G. DiPasquale, Lev N. Zakharov, Arnold L. Rheingold. " Imidazolylphosphine Ligands on Pt(0) and Pt(II): Effect of Ligand N-H Group on N-H Activation and O-H Activation" Full paper in preparation for *J. Am. Chem. Soc.*

4. Douglas B. Grotjahn, Daniel Lev, Yi Gong, Grant Boldt, Gerardo Aguirre. "Synthesis of Imidazolylphosphines with Various Substituents and Some Effects of Substituents on Reactivity." Full paper in preparation for *Organometallics.*

PRESENTATIONS

1. Yi Gong, Douglas B. Grotjahn. “Bifunctional Imidazolylphosphine Ligands as Hydrogen Bond Donors Promote N-H Activation and O-H Activation on Platinum” 232nd American Chemical Society National Meeting, Deptember 2006, San Francisco, CA.

2. Yi Gong, Douglas B. Grotjahn. “Synthesis and Study of Platinum Complexes with Bifunctional Imidazolylphosphine ligands.” 229th American Chemical Society National Meeting, March 2005, San Diego, CA.

3. Yi Gong, Douglas Grotjahn. “Palladium and Platinum Complexes with Bulky Imidazolylphosphine Ligands. Synthesis, Characterization, Reactivities and their Potentical of Catalyzing C-N and C-O Bond Formation.” 227th American Chemical Society National Meeting, March 2004, Anaheim, CA.

4. Yi Gong, Douglas Grotjahn. “Synthesis and Study of Pd(0) Complexes with Bulky Imidazolylphosphine Ligands and their Oxidative Addition Product with Arylhalides.” 4th Internation Symposium, “Chemical Research in the Border Region,” October 2002, Tijuana, Mexico.

FIELD OF STUDY

Major Field: Organic Chmemistry

Studies in Organometallics Chemistry, Catalysis.

Prefessor Douglas, B. Grotjahn

ABSTRACT OF THE DISSERTATION

Study of Bifunctional Imidazolephosphine Ligands on Pd and Pt

by

Yi Gong

Doctor of Philosophy in Chemistry

University of California, San Diego, 2007

San Diego State University, 2007

Professor Douglas B. Grotjahn, Chair

A series of three new imidazolylphosphine ligands was designed and synthesized to probe the effects of phosphorus and heterocycle substituents on coordination geometry and ligand hapticity in Pd(0) and Pd(II) complexes of these ligands. The X-ray diffraction and spectroscopic data for Pd(0) complex show that it is a two-coordinate, 14-electron species. Oxidative-addition chemistry of the two-coordinate Pd(0) complexes shows that isopropyl substituents not only allow rapid reaction but retention of both phosphine ligands. In contrast, phosphorus *tert*-butyl groups slow oxidative-addition and lead to phosphine loss and chelation by the remaining phosphine. in all of the di-*tert*-butylphosphino-substituted compounds in this study, the chelate remained closed when amines were added. Amine binding could be effected after halide ionization, but without opening of the chelate ring. Amine binding involving hydrogen bonding was seen in the isopropyl series. The results described in this dissertation show the interplay of ligand substituents in determining

ligand hapticity, coordination of other ligands, and secondary hydrogen-bonding interactions, properties of interest in study structure and catalysis of complexes featuring hybrid ligands.

Our ultimate goal is finding the catalyst for hydration and hydroamination of an unsaturated bond, resulting in terminal alcohols and amines or in a heterocyclic ring, respectively. In this dissertation, we report the syntheses of Pt complexes with various bifunctional imidazolylphosphines and look into their reactivities with small molecules which could represent the important steps in the catalysis. The reactivites of resulted Pt(0) and hydrido Pt(II) complex with RO-H compounds of acidity ranging from acids to water are very different. Pt(0) Complex reacted only with more acidic species whereas hydrido Pt(II) complex reacted with all O-H compounds tested, with O-H activation, and the product H-Pt-OR was stabilized by hydrogen bonding interactions between oxygen atom and N-H on the imidazole ring.

Bidentate phosphine ligands containing imidazolyl substituents were synthesised and studied on Pd and Pt. The combination of our ligands and Pd(0) precursor generated a catalyst for coupling reaction of bromobenzene and morpholine at room temperature. Our imidazolylphosphine and pyridylphosphine ligands were also tried on the Pt-catalyzed intromolecular hydroamination of unactivated olefins and secondary alkylamines.

CHAPTER 1

Metal-Ligand Bifunctional Catalysis Involving Ligand-Assisted Proton Transfer or Hydrogen Bonding

In Nature, hydrogen bonding and proton transfer are common in enzymatic catalysis. For example, phosphate ester hydrolysis is catalyzed by enzymes that often possess two or even more divalent metal ions in the active site.[1,2] Various roles shown for metal ions include acting as Lewis acids in the activation of substrate and nucleophile and in the stabilization of transition state and leaving group. Generally, in the phosphoesterase metalloenzymes several amino acid residues are also involved in catalysis, a phenomenon known as cooperativity. In RNase A, an ammonium group of a lysine residue activates the phosphoryl group while two histidine cooperate in the deprotonation of the nucleophile and in the protonation of the leaving group.[3,4] The catalytic role of the amino acid residue in RNase A has been mimicked with general acid-base systems,[3,4] like bisimidazoles or aqueous solutions of imidazoles or diamines.[5] Molenveld et al. reported that Calix[4]arenes functionalized with two catalytic bisimidazolyl-Cu(II) centers and two functional hydroxymethyl or aminomethyl groups can be used as models for enzymes that cleave phosphate diester bonds.[6-8] The kinetic studies showed that under neutral conditions, the catalyst with aminomethyl groups exhibited bifunctional catalytic effects. At pH = 7.4, at least one amine is protonated, which can assist as a general acid in the binding and activation of the substrate (Figure 1.01).[9]

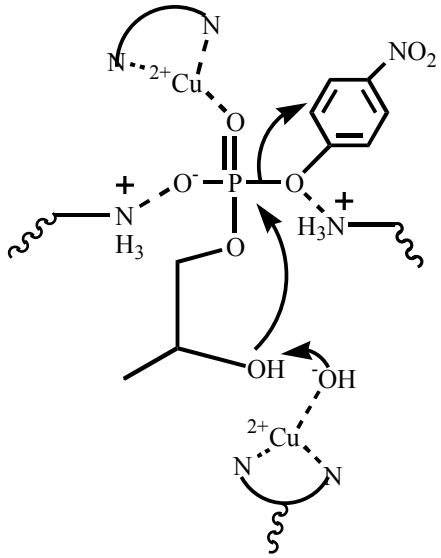

Figure 1.01. Possible mechanism for the cleavage of 2-hydroxypropyl-p-nitrophenyl phosphate catalyzed by aminomethyl functionalized Calix[4] arene copper complex.

More polarized molecules such as species containing O-H or N-H bonds are involved in stronger hydrogen bonds while the less polarized molecules are involved in weaker hydrogen bonds.[10,11] The strength of hydrogen bonds for neutral donor/acceptor pairs is in the range of 2-20 kcal/mol. Although hydrogen bonds are relatively weak, they are responsible for the major energetic contribution to enzymatic catalysis.[12-14] Strongly polarized bonds, for example, in metal hydrides, will participate in hydrogen bonding.[15-21]

Hydrogen bonding has not been intensively studied in organometallic catalysis.[22-24] There are three types of bifunctional catalyst: 1) metal-free organocatalysts; 2) those with Lewis acidic metals and Brønsted-Lowry bases; 3)

those with a transition metal which is capable of carrying out fundamental organometallic reaction and an internal base or acid.

The first type of bifunctional catalyst includes peptides[25,26] or other small molecules capable of hydrogen bonding or proton transfer.[27] In the second type of bifunctional catalyst, a Brønsted-Lowry base in a ligand is far from metal center such as Al^{III}, In^{III}, or Ti^{IV} so no coordination occurs but the base is near enough to act along with the metal on intermediates.[28-37] The third type, organometallic complexes, is the most relevant type of bifunctional catalyst in this chapter.

An example of synthetic organometallic catalysis that incorporates metal-ligand and hydrogen bonding cooperativity in the catalyst design is the Shell methoxycarbonylation of propyne to methyl methacrylate by Drent et al.[38-40] The conditions of the reaction involve a palladium(II) source and a soluble Brønsted acid and a particular phosphine ligand. The choice of the ligand was crucial for the product yield and selectivity. When a phosphine ligand contained a nitrogen proton donor/acceptor such as pyridyl, the yield of methacrylate was greater than 99% and selectivity for the branched product was 1000:1. The phosphine ligand could also contain a pyrimidyl or triazolyl group, imines and amines. On the other hand, when phosphine ligands which do not bear those N-containing groups, for example, PPh_3 and $Ph_2PCH_2CH_2PPh_2$ were used in the reaction, the result was not comparable. Moreover, when an alkyl group was placed *ortho* to the pyridyl nitrogen which blocks the chelation of the nitrogen to Pd center, the catalytic activity was increased by 2.5 times when compared to the *para* substituted ligand. Scrivanti et al. has proposed a

mechanism in which the rate determining step of the catalytic cyle is the formation of a palladium (II) vinyl complex from a η^2-propyne intermediate (Figure 1.02). In this step, pridyl nitrogen in phosphine ligand is involved in proton trasfer.[41]

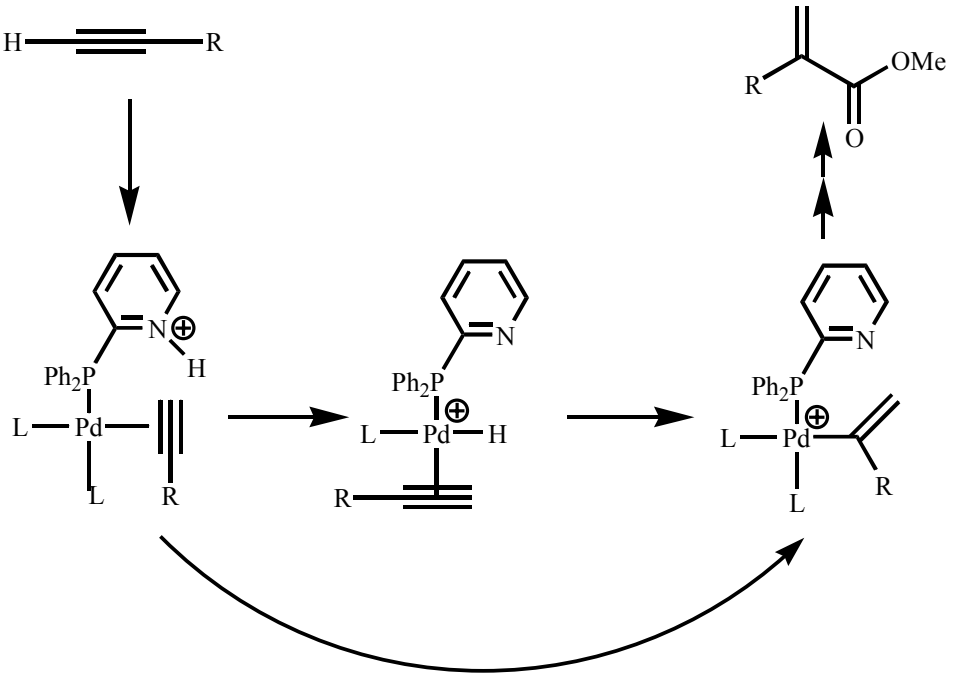

Figure 1.02. Key step in the reaction of Pd/2-pyridyldiphenylphosphine catalyzed alkoxycarbonylation of terminal alkynes.

Some of the most well-known and synthetically useful examples of hydrogen bonding in organometallic catalysis are systems of Noyori and co-workers, who have developed very active and selective ruthenium catalysts for the hydrogenation or asymmetric hydrogenation of ketones (Figure 1.03).[42,43] The ruthenium catalysts are usually generated in a 2-propanol solution by mixing a ruthenium dichloride precursor complex with an excess of a strong base such as potassium *tert*-butoxide under dihydrogen in the presense of ketone substrate. The ruthenium complexes *trans*-

$RuCl_2(PPh_3)_2$(diamine) or *trans*-$RuCl_2$(diphosphine)(diamine) contain monodentate or chiral bidentate phosphine ligands, especially the binap ligands, and also an achiral or chiral diamine ligand such as dpen = 1,2-diamino-1,2-diphenylethane or cydn = 1,2-diaminocyclohexane or tmen = $H_2NCMe_2CMe_2NH_2$.

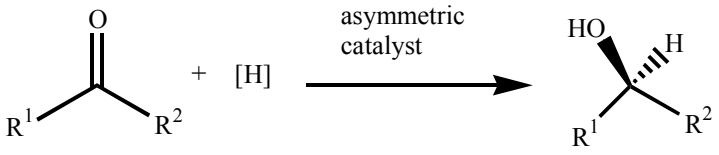

[H] = H_2 or organic hydrogen donor

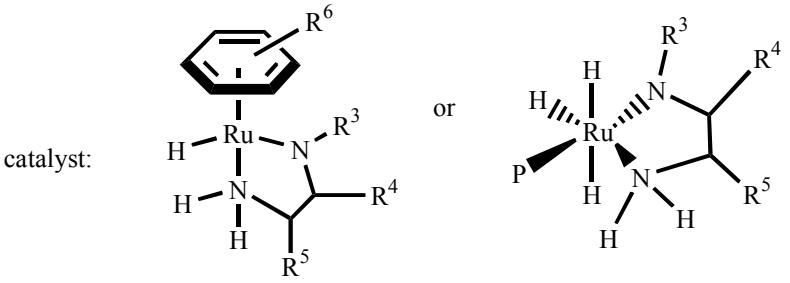

Figure 1.03. Asymmetric hydrogenation of ketone by metal-ligand bifunctional catalysts.

Noyori and co-workers have shown that an HN on the amino group is crucial to the activity of the hydrogenation catalyst, which suggests that this transfer hydrogenation takes place by a novel mechanism (Figure 1.04) rather than the widely accepted putative pathways. Usually, primary and secondary amines are relatively weak acids. However, upon complexation with a Lewis acidic metal, N-H acidity is increased and the formation of a NH···O=C hydrogen bond in a transition state could

facilitate the difficult delivery of hydride from metal to C=O. They note that at least 2 equiv of alkoxide base are needed to neutralize HCl that is formed in the catalyst activation. They speculate that a hydride complex with a *fac*-hydrido(diamine)Ru substructure of the form RuH(diamine)$(PR_3)_2(X)$, where X is hydride, alkoxide, or some other anion, is responsible for an unconventional transfer of dihydrogen from the hydride on ruthenium and a hydrogen on a diamine amino group to the ketone to give the alcohol product.[42] Noyori has called this phenomenon metal-ligand bifunctional catalysis.[43] They also suggest that the activation of dihydrogen is the turn-over limiting step in this cycle.

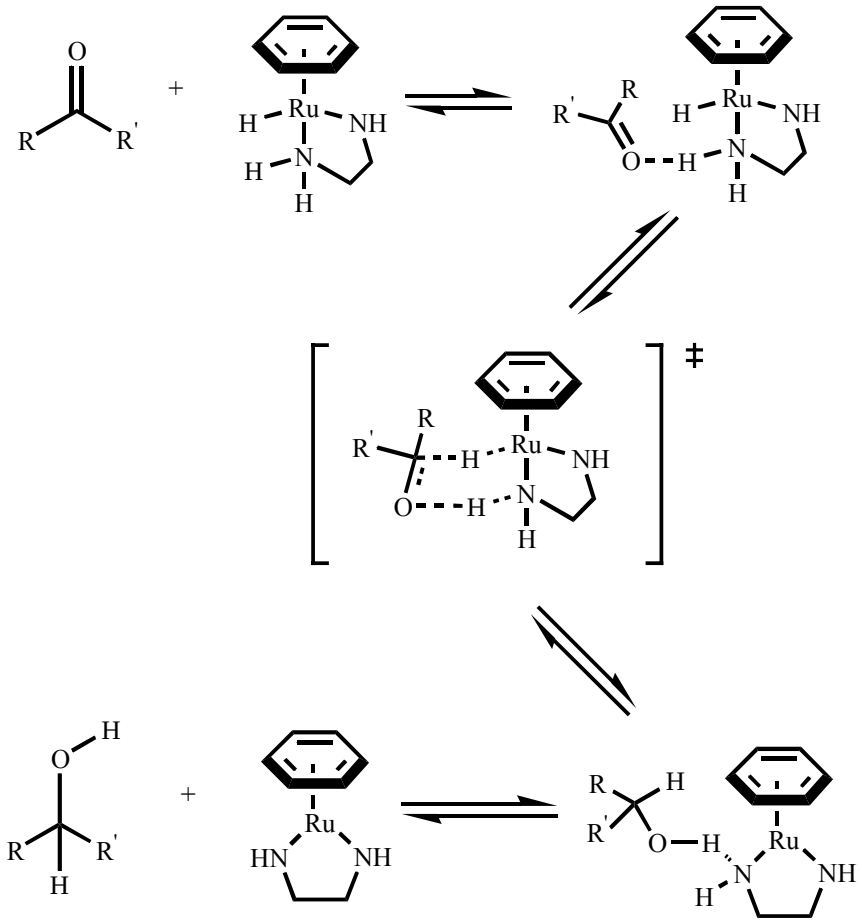

Figure 1.04. Proposed hydrogen bonding intermediates and transition state of catalytic cycle.

Late transition metal amido complexes have proven to be very reactive[44-47] and have been identified as important intermediates in both stoichiometric and catalytic reactions.[46] They were first identified in mechanisms involving base-catalyzed substitution reactions at substitution-inert amine complexes.[48] More recently they have been recognized as extremely strong bases in carbon-hydrogen bond activation

reactions[47] and as intermediates in the catalytic hydroamination of aryl halides[49] and hydrogen-transfer hydrogenation[50-54] or direct hydrogenation of imines.[42,55,56]

The reduction of C=C double bonds is one of the most fundamental synthetic transformations and plays a key role in the manufacturing of a wide variaty of bulk and fine chemicals. Highly stereoselective methods have emerged from transfer hydrogenation techniques based on the use of suitable chiral transition metal complexes in homogeneous solution.[57,58] In particular, chiral phosphine-rhodium complexes have proven effective for transfer hydrogenation of C=C double bonds.[59-61] Enantioselective transfer hydrogenation of ketones and imines can be achieved by using chiral TsDPEN-Ru(II) catalysts.[62-65] The notable feature of these catalysts is that the transfer hydrogenation is highly chemoselective for the C=O function and tolerant of alkenes.[64-66] However, it was found that the chemoselectivity could be completely switched from C=O to C=C bonds in the transfer hydrogenation of activated α, β-unsaturated ketones catalyzed by diamine-ruthenium complexes (Figure 1.05).[67] In regards to the mechanism, this transformation is believed to proceed by a stepwise conjugate reduction procedure (Figure 1.05) rather than by a concerted mechanism as in the transfer hydrogenation of ketones. In the hydrogenation of α-phenylacrylic acid or its ester, low enantioselectivity was obtained, the reason was thought to be that an asymmetric protonation of the α-carbon may preferentially occur from the acidic NH group of TsDPEN (see structure X) via six-member transition state as well as receiving a proton from achiral acid NEt_3H^+ in the reaction mixture.[67]

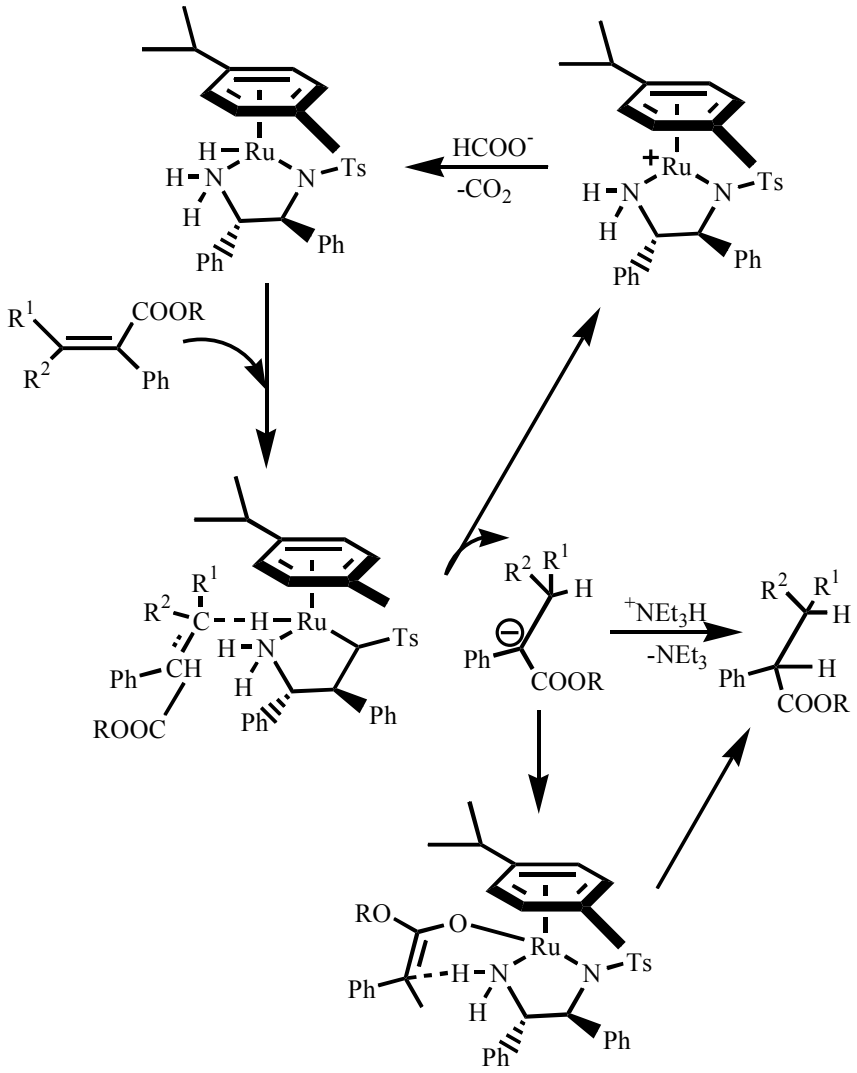

Figure 1.05. Proposed mechanism of the transfer hydrogenation of activated C=C bonds.

Lately, attention has been drawn to the more synthetically challenging and useful catalytic anti-Markovnikov hydration of terminal alkynes. Generally, hydration of terminal alkynes follows Markovnikov's rule using a number of acidic and/or metal-containing catalysts, which means the product will be corresponding methyl ketone instead of aldehyde. In order to get the anti-Markovnikov product aldehyde, stoichiometric conversions by using boranes or silanes, followed by oxidation have been required. In 1998, Tokunaga and Wakatsuki reported the first catalytic formation of aldehydes from the hydration of terminal alkynes using 10 mol% ruthenium precursor and phosphine ligand.[68] The highest ratio of aldehyde to ketone they could obtain was 67:1 and added phosphine ligand was required (Figure 1.06). Moreover, for some alkynes such as phenylacetylene, less than 2% of a 1:1 mixture of aldehyde and ketone was obtained.

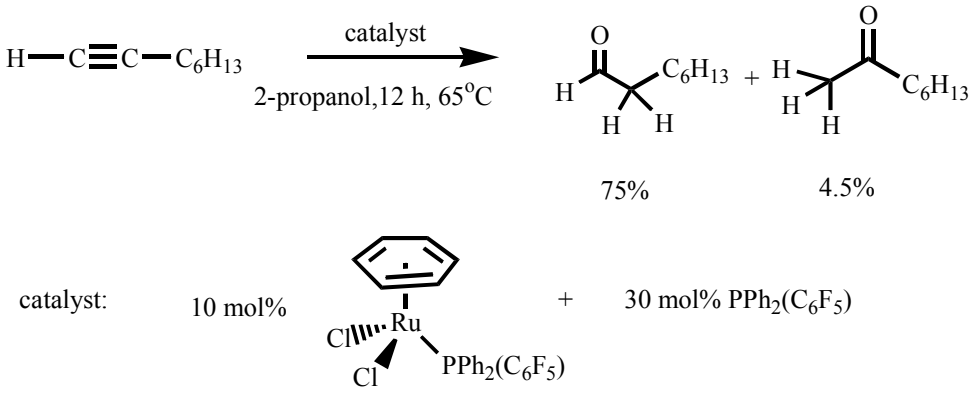

Figure 1.06. Anti-Markovnikov hydration of terminal alkynes using Tokunaga's catalyst.

In 2001, Suzuki et al. reported[69] the formation and isolation of $Ru(CO)(Cl)(Cp)(PPh_3)$ from the reaction of $Ru(Cl)(Cp)(PPh_3)_2$ (30 mol%) with 1-

octyne, in addtion to the formation of aldehyde and alkane products, which suggested that catalyst instability was due to the loss of phosphine. Therefore, it is not suprising that the chelating phosphine complex Ru(Cl)(Cp)($Ph_2PCH_2PPh_2$) (2 mol%) catalyzed formation of aldehyde at 100 ^oC in over 90% yield in many cases.

Learning from the metalloenzymes in Nature, an alkyne hydration catalyst was designed by placing an internal pendant base near the transition metal center to promote the formation of a more reactive nucleophile (Figure 1.07). The internal base could be either imidazole or pyridine. In 2001, Grotjahn reported the anti-Markovnikov hydration of terminal alkynes using a bifunctional catalyst with a CpRu fragment and imidazole containing phosphines.[70] At 70 ^oC, with environment friendly water as solvent, this resulted in the near-quantitative production of aldehydes from a variety of terminal alkynes. Compared to the other catalyst systems, the reaction is faster and requires lower temperature. More significantly, the reaction conditions are remarkably neutral, so that acid-sensitive protecting groups can be tolerated. A water complex 1a (Figure 1.07) was prepared, the crystal structure shows a water molecule in a binding pocket formed by the metal as Lewis acid and the two basic imidazole nitrogen atoms as hydrogen-bond acceptors. Then less basic pyridine was used to replace imidazole in order to reduce hydrogen bond strength and limit water coordination so that a not-too-good binding pocket for water was created (1b, Figure 1.07). In fact, 1b was 12.8 times as active as 1a and 1100 time more active than Ru(Cl)(Cp)($Ph_2PCH_2PPh_2$).[71] The mechanism of the heterocycle-assisted alkyne hydration and what role the heterocyle plays are under investigation.[72]

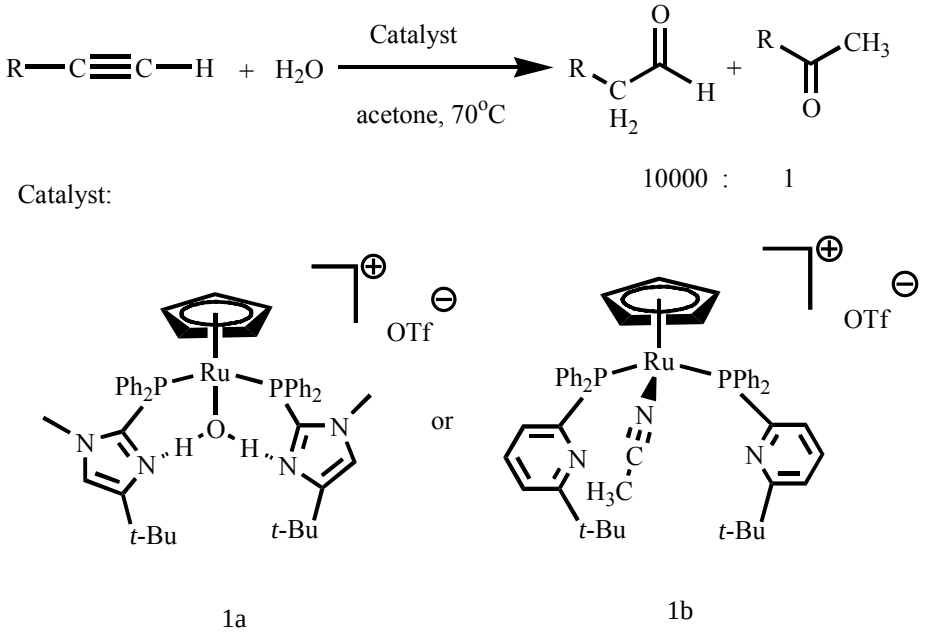

Figure 1.07. Anti-Markovnikov hydration of alkynes using bifunctional catalyst.

With many promising literature examples of the importance of proton transfer and hydrogen bonding, the goal of this thesis is to expand the use of the combination of metal-ligand and hydrogen bonding interactions or hydrogen transfer in organometallic catalysis. As in complexes 1a and 1b, part of the ligand will bind to a transition metal, while leaving the other one or more atoms free to engage in donation or acceptance of hydrogen bond(s) or proton(s). As described in further detail in the next chapter, imidazolylphosphine ligands have been less studied than pyridylphosphine ligands, yet as seen in Figure 1.08, imidazolylphosphine systems feature several positions with which to control reactivity. Other group members have been working on the study of imidazolylphosphine or pyridylphosphine ligands with a

variety of metals such as Rh,[73] Ir,[74] and Ru.[71,72] However, in this thesis, Pd and Pt complexes of imidazolylphosphines are the focus. Both are d^{10} transition metals in the zerovalent state. In this thesis both three-coordinate trigonal planar, and two-coordinate linear geometries will be seen. In addition, square-planar M^{2+} centers will also be seen. Although Pd- and Pt-catalyzed reactions have been intensively studied, Pd and Pt complexes with ligands capable of hydrogen bonding and proton transfer are still relatively rare. Our research is to conduct fundamental studies of the $M(0)/M^{2+}$ pair and lead to develop catalysts for important organic reactions.

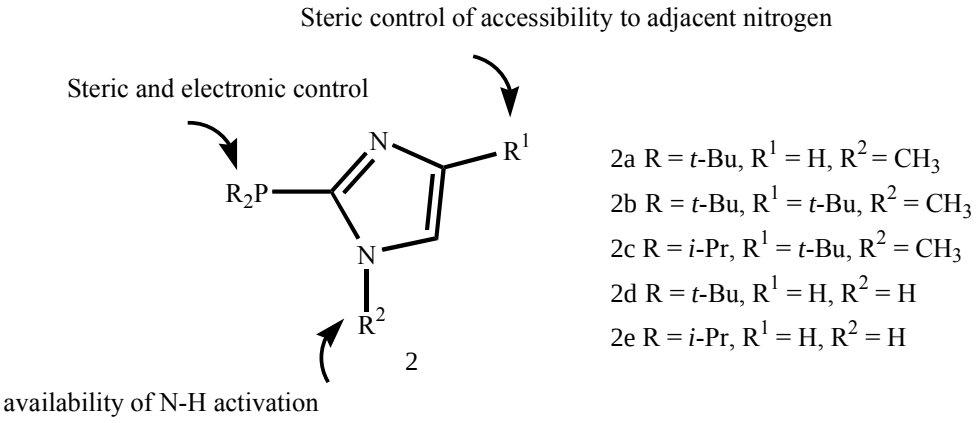

Figure 1.08. Design of bifunctional imidazolylphosphine ligand 2.

References

(1) Strater, N.; Lipsscomb, W. N.; Klablunde, T.; Krebs, B. *Angew. Chem., Int. Ed. Engl.* 1996, *35*, 2024.

(2) Wilcox, D. E.; *Chem. Rev.* 1996, *96*, 2435.

(3) Perreault, D. M.; Anslyn, E. V. *Angew. Chem., Int. Ed. Engl.* 1997, *36*, 433.

(4) Thompson, J. E.; Raines, R. T. *J. Am. Chem. Soc.* 1994, *116*, 5467.

(5) Komiyama, M.; Yoshinari, K. *J. Org. Chem.* 1997, *62*, 2155.

(6) Molenveld, P.; Kapsabelis, S.; Engbersen, J. F. J.; Reinhoudt, D. N. *J. Am. Chem. Soc.* 1997, *119*, 2948.

(7) Molenveld, P.; Stikvoort, W. M. G.; Kooijman, H.; Spek, A. L.; Engbersen, J. F. J; Reinhoudt, D. N. *J. Org. Chem.* 1999, *64*, 3896.

(8) Molenveld, P.; Engbersen, J. F. J.; Kooijman, H.; Spek, A. L.; Reinhoudt, D. N. *J. Am. Chem. Soc.* 1998, *120*, 6726.

(9) Molenveld, P.; Engbersen, J. F. J.; Reinhoudt, D. N. *J. Org. Chem.* 1999, *64*, 6337-6341.

(10) Lukin, O.; Leszczynski, J. *J. Phys. Chem. A.* 2002, *106*, 6775-6782.

(11) Toh, J. S.-S.; Jordan, M. J. T.; Husowitz, B. C.; Del Bene, J. E. *J. Phys. Chem. A.* 2001, *105*, 10906-10914.

(12) Shan, S.-O.; Herschlag, D. *Methods in Enzymology* 1999, *308*, 246-276.

(13) Shan, S.-O.; Herschlag, D. *Proceedings of the Natural Academy of Sciences of the United States of America* 1996, *93*, 14474-14479.

(14) Shan, S.-O.; Herschlag, D. *J. Am. Chem. Soc.* 1996, *118*, 5515-5518.

(15) Epstein, L. M.; Krylov, A. N.; Shubina, E. S.; *J. Mol. Struc.* 1994, *322*, 345-352.

(16) Braga, D.; Grepioni, F.; Sabatino, P.; Desiraju, G. R. *Organometallics* 1994, *13*, 3532-3543.

(17) Braga, D.; Grepioni, F.; Biradha, K.; Pedireddi, V. R.; Desiraju, G. R. *J. Am. Chem. Soc.* 1995, *117*, 3156-3166.

(18) Brammer, L.; Zhao, D.; Laido, F. T.; Braddock-Wilking, *Acta Cryst, Sect. B: Structural Science* 1995, B51, 632-640.

(19) Biradha, K.; Desiraju, G. R.; Braga, D.; Grepioni, F. *Organometallics* 1996, *15*, 1284-1295.

(20) Braga, D.; Grepioni, F.; Tedesco, E.; Biradha, K.; Desiraju, G. R. *Organometallics* 1996, *15*, 2692-2699.

(21) Braga, D.; Grepioni, F.; Tedesco, E.; Biradha, K.; Desiraju, G. R. *Organometallics* 1997, *16*, 1846-1856.

(22) Brammer, L. *Dalton Transactions* 2003, 3145-3157.

(23) Crabtree, R. H.; Loch, J. A.; Gruet, K.; Lee, D.-H.; Borgmann, C. *J. Organomet. Chem.* 2000, *600*, 7-11.

(24) Kellogg, R. M. *Pure and Applied Chemistry* 1992, *64*, 413-420.

(25) Jarvo, E. R.; Copeland, N.; Papaioannou, P. J. Miller, S. J. *J. Am. Chem. Soc.* 1999, *121*, 11638-11643.

(26) Sigman, M. S.; Vachal, P.; Jacobsen, E. N.; *Angew. Chem.* 2000, 112, 1336-1338; *Angew. Chem., Int. Ed.* 2000, *39*, 1279-1281.

(27) Okino, T.; Hoashi, Y.; Takemoto, Y. *J. Am. Chem. Soc.* 2003, *125*, 12672-12673.

(28) Hamashima, Y.; Sawada, D.; Kanai, M.; Shibasaki, M. *J. Am. Chem. Soc.* 1999, *121*, 2641-2642.

(29) Funabashi, K.; Ratni, H.; Kanai, M.; Shibasaki, M. *J. Am. Chem. Soc.* 2001, *123*, 10784-10785.

(30) Shibasaki, M.; Sasai, H.; Arai, T. *Angew. Chem*. 1997, 109, 1290-1310; *Angew. Chem., Int. Ed.* 1997, *36*, 1236-1256.

(31) Groger, H. *Chem. Eur. J.* 2001, *7*, 5246-5251.

(32) Kanai, M. *Yakugaku Zasshi* 2001, *121*, 949-960.

(33) Casas, J.; Najera, C.; Sansano, J. M.; Saa, J. M. *Org. Lett.* 2002, *4*, 2589-2592.

(34) Casas, J.; Najera, C.; Sansano, J. M.; Saa, J. M. *Tetrahedron* 2004, *60*, 10487-10496.

(35) France, S.; Wack, H.; Hafez, A. M.; Taggi, A. E.; Witsil, D. R.; Lectka, T. *Org. Lett.* 2002, *4*, 1603-1605.

(36) France, S.; Shah, M. H.; Weatherwax, A.; Wach, H.; Roth, J. P.; Lectka, T. *J. Am. Chem. Soc.* 2005, *127*, 1206-1215.

(37) Josephsohn, N. S.; Kuntz, K. W.; Snapper, M. L.; Hoveyda, A. H. *J. Am. Chem. Soc.* 2001, *123*, 11594-11599.

(38) Drent, E.; van Broekhoven, J. A. M.; Doyle, M. J. *J. Organomet. Chem.* 1991, *417*, 235-251.

(39) Drent, E.; Arnoldy, P.; Budzelaar, P. H. M. *J. Organomet. Chem*. 1993, *455*, 247-253.

(40) Drent, E.; Arnoldy, P.; Budzelaar, P. H. M. *J. Organomet. Chem.* 1994, *475*, 57-63.

(41) Scrivanti, A.; Beghetto, V.; Campagna, E.; Zanato, M.; Matteoli, U. *Organometallics* 1998, *17*, 630-635.

(42) Noyori, R.; Ohkuma, T. *Angew. Chem. Int. Ed.* 2001, *40*, 40-73.

(43) Noyori, R.; Yamakawa, M.; Hashiguchi, S. *J. Org. Chem.* 2001, *66*, 7931-7944.

(44) Bryndza, H. E.; Tam, W. *Chem. Rev.* 1988, *88*, 1163-1188.

(45) Fryzuk, M. D.; Montgomery, C. D. *Coord. Chem. Rev.* 1989, *95*, 1-40.

(46) Fulton, J. R.; Holland, A. W.; Fox, D. J.; Bergman, R. G. *Acc. Chem. Res.* 2002, *35*, 44-56.

(47) Fulton, J. R.; Bouwkamp, M. W.; Bergman, R. G. *J. Am. Chem. Soc.* 2000, *122*, 8799-8800.

(48) Basolo, F.; Pearson, R. G. *Mechanisms of Inorganic Reactions*; Wiley: New York, 1967.

(49) Alcazar-Roman, L. M.; Hartwig, J. F.; Rheingold, A. L.; Liable-Sand, L. M.; Gizei, I. A. *J. Am. Chem. Soc.* 2000, *122*, 4618-4630.

(50) Yamakawa, M.; Ito, H.; Noyori, R. *J. Am. Chem. Soc.* 2000, 122, 1466-1478.

(51) Altali, M.; Allaoud, S.; Karim, A.; Meliet, C.; Mortreux, A. *Tetrahedron*: *Asymmetry* 2000, *11*, 1367-1374.

(52) Machima, K.; Abe, T.; Tani, K. *Chem. Lett.* 1998, 1199-1200.

(53) Thorpe, T.; Blacker, J.; Brown, S. M.; Bubert, C.; Crosby, J.; Fitzjohn, S.; Muxworthy, J. P.; Williams, J. M. *J. Tetrahedron Lett.* 2001, *42*, 4041-4043.

(54) Mao, J.; Baker, D. C. *Org. Lett.* 1999, *1*, 841-843.

(55) Haack, K. J.; Hashiguchi, S.; Fujji, A.; Ikariya, T.; Noyori, R. *Angew. Chem., Int. Ed. Engl.* 1997, *36*, 285-288.

(56) Abdur-Rashid, K.; Faatz, M.; Lough, A. J.; Morris, R. H. *J. Am. Chem.* Soc. 2001, *123*, 7473-7474.

(57) Noyori, R.; Hashiguchi, S. *Acc. Chem. Res.* 1997, *30*, 97.

(58) Zassinovich, G.; Mestroni, G.; Gladiali, S. *Chem. Rev.* 1992, *92*, 1051.

(59) Brunner, H.; Leitner, W. *Angew. Chem., Int. Ed*. Engl. 1988, *27*, 1180.

(60) Brunner, H.; Leitner, W. *J. Organomet. Chem.* 1990, *387*, 209.

(61) Sinou, D.; Safi, M.; Claver, C.; Masdeu, A. *J. Mol. Catal.* 1991, *68*, L9.

(62) Yamakawa, M.; Yamada, I.; Noyori, R. *Angew. Chem., Int. Ed.* 2001, *40*, 2818. 2000, 122, 1466.

(63) Casey, C. P.; Johnson, J. B. *J. Org. Chem.* 2003, *68*, 1998.

(64) Sandoval, C. A.; Ohkuma, T.; Nuniz, K.; Noyori, R. *J. Am. Chem. Soc*. 2003, *125*, 13490.

(65) Casey, C.P.; Singer, S. W.; Powell, D. R.; Hayashi, R. K.; Kavana, M. *J. Am. Chem. Soc.* 2001, *123*, 1090.

(66) Fujii, A.; Hashiguchi, S.; Uematsu, N.; Ikariya, T.; Noyori, R. *J. Am. Chem. Soc.* 1996, *118*, 2521.

(67) Xue, D.; Chen, Y.; Cui, X.; Wang, Q.; Zhu, J.; Deng, J. *J. Org. Chem.* 2005, *70*, 3584-3591.

(68) Tokunaga, M.; Wakatsuki, Y. *Angew. Chem.* 1998, 110, 3024-3027; *Angew. Chem., Int. Ed.* 1998, *37*, 2867-2869.

(69) Suzuki, T.; Tokunaga, M.; Wakasuki, Y. *Org. Lett.* 2001, *3*, 735-737.

(70) Grotjahn. D. B.; Incarvito, C. D.; Rheingold, A. L. *Angew. Chem., Int. Ed.* 2001, *40*, 3884-3887.

(71) Grotjahn, D. B.; Lev, D. A. *J. Am. Chem. Soc.* 2004, *126*, 12232-12233.

(72) Lev, D. A. Doctoral Dissertation, *Group 8 and 9 Half Sandwich Complexes of Imidazolyl and Pyridyl Phosphines: Synthesis, Reactivity, and Catalysis*; Maontezuma Publishing, San Diego, 2004.

(73) Grotjahn, D. B.; Zeng, X.; Cooksy, A. L. *J. Am. Chem. Soc.* 2006, *128*, 2798-2799.

(74) Van S. Doctoral Dissertation, *The Search for Catalysts Using the Cooperativity of Transition Metals and Heterocyclic Ligands*" Montezuma Publishing, San Diego, 2002.

CHAPTER 2

Changes in Coordination of Sterically Demanding Hybrid Imidazolylphosphine Ligands on Pd(0) and Pd(II)

A. Introduction

Catalysis by organometallic complexes invariably involves ligand exchange and transformations.[1,2] Thus, it is not surprising that in the development of organometallic chemistry, an increasingly important role has been played by two special types of complexes, low-coordinate[3,4] and hemilabile species,[5-13] because such complexes readily undergo ligand association or exchange and can show exceptional reactivity and importance in catalytic chemistry.

There are textbook examples of the significance of low-coordinate species: although the ability of Wilkinson's catalyst $ClRh(PPh_3)_3$ (an isolable 16-electron complex) to catalyze the hydrogenation of alkenes was discovered in 1965,[14,15] it was not until eight years later that it was appreciated that the even more unsaturated 14-electron species $ClRh(PPh_3)_2$ played an important role in the catalysis, being 10,000 times more reactive than its 16-electron precursor toward oxidative addition of hydrogen.[16] Similarly, for more than 20 years, $Pd(PPh_3)_4$ has been known as a catalyst for reactions involving the activation of carbon-halogen bonds in aryl substrates and coupling of the carbon with other atoms (e. g., Heck and Suzuki[17] reactions). However, in the past ten years, using sterically demanding and electron-rich phosphines which are proposed to favor formation of low-coordinate catalytic

intermediates,[18,19] the scope of the Suzuki reaction has been remarkably extended to include aryl chlorides[20] and even alkyl halides and related substrates.[21-27] In many cases, it is clear that even minor changes in ligand can make the difference between a high-yielding catalyst and an inactive one.[21,22,28] The extent of interest in new types of ligands for Suzuki coupling catalysts is exemplified by at least 10 references in 2004 alone on new phosphines,[29-38] with focus on ones which are sterically demanding and/or hemilabile, favoring more rapid catalysis. In addition, other catalytic C-C, C-O, and C-N bond-forming reactions on C-X (X = halide or sulfonate) are facilitated by using sterically demanding phosphines.[39-44]

The large phosphines used have included P(*t*-Bu)$_3$, which can be used to make the isolable, air-stable species Pd[P(*t*-Bu)$_3$]$_2$.[45,46] There is considerable evidence that even this coordinatively unsaturated species loses a ligand, producing a catalytically active 12-electron *mono*phosphine intermediate.[18,19,47]

Hemilabile ligands offer a way to stabilize low-coordinate species with a weakly coordinating ligand which can readily be removed from the metal, facilitating catalytic reactions. The most intensive study has been on hybrid P-O and P-N based ligands, which can show large and useful differences in binding affinity of the soft P and hard O or N donors for a given metal, which may itself be hard or soft.[48] For example, on related Ni(0) complexes, the hybrid ligand (*i*-Pr)$_2$PCH$_2$CH$_2$PNMe$_2$ afforded good yields of organic products, whereas the analogous chelating bis(phosphine)(*i*-

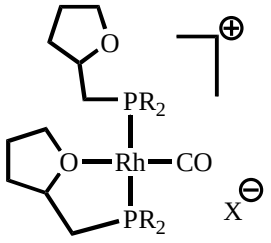

A

$Pr)_2CH_2CH_2P(i\text{-}Pr)_2$ either gave no or little product. [49,50] These differences were ascribed to the ability of the N donor in the hybrid complex to dissociate from the Ni(0) center during the catalytic cycle. In addition, the hybrid, hemilabile ligands in Rh complex A were found to facilitate the carbonylation of methyl iodide in comparison with conventional monodentate trialkylphosphines in related systems.[51] Effects of oxygen substituents on rate and selectivity of hydrogenation and hydroformylation have been noted.[6,52] Among complexes with P-N-based hybrid ligands, those with pyridyl-2-yl-modified phosphorus ligands were found to improve selectivity in hydroformylation of some olefins.[53,54]

In this chapter we describe a new group of phosphine ligands which are sterically demanding because of two large alkyl groups on P and which are hybrid because the third substituent is an imidazol-2-yl unit. For comparison, in recent years, a great deal of attention has been drawn to 2-pyridylphosphines,[55] mainly as bridging ligands; However, despite synthesis of literally hundreds of their complexes there have been surprisingly few improved catalysts using such bifunctional ligands.[56-59] By contrast, complexes of imidazolylphosphines have been much less-studied. Ligands with three imidazole groups have been used as tridentate $(N)_3$ ligands, bioinorganic models for three histidines in a protein.[60-64] In these species the phosphorus is not bound to the metal and only serves as a

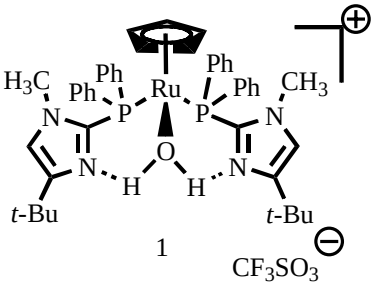

1

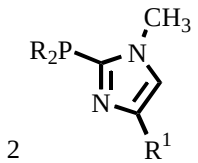

2

a R = *t*-Bu, R^1 = H
b R = *t*-Bu, R^1 = *t*-Bu
c R = *i*-Pr, R^1 = *t*-Bu

connecting element. There have been a few reports of imidazolylphosphines as bridging ligands, [65-73] bound through both P and N, but fewer of mononuclear complexes such as the ones described in this chapter.[71-77]

Our interest in imidazolylphosphines stems from our 2001 report[75] of a catalyst for anti-Markovnikov hydration of terminal alkynes to aldehydes which was more than 90 times faster than the best catalyst reported elsewhere in the literature. This species (1) contains two phosphines of general formula 2, each bearing an imidazol-2-yl group capable of hydrogen bonding or proton transfer. In our further studies both published[78] and ongoing, we seek to clarify the effects on organometallic structure and catalysis of secondary interactions between basic or acidic phosphine substituents and other ligands such as water or amines. Thus, in this report we describe the preparation of several new bulky or chelating imidazolylphosphines, their complexation to both Pd(0) and Pd(II) centers, and the effects of the heterocycles on reactivity and binding to amines, which is shown to involve hydrogen bonding as a secondary interaction.

B. Experimental Section

General Information. Reactions were performed under dry nitrogen, using a combination of Schlenk line and glovebox techniques. C_6D_6 was distilled from $LiAlH_4$ prior to use, and $CDCl_3$ was distilled from CaH_2. NMR tube reactions were performed in resealable NMR tubes (J. Young).

Unless otherwise specified, ^1H and ^{13}C data were measured at 30 °C on a 500-MHz (499.9 MHz for ^1H and 125.7 MHz for ^{13}C) and ^{31}P data were measured on a 200 MHz (80.95 MHz for ^{31}P) spectrometer and the same solvent was used for all nuclei. ^1H and ^{13}C NMR chemical shifts are reported in ppm downfield from tetramethylsilane and referenced to solvent resonances (^1H NMR: δ 7.16 for C_6HD_5, δ 7.27 for $CHCl_3$, 5.32 for CHD_2Cl_2 and ^{13}C NMR: δ 128.39 for C_6D_6 δ 77.23 for $CDCl_3$, 54.00 for CD_2Cl_2). ^1H NMR signals are given followed by multiplicity, coupling constants *J* in Hertz, integration in parentheses. For complex coupling patterns, the first coupling constant listed corresponds to the first splitting listed, e.g. for (dt, *J* = 3.2, 7.9, 1 H) the doublet exhibits the 3.2-Hz coupling constant.$^{31}P\{^1H\}$ NMR chemical shifts are referenced to an external 85% H_3PO_4 (aq) capillary placed in the solvent. IR spectra at ambient temperatures were obtained on a ThermoNicolet Nexus 670 FT-IR spectrometer. Samples were examined in C_6D_6 or CD_2Cl_2 solution in NaCl cells. Elemental analyses were performed at NuMega Laboratories in San Diego, CA for the Pd complexes and by Desert Analytics, Tucson, AZ for the ligands. Electrospray mass spectra were obtained on a Finnigan LCQ spectrometer.

Crystallographic work. Data relating to the X-ray structural determinations are collected in Table 2.01 and 2.02. All data were collected on Bruker diffractometers equipped with APEX CCD detectors. All structures were solved by direct methods and refined with anisotropic thermal parameters and idealized hydrogen atoms. All software is contained in the SMART, SAINT and SHEXTL libraries distrubted by Bruker-AXS (Madison, WI).

Preparation of CpPd(Allyl). CpPd(Allyl) was synthesized using the literature procedure.[45]

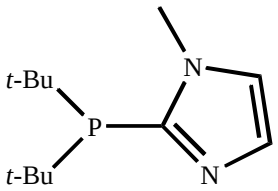

2a

Preparation of di-*tert*-butyl-(1-methyl-imidazol-2-yl)phosphine (2a). A 50 mL Schlenk flask containing a stir bar was charged with redistilled 1-methylimidazole (1.18 g, 0.014 mol) and dry, deoxygenated THF (20 mL). The reaction solution was cooled to –78 ^{o}C. A 1.6 M solution of n-BuLi (9.0 mL, 0.014 mol) was added dropwise and the reaction was allowed to stir at –78^{o}C. After 0.5 h, di-*tert*-butylchlorophosphine (2.57 g, 0.014 mol) was added dropwise. The reaction was stirred at –78 ^{o}C for 0.5 h before warming up to room temperature overnight. Deoxygenated methanol (5 mL) was added and solvents were removed on a vacuum line. Petroleum ether was added to the solid, the mixture was stirred and filtered through Celite under nitrogen. The filtrate was concentrated to a small volume (about 4 mL) and purified by radial chromatography on a 4 mm silica plate under nitrogen with hexane: ethyl acetate (8: 2). The high R_f fraction was collected and the solvent was removed on vacuum line. Pure 2a was obtained as clear

viscous oil (2.30 g, 74 %). NMR ($CDCl_3$) ^1H : 7.21 (br s, 1H), 6.96 (dd, 3, 1, 1H), 3.81 (s, 3H), 1.18 (d, 7, 18H); ^{13}C {^1H}: 158.4 (s), 129.8 (s), 122.4 (s), 34.6 (d, 18), 33.3 (d, 14), 30.1 [d, 14, $C(CH_3)_3$]; $^{31}P\{^1H\}$: 0.5 (s). Anal. Calcd for $C_{12}H_{23}N_2P$ (226.30): C, 63.69; H, 10.24; N, 12.38. Found C, 63.71; H, 10.28; N, 12.34.

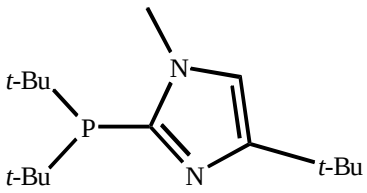

2b

Preparation of di-*tert*-butyl-(4-tert-butyl-1-methyl-imidazol-2-yl)-phosphine (2b). A 100 mL Schlenk flask was charged with 4-*tert*-butyl-1-methylimidazole[108] (3.17 g, 0.023 mol) and dry and deoxygenated THF (25 mL) and the resulting solution was cooled to -78 ^oC using a Dry Ice/acetone bath. A 1.6 M solution of n-BuLi (13.7 mL, 0.022 mol) was added dropwise over 3 min. The reaction solution was stirred at -78 ^oC. After 2 h, di-*tert*-butylchlorophosphine (4.28 g, 0.024 mol) was added dropwise. The solution was stirred at -78 ^oC for 0.5 h and then allowed to warm to room temperature overnight. The solution was quenched with deoxygenated methanol (5 mL). Solvents were removed on a vacuum line and the resulting solid was suspended in deoxygenated petroleum ether and filtered through Celite under nitrogen. The filtrate was concentrated to a small volume (5 mL) and chilled to -50 ^oC. Colorless crystals of 2b were obtained by removing the supernatant with a pipet and washing with cold petroleum ether and storing the product on a vacuum line (5.20 g, 81%). m.p. 50-51 ^oC. NMR ($CDCl_3$) ^1H : 6.63 (d, 3, 1H), 3.75 (s, 3H), 1.27 (s, 9H), 1.21 (d, 7.2, 18H); ^{13}C {^1H}: 153.2 (d, 1), 143.6 (d, 10.4), 115.7 (d, 1.4), 34.1 (d, 16.8), 33.5 [d, 14.1, $C(CH_3)_3$], 32.1 [s, $C(CH_3)_3$], 30.4 [s, $C(CH_3)_3$], 30.2 [d, 14.1, $C(CH_3)_3$]; $^{31}P\{^1H\}$: -0.4

(s).Anal. Calcd. for $C_{16}H_{31}N_2P$ (282.40): C, 68.05; H, 11.07; N, 9.92. Found C, 67.86; H, 11.11; N, 9.81.

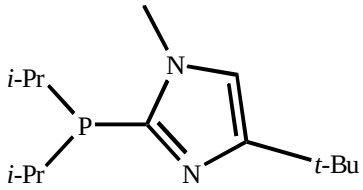

2c

Preparation of di-*iso*-propyl-(4-*tert*-butyl-1-methyl-imidazol-2-yl)phosphine (2c). To a stirred solution of 4-*tert*-butyl-1-methyl-imidazole (2.87 g, 0.021 mol) in dry and deoxygenated THF (25 mL) a 1.6 M solution of *n*-BuLi (13.0 mL, 0.021 mol) was added dropwise at room temperature. After 1 h, the solution was cooled to -78 ^{o}C, and a solution of di-*iso*-propylchlorophosphine (3.09 g, 0.020 mol) in THF (5 mL) was added dropwise. The solution was allowed to warm to room temperature and stirred for 2 h. The solution was then quenched with deoxygenated methanol (5 mL). Solvents were removed on a vacuum line and the resulting solid was suspended in deoxygenated petroleum ether and filtered through Celite under nitrogen. The filtrate was concentrated and purified by radial chromatography on a 4 mm silica plate under nitrogen with hexane:ethyl acetate (9:1). The high R_f fraction was collected and the solvent was removed on a vacuum line. Pure 2c was obtained as a clear oil (3.74 g, 73 %). NMR ($CDCl_3$) ^{1}H : 6.63 (d, 2, 1H), 3.72 (d, 1, 3H), 1.26 (s, 9H), 1.08 (dd, *J* = 7, 12, 6H), 0.96 (dd, *J* = 7, 12, 6H); ^{13}C {^{1}H}: 153.6 (d, 1), 144.9 (d, 9), 116.2 (s), 33.7 (d, 15), 32.0, 30.4, 24.44 (s, $CHMe_2$), 24.39 (s, $CHMe_2$), 20.1 (d, 18, CHMe*Me*), 19.4 (d, 8, CH*Me*Me); ^{31}P{^{1}H}: -19.3. Anal. Calcd for $C_{14}H_{27}N_2P$ (254.35): C, 66.11; H, 10.70; N, 11.01. Found C, 65.49; H, 10.45; N, 10.50.

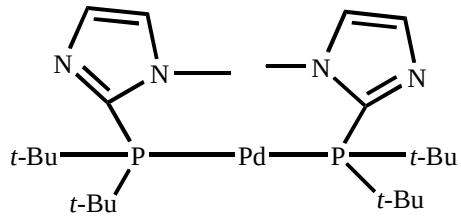

3a

Preparation of bis(di-*tert*-butyl-1-methylimidazol-2-yl-phosphine)Pd (0) (3a). Di-*tert*-butyl-1-methyl-imidazol-2-ylphosphine 2a (290.4 mg, 1.28 mmol) was added to a reaction vial containing Cp(allyl)Pd (136 mg, 0.64 mmol) and a magnetic stir bar. Deoxygenated and dry benzene (5 mL) was added to afford a dark red solution. After stirring at room temperature for 2 d, solvent was removed. The resulting residue was redissolved in THF/hexanes (about 1 mL) and filtered. The filtrate was stored in a vial at –50 ^{o}C. After 24 h, the cold supernatant was removed and the colorless crystals were washed with cold hexane and dried to give 3a (305 mg, 85%). NMR (C_6D_6) ^{1}H: 7.30 (s, 2H), 6.31 (s, 2H), 4.31 (s, 6H), 1.55 (vt, *N* = 13.8, 36H); ^{13}C{^{1}H}: 144.6 (vt, *N* = 37.7), 130.0 (vt, *N* = 6.2), 123.6 (s), 37.2 (vt, *N* = 13.8), 36.8 (vt, *N* = 14.7), 31.5 (vt, *N* = 11.7); ^{31}P{^{1}H}: 32.4 (s). Anal. Calcd. For $C_{24}H_{46}N_4P_2Pd$ (559.03): C, 51.55; H, 8.29; N, 10.02. Found: C, 51.63; H, 8.00; N, 9.98. IR (C_6D_6): 2956 (m) cm^{-1}.

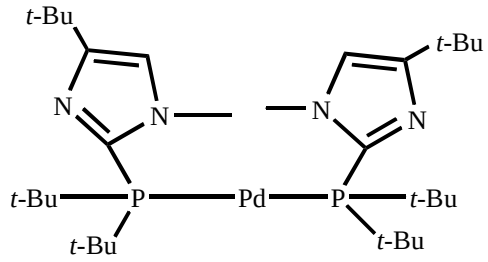

3b

Preparation of bis(di-*tert*-butyl-1-methyl-4-*tert*-butyl-imidazol-2-yl-phosphine)Pd (0) (3b). Di-*tert*-butyl-1-methyl-4-*tert*-butyl-imidazol-2-yl-phosphine 2b (440 mg, 1.56 mmol) was added to a reaction vial containing

Cp(allyl)Pd (154 mg, 0.72 mmol) and a magnetic stir bar. Deoxygenated and dry benzene (8 mL) was added to afford a dark red solution which was allowed to stir at room temperature. After 2 d, solvent was removed and the residue was redissolved in hexane (about 2 mL). After filtration, the filtrate was stored at -50 ^{o}C. After 24 h, the cold supernatant was removed and the colorless crystals were washed with cold hexane and dried to give 3b (278 mg, 62%). NMR (C_6D_6) ^{1}H: 6.37 (s, 2H), 4.34 (s, 6H), 1.56 (vt, *N* = 13.8, 36H), 1.43 (s, 18H); ^{13}C{^{1}H}: 152.8 (vt, *N* = 5.8), 143.3 (vt, *N* = 36.3), 117.4 (s), 37.2 (vt, *N* = 13.8), 36.5 (vt, *N* = 14.2), 32.5 (s), 31.6 (vt, *N* = 11.8), 30.9 (s); ^{31}P{^{1}H}: 32.1 (s).Anal. Calcd. For $C_{32}H_{62}N_4P_2Pd$ (671.24): C, 57.26; H, 9.31; N, 8.35. Found: C, 57.33; H, 9.08; N, 8.41. IR (C_6D_6): 2959 (m) cm^{-1}.

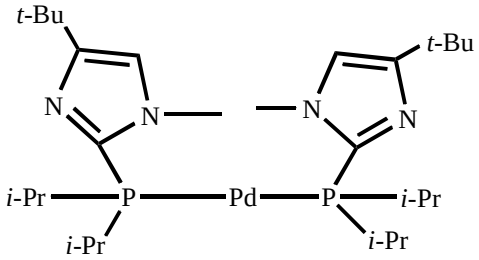

3c

Preparation of bis(di-*iso*-propyl-1-methyl-4-*tert*-butylimidazol-2-yl-phosphine)Pd(0) (3c). Di-*iso*-propyl-1-methyl-4-*tert*-butylimidazol-2-yl-phosphine 2c (493 mg, 1.94 mmol) was transferred to a reaction vial equipped with magnetic stir bar. Cp(allyl)Pd (192 mg, 0.90 mmol) was then added followed by deoxygenated benzene (8 mL). The resulting dark red solution was allowed to stir at room temperature. After 2 d, the reaction was stopped and the pale orange solution was concentrated to dryness. The residue was redissolved in hot THF/hexanes (approximately 1.5 mL) and then chilled to -50 ^{o}C. After 24 h, the cold supernatant was removed by pipet, the colorless crystals were washed with

cold hexane and dried under vacuum to give 3c (454 mg, 82%) pure by NMR spectroscopic analysis. NMR (C_6D_6) ^{1}H: 6.34 (s, 2H), 4.12 (s, 6H), 2.59 (sept, 7.0, 4H), 1.29 (dvt, *J* = 6.0, *N* = 12.5, 12H), 1.22 (dvt, *J* = 7.5, *N* = 15.0, 12H); ^{13}C{^{1}H}: 153.4 (s), 142.8 (vt, *N* = 41.0), 117.9 (s), 36.0 (broad), 32.6 (s), 30.9 (s), 27.4 (vt, *N* = 21.0), 21.1 (s, broad), 20.2 (s, sharp); ^{31}P{^{1}H}:16.2 (s).Anal. Calcd. For $C_{28}H_{54}N_4P_2Pd$ (615.12): C, 54.67; H, 8.85; N, 9.11. Found: C, 52.08; H, 8.53; N, 8.74. IR (C_6D_6): 2955 (m), 2276 (m) cm^{-1}.

Preparation of trans-bis(di-*iso*-propyl-1-methyl-4-*tert*-butyl-imidazol-2-yl-phosphine)Pd(Ph)(I) (4c-PhI). In a reaction vial, 3c (156 mg, 0.254 mmol) was weighed, then deoxygenated benzene (2 mL) was added. The reaction vial was shaken to allow everything to dissolve and a homogeneous solution was obtained. Iodobenzene (58.3 mg, 0.286 mmol) was then added via syringe. The yellow solution was allowed to stir at room temperature. After 2 d, solvent was removed and the crude product was recrystallized by slowly diffusing hexane into a benzene solution to give yellow crystals (147 mg, 71%). NMR (C_6D_6) ^{1}H: 7.16-7.18 (m, 2H), 6.87 (t, 7.1, 2H), 6.62 (t, 7.1, 1H), 6.36 (s, 2H), 3.80 (s, 6H), 2.66 (s, br, 4H), 1.39 (s, 18H), 1.39 (s, br, 12H), 1.08 (dvt, *J* = 7.6, *N* = 15.1, 12H); ^{13}C{^{1}H}: 153.2 (vt, *N* = 8.4), 153.2 (t, 4.4, C-1), 140.1 (vt, *N* = 67.5), 138.5 (t, 16.3, C-2), 127.5 (s, C-3), 123.8

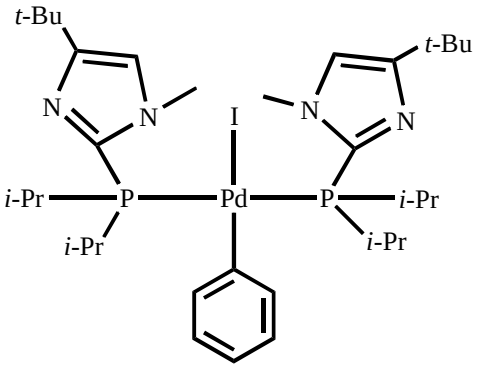

4c-PhI

(s, C-4), 118.2 (s), 37.0 (s), 32.4 (s), 30.8 (s), 27.7 (vt, *N* = 26.0), 21.0 (s, broad), 20.5 (s, sharp); $^{31}P\{^{1}H\}$: 13.7 (s). Anal. Calcd. For $C_{34}H_{59}IN_4P_2Pd$ (819.15): C, 49.85; H, 7.26; N, 6.84. Found: C, 49.52; H, 7.06; N, 6.85. IR ($CDCl_3$): 2963 (s), 1562 (s), 1470 (s) cm^{-1}.

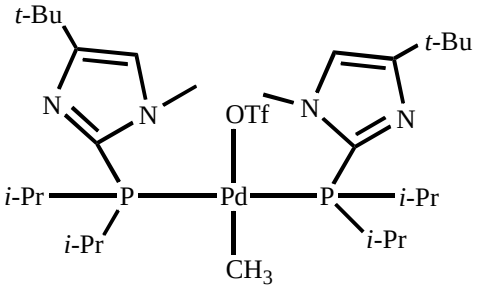

4c-MeOTf

Preparation of trans-bis(di-*iso*-propyl-1-methyl-4-*tert*-butyl-imidazol-2-ylphosphine)Pd(CH_3)(OTf) (4c-MeOTf). Palladium(0) complex 3c (73.4 mg, 0.119 mmol) and deoxygenated benzene (3 mL) were added to a reaction vial equipped with a magnetic stir bar. Methyl triflate (23.2 mg, 0.141 mmol) was added via syringe to give a slightly yellow-colored solution. After being stirred at room temperature for 1 d, solvent was removed and the solid residue was recrystallized by slowly diffusing hexane into a benzene solution. Yellow crystals (57.5 mg, 62%) were then obtained after washing and drying. NMR (C_6D_6) ^{1}H: 6.39 (s, 2H), 3.60 (s, 6H), 3.03 (s, br, 4H), 1.39 (s, 18H), 1.23 (dvt, *J* = 8.8, *N* = 16.2, 12H), 1.14 (dvt, *J* = 7.2, *N* = 14.4, 12H), 0.22 (t, 6.2, 3H); $^{13}C\{^{1}H\}$: 154.4 (vt, *N* = 8.3), 135.7 (vt, *N* = 64.9), 119.5 (s), 32.5 (s), 30.6 (s), 24.9 (vt, *N* = 24.9), 20.0 (s), 19.0 (s), -6.2 (s); $^{31}P\{^{1}H\}$: 24.5 (s). Anal. Calcd. For $C_{30}H_{57}F_3N_4O_3P_2PdS$ (779.24): C, 46.24; H, 7.37; N, 7.19. Found: C, 46.63; 6.98; 7.16. IR (C_6D_6): 2961 (s), 1315 (s) cm^{-1}.

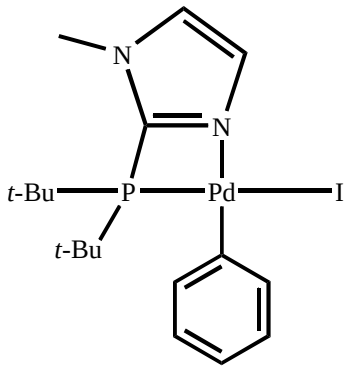

5a-PhI

Preparation of (di-*tert*-butyl-1-methylimidazol-2-yl-phosphine)Pd(Ph)(I) (5a-PhI). In a reaction vial, 3a (148 mg, 0.265 mmol) was weighed, then deoxygenated benzene (3 mL) was added. The reaction vial was shaken to allow everything to dissolve and a homogeneous solution was obtained. Iodobenzene (52.8 mg, 0.259 mmol) was then added via syringe. The resulting solution was mixed and allowed to stand still at room temperature for 24 h. The yellow crystals which formed were isolated by removing the mother liquor using a pipet, washing with benzene and drying under vacuum (134 mg, 94%). NMR (CD_2Cl_2) ^{1}H: 7.29 (s, 1H), 7.25-7.41 (m, 2H), 7.13 (s, 1H), 6.94 (t, 7.6, 2H), 6.80 (t, 7.6, 1H), 3.89 (s, 3H), 1.42 (d, 15.8, 18H); ^{13}C{^{1}H}: 147.8 (d, 27.9), 139.1 (d, 4.7, C-2), 138.3 (d, 8.9, C-1), 129.9 (d, 12.2), 126.8 (d, 2.3, C-3), 126.2 (s), 122.7 (s, C-4), 37.2 (d, 6.8), 36.9 (s), 30.3 (d, 6.0); ^{31}P{^{1}H}: 36.9 (s). Anal. Calcd. For $C_{18}H_{28}IN_2PPd$ (536.73): C, 40.28; H, 5.26; N, 5.22. Found: C, 40.52; H, 5.04; N, 5.31. IR (CH_2Cl_2): 2967 (s), 1712 (s), 1562 (s), 1470 (s) cm^{-1}.

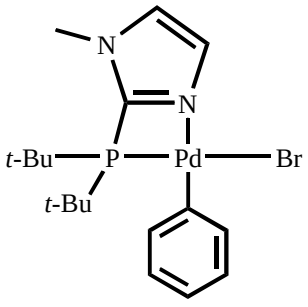

5a-PhBr

Preparation of (di-*tert*-butyl-1-methyl-imidazolylphosphine)Pd(Ph)(Br) (5a-PhBr). In a reaction vial, 3a (42.7 mg, 0.076 mmol) was weighed, then deoxygenated benzene (1 mL) was added. The reaction vial was shaken to allow everything to dissolve and a homogeneous solution was obtained.

Bromobenzene (11.9 mg, 0.076 mmol) was then added via syringe. The resulting solution was mixed and allowed to stand still at room temperature for 24 h. The yellow crystals which formed were isolated by removing the mother liquor using a pipet, washing with benzene and drying under vacuum (25 mg, 72%). %). NMR ($CDCl_3$) ^{1}H: 7.37-7.42 (m, 2H), 7.34 (s, 1H), 7.05 (s, 1H), 6.94 (t, 7.2, 2H), 6.79 (t, 7.2, 1H), 3.89 (s, 3H), 1.43 (d, 15.8, 18H); ^{31}P{^{1}H}: 43.5 (s). Anal. Calcd. For $C_{18}H_{28}BrN_2PPd$ (489.73): C, 44.15; H, 5.76; N, 5.72. Found: C, 44.14; H, 5.64; N, 5.77. IR (CH_2Cl_2): 2927 (s), 1563 (s), 1471 (s) cm^{-1}.

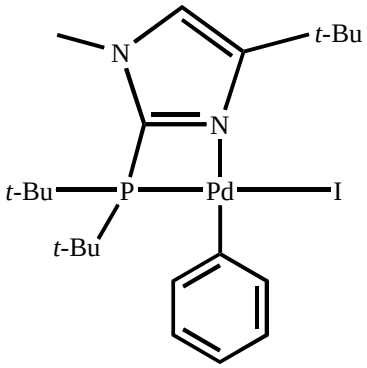

5b-PhI

Preparation of (di-*tert*-butyl-1-methyl-4-*tert*-butyl-imidazol-2-ylphosphine)Pd(Ph)(I) (5b-PhI). In a reaction vial, 3b (121 mg, 0.180 mmol) was weighed. Then deoxygenated benzene (2 mL) was added. The reaction vial was shaken to allow everything to dissolve and a homogeneous solution was obtained. Iodobenzene (36.5 mg, 0.178 mmol) was then added via syringe. The resulting solution was mixed and allowed to stand still at room temperature for 24 h. The yellow crystals which formed were isolated by removing the mother liquor using a pipet, washing with benzene and drying under vacuum (104 mg, 97%). NMR ($CDCl_3$) ^{1}H: 7.37-7.42 (m, 2H), 6.91 (t, 7.2, 2H), 6.73 (t, 7.2, 1H), 6.73 (s, 1H), 3.84 (s, 3H), 1.45 (d, 15.6, 18H), 1.37 (s, 9H); ^{13}C{^{1}H}: 154.2 (d, 11.6), 146.6 (d, 30.4), 139.0 (d, 4.5, C-2), 134.1 (d, 10.6, C-1), 126.5 (d, 2.0, C-3), 122.4 (s, C-4), 119.6 (s), 37.0 (d, 7.8), 36.7 (s), 32.0 (s), 30.5 (s), 30.3 (d, 5.8), ;

$^{31}P\{^{1}H\}$: 29.3 (s)Anal. Calcd. For $C_{22}H_{36}IN_2PPd$ (592.83): C, 44.57; H, 6.12; N, 4.73. Found: C, 44.26; H, 5.90; N, 4.76. IR ($CDCl_3$): 2963 (s), 1562 (s), 1470 (s) cm^{-1}.

Preparation of (di-*tert*-butyl-1-methylimidazol-2-ylphosphine)Pd(CH_3)[OTf] ($[6a\text{-}Me]^+[OTf]^-$). Palladium(0) complex 3a (76.8 mg, 0.137 mmol) and deoxygenated benzene (3 mL) were added to a reaction vial equipped with magnetic stir bar. Methyl triflate (22.5 mg, 0.137 mmol) was added via syringe to give a slightly yellow-colored solution. After being stirred at room temperature for 1 d, solvent was removed and the resulting solid was recrystallized by slowly diffusing diethyl ether into a dichloromethane solution. Colorless crystals (65.7 mg, 66%) were then obtained. NMR ($CDCl_3$, -50 ^{o}C) ^{1}H: 7.30 (s, 1H), 7.28 (s, 1H), 7.12 (s, 1H), 5.18 (s, 1H), 3.99 (s, 3H), 3.95 (s, 3H), 1.67 (s, br, 9H), 1.47 (vt, *N* = 16.0, 18H), 1.29 (vt, *N* = 14.4, 9H), 0.95 (t, 5.2, 3H); $^{13}C\{^{1}H\}$: 145.8 (vt, *N* = 28.8), 139.5 (vt, *N* = 56.5), 130.3 (vt, *N* = 8.2), 127.6 (vt, *N* = 13.3), 127.3 (s), 124.8 (s), 38.6 (vt, *N* = 18.0), 38.4 (vt, *N* = 16.8), 37.2 (s), 36.7 (vt, *N* = 9.5), 36.6 (s), 36.3 (vt, *N* = 9.0), 30.4 (s), 30.2 (s), -17.2 (s); $^{31}P\{^{1}H\}$: 32.1 (s). Anal. Calcd. For $C_{25}H_{49}F_3N_4O_3P_2PdS$ (723.18): C, 43.18; H, 6.83; N, 7.74. Found: C, 43.11; H, 7.13; N, 7.85. IR ($CDCl_3$): 1270 (s) cm^{-1}.

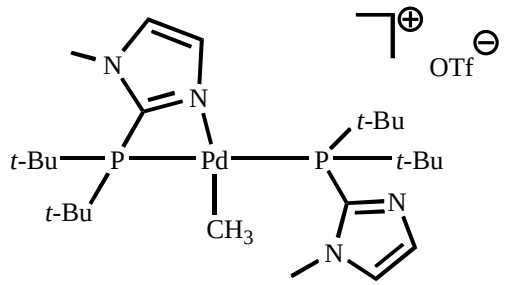

$[6a\text{-}Me]^+[OTf]^-$

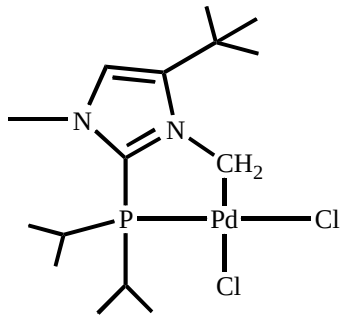

7c-CH_2Cl_2

Preparation of (di-*iso*-propyl-1-methyl-3-methylene-4-*tert*-butyl-imidazol-2-ylphosphine)$PdCl_2$ (7c-CH_2Cl_2). Palladium(0) complex 3c (33.3 mg, 0.054 mmol) was dissolved in a vial using dry and deoxygenated dichloromethane (2 mL). The resulting yellow solution was allowed to stir at room temperature. After 24 h, the reaction solution was concentrated to one third of the original volume and diethyl ether was slowly diffused into the solution. White crystals (19.2 mg, 79.8%) were so obtained. NMR (CD_2Cl_2) ^{1}H: 7.56 (s, 1H), 4.56 (d, 2.0, 2H, PdC*H*2N), 3.97 (s, 3H), 2.87 (sept of d, *J* = 7.0, 11.0, 2H), 1.56 (dd, *J* = 7.0, 19.0, 6H), 1.41 (s, 9H), 1.25 (dd, *J* = 7.5, 18.0, 6H); ^{13}C{^{1}H}: 147.5 (d, 27.7), 146.2 (d, 8.6), 129.4 (s), 45.1 (d, 5.4, Pd*C*H2N), 38.3 (s), 32.6 (s), 29.1 (s), 27.5 (d, 24.4), 20.2 (s), 19.6 (d, 5.0); ^{31}P{^{1}H}: 65.3 (s). Anal. Calcd. For $C_{15}H_{29}Cl_2N_2PPd$ (445.70): C, 40.42; H, 6.56; N, 6.29. Found: C, 40.24; H, 6.50; N, 6.58. IR (CD_2Cl_2): 2970 (m), 2298 (w), 1712 (s) cm^{-1}.

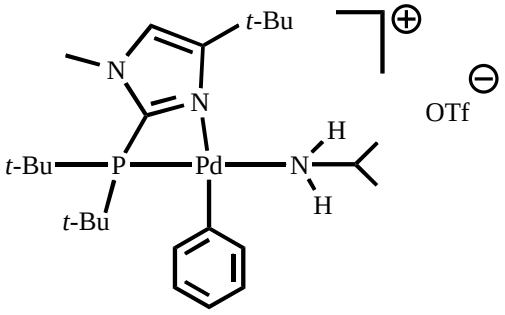

[8b-Ph]$^+$[OTf]$^-$

Preparation of (di-*tert*-butyl-1-methyl-4-*tert*-butyl-imidazol-2-ylphosphine)Pd(Ph)($NH_2CH(CH_3)_2$)[OTf] ([8b-Ph]$^+$[OTf]$^-$). Complex 5b-PhI (46.0 mg, 0.077 mmol) was transferred to a vial containing silver triflate (21.2 mg, 0.083 mmol). Degassed dichloromethane

was added followed by isopropylamine (6.25 mg, 0.106 mmol). The reaction mixture was shaken and a yellow precipitate formed right away. The upper colorless solution was isolated by filtering the suspension through cotton and Celite. The filtrate was then concentrated down to a small volume and diethyl ether was allowed to diffuse into it to give colorless crystals (22.6 mg, 56%). NMR (CD_2Cl_2) ^{1}H: 7.41 (m, 2H), 7.09 (m, 2H), 7.04 (s, 1H), 7.03 (m, 1H), 3.91 (s, 3H), 2.65-2.77 (m, 1H), 1.41 (d, 16.2, 18H), 1.31 (s, 9H), 1.27 (d, 6.2, 6H, amine CH_3); ^{13}C{^{1}H}: 153.5 (d, 10.3), 145.6 (d, 35.2), 141.4 (s), 136.7 (d, 3.9, Ph-C-1), 128.8 (d, 2.1, Ph-C-2), 124.9 (s, Ph-C-3), 121.7 (s, Ph-C-4), 46.5 (s, amine CHN), 37.5 (s), 37.4 (s), 31.6 (s), 30.4 (s), 30.3 (d, 6.3), 26.7 (s, amine CH_3); ^{31}P{^{1}H}: 39.8 (s). Anal. Calcd. For $C_{26}H_{45}F_3N_3O_3PPdS$ (674.12): C, 46.32; H, 6.73; N, 6.23. Found: C, 46.10; H, 6.95; N, 6.22. IR (CD_2Cl_2): 3327 (w), 2971 (m), 1566 (m), 1270 (s) cm^{-1}.

Preparation of (di-*tert*-butyl-1-methyl-4-*ter*t-butyl-imidazol-2-ylphosphine)Pd(Ph)(morpholine)[OTf] ([9b-Ph]$^+$[OTf]$^-$). Complex 5b-PhI (21.9 mg, 0.037 mmol) was transferred to a vial containing silver triflate (12.1 mg, 0.047 mmol). Degassed dichloromethane was added followed by the addition of morpholine (9.99 mg, 0.115 mmol). The reaction mixture was shaken and a yellow precipitate formed right away. The upper colorless solution was isolated by filtering the suspension through cotton and Celite.

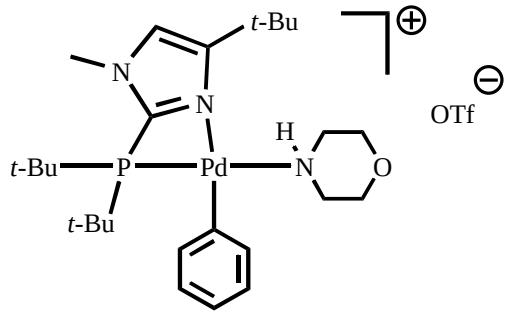

[9b-Ph]$^+$[OTf]$^-$

The filtrate was then concentrated down to a small volume and diethyl ether was allowed to diffuse into it to give colorless crystals (15.6 mg, 76%). NMR (CD_2Cl_2) ^{1}H: 7.39-7.42 (m, 2H), 7.10 (t, 8.0, 2H), 7.10 (s, 1H), 7.04 (t, 7.5, 1H), 3.92 (s, 3H), 3.78 (d, 13.0, 2H), 3.50 (t, 11.5, 2H), 3.34 (t, br, 12.0, 1H), 3.04 (d, 13.5, 2H), 2.74 (dt, 11.0, 12.0, 2H), 1.39 (d, 16.5, 18H), 1.34 (s, 9H); ^{13}C{^{1}H}: 153.0 (d, 10.0), 145.5 (d, 36.7), 143.3 (s), 136.6 (d, 3.9, Ph-C-1), 128.6 (d, 2.0, Ph-C-2), 125.2 (s, Ph-C-3), 122.1 (s, Ph-C-4), 68.2 (s, amine C-2), 49.3 (s, amine C-3), 37.6 (s), 37.5 (s), 31.5 (s), 30.3 (d, 4.8), 30.3 (s); ^{31}P{^{1}H}: 42.3 (s). Anal. Calcd. For $C_{27}H_{45}F_3N_3O_4PPdS$ (702.12): C, 46.19; H, 6.46; N, 5.98. Found: C, 42.51; H, 5.56; N, 6.15. Anal. Calcd. For $C_{27}H_{45}F_3N_3O_4PPdS$ + CH_2Cl_2 (702.12 + 84.93): C, 42.73; H, 6.02; N, 5.34. IR (CD_2Cl_2): 2970 (m), 1565 (m), 1271 (s) cm^{-1}.

Preparation of trans-bis(di-*iso*-propyl-1-methyl-4-*tert*-butyl-imidazol-2-ylphosphine)$_2$Pd(CH_3)(NH_2CH_2Ph)[OTf] ([10c-Me]$^+$[OTf]$^-$). Complex 4c-MeOTf (36.0 mg, 0.058 mmol) was dissolved in dichloromethane (1 mL) to give a clear solution. Benzylamine (6.27 mg, 0.058 mmol) was added via syringe. The reaction mixture was allowed to stir at room temperature. After 24 h, the solution was concentrated to dryness and the resulting solid was recrystallized by slowly diffusing diethyl ether into a dichloromethane solution. The colorless crystals were washed with cold diethyl ether and dried under vacuum (33.7 mg, 65%). NMR

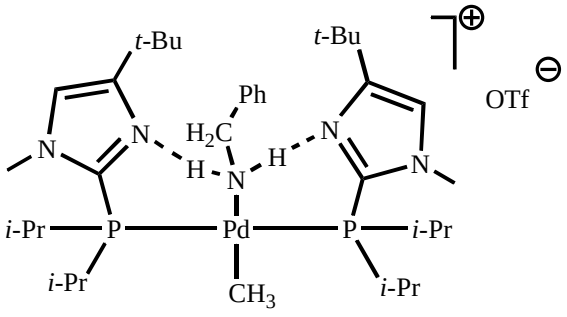

[10c-Me]$^+$[OTf]$^-$

(CD_2Cl_2) ^1H: 7.10-7.22 (m, 3H), 6.69 (s, 2H), 6.29(sl br d, 6, 2H), 4.00 (s, 6H), 3.44 (br s, 2H), 2.95-3.10 (m, 2H), 2.80-3.05 (m, 4H), 1.18-1.38 (m, 24H), 1.12 (s, 18H), 0.51 (t, 6.2, 3H); $^{13}C\{^1H\}$: 154.3 (d, 10.0), 139.8 (s, ipso), 134.2 (vt, *N* = 56.6), 129.5 (s, ortho), 128.7 (s, para), 127.7 (s, meta), 121.3 (s), 49.1 (s, CH_2), 35.8 (s), 31.7 (s), 29.8 (s), 23.9 (vt, *N* = 24.6), 19.2 (s), -10.4 (s, Pd-CH_3); $^{31}P\{^1H\}$: 30.3 (s); ($CDCl_3$): 7.11-7.20 (m, 3H), 6.93 (s, 2H), 6.33 (sl br d, 7.0, 2H), 4.04 (s, 6H), 3.30 (br s, 2H), 3.03 (t, 7.0, 2H), 2.92 (sept, 6.5, 4H), 1.25-1.32 (m, 24H), 1.11 (s, 18H), 0.47 (t, 6.0, 3H); $^{31}P\{^1H\}$: 28.8 (s). Anal. Calcd. For $C_{37}H_{66}F_3N_5O_3P_2PdS$ (885.33): C, 50.14; H, 7.51; N, 7.90. Found: C, 50.03; H, 6.54; N, 8.07. IR (CD_2Cl_2): 2966 (m), 1515 (s), 1270 (s) cm^{-1}.

Preparation of trans-bis(di-*iso*-propyl-1-methyl-4-*tert*-butyl-imidazol-2-ylphosphine)$_2$Pd(CH_3)(NH_2CH_2Ph)[$B(Ar_F')_4$] ([10c-Me]$^+$[$B(Ar_F')_4$]$^-$). Palladium(0) complex 3c (58.3 mg, 0.095 mmol) was dissolved in benzene (1 mL) to give a clear solution. Iodomethane (13.5 mg, 0.095 mmol) was added with gentle shaking, giving a slightly yellow solution. After 20 min, solvent was removed and dichloromethane was added to the residue to a homogeneous solution. Benzylamine (10.2 mg, 0.095 mmol) was added to the solution followed by salt potassium tetra(pentafluorophenyl)borate (67.3 mg, 0.094 mmol). The sequential addition resulted in the formation of a yellow precipitate.

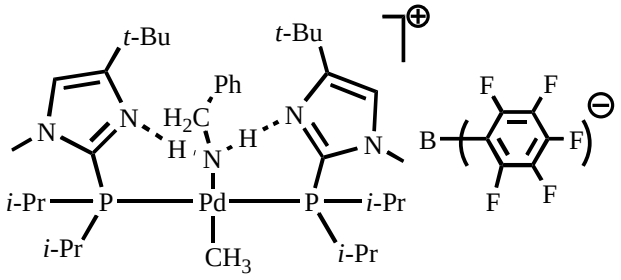

[10c-Me]$^+$[$B(Ar_F')_4$]$^-$

After the reaction mixture was filtered through cotton and Celite, the filtrate was concentrated to dryness and the residue was recrystallized from a diethyl ether/dichloromethane mixture. Yellow crystals were obtained after washing with cold diethyl ether and drying under vacuum (72.7 mg, 46%). NMR ($CDCl_3$) ^{1}H: 7.18 (t, 7.5, 1H), 7.11 (t, 7.5, 2H), 6.87 (s, 2H), 6.20 (d, 7.5, 2H), 3.94 (s, 6H), 3.41 (s, br, 2H), 3.00 (t, 7.5, 2H), 2.89 (sept, 6.5, 4H), 1.25-1.32 (m, 24H), 1.11 (s, 18H), 0.50 (t, 6.0, 3H); $^{13}C\{^{1}H\}$: 154.7 (vt, *N* = 10.8), 138.8 (s, ipso), 134.3 (vt, *N* = 56.3), 129.0 (s, ortho), 128.3 (s, para), 126.8 (s, meta), 121.3 (s), 48.5 (s, CH_2), 35.3 (s), 31.8 (s), 29.7 (s), 23.9 (vt, N = 24.6), 19.1 (s), -10.1 (s, Pd-CH_3); $^{31}P\{^{1}H\}$: 30.5 (s). Anal. Calcd. For $C_{60}H_{66}BF_{20}N_5P_2Pd$ (1415.36): C, 50.88; H, 4.70; N, 4.94. Found: C, 45.26; H, 4.10; N, 4.42. Anal. Calcd. for $C_{60}H_{66}BF_{20}N_5P_2Pd + 3CH_2Cl_2$ (1670.16): C, 45.28; H, 4.34; N, 4.19. IR (CD_2Cl_2): 2967 (m), 1513 (s), 1464 (s) cm^{-1}.

Table 2.01. Collection Data for Crystal Structures of the Complexes 3a, 4c-MeOTf, 4c-PhI, 5a-PhBr, 5a-PhI.

	3a	4c-MeOTf	4c-PhI	5a-PhBr	5a-PhI
Formula	$C_{24}H_{46}N_4P_2Pd$	$C_{30}H_{57}F_3N_4O_3P_2PdS$	$C_{34}H_{59}I\ N_4P_2Pd$	$C_{18}H_{28}BrN_2PPd$	$C_{18}H_{28}IN_2PPd$
Mw	558.99	779.24	819.09	489.70	536.69
Crystal system	Monoclinic	Orthorhombic	Monoclinic	Monoclinic	Monoclinic
Space group	P21/n	P212121	P21/c	P21/n	P21/n
Crystal dim (mm)	0.3x0.3x0.25	0.30x0.25x.015	0.40 x 0.15 x 0.08	0.40 x 0.30 x 0.10	0.50 x 0.25 x 0.10
Color	Colorless	Colorless	Colorless	Colorless	Colorless
a [Å]	15.9009	9.6134	14.3428	9.5657	9.9008
b [Å]	11.4188	16.0484	10.4371	16.3449	16.7186
c [Å]	16.5897	25.4098	26.6199	12.8255	12.9150
α [°]	90	90	90	90	90
β [°]	110.4000	90	97.0240	99.8240	102.8490
γ [°]	90	90	90	90	90
V [$Å^3$]	2823.3	3920.2	3955.0	1975.9	2084.26
Z	4	4	4	4	4
D_{calcd} (g cm^{-3})	1.315		1.376	1.646	1.710
λ [Å]	0.71073	0.71070	0.71047	0.71076	0.71108
T [^{o} K]	223	100	218	147	147
$2\theta_{max}$ [°]	28.27	27.50	28.15	28.30	28.26
Measured reflections	20705	23881	28863	12128	12908
Independent reflections	6800	8900	9506	4542	4808
No. of parameters	280	626	398	208	208
R(F) (I>2σ(I)), %[a]	2.78	2.59	3.88	2.73	2.30
$R(wF^2)$ (I>2σ(I)), %[b]	9.47	6.02	9.20	7.12	5.88
GOF	1.069	1.099	1.028	1.079	1.022

Table 2.01.
(Continued)

Res. electron density	0.836	0.650	0.235	0.864	1.129

[a] $R = \sum||F_o|-|F_c||/\sum|F_o|$. [b] $R(wF^2)=\{\sum[\omega(F_o^2-F_c^2)^2]/\sum[\omega(F_o^2)^2]\}^{1/2}$; $\omega=1/[\sigma^2(F_o^2)+(aP)^2+bP]$, $P=[2F_c^2+\max(F_o,0)]/3$.

Table 2.02. Collection data for crystal structures of the complexes 5b-PhI, [6a-Me]$^+$[OTf]$^-$, 7c-CH_2Cl_2, [8b-Ph]$^+$[OTf]$^-$, [10c-Me]$^+$[OTf]$^-$, [10c-Me]$^+$[B(Ar$_F$')$_4$]$^-$.

	5b-PhI	[6a-Me]$^+$[OTf]$^-$	7c-CH_2Cl_2	[8b-Ph]$^+$[OTf]$^-$	[10c-Me]$^+$[OTf]$^-$	[10c-Me]$^+$[B(Ar$_F$')$_4$]$^-$
Formula	$C_{22}H_{36}IN_2PPd$	$C_{26}H_{49}F_3N_4O_3P_2PdS$	$C_{20}H_{29}Cl_2N_2P_2Pd$	$C_{26}H_{45}F_3N_3O_3PPdS$	$C_{37}H_{66}F_3N_5O_3P_2PdS$	$C_{60}H_{66}BF_20N_5P_2Pd$
Mw	592.80	723.09	445.67	674.08	885.33	1416.33
Crystal system	Monoclinic	Triclinic	Monoclinic	Triclinic	Triclinic	Monoclinic
Space group	P21/n	P-1	P2(1)/n	P-1	P-1	P21/n
Crystal dim (mm)	0.35 x 0.30 x 0.15	0.20 x 0.15 x 0.10	0.20 x 0.15 x 0.10	0.32 x 0.30 x 0.15	0.40 x 0.35 x 0.30	0.28 x 0.08 x 0.07
Color	Colorless	Colorless	Yellow	Yellow	Colorless	Colorless
a [Å]	10.3039	8.5573	9.9919	10.7472	13.2846	23.6456
b [Å]	20.2485	13.3881	17.5170	11.485	13.6817	9.9940
c [Å]	12.1211	15.2667	11.0258	14.9802	13.7439	26.4930
α [°]	90	103.0040	90	19.3880	109.5820	90
β [°]	103.8140	101.7090	98.5320	83.3990	91.5240	96.8290
γ [°]	90	94.4640	90	62.8250	105.1180	90
V [Å^3]	2455.8	1650.35	1908.47	1615.80	2254.2	6216.3
Z	4	2	4	2	2	4
D_{calcd} (g cm^{-3})	1.603					1.513
λ [Å]	0.71073	0.71094	0.71067	0.70964	0.71073	0.71077
T [^{o} K]	150	150	150	218	213	100
$2\theta_{max}$ [°]	28.25	28.16	28.27	28.29		26.00
Measured reflections	14972	10245	11711	10107	15104	12187
Independent reflections	5592	7142	4395	6661	8765	9499
No. of parameters	244	557	306	523		827
R(F) (I>2σ(I)), %[a]	2.32	2.62	2.11	3.38	4.02	4.32
R(wF^2) (I>2σ(I)), %[b]	5.84	6.50	5.25	8.76	10.39	8.77

Table 2.02. (Continued)

GOF	1.045	1.055	1.050	1.001	1.027
Res. electron density	0.700	0.813	0.647	0.622	0.615

[a] $R = \sum||F_o|-|F_c||/ \sum|F_o|$. [b] $R(wF^2)=\{\sum[\omega(F_o^2-F_c^2)^2]/\sum[\omega(F_o^2)^2]\}^{1/2}$; $\omega=1/[\sigma^2(F_o^2)+(aP)^2+bP]$, $P=[2F_c^2+\max(F_o,0)]/3$.

C. Results and Discussion

Synthesis and structures of two-coordinate complexes. Hindered phosphines of type 2 were made by lithiating the appropriate 1-methylimidazole derivative with n-BuLi in THF,[79,80] followed by quenching with the requisite chloro(dialkyl)phosphine, as others have done using chloro(diphenyl)phosphine.[65] Our initial efforts to make Pd(0) species 3 used two moles of hindered phosphines 2 and $Pd(dba)_2$ (dba = dibenzylideneacetone). Monitoring these reactions by ^{1}H and $^{31}P\{^{1}H\}$ NMR suggested that indeed zerovalent Pd complexes were formed cleanly, but efforts to remove the byproduct dba by recrystallization were never completely successful. Some previous literature efforts to make Pd-phosphine complexes $Pd(dba)_2$ have led to Pd-bis(phosphine) species but others have led to Pd-phosphine-dba complexes.[81,82] Thus, the Pd(II) precursor CpPd(allyl) was used as done by Otsuka et. al,[45,46] forming volatile and very soluble hydrocarbon byproducts presumed to be isomers of allylcyclopentadiene. These byproducts could be completely and easily removed from crystalline, nonvolatile 3, isolated in 62 to 85% yield (Figure 2.01).

Elemental analyses for 3a, b, c were consistent with ML_2 species. Spectroscopic data for 3a, b, c (Tables 2.03 and 2.06) were consistent with formation of species with two equivalent phosphines mutually trans: the $^{31}P\{^{1}H\}$ NMR spectra exhibited one sharp singlet in each case, and the ^{1}H and $^{13}C\{^{1}H\}$ resonances for the atoms of the alkyl substituents on phosphorus and C-2 of the imidazol-2-yl groups appeared as virtual triplets. For example, the proton resonances for the *t*-butyl groups

in 3a appeared at δ 1.55 ppm (vt, N = 13.8 Hz), and the carbon resonance for C-2 appeared at 144.6 ppm (vt, N = 37.7 Hz).[83]

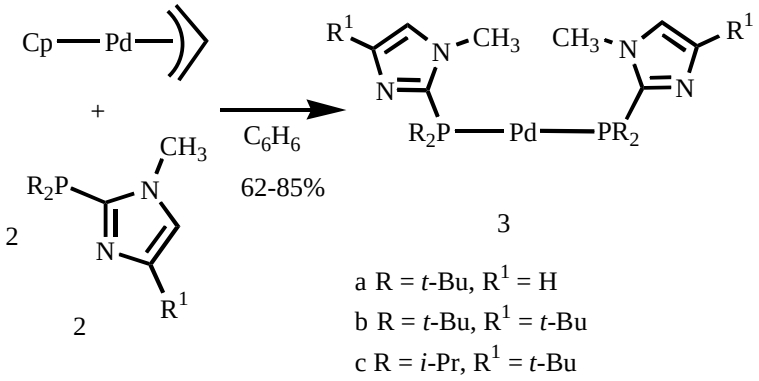

Figure 2.01. Preparation of Pd(0) complexes 3.

Table 2.03. ^{1}H and $^{31}P\{^{1}H\}$ NMR data for ligands 2 and Pd complexes 3 and 4.[a]

compound	solvent	^{1}H					$^{31}P\{^{1}H\}$
		Imi-H5	H4 or R^{1} at C-4	N-CH_3	R_2P	Other ligand(s) on Pd	
2a	$CDCl_3$	6.96 (dd, 3, 1, 1H)	7.21 (br s, 1H)	3.81 (s, 3H)	1.18 (d, 7, 18H)	--	0.5 (s)
2b	$CDCl_3$	6.63 (d, 3, 1H)	1.27 (s, 9H)	3.75 (s, 3H)	1.21 (d, 7.2, 6H)	--	-0.4 (s)
2c	$CDCl_3$	6.63 (d, 2, 1H)	1.26 (s, 9H)	3.72 (s, 3H)	0.96 (dd, 7, 12, 6H) 1.08 (dd, 7, 16, 6H) 2.32 (sept of d, 7, 2, 2H)	--	-19.3 (s)
3a	C_6D_6	6.31 (s, 2H)	7.30 (s, 2H)	4.31 (s, 6H)	1.55 (vt, N =13.8, 36H)	--	32.4 (s)
3b	C_6D_6	6.37 (s, 2H)	1.43 (s, 18H)	4.34 (s, 6H)	1.56 (vt, N = 13.8, 36H)	--	32.1 (s)
3c	C_6D_6	6.34 (s, 2H)	1.45 (s, 18H)	4.12 (s, 6H)	1.22 (dvt, J = 7.5, N = 15.0, 12H) 1.29 (dvt, J = 6.0, N = 12.5, 12H) 2.59 (sept, 7.0, 4H)	--	16.2 (s)
4c-PhI	C_6D_6	6.36 (s, 2H)	1.39 (s, 18H)	3.80 (s, 6H)	1.08 (dvt, J = 7.6, N = 15.1, 12H) 1.39 (br s, 12H) 2.66 (br s, 4H)	6.62 (t, 7.1, 1H) 6.87 (t, 7.1, 2H) 7.16-7.18 (m, 2H)	13.7 (s)
4c-MeOTf	C_6D_6	6.39 (s, 2H)	1.39 (s, 18H)	3.60 (s, 6H)	1.14 (dvt, J = 7.2, N = 14.4, 12H) 1.23 (dvt, J = 8.8, N = 16.2, 12H) 3.03 (br s, 4H)	0.22 (t, 6.2, 3H)	24.5 (s)
4c-MeI	CD_2Cl_2	6.78 (s, 2H)	1.27 (s, 18H)	3.86 (s, 6H)	1.15 (dvt, J = 7.2, N = 14.4, 12H) 1.30 (dvt, J = 7.2, N = 14.4, 12H) 3.39 (br s, 4H)	0.20 (t, 6.0, 3H)	21.4 (s)

[a] Measured at 30 °C unless otherwise specified. Chemical shifts in ppm, δ scale. Unless otherwise stated, value after multiplicity is *J* in Hz, br = broad.

Table 2.04. ^{1}H and $^{31}P\{^{1}H\}$ NMR data for Pd complexes 5, 6 and 7.[a]

compound	solvent	^{1}H					$^{31}P\{^{1}H\}$
		Imi-H5	H4 or R^{1} at C-4	N-CH_3	R_2P	Other ligand(s) on Pd	
5a-PhBr	$CDCl_3$	7.05 (s, 1H)	7.34 (s, 1H)	3.89 (s, 3H)	1.43 (d, 15.8, 18H)	6.79 (t, 7.2, 1H) 6.94 (t, 7.2, 2H) 7.37-7.42 (m, 2H)	43.5 (s)
5a-PhI	CD_2Cl_2	7.13(s, 1H)	7.39 (s, 1H)	3.89(s, 3H)	1.42 (d, 15.8, 18H)	6.80 (t, 7.6, 1H) 6.94 (t, 7.6, 2H) 7.25-7.41 (m, 2H)	36.9 (s)
5b-PhI	$CDCl_3$	6.73 (s, 1H)	1.37 (s, 9H)	3.84 (s, 3H)	1.45 (d, 15.6, 18H)	6.73 (t, 7.2, 1H) 6.91 (t, 7.2, 2H) 7.37-7.42 (m, 2H)	29.3 (s)
$[6a\text{-}Me]^{+}[OTf]^{-}$	$CDCl_3$	7.12 (s, 1H) 7.29 (br s, 2H)[b]	5.18(s, 1H)	3.97 (s, 6H)	1.29-1.73 (m, 36H)	0.95 (t, 5.2, 3H)	32.4 (s)
	$CDCl_3$[c]	7.12 (s, 1H) 7.28 (s, 1H)	5.18 (s, 1H) 7.30 (s, 1H)	3.95 (s, 3H) 3.99 (s, 3H)	1.29 (vt, N = 14.4, 9H) 1.47 (vt, N = 16.0, 18H) 1.67 (brs, 9H)	0.95 (t, 5.2, 3H)	
7c-CH_2Cl_2	CD_2Cl_2	7.56 (s, 1H)	1.41 (s, 9H)	3.97 (s, 3H)	1.25 (dd, 7.5, 18.0, 6H) 1.56 (dd, 7.0, 19.0, 6H) 2.87(sept of d, 7.0, 11.0, 2H)	4.56 (d, 2.0, 2H, $PdCH_2N$)	65.3 (s)

[a] Measured at 30 °C unless otherwise specified. Chemical shifts in ppm, δ scale. Unless otherwise stated, value after multiplicity is *J* in Hz, br = broad.
[b] Peak for H-4 and H-5 overlapping at this temperature but separated at –50 °C.
[c]Measured at –50 °C.

Table 2.05. ^{1}H and $^{31}P\{^{1}H\}$ NMR data for Pd complexes 8, 9 and 10.[a]

compound	solvent	^{1}H					$^{31}P\{^{1}H\}$
		Imi-H5	H4 or R^{1} at C-4	N-CH_3	R_2P	Other ligand(s) on Pd	
[8b-Ph]$^{+}$[OTf]$^{-}$	CD_2Cl_2	7.04 (s, 1H)	1.31 (s, 9H)	3.91 (s, 3H)	1.41 (d, 16.2, 18H)	7.03 (m, 1H), 7.09 (m, 2H) 7.41 (m, 2H), 1.27 (d, 6.2, 6H, amine CH_3), 2.65-2.77 (m, 1H).	39.8 (s)
[8a-Ph]$^{+}$[B(Ar_F')$_4$]$^{-}$	CD_2Cl_2	7.17(s, 1H)	7.22 (s, 1H)	3.92 (s, 3H)	1.41 (d, 16.4, 18H)	1.35 (d, 7.8, 6H), 2.57 (br s, 2H), 3.28 (sept, 6.6, 1H), 7.00 (t, 7.0, 1H), 7.08 (t, 7.2, 2H), 7.29-7.37 (m, 2H).	45.4 (s)
[9b-]$^{+}$[OTf]$^{-}$	CD_2Cl_2	7.10 (s, 1H)	1.34 (s, 9H)	3.92 (s, 3H)	1.39 (d, 16.5, 18H)	2.74 (dt, 11.0, 12.0, 2H), 3.04 (d, 13.5, 2H), 3.34 (br t, 12.0, 1H), 3.50 (t, 11.5, 2H), 3.78 (d, 13.0, 2H), 7.04 (t, 7.5, 1H), 7.10 (t, 8.0, 2H) 7.39-7.42 (m, 2H).	42.3 (s)
[10c-Me]$^{+}$[OTf]$^{-}$	CD_2Cl_2	6.69 (s, 2H)	1.12 (s, 18H)	4.00 (s, 6H)	1.18-1.38 (m, 24H) 2.80-3.05 (m, 4H)	0.51 (t, 6.2, 3H), 2.95-3.10 (m, 2H), 3.44 (br s, 2H), 6.29 (sl br d, 7.0, 2H), 7.10-7.22 (m, 3H).	30.3 (s)
	$CDCl_3$	6.93 (s, 2H)	1.11 (s, 18H)	4.04 (s, 6H)	1.25-1.32 (m, 24H) 2.92 (sept, 6.5, 4H)	0.47 (t, 6.0), 3.03 (t, 7.0, 2H), 3.30 (br s, 2H), 6.33 (sl br s, 7.0, 2H), 7.11-7.20 (m, 3H).	28.8 (s)
[10c-Me]$^{+}$[B(Ar_F')$_4$]$^{-}$	$CDCl_3$	6.87 (s, 2H)	1.11 (s, 18H)	3.94 (s, 6H)	1.25-1.32 (m, 24H) 2.89 (sept, 6.5, 4H)	0.50 (t, 6.0, 3H), 3.00 (t, 7.5, 2H), 3,41 (br s, 2H), 6.20 (d, 7.5, 2H), 7.11 (t, 7.5, 2H), 7.18 (t, 7.5, 1H).	30.5 (s)

[a] Measured at 30 °C unless otherwise specified. Chemical shifts in ppm, δ scale. Unless otherwise stated, value after multiplicity is *J* in Hz, br = broad.

Table 2.06. $^{13}C\{^{1}H\}$ NMR data for ligands 2 and Pd complexes 3 and 4.[a]

compound	C-2	C-4	C-5	R^1 at C-4	CH_3 at N-1	R_2P	Other ligands on Pd
2a	158.4 (s)	129.8 (s)	122.4 (s)	--	33.3 (d, 14)[b]	30.1 [d, 14, C(*C*H_3)$_3$] 34.6 (d, 18)[b]	--
2b	153.2 (d, 1)	143.6 (d, 10.4)	115.7 (d, 1.4)	30.4 [s, C(*C*H_3)$_3$] 32.1 [s, *C*(CH_3)$_3$]	34.1 (d, 16.8)	30.2 [d, 14.1, C(*C*H_3)$_3$] 33.5 [d, 14.1, *C*(CH_3)$_3$]	--
2c	153.6 (d, 1)	144.9 (d, 9)	116.2 (s)	30.4 [s, C(*C*H_3)$_3$] 32.0 [s, *C*(CH_3)$_3$]	33.7 (d, 15)	19.4 (d, 8, CH*M*eMe) 20.1 (d, 18, CHMe*Me*) 24.39 (s, one *C*HMe_2) 24.44 (s, other CHMe_2)	--
3a	144.6 (vt, *N* = 37.7)	130.0 (vt, *N* = 6.2)	123.6 (s)	--	37.2 (vt, *N* = 13.8)	31.5 (vt, *N* = 11.7) 36.8 (vt, *N* = 14.7)	--
3b	143.3 (vt, *N* = 36.3)	152.8 (vt, *N* = 5.8)	117.4 (s)	30.9 (s) 32.5 (s)	37.2 (vt, *N* = 13.8)	31.6 (vt, *N* = 11.8) 36.5 (vt, *N* = 14.2)	--
3c	142.8 (vt, *N* = 41.0)	153.4 (s)	117.9 (s)	30.9 (s) 32.6 (s)	36.0 (br s)	21.2 (br s), 20.2 (sh s), 21.0 (br s), 27.7 (vt, *N* = 26.0).	--
4c-PhI	140.1 (vt, *N* = 41.0)	153.2 (vt, *N* = 8.4)	118.2 (s)	30.8 (s) 32.4 (s)	37.0 (s)	20.5 (sh s) 21.0 (br s) 27.7 (vt, *N* = 26.0)	123.8 (s, C-4) 127.5 (s, C-3) 138.5 (t, 16.3, C-2) 153.2 (t, 4.4, C-1)
4c-MeOTf	135.7 (vt, *N* = 64.9)	154.4 (vt, *N* = 8.3)	119.5 (s)	30.6 (s) 32.5 (s)	35.4 (s)	19.0 (s), 20.0 (s), 27.7 (vt, *N* = 21.0)	-6.2 (s)

[a] Measured at 30 °C in the same solvent as listed in Table 2.03. Chemical shifts in ppm, δ scale. Unless otherwise stated, value after multiplicity is *J* in Hz, br = broad, Sh = sharp, sl = slightly.
[b] Assignment of 33.3 and 34.6 ppm peaks not completely certain.

Table 2.07. $^{13}C\{^{1}H\}$ NMR data for Pd complexes 5, 6 and 7.[a]

Compound	C-2	C-4	C-5	R^1 at C-4	CH_3 at N-1	R_2P	Other ligands on Pd
5a-PhI	147.8 (d, 27.9)	129.9 (d, 12.2)	126.2 (s)	--	36.9 (s)	30.3 (d, 6.0) 37.2 (d, 6.8)	122.7 (s, C-4) 126.8 (d, 2.3, C-3) 138.3 (d, 8.9, C-1) 139.1 (d, 4.7, C-2)
5b-PhI	146.6 (d, 30.4)	154.2 (d, 11.6)	119.6 (s)	30.5 (s) 32.0 (s)	36.7 (s)	30.3 (d, 5.8) 37.0 (d, 7.8)	122.4 (s, C-4) 126.5 (d, 2.0, C-3) 134.1 (d, 10.6, C-1) 139.0 (d, 4.5, C-2)
$[6a\text{-}Me]^+[OTf]^-$[b]	139.5 (vt, N = 56.5) 145.8 (vt, N = 28.8)	127.6 (vt, N = 13.3) 130.3 (vt, N = 8.2)	124.8 (s) 127.3 (s)	--	36.6 (s) 37.2 (s)	30.2 (s) 30.4 (s) 36.3 (vt, N = 9.0) 36.7 (vt, N = 9.5) 38.4 (vt, N = 16.8) 38.6 (vt, N = 18.0)	-17.2 (s)
7c-CH_2Cl2	147.5 (d, 27.7)	146.2 (d, 8.6)	129.4 (s)	38.3 (s)	38.3 (s)	19.6 (d, 5.0) 20.2 (s) 27.5 (d, 24.4)	45.1 (d, 5.4, Pd CH_2N)

[a] Measured at 30 °C in the same solvent as listed in Table 2.03. Chemical shifts in ppm, δ scale. Unless otherwise stated, value after multiplicity is *J* in Hz, br = broad.
[b] Measured at 0 °C.

Table 2.08. $^{13}C\{^{1}H\}$ NMR data for Pd complexes 8, 9 and 10.[a]

Compound	C-2	C-4	C-5	R^1 at C-4	CH_3 at N-1	R_2P	Other ligands on Pd
[8b-Ph]$^+$[OTf]$^-$	145.6 (d, 35.2)	153.5 (d, 10.3)	141.4 (s)	30.4 (s) 31.6 (s)	37.4 (s)	30.3 (d, 6.3) 37.5 (s)	25.7 (s, amine CH_3), 46.5 (s, amine CHN), 121.7 (s, Ph-C4), 124.9 (s, Ph-C3), 128.8 (d, 2.1, Ph-C2), 136.7 (d, 3.9, Ph-C1).
[9b-Ph]$^+$[OTf]$^-$	145.5 (d, 36.7)	153.0 (d, 10.0)	143.3 (s)	30.3 (s) 31.5 (s)	37.5 (s)	30.3 (d, 4.8) 37.6 (s)	49.3 (s, amine-C3), 68.2 (s, amine-C2), 122.1 (s, Ph-C4), 125.2 (s, Ph-C3), 128.6 (d, 2.0, Ph-C2), 136.6 (d, 3.9, Ph-C1).
[10c-Me]$^+$[OTf]$^-$	134.2 (vt, N = 56.6)	154.3 (vt, N = 11.3)	121.3 (s)	29.8 (s) 31.7 (s)	35.8 (s)	19.2 (s) 23.9 (vt, N = 24.6)	-10.4 (s, Pd-CH_3), 49.1 (s, CH_2), 127.7 (s, meta), 128.7 (s, para), 129.5 (s, ortho), 139.8 (s, ipso).
[10c-Me]$^+$[B(Ar_F')$_4$]$^-$[b]	134.3 (vt, N = 56.3)	154.7 (vt, N = 10.8)	121.3 (s)	29.7 (s) 31.8 (s)	35.3 (s)	19.1 (s) 23.9 (vt, N = 24.6)	-10.1 (s, Pd-CH_3), 48.5 (s, CH_2), 126.8 (s, meta), 128.3 (s, para), 129.0 (s, ortho), 138.8 (s, ipso).

[a] Measured at 30 °C in the same solvent as listed in Table 2.03. Chemical shifts in ppm, δ scale. Unless otherwise stated, value after multiplicity is *J* in Hz, br = broad.

[b] Resonances for the anion: 148.2 (d of narrow m, *J* = 242, ortho C- furthest downfield), 138.2 (d of narrow m, *J* = 240, para C- about half the intensity of the signal at 136.2), 136.2 (d of narrow m, *J* = 240, meta C), 124.0 (very broad, ipso C).

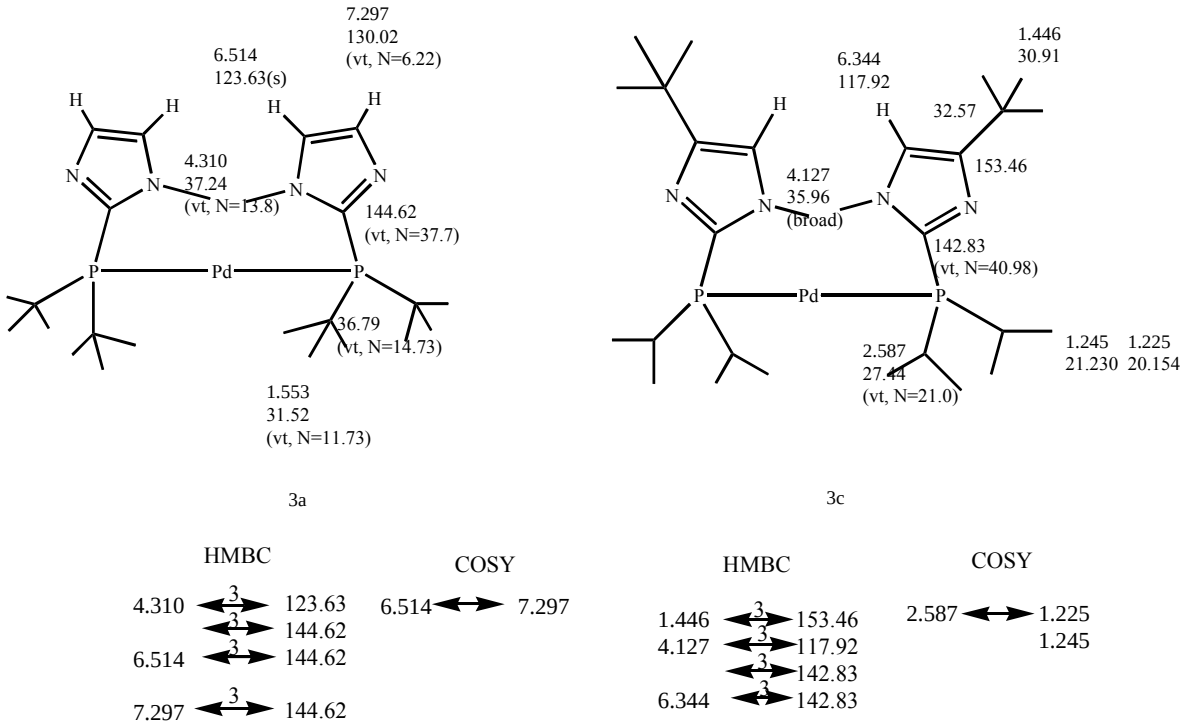

Figure 2.02. Two-dimensional NMR lead to the assignments of proton and carbon signals for 3a and 3c.

One key question unanswered by the spectroscopic data was whether the imidazole nitrogens were interacting with the metal. Intriguingly, for Pd(0) species 3a, b, c, the protons of the N-methyl groups resonanted as sharp singlets about 1 ppm downfield compared with the free ligands. Additional information about the bonding of the ligands required X-ray diffraction studies.

Crystals of 3a were grown for analysis by X-ray diffraction. The data for refinement are given in Table 2.01 in the Experimental Section, selected bond lengths and angles are shown in Table 2.09, and the ORTEP diagram of the structure is shown in Figure 2.03.

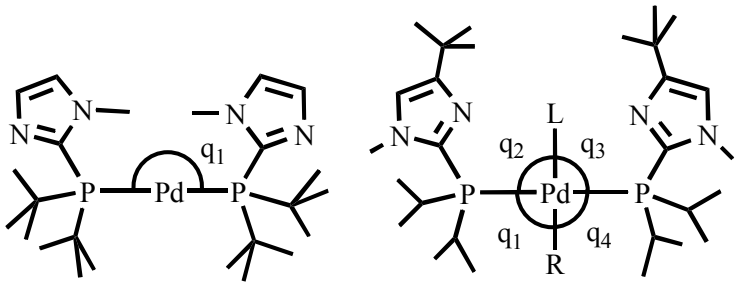

3a 4c, 10c

Table 2.09. Selected bond lengths (Å) and bond angles (deg) for complexes 3a, 4c, and 10c.

	3a	4c-PhI	4c-MeOTf	$[10c\text{-}Me]^+[OTf]^-$	$[10c\text{-}Me]^+[B(Ar_F')_4]^-$
R	---	Ph	Me	Me	Me
L	---	I	OTf	NH_2CH_2Ph	NH_2CH_2Ph
Pd-P(1)	2.2836(4)	2.3430(8)	2.3328(5)	2.3448(7)	2.3387(8)
Pd-P(2)	2.2886(4)	2.3405(8)	2.3356(5)	2.3284(7)	2.3287(8)
Pd-L	---	2.6904(3)	2.2161(13)	2.148(2)	2.137(2)
Pd-R	---	2.021(3)	2.0436(19)	2.059(3)	2.077(3)
θ_1	173.964(14)	93.00(2)	91.27(4)	94.49(6)	93.59(8)
θ_2	---	88.88(8)	88.78(8)	86.86(9)	87.29(9)
θ_3	---	88.71(8)	89.02(8)	86.81(9)	88.08(9)
θ_4	---	91.98(2)	91.48(4)	93.11(6)	92.34(8)
N(Im)-N(amine)	---	---	---	2.883(5), 2.943(5)	2.885(4) 2.920(4)

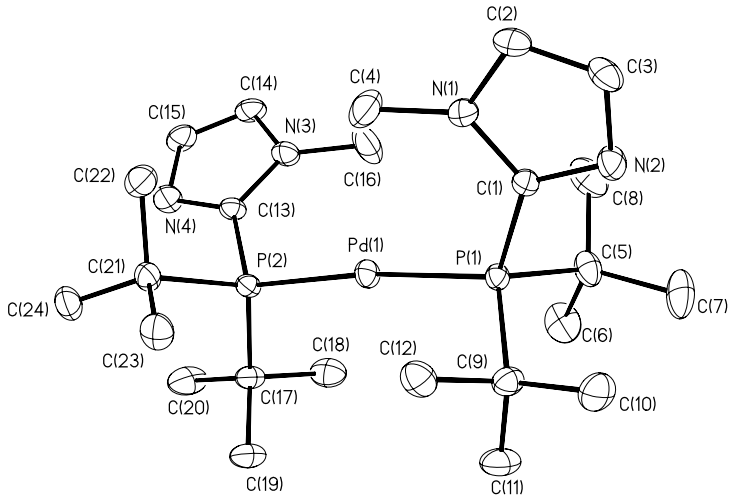

Figure 2.03. Molecular structure of 3a. Ellipsoids are shown at 30% probability.

As shown in Figure 2.03, the Pd(0) complex 3a adopted a nearly linear configuration (P-Pd-P angle, 174.0^{o}), and when viewed down the P-P axis, the two imidazole rings are essentially gauche to each other, rather than anti. Interestingly, both of the imidazole *N*-methyl groups were pointed toward the Pd atom, consistent with agostic interactions. The distances between Pd atom and H atoms on the *N*-methyl group fell within the range of M-H distance for agostic interaction (1.85 to 2.4 Å). However, in general, a hydrogen involved in an agostic interaction shows some spectral data resembling those of a metal hydride, for example, in upfield ^{1}H NMR resonances[84,85] or low-frequency C-H stretching absorptions in IR spectra (2300 – 2700 cm^{-1}).[86] Evidence against agostic interactions includes the 1.0 ppm-*downfield* ^{1}H NMR chemical shift of the *N*-methyl protons on complexation of the ligand, and

normal C-H stretching absorptions, between 2860 to 2960 cm^{-1}. Thus, although Figure 2.02 shows that the solid-state orientation of the methyl groups is consistent with agostic interaction with a 14-electron metal center, all the spectroscopic evidence lead us to the conclusion that there are no agostic interactions between Pd and H atoms of the *N*-methyl groups in solution. Rather, the orientations seen for the imidazole rings may be a way for the system to avoid steric interactions between the two bulky *tert*-butyl groups on the phosphorus atom and the *N*-methyl group on the imidazole. A similar orientation was seen by Otsuka et al. in their crystal structure of (t-$Bu_2PPh)_2Pd$,[46] and Milstein and co-workers recently reported a two-coordinate Pd(0) complex in which the ether oxygens are positioned to interact with the soft Pd(0) center but do not.[36] Clearly, a combination of structural and spectroscopic data are needed to establish whether a potentially coordinating ligand is truly hemilabile.

Reactivities of Pd(0) complexes with aryl halides. In the coupling reaction between aryl halides and amines, oxidative addition of aryl halides is usually involved in the early stage of the catalytic cycle, generally following the dissociation of one ligand from the catalyst.[18,19,47]

The oxidative addition products are likely intermediates in metal-catalyzed cross-coupling reactions. The low-coordinate, electron-rich Pd(0) complexes prepared above were expected to readily undergo oxidative-addition with aryl halides.

Significantly, for reactions of Pd(0) complexes 3a, b, c with aryl halides, reaction rates and product structures could be controlled by changing the X group on the aryl halide and the alkyl substituents on phosphorus (Figure 2.04).

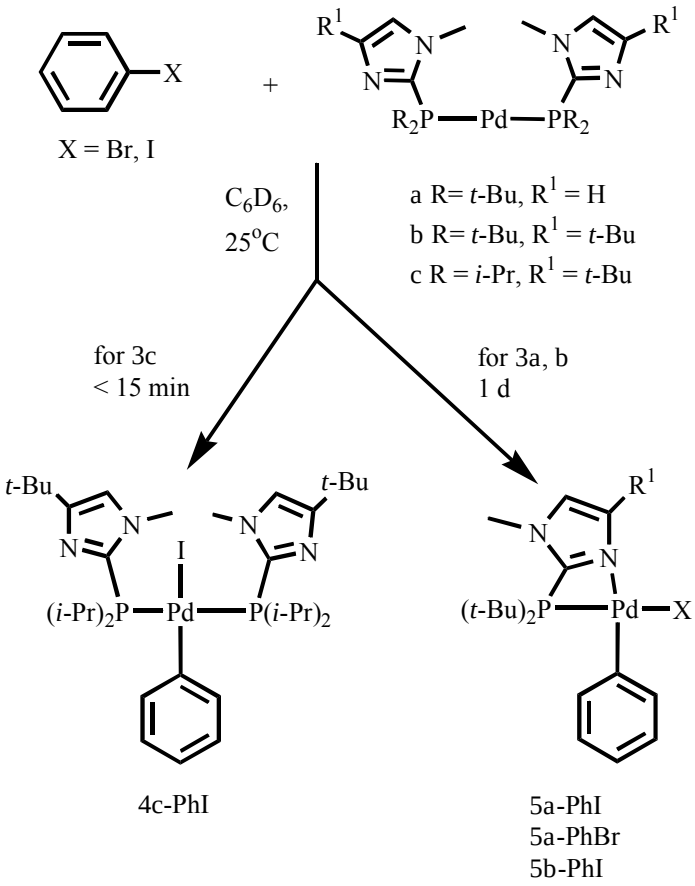

Figure 2.04. Reactivity with aryl halides as a function of phosphine.

When the less crowded Pd(0) complex 3c was treated with iodobenzene at room temperature, oxidative addition was complete within a remarkably short time, 15 minutes. The product, 4c-PhI was soluble in benzene and was isolated by recrystallization in 71% yield. The molecular formula of the product was confirmed by

elemental analysis, and the trans orientation of the two equivalent phosphines was determined by a $^{31}P\{^{1}H\}$ singlet and the appearance of certain proton and carbon resonances as virtual triplets. For example, the proton resonances for the methyl group on isopropyl substituent appeared at 1.08 ppm as a doublet of a virtual triplet, and the carbon resonance for C-2 of the imidazol-2-yl group appeared at 140.1 ppm (vt, N = 67.5 Hz). Moreover, the $^{31}P\{^{1}H\}$ NMR spectrum of 4c-PhI showed a singlet, consistent with a trans geometry. In confirmation, the molecular structure as confirmed by X-ray diffraction is shown in Figure 2.05a.

As expected, complex 4c-PhI features a square-planar Pd center (the sum of the four L-Pd-L angles is 362^{o}, Table 2.09), on which both of the phosphine ligands are located trans to each other, whereas the aryl and halide ligands occupied the other two coordination sites. Distortions in this symmetrical but crowded complex include a P-Pd-P angle of 163.71(3)^{o}, which may be ascribed to interactions between isopropyl substituents on phosphines and the ring of the phenyl ligand (Figure 2.05.a).

The reactions of aryl halides with Pd(0) complexes 3a, 3b with more hindered phosphine ligands are different from that with 3c. The rate of the reactions was quite a bit slower, requiring a period of 24 h. Iodobenzene reacted somewhat faster than bromobenzene and gave a better yield, 94-97% vs 72%. Most significantly, the structures of products from 3a and 3b were different than that of the product obtained from 3c, and reactions followed different stoichiometry. The reactions of 3a with either PhBr or PhI or of 3b with PhI in C_6D_6 were monitored by NMR.

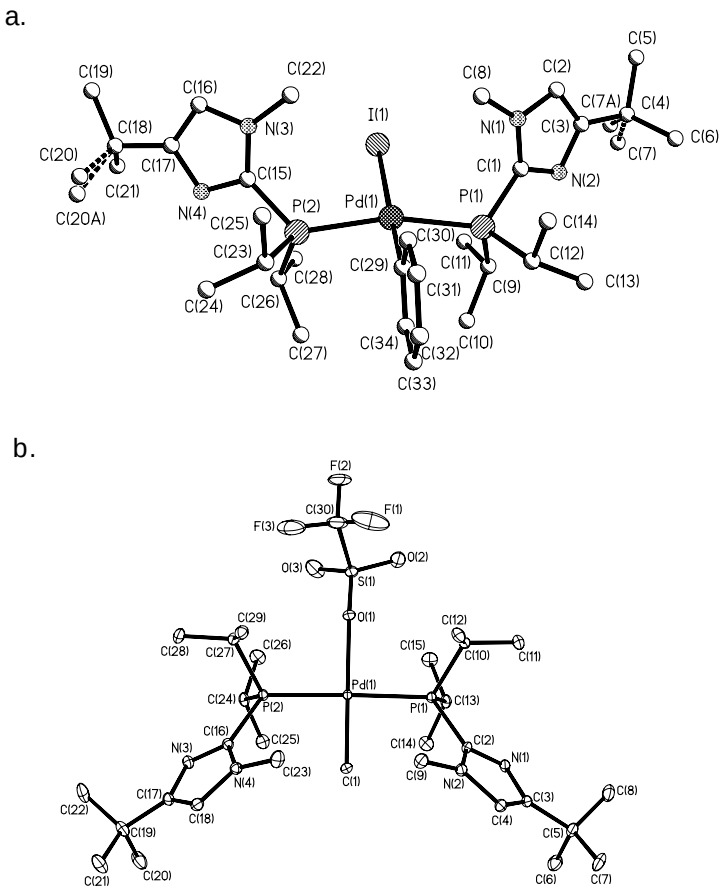

Figure 2.05. X-ray crystal structures of (a) 4c-PhI and (b) 4c-MeOTf. Ellipsoids are shown at 30% probability.

Surprisingly, as the reaction proceeded, signals for the free phosphine appeared and grew until all the signals for complex 3a or 3b had disappeared. At the same time, yellow crystals precipitated out of the solution. The proton NMR spectra of a solution from the crystals in either CD_2Cl_2 or $CDCl_3$ revealed resonances for a phenyl ligand in the range 6.7 to 7.5 ppm. The singlet for the three *N*-methyl protons on the oxidative addition products shifted 0.4 ppm upfield compared to that of Pd(0) complexes.

Significantly, the signals for the imidazole ring and the *tert*-butyl groups of the phosphine (in the case of reaction of 3a with PhI, singlets at 7.13 and 7.29 ppm and doublet at 1.42 ppm) integrated for only 1, 1 and 18 protons, respectively, indicating that there was only one phosphine ligand in each complex, hence the empirical formula would be (phosphine)PdPhI. This composition was verified by elemental analysis in each case. However, we needed X-ray diffraction data to assign the hapticity of the imidazolylphosphine, the stereochemistry about the metal, and even the nuclearity of the complex.

Many previous arylpalladium halide complexes with a single hindered ligand, such as P(o-tol)$_3$, have been dimeric.[81,87] Since the bridging halide palladium dimer has the same ratio of ligands as that of monomeric one, it is not possible to tell one from the other only based on NMR spectroscopic data. However the X-ray diffraction data of 5a-PhBr, 5a-PhI and 5b-PhI showed that the complexes are indeed monomeric in the solid state. The structure of complex 5b-PhI is shown in Figure 2.06 and selected bond lengths and angles are shown in Table 2.10, along with data for structures of 5a-PhBr and 5a-PhI. The structures of the 5a-PhBr and 5a-PhI are shown in Figure 2.07 and Figure 2.08.

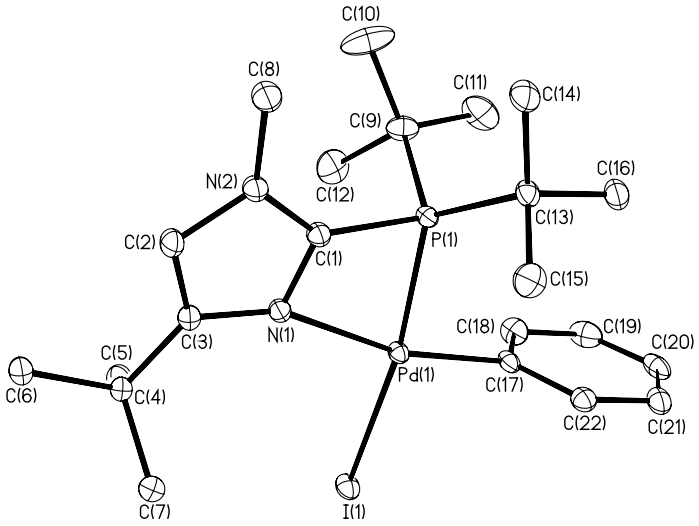

Figure 2.06. Molecular structure of 5b-PhI. Ellipsoids are shown at 30% probability.

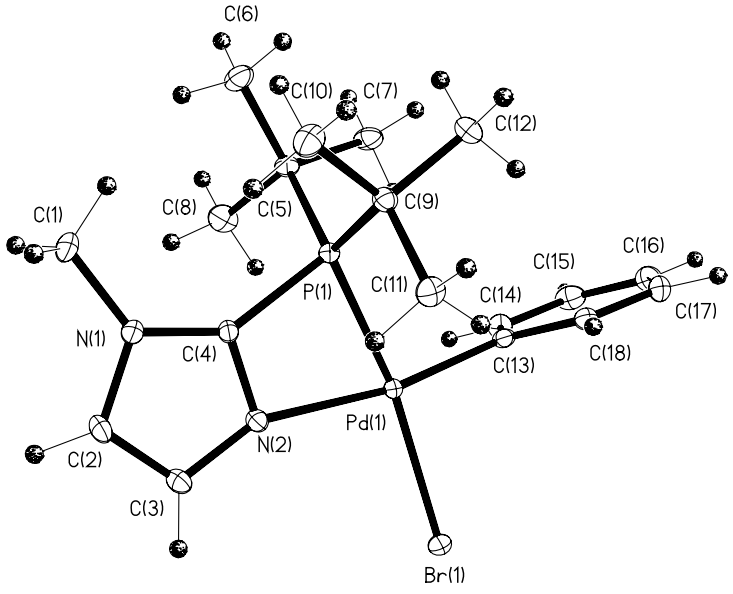

Figure 2.07. Molecular structure of 5a-PhBr. Ellipsoids are shown at 30% probability.

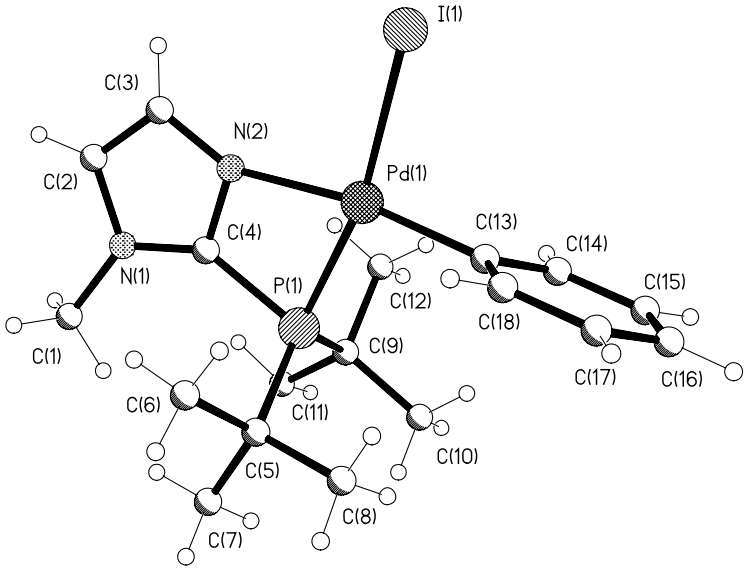

Figure 2.08. Molecular Structure of 5a-PhI. Ellipsoids are shown at 30% probability.

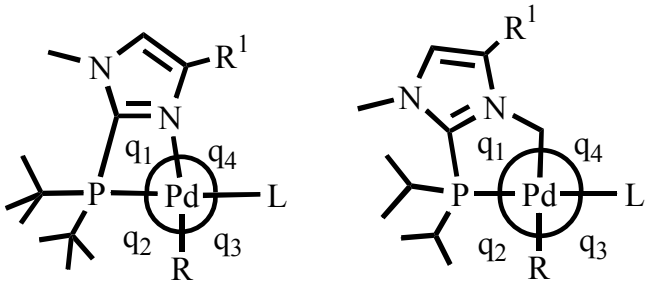

5, 6, 8 7c-CH_2Cl_2

Table 2.10. Selected bond lengths (Å) and bond angles (deg) for chelate complexes 5-8.

	5a-PhBr	5a-PhI	5b-PhI	$[6a\text{-}Me]^+[OTf]^-$	$7c\text{-}CH_2Cl_2$	$[8b\text{-}Ph]^+[OTf]^-$
R^1	H	H	t-Bu	H	t-Bu	t-Bu
R	Ph	Ph	Ph	Me	Cl	Ph
L	Br	I	I	2a	Cl	$NH_2CH(CH_3)_2$
Pd-P(1)	2.2748(6)	2.2936(6)	2.2890(6)	2.3496(5)	2.1878(4)	2.2639(6)
Pd-L	2.4729(3)	2.6245(3)	2.6368(2)	2.3337(5)	2.3769(4)	2.129(2)
Pd-N(Im)	2.170(2)	2.1639(18)	2.2626(17)	2.1735(16)	2.0236(17)[a]	2.198(2)
Pd-R	1.988(2)	1.997(2)	1.995(2)	2.051(2)	2.4124(4)	1.979(2)
θ_1	69.98(6)	69.76(5)	69.01(5)	68.96(5)	86.63(5)	70.14(5)
θ_2	100.02(7)	100.18(7)	96.60(6)	97.71(6)	91.203(15)	99.01(6)
θ_3	90.47(7)	91.55(7)	88.42(6)	94.13(6)	96.312(15)	86.43(10)
θ_4	99.64(5)	98.50(5)	106.10(5)	99.07(5)	86.02(5)	104.78(9)

[a] Length of bond between Pd and attached CH_2 carbon.

Figure 2.06 shows that 5b-PhI has a distorted square planar geometry, with the P and N atoms on the chelating phosphine ligand occupying two adjacent coordination sites while the phenyl ligand and halide ligands filling the other two, with phenyl trans to N atom and halide trans to P atom. The sum of the four intraligand angles is equal to 360.0° within experimental uncertainty, but the four-membered chelate ring has a narrow P-Pd-N angle [69.01(5)°], creating a large adjacent N-Pd-I angle [106.10(5)°].

Steric interactions between ligands become especially apparent (Table 2.10) in comparing the structure of 5a-PhI which lacks the imidazole *tert*-butyl substituent (R^1)

with that of 5b-PhI, just discussed. Looking at Table 2.10, in going from 5a-PhI to 5b-PhI one sees essentially no change in bond lengths between Pd and the four ligands, with the important exception of the Pd-N(Im) distance, which is about 0.1 Å longer in the *tert*-butyl-substituted case. Similarly, ligand substitution has the largest effect on θ_4, the N(Im)-Pd-I angle, increasing it by 7.6^o on going from 5a-PhI to 5b-PhI. This movement of the iodide ligand away from the coordinated heterocycle is compensated by closing of intraligand angles θ_3 and θ_2 by 3.1 and 3.6^o, respectively, with the remaining chelate bite angle hardly changing at all.

Not long after we isolated and resolved the structure of these monomeric complexes, Hartwig's group published a structure of a monomeric, three-coordinate T-shaped species (phosphine)PdPhX with a hindered phosphine.[19] As in our structures, the phosphine and halide ligands are trans to each other. Their structure features the phenyl group located trans to the open coordination site of the metal, whereas ours has the imidazole nitrogen in this position. The observed geometry of the T-shaped system allows the ligand with the greatest steric demand to bind in the least hindered position and the covalent ligand with the largest trans effect to bind trans to the open site. A similar reaction course (loss of one bulky ligand) and geometrical preference (high-trans effect P and aryl ligands cis to each other) was seen recently by Milstein, et al.[36]

Comparing reactivities of 3a-3c briefly at this point, we believe that changing steric demands of phosphine substituents (*iso*-propyl in 3c vs. *tert*-butyl in 3a or 3b) determine not only the rate of oxidative-addition (a phenomenon well-documented for other complexes elsewhere [88]) but also the structure of the resulting oxidative addition

products, a bis(phosphine) complex of type of 4c-PhI or a monophosphine species such as 5a- or 5b-PhX with chelated phosphine. In addition, more subtle changes accompany heterocycle substitution. The ability of large substituents on phosphorus (e.g. R = *tert*-butyl in R_2PR') to promote interactions such as cyclometalation between atoms on R' and a metal coordinated to R_2PR' has been seen before, notably by Shaw and coworkers.[89] The work here shows that the same effects come to play in hemilabile systems.

Reactivities of Pd(0) complexes with Methyl Triflate. Similar to the reaction of 3c with iodobenzene, reaction between 3c and methyl triflate was fast and clean at room temperature (Figure 2.09). The product 4c-MeOTf is symmetrical, with the two phosphine ligands trans to each other, and the remaining methyl and triflate ligands trans to each other. In the ^{1}H NMR spectrum, the resonances for methyl groups on each isopropyl substituent appeared at 1.14 and 1.23 ppm (each a doublet of virtual triplet), and the resonance for methyl protons on Pd-Me appeared at 0.22 ppm as a triplet ($J_{P\text{-}H}$ = 6.2 Hz). The product was fairly soluble in benzene, suggesting a neutral species rather than ionic one, a proposal confirmed by observation in the infrared spectrum of an S-O stretch absorption band at 1316 cm^{-1} for a bound triflate rather than free triflate ion.[90] Elemental analysis and ultimately X-ray diffraction data were consistent with the structure (Figure 2.05.b). The average Pd-P bond lengths in 4c-MeOTf are 0.007 Å shorter in this complex than in 4c-PhI, perhaps a reflection of the smaller sizes of the two anionic ligands. Consistent with this, in 4c-MeOTf , the P-Pd-

P angle is 173.353(18)°, whereas in 4c-PhI it is 163.71(3)°, suggesting greater distortion in the latter complex.

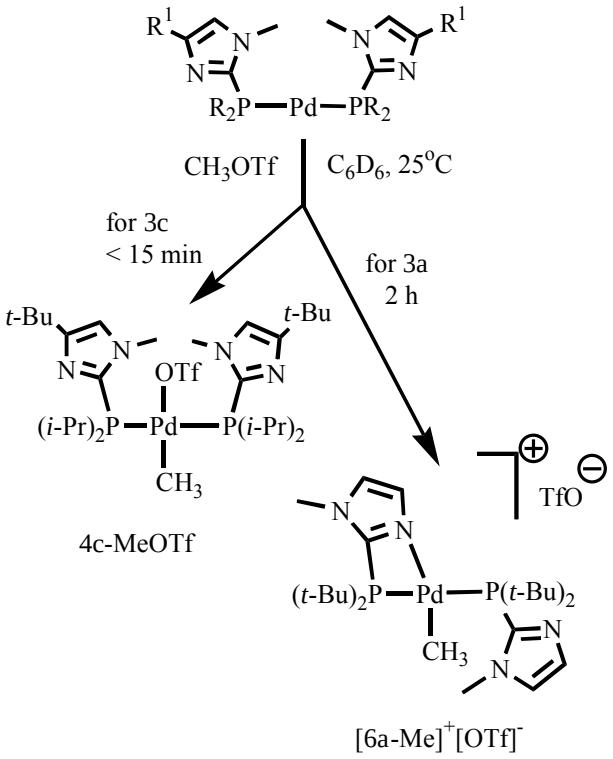

Figure 2.09. Reactivity with methyl triflate and product structure as a function of phosphine.

The reaction between 3a with methyl triflate in benzene required 2 h at room temperature, several times longer than the reaction with 3c, consistent with the larger size of the ligands. Elemental analysis of the product was consistent with an oxidative addition product in which the two phosphines were retained, in distinct contrast to results from oxidative-addition of haloarenes to 3a, in which one phosphine was lost. To a first approximation, the proton and phosphorus NMR data for the product from 3a suggested a structure similar to 4c-MeOTf, but the product resulting from 3a was

much less soluble in benzene than the corresponding one from 3c, and also the appearance of a strong IR absorption at 1271 cm^{-1} suggested an ionic triflate rather than a bound one.[90]

At 30°C, in $CDCl_3$, the ^1H NMR spectrum (Table 2.04) showed a sharp triplet at 0.95 ppm (3H) and a sharp singlet at 3.97 ppm (6H) which were assigned to the methyl ligand on Pd and the imidazole *N*-methyl protons, respectively. One singlet at δ 32.1 ppm was found in the $^{31}P\{^1H\}$ NMR spectrum. On the basis of these NMR data, we would expect that the structure of the product is similar to that of 4c-MeOTf, which is symmetrical. However, for the *tert*-butyl substituents on the phosphorus atoms were seen three broad peaks in the range δ 1.29-1.73 ppm. The unusual appearance of these proton resonances, and in comparison with 4c-MeOTf, the different solubility and the IR absorption led us to question this conclusion. Therefore, we grew crystals for X-ray analysis.

The X-ray data (Figure 2.10 and Table 2.10) showed that the product is the ionic species $[6a\text{-}Me]^+[OTf]^-$, indeed quite different from 4c-MeOTf, explaining the different solubility and IR absorption spectra. The four angles around Pd center are added up to 359.9° indicating a square-planar geometry. The two phosphine ligands are located trans to each other, with one phosphine ligand chelating to the Pd center with an imidazole N atom and Pd-methyl ligand trans to the coordinated N atom. The angle N-Pd-P(1) is small (68.96°) because of the four-membered chelate ring. The triflate was found as a free ion rather than coordinating to the Pd as it does in 4c-MeOTf, in accord with solution-phase IR data for both complexes. The Pd-P bond

lengths are significantly longer (about 0.05 Å) than those of 3a, consistent with increased steric demand about the metal center and reduced back-bonding to the phosphines. In addition, the Pd-P bond lengths are longer (about 0.05 Å) than in 5a-PhX and 5b-PhI, perhaps because of the higher trans influence of the second phosphine in $[6a\text{-}Me]^{+}[OTf]^{-}$.

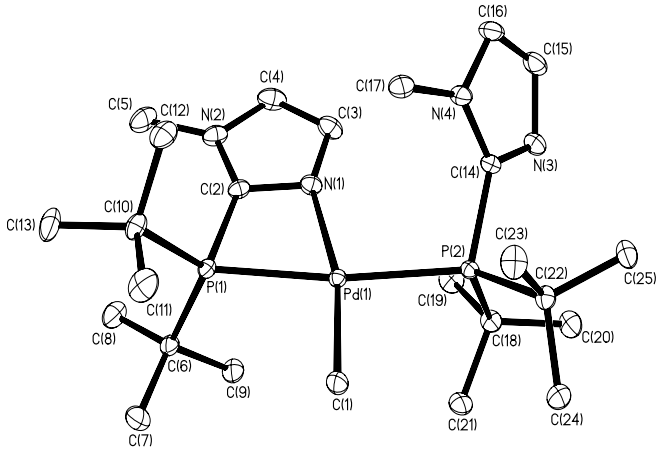

Figure 2.10. Molecular structure of $[6a\text{-}Me]^{+}[OTf]^{-}$. Only the cation is shown. Ellipsoids are shown at 30% probability.

According to the solid state structure, the two phosphine ligands are inequivalent so that two sets of ligand resonances would be expected in ^{1}H NMR spectra, and two different phosphorus signals would be expected in $^{31}P\{^{1}H\}$NMR spectra. Our NMR data collected at 30 ^{o}C did not meet these expectations; in particular, resonances for imidazole aromatic hydrogens appeared broad and more intriguingly, one of these resonances had an unusually high-field chemical shift of δ 5.18 ppm, suggesting an unusual environment for this unique proton. All these

unexpected spectroscopic data raised the following questions: Is the structure of the complex in solution the same as that of complex in solid state? Is there an equilibrium of two or more species in solution? To which phosphine (chelated or unchelated) does the aromatic proton with high-field chemical shift belong?

To answer these questions, variable-temperature ^{1}H, $^{31}P\{^{1}H\}$ and $^{13}C\{^{1}H\}$ NMR spectra were taken, as well as NOE, DEPT and COSY, HMQC and HMBC spectra. The ^{1}H NMR spectra at selected temperature aree shown in Figure 2.11. While the sample temperature was lowered, the broad signals for the *tert*-butyl groups in the ^{1}H NMR sharpened. At –50 ^{o}C, all signals were sharp and the presence of the two different phosphine ligands was suggested by two singlets for *N*-methyl protons and four singlets for imidazolyl protons, consistent with the solid state structure. Rather remarkably, at –50 ^{o}C four virtual triplets for *tert*-butyl substituents were seen, consistent with each large alkyl group being in a unique environment both in the solid state and in solution. Our interpretation of these data is that at lower temperature the rotation of each ligand about the Pd-P axis is slowed to the point where four individual virtual triplets could be seen. On the other hand, when the temperature was increased, the resonances of aromatic protons on imidazole and *tert*-butyl substituents became broader and started to coalesce, while the resonances of imidazole *N*-methyl proton and methyl-Pd ligand protons always stayed sharp. However, over the temperature range -50 to +55 ^{o}C, only one singlet was detected in the $^{31}P\{^{1}H\}$ NMR spectrum.

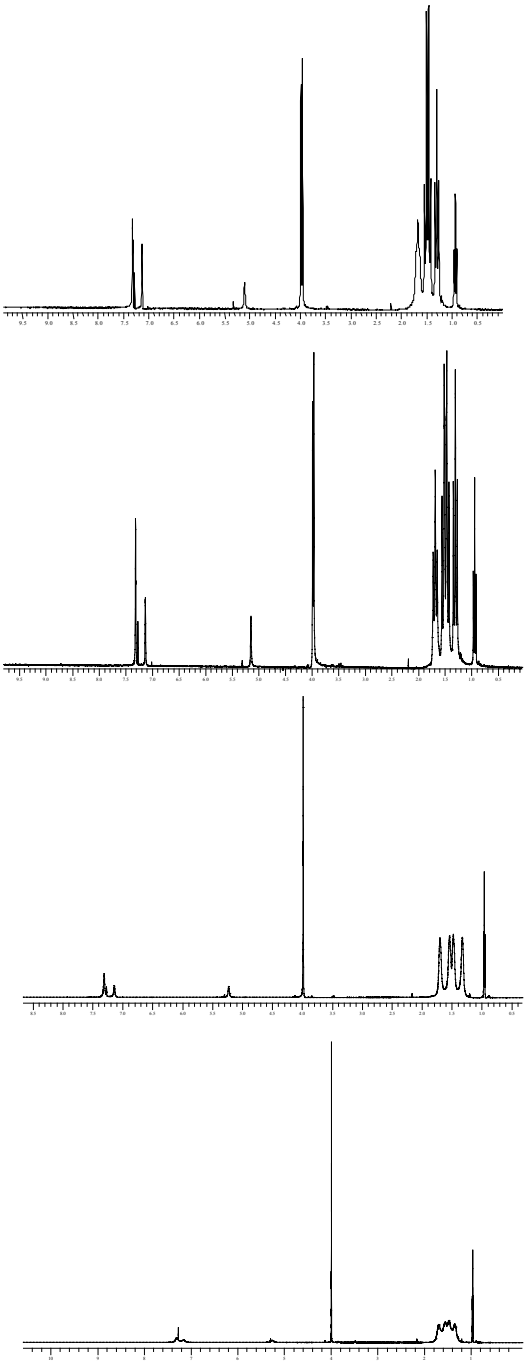

Figure 2.11. ^{1}H NMR spectra of $[6a\text{-}Me]^{+}[OTf]^{-}$ at –30 ^{o}C, -10 ^{o}C, 30 ^{o}C and 50 ^{o}C (from top to bottom).

The interesting dynamic behavior of $[6a\text{-}Me]^+[OTf]^-$ in solution (Figure 2.12) can be explained by invoking a windshield-wiper exchange of the chelating and non-chelating ligands, either in a concerted process or through a three-coordinate T-shaped intermediate B. By simulating the appearance of that portion of the spectrum for the four imidazole aromatic hydrogens, we determined for the site exchange of chelating and nonchelating imidazoles the following parameters: $E_a = 6 \pm 2$ kcal mol^{-1} and $\Delta S^{\ddagger} = -6 \pm 4$ cal mol^{-1} K^{-1}.[91] We are aware of only a single recent report on such a process in imidazolylphosphine complexes, however, no data on the activation parameters.[73] There are a few examples in pyridylphosphine chemistry of complexes with one chelating and one non-chelating phosphine, some without exchange[92-94] and others with some evidence of exchange.[95-97] There are examples of other hemilabile Pd complexes, for example ones with pyridylphosphines in which the heterocycle and the phosphine are separated by several atoms,[98-100] or complexes with phosphines containing ethers[101] as well as other functional groups.[10] However, in most cases activation energies were not reported, or in the cases where this information is available,[99,102] the differences in ligand type or metal preclude any meaningful comparison. Nonetheless, the slightly negative value obtained for $\Delta S^{\ddagger}$ would suggest involvement of either an associative or interchange ligand exchange mechanism rather than a dissociative mechanism via intermediate B.

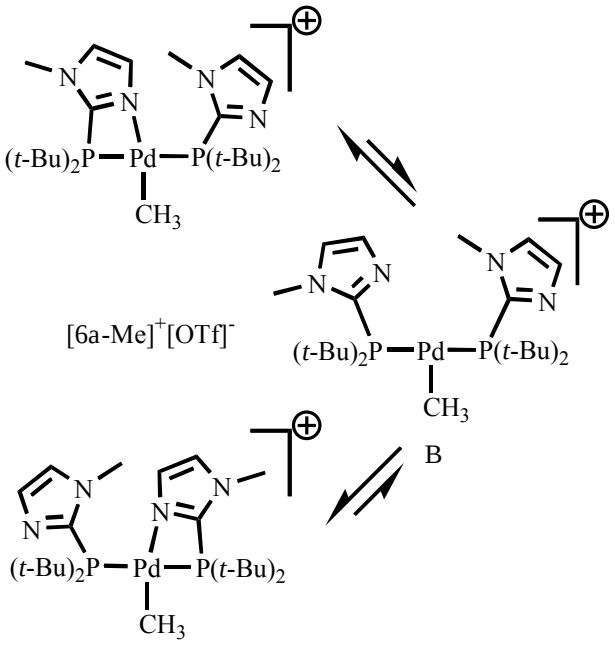

Figure 2.12. Fluxionality in $[6a\text{-}Me]^{+}[OTf]^{-}$.

It is surprising that at the low-temperature limit there are four individual proton resonances for each of the four *tert*-butyl substituents; the rotation of the non-chelating phosphine ligand about the Pd-P axis must be hindered by the bulkiness of the *tert*-butyl groups.[91] The situation in the solid (Figure 2.10) suggests the barrier to rotation in solution.

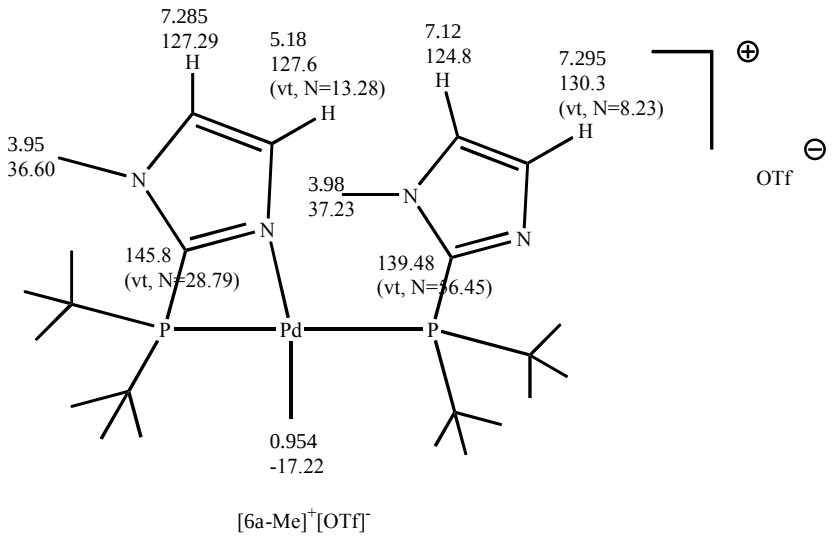

[6a-Me]$^{+}$[OTf]$^{-}$

HMBC

3.95	3	145.8
	3	127.29
3.98	3	139.48
	3	124.8
5.18	3	145.8
7.12	3	139.48
7.285	3	145.8
7.295	2	124.8

COSY

5.18	7.285
7.12	7.295

t-Bu Group HMQC results

Four methyl groups

1.30	30.23
1.46	36.26 (vt, N=9.04)
1.50	36.72 (vt, N=9.52)
1.67	30.39

Quantenary carbons

38.44 (vt, N=16.82)
38.55 (vt, N=17.95)

Figure 2.13. Two dimensional NMR leads to the assignments of proton and carbon signal for [6a-Me]$^{+}$[OTf]$^{-}$.

Because [6a-Me]$^{+}$[OTf]$^{-}$ features the same ligand in chelating and nonchelating mode and because it is obvious by looking at NMR data shown in Tables 2.04 and 2.07 that there are unusual differences in the NMR data for the same ligand in two coordination modes, a total assignment of all proton and carbon NMR resonances was made using a combination of several experiments. A graphical summary of the results is presented in Figure 2.13. HMQC was first used to determine the correlation between proton and carbon, then COSY used to identify which two

aromatic protons are in the same imidazole ring, and finally, HMBC was used to locate other pairs of protons and carbons in each imidazole ring. Once the pairs of proton and carbon were divided into two sets, the only question then left was to assign which set belongs to which imidazole, the one on the non-chelating or chelating phosphine. Although it was impossible to assure this last assignment in the absence of a P-C correlation experiment, it seems reasonable to assign the unusually high-field proton resonance at δ 5.18 ppm to the proton on the unusual ring, the one involved in chelation. The 2D-NMR work suggests that this proton is next to the nitrogen in the chelating ring. Examination of the solid-state structure (Figure 2.10) suggests that this proton is shielded by the imidazole ring of the nonchelating ligand. In looking for spectroscopic evidence for bonding differences between the two ligands, we note that the magnitude of virtual coupling between imidazole C-2 and the two phosphorus nuclei in the unusual chelate ring is about half that in the nonchelated phosphine (N = 28.8 Hz for the signal at 145.8 ppm and 56.5 Hz for the signal at 139.5 ppm).

Reaction between 3b and MeOTf gave a similar product along with another major product with almost the same amount when monitored by NMR. The attempts at isolating and purifying the product were not successful, since the two products have very similar solubility. We could speculate that the product is less stable because the big *tert*-butyl group on the ligand make chelation harder.

Reactivity toward solvents, particularly CH_2Cl_2. Both of the Pd(0) complexes 3a, 3b were quite stable either in solid state or in the solution, where there

was no reaction with solvents such as benzene, dichloromethane or chloroform. On the other hand, initially colorless solutions of the Pd(0) complex 3c with less hindered phosphine ligands deposited some dark solid, presumably Pd black, when left at room temperature for a period of weeks. Although the major component was still the Pd(0) complex, some minor unidentified impurities were detected by NMR. In solution of benzene, 3c was relatively stable, but in dichloromethane, a completely new complex 7c-CH_2Cl_2 was formed (Figure 2.14).

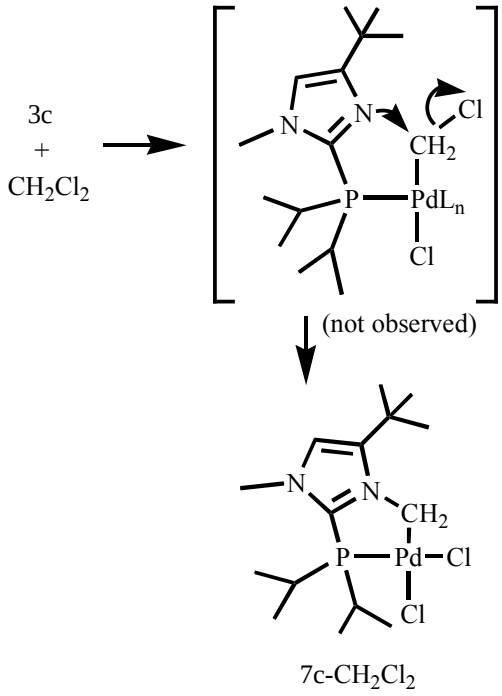

Figure 2.14. Reaction between 3c and dichloromethane.

Elemental analysis was consistent with the species shown, and the structure of this new complex was confirmed by X-ray diffraction data (Figure 2.15). The novel

square planar Pd(II) complex bears two chloride ligands and only one phosphine ligand which was alkylated with the CH_2 unit from dichloromethane. The Pd-P bond length in 7c-CH_2Cl_2 (Table 2.10, 2.1878 Å) is ca. 0.15 Å shorter than those in 4c-PhI and 4c-MeOTf, probably a reflection of the weaker trans influence of chloride in 7c-CH_2Cl_2. Oxidative additions of dichloromethane to Pd(0) species are known,[103,104] and the X-ray diffraction structure of $[Cy_2PCH_2CH_2PCy_2]Pd(CH_2Cl)(Cl)$ shows Pd-C = 2.101(9) Å, Pd-P trans to Cl = 2.225(2) and trans to CH_2Cl = 2.317(2) Å, respectively.[104]

Another interesting structural feature revealed by the data for Pd-Cl bond length in Table 2.10 is that the Pd-Cl bond trans to phosphine (2.3769 Å) is significantly shorter than the Pd-Cl bond trans to carbon (2.4124 Å).

A likely mechanism for the formation of 7c-CH_2Cl_2 would involve oxidative-addition of a C-Cl bond to Pd(0) as suggested in Figure 2.14, followed by displacement of the remaining chloride on carbon by the imidazole nitrogen. It is worth noting that despite the presence of the large *tert*-butyl group adjacent to nitrogen, attack on the putative Pd-CH_2Cl intermediate seems to occur readily. Formation of 7c-CH_2Cl_2 from 3c may be considered a bifunctional double activation of the substrate CH_2Cl_2.

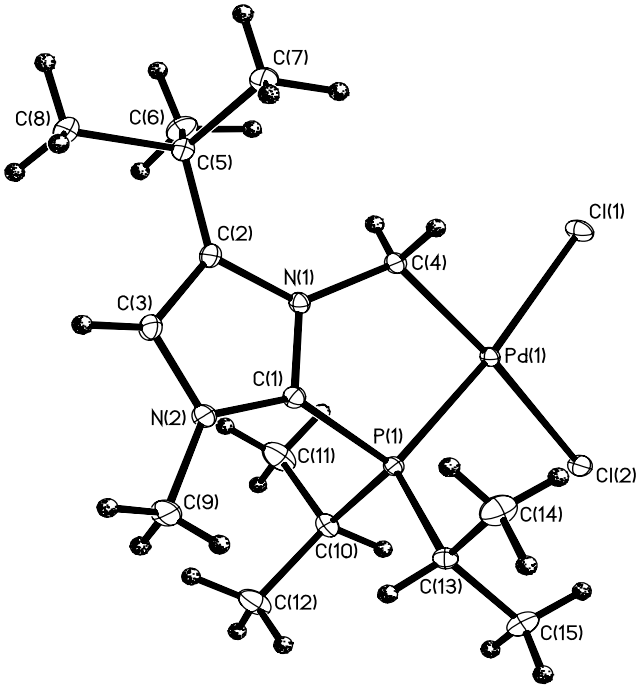

Figure 2.15. Molecular structure of 7c-CH_2Cl_2. Ellipsoids are shown at 30% probability.

In the ^{1}H NMR spectrum, the most affected resonance is that of the imidazole-H which shifted 1.5 ppm downfield from that of 3c. Similarly, the resonance for protons of the isopropyl substituents on phosphorus shifted downfield, whereas the peaks for the methyl hydrogens on the isopropyl substituents appear as two doublet of doublets because the methyl groups are diastereotopic. These chemical shift changes may be due to the two new trans ligands (chlorides) as well as alkylation of the imidazole ring, which changes the distribution of the formal charge on the aromatic ring.

Addition of amines or other polar ligands to chelated oxidative-addition products without opening of the chelate. In the process of coupling between aryl halides and amines, the step which follows oxidative-addition is believed to be coordination of the amine to an open site on the Pd center. Although there was no open site on complex 5a-PhX and 5b-PhI, our expectation was that the chelate ring would open, with the amine nitrogen coordinating to Pd. We expected that this process would be facilitated not only by relief of any strain in the chelate but also by hydrogen bonding between one of the N-H bonds of the coordinated amine and the now-free imidazole nitrogen, an interaction we saw between coordinated water and imidazole substituent in Ru complex 1.[75]

Surprisingly, in 5a-PhX (X = Br, I) and 5b-PhI the chelate ring stayed closed when primary and secondary amines were added; no binding of amine was detected as evidenced by lack of changes in ^{1}H or ^{31}P NMR spectral data. The same result was obtained when H_2O was added. Similarly, when complex $[6a\text{-}Me]^{+}[OTf]^{-}$ was treated individually with isopropylamine, water or 2-propanol, the chelate ring stayed closed also, and if any coordination of the ligands took place it was to an indetectable extent.

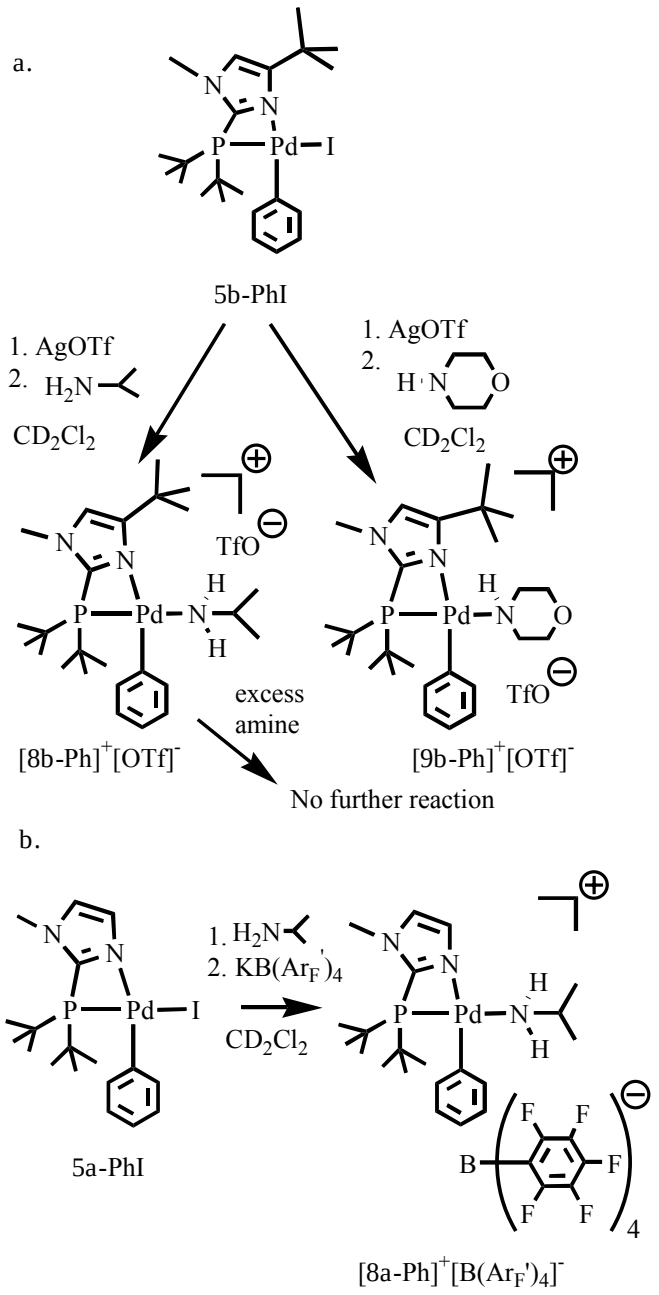

Figure 2.16. Amine binding without chelate opening.

One way of opening a coordination site in a halopalladium complex would be to abstract halide ion. Thus, the oxidative-addition product with one chelating

phosphine ligand 5b-PhI was ionized by silver triflate in dichloromethane (Figure 2.16), forming a yellow precipitate assumed to be silver iodide. After the yellow precipitate was removed, one equivalent of the primary amine, *iso*-propylamine was added to the filtrate. The $^{31}P\{^{1}H\}$ NMR spectrum showed there was only one major species in the NMR solution. After isolation, purification and characterization, the product was found to be $[8b\text{-}Ph]^{+}[OTf]^{-}$ (Figure 2.16a). The elemental analysis data were consistent with the formula (phosphine)Pd(Ph)(*iso*-propylamine)(triflate). The strong absorption at 1270 cm^{-1} indicated the S-O stretch in the free triflate ion. A square-planar Pd(II) cation in this formula would reasonably contain a chelated phosphine in addition to phenyl and amine ligands. The NMR data were consistent with this structure though not diagnostic. In the ^{1}H NMR spectrum, the resonance for the N-H protons in *iso*-propylamine appeared at 2.83 ppm as a slightly broad singlet, whereas in the $^{31}P\{^{1}H\}$ NMR spectrum, the singlet at +39.8 ppm was shifted 10 ppm downfield from that of 5b-PhI, either because of the change of the trans ligand to the phosphorus atom or the overall charge on the metal. We could not tell the precise bonding in the product from the spectral data, but the molecular structure was clarified by X-ray diffraction. The crystal structure shown in Figure 2.17 demonstrated the binding of isopropyl amine, where the Pd-N bond length [Table 2.10, 2.129(2) Å] falls in the range of that in Pd complex with bound amine.[105,106] Looking at Table 2.10, it is interesting to compare the structures of 5b-PhI and $[8b\text{-}Ph]^{+}OTf^{-}$: in going from the neutral to the ionic species, the Pd-P(1) and Pd-N(Im) bond lengths decrease by 0.025(1) and 0.065(4) Å, respectively, with a concomitant increase in the P(1)-Pd-

N(Im) angle of 1.1(1)°. The four interligand bond angles shown in Table 2.10 change by at most 2.4°, with θ_1 and θ_2 together increasing by a total of 3.5° and the opposite angles θ_3 and θ_4 together decreasing by the same amount. These changes may reflect both the increase in positive charge on the complex (tightening the chelate) and the reduced size of the ligand cis to phenyl (from I to H_2NR). Since amine and phenyl ligands are located cis to each other, the release of arylated amine through reductive elimination is conceivable. However, the addition of excess amine to pure [8b-Ph]$^+$[OTf]$^-$ did not open the chelate ring.

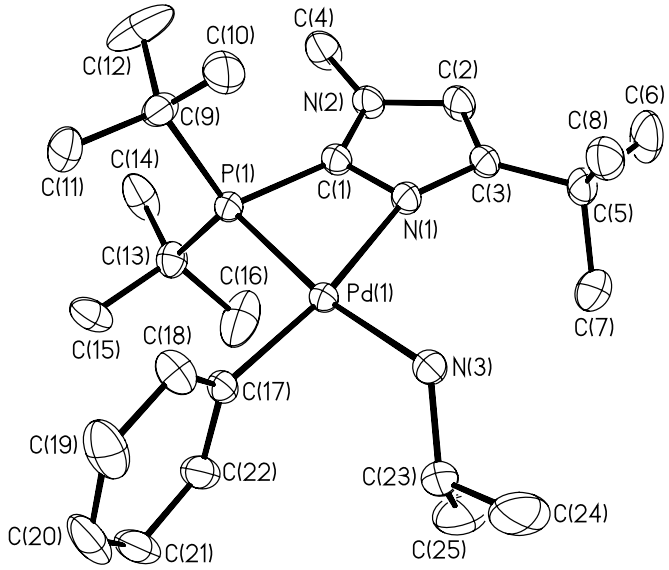

Figure 2.17. Molecular structure of [8b-Ph]$^+$[OTf]$^-$. Only the cation is shown. Ellipsoids are shown at 30% probability.

A product with similar spectral data was obtained when the secondary amine morpholine was used instead of isopropyl amine to react with 5b-PhI and silver triflate (Figure 2.16a), so we assume a similar structure, $[9b\text{-}Ph]^{+}[OTf]^{-}$.

The analogous reaction with 5a-PhI gave slightly different results. The use of an ionizing agent, silver triflate and the subsequent addition of amine yielded a mixture with many minor species. However, when the ionizing reagent was changed to potassium tetrakis(pentafluorophenyl)borate [$KB(Ar_F')_4$] and amine was added prior to the addition of ionizing reagent, the reaction was cleaner, with a major species assigned structure $[8a\text{-}Ph]^{+}$ $[B(Ar_F')_4]^{-}$ on the basis of spectral data similar to those of $[8b\text{-}Ph]^{+}[OTf]^{-}$ (Figure 2.16b).

In summary, the products from the reactions between 5a-PhI, 5b-PhI with ionizing reagents and amine had very similar structures. In the resulting complexes, the amine coordinated to Pd as a neutral ligand, oriented cis to the phenyl ligand. In the case of 5a-PhI, the sequence of adding ionizing reagents and amine was essential, and the choice of ionizing reagent was also important.

Binding of amines with hydrogen bonding. Whereas $[6a\text{-}Me]^{+}[OTf]^{-}$ did not react with an amine, neutral but less hindered 4c-MeOTf did react with benzylamine to give an ionic product in which the weakly coordinating triflate ion was replaced by the amine (Figure 2.18). When the amine binding reaction was carried out in dichloromethane, only $[10c\text{-}Me]^{+}[OTf]^{-}$ was observed and isolated. IR absorption suggested an ionic triflate rather than bound triflate, but ultimately X-ray diffraction was used to verify the structure (Figure 2.19). Interestingly, when the reaction of 4c-

MeOTf and benzylamine was carried out in C_6D_6, a mixture containing four species was observed, three being unreacted 4c-MeOTf, free phosphine 2c, and [10c-Me]$^+$[OTf]$^-$ as shown by $^{31}P\{^1H\}$ NMR peaks at δ 24.4, -17.7, and 28.6 ppm, respectively. The appearance of free ligand 2c and the fourth species ($^{31}P\{^1H\}$ NMR δ 33.4 ppm) in a molar ratio of approximately 1 to 1 suggests that the latter compound is the monophosphine complex [11c-Me]$^+$[OTf]$^-$, though we were unable to isolate it from this mixture and it was not characterized further. The nature of hydrogen bonding in purified [10c-Me]$^+$[OTf]$^-$ was not clearly revealed in its infrared spectrum, which exhibited several weak bands in the region 3000 to 3400 cm^{-1}.

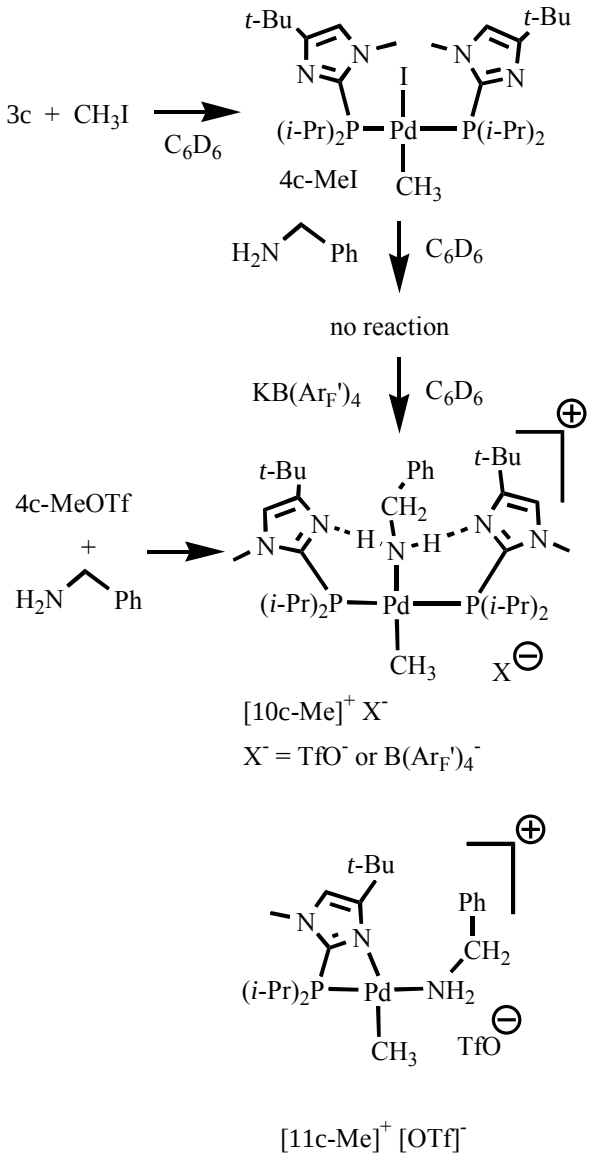

Figure 2.18. Amine binding with hydrogen bonding.

Therefore, crystals of $[10c\text{-}Me]^{+}[OTf]^{-}$ were grown for X-ray diffraction study, the results of which are shown in Figure 2.19. The two phosphine ligands are located trans to each other and the benzylamine is coordinated to Pd trans to methyl ligand. Significantly, the benzylamine fits into a binding pocket created by the two

heterocyclic phosphine ligands acting as hydrogen bond acceptors to the amine. The distances between the amine hydrogens and the interacting nitrogens on the imidazole rings were 2.05 Å and 2.09 Å which was in the range of N-H distance involved in hydrogen bonding.[107]

The same cation could be created in three steps, first by performing oxidative-addition of iodomethane to 3c to give 4c-MeI, in a fast and clean reaction like that with iodobenzene. Subsequent addition of benzylamine followed by potassium tetra(pentafluorophenyl)borate resulted in the formation of $[10c\text{-}Me]^+[B(Ar_F')_4]^-$ (Figure 2.19). The X-ray crystal structure of this complex obtained from Et_2O/CH_2Cl_2 (Figure 2.20) also showed a hydrogen bond between each amine N-H and the nitrogen atom on closest imidazole ring. The only difference between $[10c\text{-}Me]^+[OTf]^-$ and $[10c\text{-}Me]^+[B(Ar_F')_4]^-$ is the anion, thus the corresponding bond lengths and bond angles are comparable (Table 2.10).

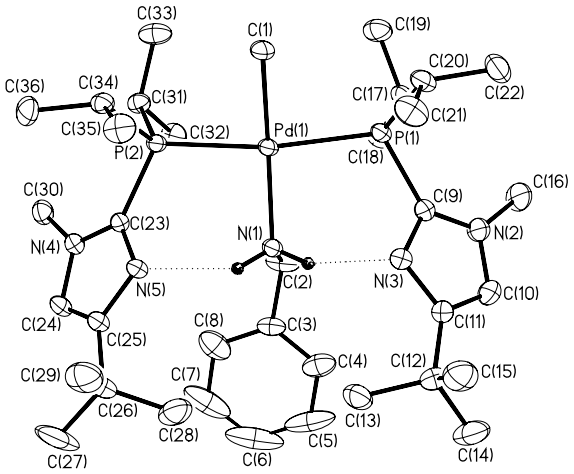

Figure 2.19. Molecular structure of the cation of $[10c\text{-}Me]^{+}[OTf]^{-}$. Ellipsoids are shown at 30% probability.

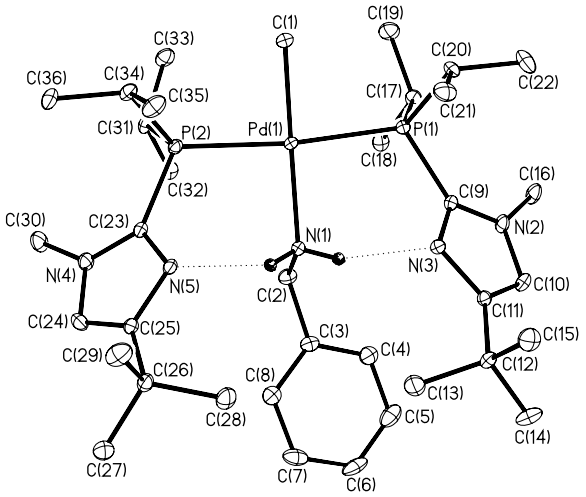

Figure 2.20. Molecular structure of $[10c\text{-}Me]^{+}[B(Ar_F')_4]^{-}$, only cation is shown.

D. Conclusion

A series of three new imidazolylphosphine ligands was designed and synthesized to probe the effects of phosphorus and heterocycle substituents on coordination geometry and ligand hapticity in Pd(0) and Pd(II) complexes of these ligands. In verification of the HSAB concept,[48] the X-ray diffraction and spectroscopic data for Pd(0) complex 3a show that it is a two-coordinate, 12-electron species despite the availability of the heterocyclic nitrogens to enter into chelation, and the proximity of hydrogens on the *N*-methyl groups to enter into agostic interactions.

Oxidative-addition chemistry of the two-coordinate Pd(0) complexes 3a-3c shows that isopropyl substituents not only allow rapid reaction but retention of both phosphine ligands in 4c-PhI and 4c-MeOTf. In contrast, phosphorus *tert*-butyl groups slow oxidative-addition and lead to phosphine loss and chelation by the remaining phosphine in 5a-PhBr, 5a-PhI, and 5b-PhI. Unlike isopropyl-substituted complex 4c-MeOTf, which features a metal-bound triflate ion, *tert*-butyl substituted analog [6a-Me]$^{+}$[OTf]$^{-}$ is ionic because the triflate ligand has been displaced by one imidazole nitrogen in forming a chelate. Taken together, these results show a strong enforcement of chelation by larger substituents R in R_2PR' (R' = imidazol-2-yl). This preference is reminiscent of the trends noted in the past for metalation of R' when R is large. Comparing 5a-PhI and 5b-PhI one can see the effects of increasing steric hindrance at the chelating imidazole nitrogen, notably a lengthening of the Pd-N(Im) bond, yet this is insufficient to allow opening of the chelate by amines. In fact, in all of the di-*tert*-

butylphosphino-substituted compounds in this study, the chelate remained closed when amines were added. Amine binding could be effected after halide ionization, but without opening of the chelate ring in $[8b\text{-}Ph]^+[OTf]^-$, $[9b\text{-}Ph]^+[OTf]^-$, and $[8a\text{-}Ph]^+[OTf]^-$. Amine binding involving hydrogen bonding was seen in the isopropyl series by looking at the crystal structures of $[10c\text{-}Me]^+[OTf]^-$ and its $[B(Ar_F')_4]^-$ analog. The results described here show the interplay of ligand substituents in determining ligand hapticity, coordination of other ligands, and secondary hydrogen-bonding interactions, properties of interest in study structure and catalysis of complexes featuring hybrid ligands.

E. References

(1) Collman, J. P.; Hegedus, L. S.; Norton, J. R.; Finke, R. G. *Principles and Applications of Organotransition Metal Chemistry*; University Science Books: Mill Valley, CA, 1987.

(2) Crabtree, R. H. *The Organometallic Chemistry of the Transition Metals*; 3rd ed.; Wiley: New York, 2000.

(3) Cummins, C. C. *Prog. Inorg. Chem.* 1998, *47*, 685-836.

(4) Cummins, C. C. *Chem. Comm.* 1998, 1777-1786.

(5) Braunstein, P.; Naud, F. *Angew. Chem., Int. Ed. Engl.* 2001, *40*, 680-699.

(6) Börner, A. *Eur. J. Inorg. Chem.* 2001, 327-337.

(7) Schneider, J. J. *Nachr. aus der Chemie* 2000, *48*, 614-616, 618-620.

(8) Müller, C.; Vos, D.; Jutzi, P. *J. Organomet. Chem.* 2000, *600*, 127-143.

(9) Slone, C. S.; Weinberger, D. A.; Mirkin, C. A. *Prog. Inorg. Chem.* 1999, *48*, 233-350.

(10) Bader, A.; Lindner, E. *Coord. Chem. Rev.* 1991, *108*, 27-110.

(11) Jeffrey, J. C.; Rauchfuss, T. B. *Inorg. Chem.* 1979, *18*, 2658-2666.

(12) Okuda, J. *Comm. Inorg. Chem.* 1994, *16*, 185-205.

(13) Werner, H. *Dalton Transactions* 2003, 3829-3837.

(14) Young, J. F.; Osborn, J. A.; Jardine, F. H.; Wilkinson, G. *J. Chem. Soc., Chem. Comm.* 1965, 131-132.

(15) Osborn, J. A.; Jardine, F. H.; Young, J. F.; Wilkinson, G. *J. Chem. Soc., Dalton Trans.* 1966, 1711-1732.

(16) Halpern, J.; Wong, C. S. *J. Chem. Soc., Chem. Comm.* 1973, 629-630.

(17) Miyaura, N.; Yanagi, T.; Suzuki, A. *Synth. Comm.* 1981, *11*, 513-519.

(18) Littke, A. F.; Dai, C.; Fu, G. C. *J. Am. Chem. Soc.* 2000, *122*, 4020-4028.

(19) Stambuli, J. P.; Bühl, M.; Hartwig, J. F. *J. Am. Chem. Soc.* 2002, *124*, 9346-9347.

(20) Littke, A. F.; Fu, G. C. *Angew. Chem., Int. Ed. Engl.* 2002, *41*, 4176-4211.

(21) Netherton, M. R.; Dai, C.; Neuschütz, K.; Fu, G. C. *J. Am. Chem. Soc.* 2001, *123*, 10099-10100.

(22) Kirchhoff, J. H.; Dai, C.; Fu, G. C. *Angew. Chem., Int. Ed. Engl.* 2002, *41*, 1945-1947.

(23) Kirchhoff, J. H.; Netherton, M. R.; Hills, I. D.; Fu, G. C. *J. Am. Chem. Soc.* 2002, *124*, 13662-13663.

(24) Netherton, M. R.; Fu, G. C. *Angew. Chem., Int. Ed. Engl.* 2002, *41*, 3910-3912.

(25) Menzel, K.; Fu, G. C. *J. Am. Chem. Soc.* 2003, *125*, 3718-3719.

(26) Lee, J.-Y.; Fu, G. C. *J. Am. Chem. Soc.* 2003, *125*, 5616-5617.

(27) Zhou, J.; Fu, G. C. *J. Am. Chem. Soc.* 2003, *125*, 12527-12530.

(28) Hills, I. D.; Netherton, M. R.; Fu, G. C. *Angew. Chem., Int. Ed. Engl.* 2003, *42*, 5749-5752.

(29) DeVasher, R. B.; Moore, L. R.; Shaughnessy, K. H. *J. Org. Chem.* 2004, *69*, 7919-7927.

(30) Smith, R. C.; Woloszynek, R. A.; Chen, W.; Ren, T.; Protasiewicz, J. D. *Tet. Lett.* 2004, *45*, 8327-8330.

(31) Baillie, C.; Zhang, L.; Xiao, J. *J. Org. Chem.* 2004, *69*, 7779-7782.

(32) Brenstrum, T.; Gerristma, D. A.; Adjabeng, G. M.; Frampton, C. S.; Britten, J.; Robertson, A. J.; McNulty, J.; Capretta, A. *J. Org. Chem.* 2004, *69*, 7635-7639.

(33) Colacot, T. J.; Shea, H. A. *Org. Lett.* 2004, *6*, 3731-3734.

(34) Kwong, F. Y.; Lam, W. H.; Yeung, C. H.; Chan, K. S.; Chan, A. S. C. *Chem. Comm.* 2004, 1922-1923.

(35) Weng, Z.; Teo, S.; Koh, L. L.; Hor, T. S. A. *Organometallics* 2004, *23*, 4342-4345.

(36) Weissman, H.; Shimon, L. J. W.; Milstein, D. *Organometallics* 2004, *23*, 3931-3940.

(37) Wang, A.-E.; Zhong, J.; Xie, J.-H.; Li, K.; Zhou, Q.-L. *Adv. Synth. Catal.* 2004, *346*, 595-598.

(38) Harkal, S.; Rataboul, F.; Zapf, A.; Fuhrmann, C.; Riermeier, T.; Monses, A.; Beller, M. *Adv. Synth. Catal.* 2004, *346*, 1742-1748.

(39) Hartwig, J. F. *Acc. Chem. Res.* 1998, *31*, 852-860.

(40) Hartwig, J. F. *Angew. Chem., Int. Ed. Engl.* 1998, *37*, 2046-2067.

(41) Hartwig, J. F. In *Modern Amination Methods*; Ricci, A., Ed.; Wiley-VCH: Weinheim, Germany, 2000.

(42) Hartwig, J. F. In *Handbook of Organopalladium Chemistry for Organic Synthesis*; Negishi, E., Ed.; Wiley: Hoboken, N. J., 2002, p 1051-1096.

(43) Wolfe, J. P.; Wagaw, S.; Marcoux, J.-F.; Buchwald, S. L. *Acc. Chem. Res.* 1998, *31*, 805-818.

(44) Yang, B. H.; Buchwald, S. L. *J. Organomet. Chem.* 1999, *576*, 125-146.

(45) Matsumoto, M.; Yoshioka, H.; Nakatsu, K.; Yoshida, T.; Otsuka, S. *J. Am. Chem. Soc.* 1974, *96*, 3322-3324.

(46) Otsuka, S.; Yoshida, T.; Matsumoto, M.; Nakatsu, K. *J. Am. Chem. Soc.* 1976, *98*, 5850-5858.

(47) Hartwig, J. F.; Paul, F. *J. Am. Chem. Soc.* 1995, *117*, 5373-5374.

(48) Pearson, R. G.; Scott, A. In *Survey of Progress in Chemistry*; Academic Press: New York, 1969, p Chapter 1.

(49) Müller, C.; Lachicotte, R. J.; Jones, W. D. *Organometallics* 2002, *21*, 1975-1981.

(50) Perthuisot, C.; Edelbach, B. L.; Zubris, D. L.; Simhai, N.; Iverson, C. N.; Müller, C.; Satoh, T.; Jones, W. D. *J. Mol. Catal. A: Chemical* 2002, *189*, 157-168.

(51) Lindner, E.; Andres, B. *Chem. Ber.* 1988, *121*, 829-832.

(52) Horner, L.; Simons, G. *Zeitschrift für Naturforschung, Teil B* 1984, *39B*, 497-503.

(53) Basoli, C.; Botteghi, C.; Cabras, M. A.; Chelucci, G.; Marchetti, M. *J. Organomet. Chem.* 1995, *488*, C20-C22.

(54) Kurtev, K.; Ribola, D.; Jones, R. A.; Cole-Hamilton, D. J.; Wilkinson, G. *J. Chem. Soc. Dalton Trans.* 1980, 55-58.

(55) Newkome, G. R. *Chem. Rev.* 1993, *93*, 2067-2089.

(56) Drent, E.; Arnoldy, P.; Budzelaar, P. H. M. *J. Organometal. Chem.* 1994, *475*, 57-63.

(57) Drent, E.; Arnoldy, P.; Budzelaar, P. H. M. *J. Organomet. Chem.* 1993, *455*, 247-253.

(58) Drent, E.; Van Broekhoven, J. A. M.; Doyle, M. J. *J. Organomet. Chem.* 1991, *417*, 235-251.

(59) 3- and 4-Pyridylphosphines have been used recently as bridging ligands to assemble polynuclear catalysts: Slagt, V. F.; Kamer, P. C. J.; Van Leeuwen, P. W. N. M.; Reek, J. N. H. *J. Am. Chem. Soc.* 2004, *126*, 1526-1536. Slagt, V. F.; Reek, J. N. H.; Kamer, P. C. J.; Van Leeuwen, P. W. N. M. *Angew. Chem., Int. Ed.* 2001, *40*, 4271-4274. Kleij, A. W.; Lutz, M.; Spek, A. L.; van Leeuwen, P. W. N. M.; Reek, J. N. H. *Chem. Comm. (Cambridge)* 2005, 3661-3663.

(60) Slebocka-Tilk, H.; Cocho, J. L.; Frackman, Z.; Brown, R. S. *J. Am. Chem. Soc.* 1984, *106*, 2421-2431.

(61) Brown, R. S.; Zamkanei, M.; Cocho, J. L. *J. Am. Chem. Soc.* 1984, *106*, 5222-5228.

(62) Sorrell, T. N.; Allen, W. E.; White, P. S. *Inorg. Chem.* 1995, *34*, 952-960.

(63) Kimblin, C.; Bridgewater, B. M.; Churchill, D. G.; Parkin, G. *Dalton* 2000, 2191-2194.

(64) Kimblin, C.; Murphy, V. J.; Hascall, T.; Bridgewater, B. M.; Bonanno, J. B.; Parkin, G. *Inorg. Chem.* 2000, *39*, 967-974.

(65) Burini, A.; Pietroni, B. R.; Galassi, R.; Valle, G.; Calogero, S. *Inorg. Chim. Acta* 1995, *229*, 299-305.

(66) Burini, A.; Galassi, R.; Pietroni, B. R.; Rafaiani, G. *J. Organomet. Chem.* 1996, *519*, 161-167.

(67) Bachechi, F.; Burini, A.; Galassi, R.; Macchioni, A.; Pietroni, B. R.; Ziarelli, F.; Zuccaccia, C. *J. Organomet. Chem.* 2000, *593-594*, 392-402.

(68) Done, M. C.; Rüther, T.; Cavell, K. C.; Kilner, M.; Peacock, E. J.; Braussaud, N.; Skelton, B. W.; White, A. *J. Organomet. Chem.* 2000, *607*, 78-92.

(69) Bachechi, F.; Burini, A.; Fontani, M.; Galassi, R.; Macchioni, A.; Pietroni, B. R.; Zanello, P.; Zuccaccia, C. *Inorg. Chim. Acta* 2001, *323*, 45-54.

(70) Jalil, M. A.; Yamada, T.; Fujinami, S.; Honjo, T.; Nishikawa, H. *Polyhedron* 2001, *20*, 627-633.

(71) Tejel, C.; Bravi, R.; Ciriano, M. A.; Oro, L. A.; Bordonaba, M.; Graiff, C.; Tiripicchio, A.; Burini, A. *Organometallics* 2000, *19*, 3115-3119.

(72) Tejel, C.; Ciriano, M. A.; Bravi, R.; Oro, L. A.; Graiff, C.; Galassi, R.; Burini, A. *Inorg. Chim. Acta* 2003, *347*, 129-136.

(73) Espino, G.; Jalon, F. A.; Maestro, M.; Manzano, B. R.; Perez-Manrique, M.; Bacigalupe, A. C. *Eur. J. Inorg. Chem.* 2004, 2542-2552.

(74) Moore, S. S.; Whitesides, G. M. *J. Org. Chem.* 1982, *47*, 1489-1493.

(75) Grotjahn, D. B.; Incarvito, C. D.; Rheingold, A. L. *Angew. Chem., Int. Ed. Engl.* 2001, *40*, 3884-3887.

(76) Caballero, A.; Jalon, F. A.; Manzano, B. R.; Espino, G.; Perez-Manrique, M.; Mucientes, A.; Poblete, F. J.; Maestro, M. *Organometallics* 2004, *23*, 5694-5706.

(77) For a recent report on the use of N-aryl-2-phosphino(benz)imidazoles as ligands in Suzuki couplings and aryl aminations, see reference 38.

(78) Grotjahn, D. B.; Lev, D. A. *J. Am. Chem. Soc.* 2004, *126*, 12232-12233.

(79) Shirley, D. A.; Alley, P. W. *J. Am. Chem. Soc.* 1957, *79*, 4922-4927.

(80) Curtis, N. J.; Brown, R. S. *J. Org. Chem.* 1980, *45*, 4038-4040.

(81) Paul, F.; Patt, J.; Hartwig, J. F. *Organometallics* 1995, *14*, 3030-3039.

(82) Herrmann, W. A.; Thiel, W. R.; Brossmer, C.; Oefele, K.; Priermeier, T.; Scherer, W. *J. Organomet. Chem.* 1993, *461*, 51-60.

(83) The proton and carbon resonances for this complex were assigned using COSY, HMQC, and HMBC spectra, results summarized in Supporting Information.

(84) Brookhart, M.; Green, M. L. H. *J. Organomet. Chem.* 1983, *250*, 395-408.

(85) Brookhart, M.; Green, M. L. H.; Wonk, L.-L. *Prog. Inorg. Chem.* 1988, *36*, 1-124.

(86) Elschenbroich, C.; Salzer, A. *Organometallics: A Concise Introduction*; second ed.; VCH: Weinheim, 1992.

(87) Widenhoefer, R. A.; Zhong, H. A.; Buchwald, S. L. *Organometallics* 1996, *15*, 2745-2754.

(88) For older examples, see Tolman, C. A. *Chem. Rev.* 1977, *77*, 313-348, and for more recent examples, see Mann, G.; Shelby, Q.; Roy, A. H.; Hartwig, J. F. *Organometallics* 2003, *22*, 2775-2789 and Caporali, M.; Müller, C.; Staal, B. B. P.; Tooke, D. M.; Spek, A. L.; van Leeuwen, P. W. N. M. *Chem. Comm. (Cambridge)* 2005, 3478-3480.

(89) Shaw, B. L. *J. Organomet. Chem.* 1980, *200*, 307-318.

(90) Stang, P. J.; Huang, Y. H.; Arif, A. M. *Organometallics* 1992, *11*, 231-237.

(91) No attempt was made to determine the rotational barriers around the P-imidazole axes because of the complications of simulating spectra containing virtual triplets.

(92) Farr, J. P.; Olmstead, M. M.; Wood, F.; Balch, A. L. *J. Am. Chem. Soc.* 1983, *105*, 792-798.

(93) Jain, V. K.; Jakkal, V. S.; Bohra, R. *J. Organometal. Chem.* 1990, *389*, 417-426.

(94) Nicholson, T.; Hirsch-Kuchma, M.; Shellenbarger-Jones, A.; Davison, A.; Jones, A. G. *Inorg. Chim. Acta* 1998, *267*, 319-322.

(95) Farr, J. P.; Wood, F. E.; Balch, A. L. *Inorg. Chem.* 1983, *22*, 3387-3393.

(96) Suzuki, T.; Kita, M.; Kashiwabara, K.; Fujita, J. *Bull. Chem. Soc. Jpn.* 1990, *63*, 3434-3442.

(97) Some examples of fluxionality in pyridylphosphine complexes stem from interchange of two heterocycles attached to the same phosphorus center, for example, in tri(2-pyridyl)- or di(2-pyridyl)-phosphines: Wajda-Hermanowicz, K.; Pruchnik, F. P. *Transition Metal Chem. (London)* 1988, *13*, 101-103. Espinet, P.; Hernando, R.; Iturbe, G.; Villafane, F.; Orpen, A. G.; Pascual, I. *Eur. J. Inorg. Chem.* 2000, 1031-1038. On some clusters, fluxionality even involves disruption of the pyridylphosphine: Deeming, A. J.; Smith, M. B. *J. Chem. Soc., Chem. Commun.* 1993, 844-846.

(98) Heßler, A.; Fischer, J.; Kucken, S.; Stelzer, O. *Chem. Ber.* 1994, *127*, 481-488.

(99) Yang, H.; Lugan, N.; Mathieu, R. *Organometallics* 1997, *16*, 2089-2095.

(100) Del Zotto, A.; Nardin, G.; Rigo, P. *J. Chem. Soc., Dalton Trans.* 1995, 3343-3351.

(101) Lindner, E.; Speidel, R.; Fawzi, R.; ller, W. *Chem. Ber.* 1990, *123*, 2255-2260.

(102) Espinet, P.; Hernando, R.; Iturbe, G.; Villafane, F.; Orpen, A. G.; Pascual, I. *Eur. J. Inorg. Chem.* 2000, 1031-1038.

(103) Leoni, P. *Organometallics* 1993, *12*, 2432-2434.

(104) Doehring, A.; Goddard, R.; Hopp, G.; Jolly, P. W.; Kokel, N.; Krueger, C. *Inorg. Chim. Acta* 1994, *222*, 179-192.

(105) Kumar, J. S.; Singh, A. K.; Yang, J.; Drake, J. E. *J. Coord. Chem.* 1998, *44*, 217-223.

(106) Zhao, G.; Lina, H.; Yub, P.; Suna, H.; Zhua, S.; Sua, X.; Chen, Y. *J. Inorg. Biochem.* 1999, *73*, 145-149.

(107) Jeffery, G. A. *An Introduction to Hydrogen Bonding*; Oxford: New York, 1997.

(108) Lipshutz, B. H.; Morey, M. C. *J. Org. Chem.* 1983, *48*, 3745-3750.

CHAPTER 3

Imidazolylphosphine Ligands on Pt(0) and Pt(II): Effect of Ligand N-H Group on N-H activation and O-H activation by Hydrogen Bonding

A. Introduction

Platinum complexes have recieved a lot of attention due to the important role they play in the catalysis of transformation of organic compounds. For example, some of the most promising approches to the selective functionalization of alkanes involve platinum catalysts.[1,2] Significant recent progress has been made in the development of catalytic systems for alkane oxidation,[3-5] as well as in the understanding of the mechanism of these platinum(II/IV) based systems.[6-10] In addition, although the attack of nucleophiles on olefins on Pt(II) has been known for almost a century,[11] it is not until recently that the effective Pt(II)-catalyzed protocols for alkylation of indoles,[12] intramolecular hydroamination[13,14] and intramolecular hydroalkoxylation[15] with unactivated olefins have been reported.

One of our goals is to catalyze alkene hydration or amination. Direct hydration of an alkene is a commercial process for the synthesis of alcohols.[16] The catalysts used require moderate to high temperatures and pressures. They are of limited use because primary alcohols are not obtained, following Markovnikov's rule. Straight-chain primary alcohols are used widely in surfactants, plasticizers, and detergent precursors. Palladium-catalyzed telomerization of dienes to isomeric mixtures of dienols is an

example of direct catalytic hydration of alkenes to primary alcohols,[17-22] however, the selectivity is low.

In 1986, the selective hydration of unactivated terminal alkenes to primary alcohols catalyzed by trans-$PtH(OH_2)(PMe_3)_2$ under mild conditions was reported by Jensen and Trogler, as well as mechanistic studies of this transformation.[23] This would represent a revolutionary improvement over current methods of manufacturing primary alcohols. However, two years later, Ramprasad and Marsella et al. reported that their attempts to hydrate 1-hexene in a basic aqueous medium in the presence of a phase-transfer agent or surfactant and pure trans-$(PMe_3)_2PtHCl$ failed to yield any alcohol products, instead, the predominant reaction was olefin isomerization.[24] Therefore, the process of olefin hydration is complex, requires further studies and still is an un-met goal in catalysis.

Although several mechanisms can be imagined for metal-catalyzed alkene hydration as proposed by Jensen and Trogler, one key step could be O-H activation of water by oxidative addition. C-H activation by transition metal complexes has received intense scrutiny over the past 25 years.[25-29] Though less studied, N-H[30-41] or O-H[42-47] bond activation is of great interest in connection with functionalization of organic substrates with nitrogen- or oxygen-containing functional groups. Among reactants which may undergo O-H activation, water is of special interest because of its importance in useful process such as the Wacker oxidation and hydration of unsaturated species.

Our ultimate goal is finding the catalyst for hydration and hydroamination of an unsaturated bond, in an intermolecular or intramolecular sense, resulting in terminal alcohols and amines or in a heterocyclic ring, respectively. In chapter 2, we studied imidazolylphosphine ligands **2** containing different R and R^1 groups on Pd. In this Chapter, we report the syntheses of Pt complexes with various bifunctional imidazolylphosphines **2** containing different R and R^2 groups (H vs CH_3) and look into their reactivities with small molecules which could represent the important steps in the catalysis.

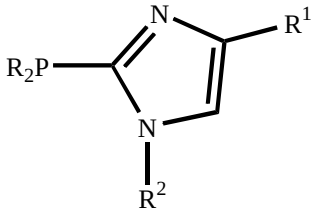

2a R = *t*-Bu, R^1 = H, R^2 = CH_3
2b R = *t*-Bu, R^1 = *t*-Bu, R^2 = CH_3
2d R = *t*-Bu, R^1 = H, R^2 = H

B. Experimental Section

General information. Reactions were performed in resealable NMR tubes (J. Young) under dry nitrogen, using a combination of Schlenk line and glovebox techniques. C_6D_6 was distilled from $LiAlH_4$ prior to use.

Unless otherwise specified, ^1H and ^{13}C data were measured at 30 °C on a 500-MHz (499.9 MHz for ^1H and 125.7 MHz for ^{13}C) spectrometer and ^{31}P data were measured on a 200-MHz (80 MHz for ^{31}P) spectrometer and the same solvent was used for all nuclei. ^1H and ^{13}C NMR chemical shifts are reported in ppm downfield from tetramethylsilane and referenced to solvent resonances (^1H NMR: δ 7.16 for C_6HD_5, δ 7.27 for $CHCl_3$ and δ 3.31 for CHD_2OD; ^{13}C NMR: δ 128.39 for C_6D_6 and δ 77.23 for $CDCl_3$). ^1H NMR signals are given followed by multiplicity, coupling constants *J* in Hertz, integration in parentheses. For complex coupling patterns, the first coupling constant listed corresponds to the first splitting listed, e.g. for (dt, *J* = 3.2, 7.9, 1 H) the doublet exhibits the 3.2-Hz coupling constant.$^{31}P\{^1H\}$ NMR chemical shifts are referenced to an external 85% H_3PO_4 (aq) capillary placed in C_6D_6. IR spectra at ambient temperatures were obtained on a ThermoNicolet Nexus 670 FT-IR spectrometer. Samples were examined in C_6D_6 or CD_3OD solution in NaCl cells. Elemental analyses were performed at NuMega Laboratories in San Diego, CA.

Crystallographic work. Data relating to the X-ray structural determinations are collected in Table 2.01 and 2.02. All data were collected on Bruker

diffractometers equipped with APEX CCD detectors. All structures were solved by direct methods and refined with anisotropic thermal parameters and idealized hydrogen atoms. All software is contained in the SMART, SAINT and SHEXTL libraries distrubted by Bruker-AXS (Madison, WI).

Pt(0)-1,3-dininyl-1,1,3,3,-tetramethyldisiloxane. 3 wt % solution in xylene was purchased from Sigma Aldrich.

Preparation of $Pt(cod)_2$. $Pt(cod)_2$ was prepared according to the literature procedure.[48]

Preparation of $PtCl_2(PhCN)_2$. Procedure used is similar to the literature procedure.[49] Potassium tetrachloroplatinate (3.38 g, 0.0081 mol) was weighed in a round-bottom flask containing a stir bar, then deionized water (15 mL) was added to the flask and a red solution was obtained. Benzonitrile (60 mL, 0.588 mol) was also added to the reaction mixture before it was allowed to stir at room temperature overnight. After the reaction was stopped, the flask containing the reaction mixture was chilled in an ice bath, the yellow precipatate formed was collected by vacuum filtration and washed with 100 mL cold hexane (3 x 100 mL). The yellow solid obtained was dried in the dessicator (2.88 g, 75%).

Preparation of $Pt(C_7H_{10})_3$. The procedure used is similar to the lierature procedure.[50] The reaction was set up in the glovebox and all the glasswear were dried in the oven prior to use. Samarium iodide solution (60 mL, 0.1 M in THF, purchased from Sigma-Aldrich) was concentrated to dryness and the residue was dissolved in acetonitrile (60 mL). Platinum-dichloro-dibenzonitrile (0.87 g, 1.85 mmol) and

norbornene (5.27 g, 0.056 mol) were transferred to a 250 mL Schlenk flask followed by the addition of acetonitrile (100 mL). The samarium iodide solution (60 mL, 0.1 M in CH_3CN) was added dropwise after the flask was cooled to –20 ^oC in an acetone-Dry Ice bath. During the addition, the intense color of SmI_2 went away then persisted. After the addition was complete, the reaction mixture was slowly warmed to room temperature and stirred overnight. The reaction mixture was concentrated to dryness and the residue was extracted with pentane (2 x 20 mL) and hexane (2 x 20 mL). All the extracts were filtered and combined, solvent was evaporated on a vacuum line to afford a white solid (88 mg, 10%).

Preparation of di-*tert*-butyl-(imidazol-2-yl)phosphine (2d). To a stirred solution of 1-(diethoxymethyl)imidazole (7.64 g, 0.045 mol) in dry and deoxygenated THF (60 mL) a 1.65 M solution of n-BuLi (27.5 mL, 0.045 mol) was then added dropwise at –35- 40 ^oC. After 15 min, di-*tert*-butyl-chlorophosphine (8.21 g, 0.045 mol) was added dropwise at –35- 40 ^oC. The solution was allowed to warm to room temperature and stirred for 2 h. The solution was then quenched with deoxygenated methanol (15 mL). The solvent was removed on a vacuum line and the resulting solid was suspended in deoxygenated pentane and filtered through Celite under nitrogen. The filtrate was concentrated to dryness, and methanol (5 mL) was added to the residue, followed by addition of a few drops of chlorotrimethylsilane. After sitting at room temperature overnight, crude product formed and was purified by recrystallization in hot acetone. Pure di-tert-butyl-

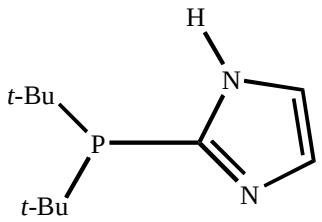

2d

(imidazol-2-yl)phosphine was obtained as colorless crystals (8.11 g, 85%). NMR (C_6D_6) ^{1}H: 8.85 (br s, 1H), 6.89 (s, 2H), 1.27 (d, 12.2, 18H); ^{31}P{^{1}H}: 16.1 (s). Anal. Calcd. for $C_{11}H_{21}N_2P$ (212.28): C, 62.24; H, 9.97; N, 13.20. Found: C, 61.36; H, 9.57; N, 13.08.

Preparation of di-*iso*-propyl-(imidazol-2-yl)phosphine (2e). To a –60 ^{o}C solution of 1-(diethoxymethyl)imidazole (6.19 g, 36.4 mmol) in dry THF (75 mL) (immersion thermometer) was added *n*-BuLi (22.0 mL of solution in hexanes, 1.65 M, 36.3 mmol) over 10 min, keeping the reaction temperature between -50 and –60 ^{o}C. At the end of the addition the temperature was –55 ^{o}C, and this was allowed to rise to –40 ^{o}C over the course of 1 h, at which point chloro-diisopropylphoshine was added dropwise over 5 min. The temperature rose to –25 ^{o}C, then dropped to –32 ^{o}C, and the mixture was stirred for 15 h as the cooling bath was allowed to warm to room temperature. Deoxygenated ethanol (5 mL) was added and the mixture was concentrated on the vacuum line. In the glovebox, the residue was stirred with pentane (50 mL) and the mixture filtered. The solid filter cake was washed with fresh pentane (2 x 50 mL). Combined filtrates were concentrated in vacuo, leaving the protected intermediate as an oil (9.85 g). ^{1}H NMR ($CDCl_3$, 200 MHz): δ 7.32 (t, 1.6, 1H), 7.22 (d, 1.2, 1H), 6.62 (d, 6.6, 1H), 3.40-3.74 (m, 4H), 2.34 (d of septet, 2.4, 7.0, 2H), 1.20 (t, 7.1, 6H), 1.09 (dd, 7.1, 16.0, 6H), 0.97 (dd, 6.8, 12.6, 6H). ^{31}P{^{1}H}: δ -18.0; ^{13}C{^{1}H}: δ 130.7, 117.6, 101.5 (d, 1.0), 62.5, 24.6 (d, 6.5), 20.0 (d, 18.3), 19.6 (d, 8.7), 15.0. Deprotection was

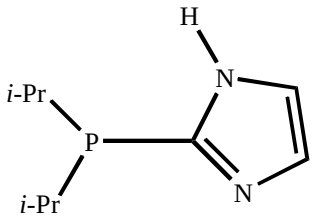

2e

effected by dissolving the crude acetal in pentane (20 mL), adding methanol (10 mL), followed by chlorotrimethylsilane (0.25 mL). Analysis of an aliquot by NMR spectroscopy after 0.5 h indicated that deprotection was complete. After a total reaction time of 1.5 h, the mixture was concentrated and the residue crystallized from a solution in CH_2Cl_2 (20 mL) by diffusing petroleum ether into it, a process completed at –50 ^oC in the glovebox freezer. The mixture was filtered through a precooled glass frit and rinsed with cold hexanes. Drying in vacuo left **2e** (4.50 g, 67%). ^1H NMR ($CDCl_3$, 200 MHz): δ 11.78 (sl br s, 1H), 7.27 (s, 2H), 2.37 (d of septet, 2.4, 7.0, 2H), 1.12 (dd, 7.0, 16.0, 6H), 1.01 (dd, 7.0, 12.4, 6H); $^{31}P\{^1H\}$ δ -8.4; $^{13}C\{^1H\}$: δ 145.5 (d, 18.0), 124.1 (d, 3.0), 24.0 (d, 7.6), 20.2 (d, 18.7), 19.8 (d, 8.4). Anal. Calcd. for $C_9H_{17}N_2P$ (184.22): C, 58.68; H, 9.30; N, 15.20. Found: C, 58.46; H, 9.49; N, 15.39.

Preparation of bis(di-*tert*-butyl-1-methylimidazol-2-yl-phosphine)platinum complex (0) (12a). Di-*tert*-butyl-1-methyl-imidazol-2-ylphosphine **2a** (82.7 mg, 0.37 mmol) was added to a reaction vial containing $Pt(cod)_2$ (67.6 mg, 0.16 mmol) and a magnetic stir bar. Deoxygenated and dry benzene (2 mL) was added to afford a slightly yellow solution. After stirring at room temperature for 1 d, solvent was removed. The resulting solid was redissolved in hot toluene (about 1 mL) and cooled to room temperature, then chilled at –50 ^oC. After 24 h, the cold supernatant was removed and the colorless crystals were washed with cold hexane and dried to give **12a** (69.8 mg, 66%). NMR

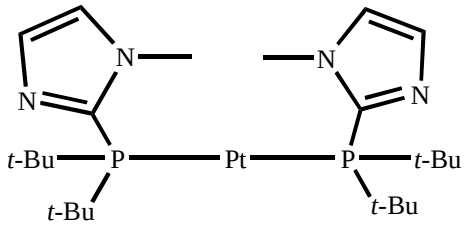

12a

(C_6D_6) ^{1}H : 7.27 (s, 2H), 7.27 (s, 2H), 4.51 (s, 6H), 1.60 (vt, *N* = 14.3, 36H); ^{13}C {^{1}H}: 143.5 (vt, *N* = 52.5), 130.1 (vt, *N* = 8.0), 124.1 (s), 39.2 (vt, *N* = 25.5), 37.5 (vt, *N* = 4.9), 31.3 (vt, *N* = 8.3); ^{31}P{^{1}H}: 55.7 (s, J_{Pt-P} = 4247.1). Anal. Calcd. For $C_{24}H_{46}N_4P_2Pt$ (647.69): C, 44.51; H, 7.16; N, 8.65. Found: C, 44.80; H, 6.83; N, 8.66. IR (C_6D_6): 2941 (s), 2894 (m) cm^{-1}.

Preparation of (η^2-P,N-di-*tert*-butyl-imidazol-2-ylphosphine)(η^1-P-di-*tert*-butyl-imidazol-2-ylphosphine)Pt(H) complex (13) (method 1). Di-*tert*-butyl-imidazol-2-yl-phosphine **2c** (62.1 mg, 0.29 mmol) was added to a reaction vial containing Pt(cod)$_2$ (51.3 mg, 0.12 mmol) and a magnetic stir bar. Deoxygenated and dry benzene (2 mL) was added to afford a slightly yellow solution which was allowed to stir at room temperature. After 1 d, solvent was removed and the crude product was recrystallized by slowly diffusing hexane into a benzene solution to give colorless crystals (53.4 mg, 70%). NMR (C_6D_6) ^{1}H: 10.57 (s, bd, 1H), 7.52 (s, 1H), 7.33 (s, 1H), 7.04 (d, 2.4, J_{Pt-H} = 7.8, 1H), 6.44 (s, 1H), 1.39 (vt, *N* = 11.2, 18H), 1.37 (vt, *N* = 11.2, 18H), -19.17 (d, J_{P-H} = 20.5, J_{Pt-H} = 1169.3); ^{13}C{^{1}H}: 155.8 (d, 75.4), 139.7 (dd, 3.9, 63.4), 132.6 (d, 8.0), 130.4 (d, 10.3), 117.6 (s), 117.6 (s), 37.0 (d, 1.6), 36.8 (d, 1.8), 33.9 (d, 3.8), 33.8 (d, 3.6); ^{31}P{^{1}H}: 52.6 (d, $J_{P-P-trans}$ = 327.8, J_{Pt-P} = 2940.3), 39.4 (d, $J_{P-P-trans}$ = 327.8, J_{Pt-P} = 2341.2). Anal. Calcd.

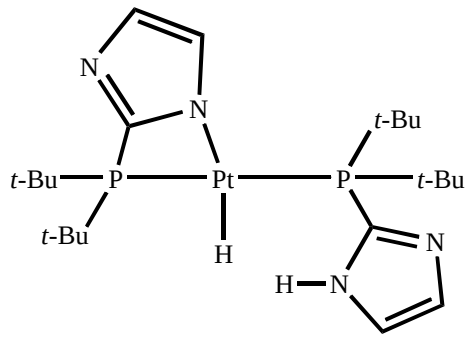

13

For $C_{22}H_{42}N_4P_2Pt$ (618.61): C, 42.64; H, 6.83; N, 9.04. Found: C, 42.84; H, 6.51; N, 9.10. IR (C_6D_6): 3373 (m), 2946 (s), 2213 (m) cm^{-1}.

(method 2) Di-tert-butyl-imidazol-2-yl-phosphine **2c** (650 mg, 3.06 mmol) was added to a reaction vial containing platinum(0)-1,3-divinyl-1,1,3,3-tetramethyldisiloxane 3 wt% solution in xylene (15 mL, 1.01 mmol) and a magnetic stir bar. The colorless solution was allowed to stir at room temperature. After 1 d, the reaction mixture was concentrated *in vacuo* to give crude product which was recrystallized from hot toluene (1 mL) to yield colorless crystals (375 mg, 60%).

Preparation of trans-bis(di-*tert*-butyl-1-methylimidazol-2-yl-phosphine)$PtCl_2$ (14a). Di-*tert*-butyl-N-methyl-imidazol-1-yl-phosphine **2a** (793.2 mg, 3.50 mmol) was weighed in a 50 mL Schlenk flask. Potassium tetrachloroplatinate (710.6 mg, 1.71 mmol) was trasferred to the flask followed by the addition of water (4 mL) and ethyl alcohol (8 mL). The resulting red solution was allowed to stir at room temperature. After 24 h, the reaction mixture was filtered and the slightly yellow solid thus obtained was dried (742.5 mg, 60%). NMR (the ratio of two rotamers is 50:50) ($CDCl_3$) ^1H: 7.45, 7.40 (s, 2H), 7.28, 7.22 (s, 2H), 4.59, 4.45 (s, 6H), 1.90 (vt, *N* = 13.8, 36H). $^{31}P\{^1H\}$: 26.5, 25.5 (s, $J_{Pt\text{-}P}$ = 2401.2).

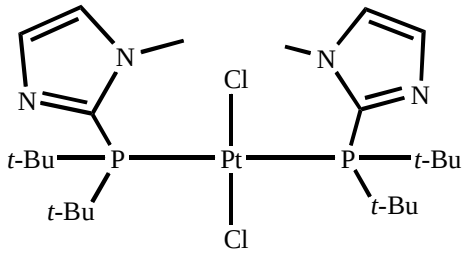

14a

Preparation of bis(di-*tert*-butyl-1-methylimidazol-2-yl-phosphine)Pt(0) complex (12a). Complex **14a** (742.5 mg, 1.03 mmol) was dissolved in dry and

deoxygenated THF (15 mL) and added to a Schlenk flask containing freshly made 1% sodium amalgam (Na, 765.1 mg, 33.3 mmol). The grey suspension was stirred at room temperature for 24 h, then the THF phase was filtered through Celite, and additional THF (10 mL) was added to wash the amalgam. The washes were filtered and all the filtrates were combined and dried in vacuo to give grey crude product which was then recrystallized from hot toluene. Finally, chilling in the freezer (-50 ^{o}C) afforded colorless crystals (408.4 mg, 61%). (see preparation above for characterization)

Preparation of trans-bis(di-*tert*-butyl-1-methyl-4-*tert*-butyl-imidazol-2-yl-phosphine)$PtCl_2$ (14b). Di-*tert*-butyl-N-methyl-4-tert-butyl-imidazol-1-yl-phosphine

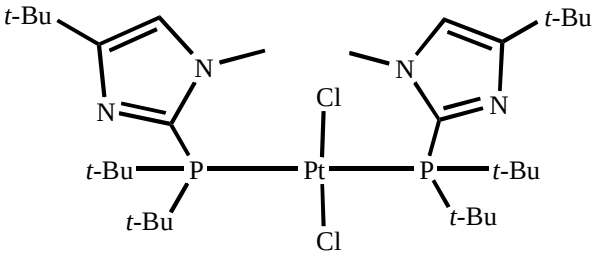

14b

2b (862.5 mg, 3.05 mmol) was weighed in a 50 mL Schlenk flask. Potassium tetrachloroplatinate (629.5 mg, 1.52 mmol) was transferred to the flask followed by the addition of water (5 mL) and ethyl alcohol (10 mL). The resulting red solution was allowed to stir at room temperature. After 24 h, the reaction mixture was filtered and the slightly yellow solid thus obtained was dried (913.6 mg, 72%). NMR ($CDCl_3$) (two rotamers in 45:55 ratio) ^{1}H: 6.66, 6.60 (s, 2H), 4.22, 4.10 (s, 6H), 1.62 (vt, N = 13.4, 36H), 1.25, 1.22 (s, 18H); $^{31}P\{^{1}H\}$: 25.7, 24.7 (s, $J_{Pt\text{-}P}$ = 2383.9).

Preparation of bis(di-*tert*-butyl-1-methyl-4-*tert*-butyl-imidazol-2-yl-phosphine)Pt(0) complex (12b). Complex **14b** (1250 mg, 1.50 mmol) was dissolved in dry and deoxygenated THF (15 mL) and added to a Schlenk flask containing freshly made 1% sodium amalgam (Na, 765.1 mg, 33.3 mmol). The grey suspension was stirred at room temperature for 24 h, then the THF phase was filtered through Celite, and additional THF (10 mL) was added to wash the amalgam. The washes were filtered and all the filtrates were combined and dried in vacuo to give grey crude product which was then recrystallized from hexane. Finally, chilling in the freezer (-50 ^{o}C) afforded colorless crystals (733.0 mg, 64%). NMR (C_6D_6) ^{1}H : 7.27 (s, 2H), 4.51 (s, 6H), 1.60 (vt, *N* = 14.3, 36H), 1.41 (s, 18H); ^{13}C{^{1}H}: 143.5 (vt, *N* = 52.5), 130.1 (vt, *N* = 8.0), 124.1 (s), 39.2 (vt, *N* = 25.5), 37.5 (vt, *N* = 4.9), 31.3 (vt, *N* = 8.3); ^{31}P{^{1}H}: 55.7 (s, J_{Pt-P} = 4247.1). Anal. Calcd. For $C_{24}H_{46}N_4P_2Pt$ (647.69): C, 44.51; H, 7.16; N, 8.65. Found: C, 44.80; H, 6.83; N, 8.66. IR (C_6D_6): 2941 (s), 2894 (m) cm^{-1}.

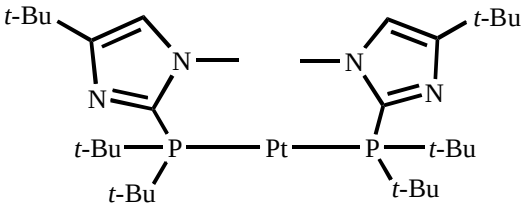

12b

Preparation of trans-bis(di-*iso*-propyl-imidazol-2-yl-phosphine)PtCl$_2$ (14e). Di-isopropyl-imidazol-2-yl-phosphine **2e** (290.0 mg, 1.57 mmol) was weighed in a reaction vial inside the glovebox. Potassium tetrachloroplatinate (325.8 mg, 0.78 mmol)

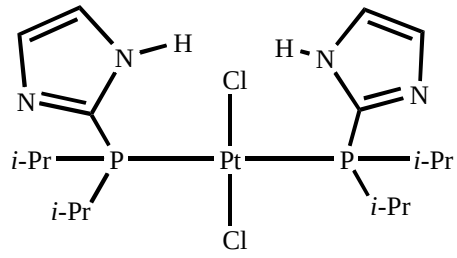

14e

was transfered to the vial followed by the addition of water (3 mL) and ethyl alcohol (6 mL). The resulting red solution was allowed to stir at room temperature. After 24 h, reaction mixture was filtered and a slightly yellow solid was obtained and dried (348.2 mg, 70%). NMR (CD_3COCD_3) ^{1}H: 11.70 (br s, 2H), 7.33 (s, 2H), 7.24 (s, 2H), 3.05-3.19 (m, 4H), 1.08-1.33 (m, 24H); ^{31}P{^{1}H }: 23.6 (s, J_{Pt-P} = 2487.0).

Preparation of {(η^2-P,N-di-*tert*-butyl-imidazol-2-ylphosphine)(η^1-di-*tert*-butyl-imidazol-2-ylphosphine)Pt(Cl)}$^+$[Cl]$^-$ ([15-Cl]$^+$[Cl]$^-$). Di-*tert*-butyl-N-methyl-imidazol-2-yl-phosphine **2d** (846.6 mg, 3.64 mmol) was weighed in a clean reaction vial, then potassium tetrachloroplatinate (750.1 mg, 1.81 mmol) was transferred to the vial followed by the addition of water (5 mL) and ethyl alcohol (10 mL). The red-colored reaction mixture was allowed to stir at room temperature. The reaction was stopped after 2 d and the reaction mixture was filtered. White solid was obtained and dried on the vacuum line (792 mg, 63.3%). NMR (CD_3OD) ^{1}H: 7.37 (d, 0.8, 2H), 7.16 (d, 1.6, J_{Pt-H} = 10.0, 1H), 5.02 (t, 1.8, J_{Pt-H} = 14.8, 1H), 4.82 (s, 2H), 1.64 (d, 4.2, 18H), 1.56 (d, 6.2, 18H); ^{13}C {^{1}H}: 151.9 (dd, 2.5, 41.5), 138.1 (dd, 2.8, 67.9), 127.8 (d, 8.9), 122.0, 39.8 (d, 2.8), 39.6 (d, 3.0), 37.7 (d, 3.9), 37.6 (d, 3.7), 30.8 (d, 2.1), 29.9 (dd, 1.6, 3.8); ^{31}P {^{1}H}: 25.0 (d, $J_{P-P-trans}$ = 375.8, J_{Pt-P} = 2765.8), 12.1 (d, $J_{P-P-trans}$ = 375.8, J_{Pt-P} = 1923.6).

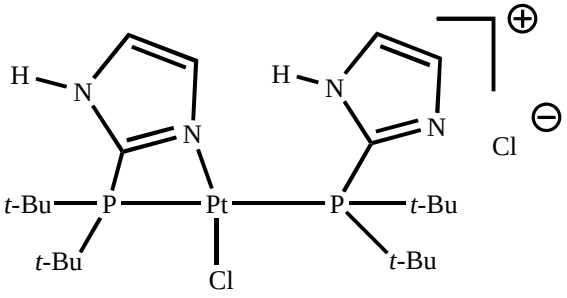

[**15**-Cl]$^+$[Cl]$^-$

Preparation of {(η^2-P,N-di--*tert*-butyl-imidazol-2-ylphosphine)(η^1-P-di-*tert*-butyl-imidazol-2-ylphosphine)Pt(Cl)}$^+$[PF_6]$^-$ ([15-Cl]$^+$[PF_6]$^-$). Complex [**15**-Cl]$^+$[Cl]$^-$ (49.0 mg, 0.071 mmol) was dissolved in dry and deoxygenated methanol (1 mL), then potassium hexafluorophosphinate (12 mg, 0.065 mmol) was added. White precipitate formed right away and was removed by filtering through Celite, the filtrate was concentrated to dryness and resulting solid was recrystallized by slowly diffusing diethyl ether into a methanol solution to afford slightly yellow crystals (40 mg, 77%). NMR (CD_3OD) ^{1}H: 7.37 (d, 0.8, 2H), 7.16 (d, 1.6, J_{Pt-H} = 10.0, 1H), 5.02 (t, 1.8, J_{Pt-H} = 14.8, 1H), 4.82 (s, 2H), 1.64 (d, 4.2, 18H), 1.56 (d, 6.2, 18H); ^{13}C {^{1}H}: 151.9 (dd, 2.5, 41.5), 138.1 (dd, 2.8, 67.9), 127.8 (d, 8.9), 122.0, 39.8 (d, 2.8), 39.6 (d, 3.0), 37.7 (d, 3.9), 37.6 (d, 3.7), 30.8 (d, 2.1), 29.9 (dd, 1.6, 4.0); ^{31}P {^{1}H}: 25.0 (d, $J_{P-P-trans}$ = 375.8, J_{Pt-P} = 2765.8), 12.1 (d, $J_{P-P-trans}$ = 375.8, J_{Pt-P} = 1923.6).

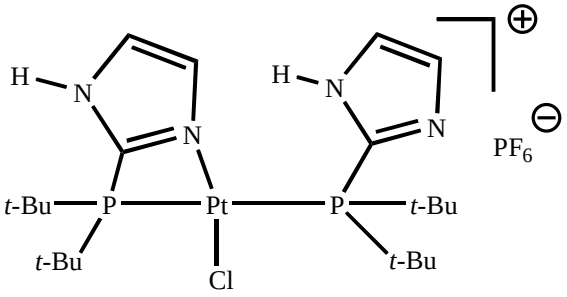

[**15**-Cl]$^+$[PF_6]$^-$

Reduction of complex [15-Cl]$^+$[Cl]$^-$ by Na/Hg. Complex [**15**-Cl]$^+$[Cl]$^-$ (1043.3 mg, 1.51 mmol) was dissolved in dry and deoxygenated THF (15 mL) and added to a Schlenk flask containing freshly made 1% sodium amalgam (Na, 765.1 mg, 33.3 mmol). The grey suspension was stirring at room temperature for 24 h. The THF phase was filtered through Celite, and additional THF (10 mL) was added to

wash the amalgam. The washes were filtered and all the filtrates were combined and dried in vacuo to give grey solid residue. The crude grey residue was dissolved in $CDCl_3$ and NMR was taken on a 200 MHz NMR spectrometer, NMR ($CDCl_3$) $^{31}P\{^1H\}$: Major signals: 51.1 (d, $J_{P\text{-}P\text{-}trans}$ = 329.2 Hz, $J_{Pt\text{-}P}$ = 2944.7 Hz), 38.1 (d, $J_{P\text{-}P\text{-}trans}$ = 327.8 Hz, $J_{Pt\text{-}P}$ = 2366.0 Hz), 63.1 (s, $J_{Pt\text{-}P}$ = 2859.5 Hz) and minor signals. The crude solid was recrystallized from THF/hexane but no pure compound was obtained.

Reduction of complex 14e by Na/Hg. Complex **14e** (252 mg, 0.40 mmol) was dissolved in dry and deoxygenated THF (10 mL) and added to a Schlenk flask containing freshly made 1% sodium amalgam (Na, 765.1 mg, 33.3 mmol). The grey suspension was stirred at room temperature for 24 h. The THF phase was filtered through Celite and additional THF (10 mL) was added to wash the amalgam. The washes were filtered and all the filtrates were combined and dried in vacuo to give grey solid residue. The crude grey residue was not soluble in benzene or dichloromethane, but soluble in THF and methanol. The crude product was then recrystallized from diethyl ether/methanol and the crystals obtained were then dissolved in CD_3OD and NMR was taken on 200 MHz NMR spectrometer, NMR (CD_3OD) $^{31}P\{^1H\}$: 29.3 (s, $J_{Pt\text{-}P}$ = 3300.3 Hz), 40.9 (s, $J_{Pt\text{-}P}$ = 2614.0 Hz) and minor signals. Further purification such as recrystallization was not successful in obtaining a pure single compound.

General procedure for the reaction of K_2PtCl_4 with ligand 2, attempts to make Pt(0) complex 12a and 12b. Phosphine ligand **2a** (208 mg, 0.92 mmol) or **2b** (260 mg, 0.92 mmol) was weighed in 50 mL round-bottom flask then potassium

tetrachloroplatinate (190 mg, 0.46 mmol) and potassium hydroxide (40 mg, 0.71 mmol) were transferred to the flask followed by the addition of dry and deoxygenated ethyl alcohol, the reaction mixture was allowed to stir at 70 ^{o}C.

With ligand 2a. After 1 d, a reaction aliquot was taken and solvent was removed, and the residue was dissolved in C_6D_6. NMR (C_6D_6) ^{1}H: 7.33 (s, 1H), 6.46 (dd, 3, 1, 1H), 3.30 (s, 3H), 1.31 (d, 5.0, 18H); ^{31}P{^{1}H} NMR: 1.96 (s) (resonances for ligand **2a**). After 10 d, the reaction mixture turned black and NMR spectra of a reaction aliquot showed no change.

With ligand 2b. After 1 d, a reaction aliquot was taken and the solvent was removed. The residue was dissolved in C_6D_6. NMR (C_6D_6) ^{1}H: 6.30 (d, 3.0, 1H), 3.32 (s, 3H), 1.43 (s, 9H), 1.30 (d, 12.4, 18H); ^{31}P{^{1}H}: 1.80 (s) (resonances for ligand **2b**). ^{1}H: 6.35 (s, 2H), 4.54 (s, 6H), 1.62 (vt, N = 14.2, 36H), 1.41 (s, 18H); ^{31}P{^{1}H}: 57.7 (s, $J_{Pt\text{-}P}$ = 4235.7 Hz) (resonances for product **12b**). Ratio of **12b** to **2b** was 1:12 which was determined by the integrals of the proton resonances. After 2 d, NMR of another aliquot was taken again, showing no new resonances, but the ratio of **12b** to **2b** has changed to 1:1.8. After 5 d, NMR of a third aliquot was taken, and new resonances appeared shown as follows: NMR (C_6D_6) ^{1}H: 6.30 (s, 2H), 4.06 (s, 6H), 1.57 (vt, N = 14.6, 36H), 1.36 (s, 18H), -17.2 (t, $J_{P\text{-}H}$ = 13.6 Hz, $J_{Pt\text{-}H}$ = 1167.4 Hz, 1H); ^{31}P{^{1}H}: 46.1 (s, $J_{Pt\text{-}P}$ = 2827.3 Hz) (resonances for complex **D**). Ratio of **12b** to **D** to **2b** was 1:0.88:0.85 which was

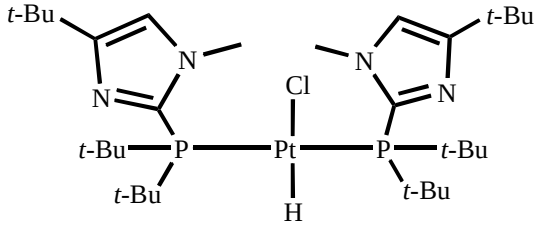

D

determined by the integrals of the corresponding proton resonances. The reaction was stopped after 10 d and the solid residue from concentration of the reaction mixture was recrystallized by first dissolving it in hexane at room temperature, then chilling at –50^{o}C. No pure crystals were isolated.

Preparation of (η^2-P,N-di-*tert*-butyl-imidazol-2-ylphosphine)(η^1-P-di-*tert*-butyl-imidazol-2-ylphosphine)Pt(Cl) (16). In a reaction vial, complex [**15**-Cl]$^{+}$[Cl]$^{-}$ was weighed (71.4 mg, 0.103 mmol), then triethylamine (10.4 mg, 0.103 mmol) was added followed by the addition of dry and deoxygenated methanol (1.5 mL). White precipitate started to form and reaction mixture was allowed to stir at room temperature in the glovebox. After 24 h, reaction was stopped and white precipitate was removed by filtration, the solvent of the filtrate was removed and complex **16** was obtained as white solid (45.1 mg, 67%). NMR (C_6D_6) ^{1}H: 9.12 (br s, 1H), 7.18 (s, 1H), 7.00 (s, 1H), 6.22 (s, 1H), 5.56 (d, 2.2, 1H), 1.58 (d, 14.8), 1.48 (d, 15.4); ^{31}P {^{1}H}: 27.9 (d, $J_{P\text{-}P\text{-}trans}$ = 377.9, $J_{Pt\text{-}P}$ = 2683.9), 13.1 (d, $J_{P\text{-}P\text{-}trans}$ = 377.5, $J_{Pt\text{-}P}$ = 2038.3).

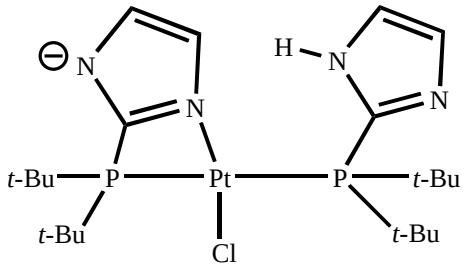

16

Reaction of complex [15-Cl]$^{+}$[Cl]$^{-}$ with triethylsilane ($HSiEt_3$). Complex [**15**-Cl]$^{+}$[Cl]$^{-}$ (46.0 mg, 0.067 mmol) was dissolved in CD_3OD in J-Young NMR tube, then triethylsilane (7.28 mg, 0.063 mmol) was added to the NMR tube via syringe. NMR tube was heated at 60 ^{o}C in the oil bath. After 10 d,

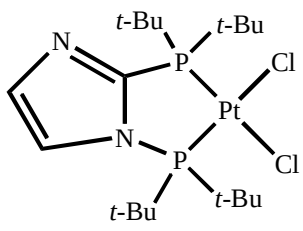

17

the NMR tube was removed from the heating source and the colorless crystals on the bottom of the NMR tube were isolated and washed with CH_3OH twice then dried on vacuum line. The colorless crystals (complex **17**) obtained were not soluble in C_6D_6, but NMR data were collected in $CDCl_3$. NMR ($CDCl_3$) ^1H: 7.83 (t, 16.4, 1H), 7.50 (s, 1H), 1.58 (d, 16.0, 36H); $^{31}P\{^1H\}$: 97.8 (s, $J_{Pt\text{-}P}$ = 3863.7), 35.8 (s, $J_{Pt\text{-}P}$ = 3352.4).

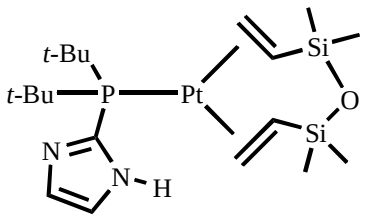

E

NMR data for intermediate E. NMR (C_6D_6) ^1H: 9.35 (s, 1H), 7.29 (s, 1H), 6.56 (s, 1H), 2.44-2.74 (m, 6H), 1.28 (d, 6.4, 18H), 0.60 (s, 6H), -0.06 (s, 6H); $^{31}P\{^1H\}$: 47.7 (s, $J_{Pt\text{-}P}$ = 3467.4).

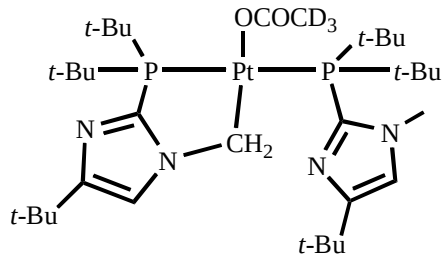

18

NMR data for complex 18. NMR (CD_3COOD) ^1H: 7.30 (s, 1H), 6.83 (s, 1H), 4.26 (s, $J_{Pt\text{-}H}$ = 46.2 Hz, 2H), 4.01 (s, 3H), 1.29 (s, 18H), 1.43 (d, 14.6, 36H); $^{31}P\{^1H\}$: 88.5 (d, $J_{P\text{-}P\text{-}trans}$ = 346.2 Hz, $J_{Pt\text{-}P}$ = 2799.9 Hz), 42.6 (d, $J_{P\text{-}P\text{-}trans}$ = 346.2 Hz, $J_{Pt\text{-}P}$ = 2875.8 Hz).

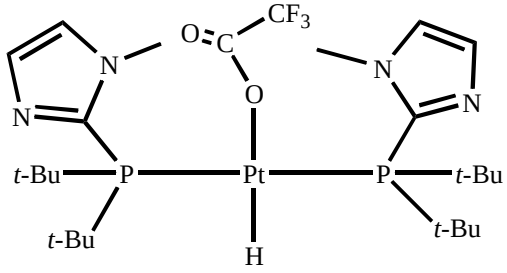

21a

Preparation of trans-bis(di-*tert*-butyl-1-methylimidazol-2-ylphosphine)Pt(H)(CF_3COO) (21a). Bis(di-*tert*-butyl-1-methyl-imidazol-2-yl-phosphine)Pt(0) complex **12a** (63.6 mg, 0.10 mmol) was weighed in a clean vial containing a magnetic stir bar, and trifluoroacetic acid (11.2 mg, 0.10 mmol) was

added to the reaction vial followed by the addition of dry and deoxygenated benzene (1 mL). The resulted colorless solution was allowed to stir at room temperature, after 0.5 h, solvent was removed and the crude solid was recrystallized by diffusing hexane into a toluene solution, the colorless crystals were separated from the supernant, washed with cold hexane and dried to give pure **21a** (44.9 mg, 59%). NMR (C_6D_6) ^{1}H : 7.21 (s, 2H), 6.51 (s, 2H), 4.07 (s, 6H), 1.45 (vt, *N* = 15.0, 36H), -23.22 (t, $J_{P\text{-}H}$ = 14.5, $J_{Pt\text{-}H}$ = 1176.8); ^{13}C {^{1}H}: 139.6 (vt, *N* = 66.5), 130.5 (vt, *N* = 9.9), 125.0 (s), 39.1 (vt, *N* = 27.9), 37.0, 30.5 (vt, *N* = 5.76) (peaks for CF_3COO unit not observed due to low density or overlap with solvent resonances); ^{31}P{^{1}H}: 45.3 (s, $J_{Pt\text{-}P}$ = 2884.7). Anal. Calcd. For $C_{26}H_{47}F_3N_4O_2P_2Pt$ (761.71): C, 41.00; H, 6.22; N, 7.36. Found: C, 40.02; H, 5.78; N, 6.77. IR (C_6D_6): 2965 (m), 2298 (w), 1712 (s) cm^{-1}.

Preparation of (di-*tert*-butyl-imidazol-2-ylphosphine)Pt(H)(OH) (29). To Pt(II) complex **13** (63 mg, 0.10 mmol) in a vial was added dry and degassed benzene (1 mL) followed by water (43.2 mg, 2.04 mmol). The mixture was sonicated and resulted in an emulsion. After 15 min, the shaking was stopped and hexane was then allowed to slowly diffuse into benzene solution. Colorless crystals formed and some of them were packed in hexane and sent for X-ray diffraction study. The rest of the crystals were washed with hexane and dried on a vacuum line. NMR study of the dry crystals showed the presence of a mixture of

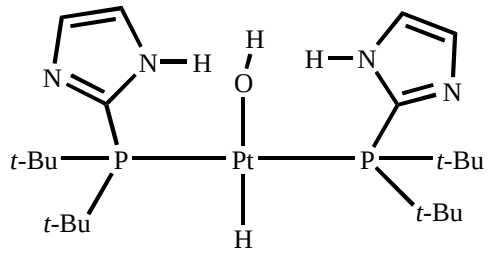

29

product **29** and starting complex **13** in a ratio of 40:60. Because a mixture was present, no elemental analysis was obtained, nor was yield calculated.

General procedure for reactivity studies. In a J-Young tube, complex **12a** (32 mg, 0.05 mmol) or **12b** (38 mg, 0.05 mmol) or **13** (31 mg, 0.05 mmol) was dissolved in C_6D_6 (1 mL). Stock solutions of CH_3COOH, CF_3COOH, PhOH and CH_3OH was prepared in C_6D_6, then they were added to the J-Young tube via syringe. Reactions were carried out at room temperature in most cases, or when elevated temperature was needed, using a temperature-controlled oil bath as the heating source. Reactions were monitored by NMR spectroscopy and ratios were determined by the integrals in the NMR spectra.

NMR data of complexes 19-29:

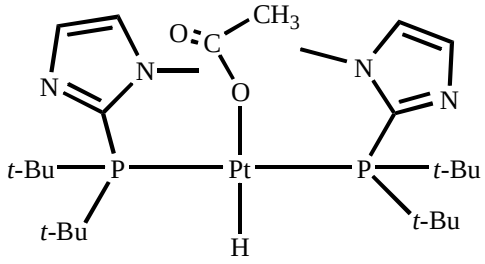

19a

Trans-bis(di-*tert*-butyl-1-methylimidazol-2-ylphosphine)Pt(H)(CH_3COO) (19a). NMR(C_6D_6) ^{1}H: 7.21 (s, 2H), 6.63 (s, 2H), 4.19 (s, 6H), 1.81 (s, 3H), 1.48 (vt, N = 14.6, 36H), -22.60 (t, J_{P-H} = 14.6, J_{Pt-H} = 1077.4, 1H); ^{31}P{^{1}H}: 42.6 (s, J_{Pt-P} = 2949.7).

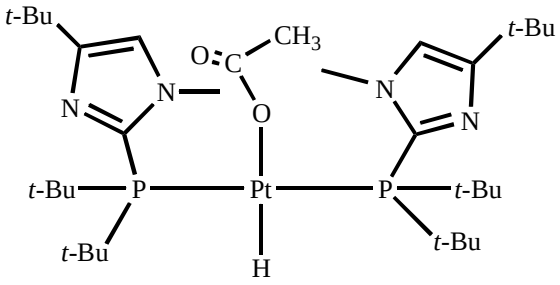

19b

Trans-bis(di-*tert*-butyl-1-methyl-4-*tert*-butyl-imidazol-2-ylphosphine)Pt(H)(CH_3COO) (19b). NMR(C_6D_6) ^{1}H: 6.47 (s, 2H), 4.20 (s, 6H), 1.84 (s, 3H), 1.49 (vt, *N* = 14.8, 36H), 1.37 (s, 18H), -22.73 (t, $J_{P\text{-}H}$ = 14.8, $J_{Pt\text{-}H}$ = 1089.8, 1H); ^{31}P{^{1}H}: 42.0 (s, $J_{Pt\text{-}P}$ = 2940.3).

{(η^2-P,N-di-*tert*-butyl-1-methylimidazol-2-ylphosphine)(η^1-P-di-*tert*-butyl-1-methylimidazol-2-ylphosphine)Pt(H)}$^+$[CH_3COO]$^-$ (20a). NMR(C_6D_6) ^{1}H: 7.58 (s, 1H), 7.27 (s, 1H), 7.00 (s, 1H), 6.14 (s, 1H), 3.95 (s, 3H), 3.81 (s, 3H), 1.73 (s, 3H), 1.30 (d, *J* = 15.0, 18H), 1.11 (d, *J* = 16.0, 18H), -20.09 (d, $J_{P\text{-}H}$ = 19.0, $J_{Pt\text{-}H}$ = 1262.8, 1H); ^{31}P{^{1}H}: 52.5 (d, $J_{P\text{-}P\text{-}trans}$ = 321.8, $J_{Pt\text{-}P}$ = 2348.2), 43.9 (d, $J_{P\text{-}P\text{-}trans}$ = 321.8, $J_{Pt\text{-}P}$ = 2938.8).

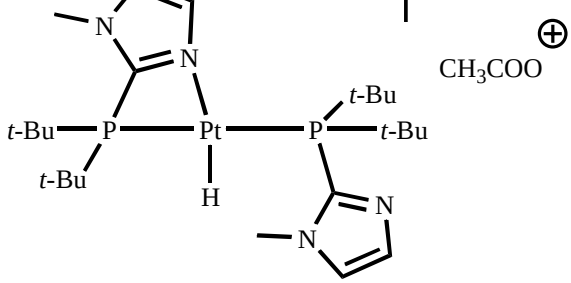

20a

Trans-bis(di-*tert*-butyl-1-methylimidazol-2-ylphosphine)Pt(H)(CF_3COO) (21a). %). NMR (C_6D_6) ^{1}H : 7.21 (s, 2H), 6.51 (s, 2H), 4.07 (s, 6H), 1.45 (vt, *N* = 15.0, 36H), -23.22 (t, $J_{P\text{-}H}$ = 14.5, $J_{Pt\text{-}H}$ = 1176.8); ^{13}C {^{1}H}: 139.6 (vt, *N* = 66.5), 130.5 (vt, *N* =

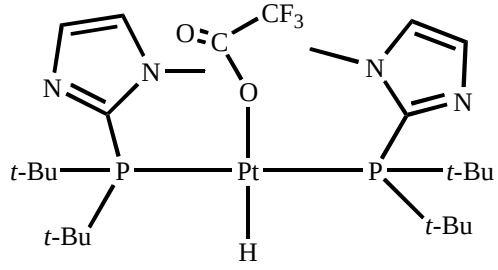

21a

9.9), 125.0 (s), 39.1 (vt, *N* = 27.9), 37.0, 30.5 (vt, *N* = 5.76, J_{Pt-C} = 21.4) (peaks for CF_3COO unit not observed due to low density or overlap with solvent resonances); $^{31}P\{^1H\}$: 45.3 (s, J_{Pt-P} = 2884.7).

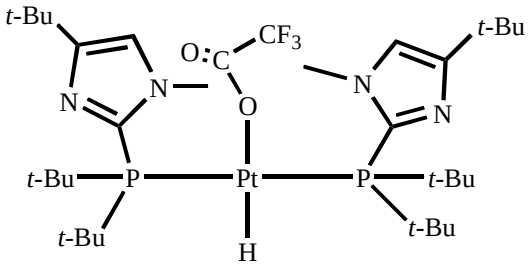

21b

Trans-bis(di-*tert*-butyl-1-methy-4-*tert*-butyl-limidazol-2-ylphosphine)Pt(H)(CF_3COO) (21b). NMR(C_6D_6) ^1H: 6.40 (s, 2H), 4.10 (s, 6H), 1.46 (vt, *N* = 14.8, 36H), 1.35 (s, 18H), -22.34 (t, $^2J_{P-H}$ = 14.8, J_{Pt-H} = 1089.8, 1H); $^{31}P\{^1H\}$: 44.4 (s, J_{Pt-P} = 2876.3).

{(η^2-P,N-di-*tert*-butyl-1-methylimidazol-2-ylphosphine)(η^1-P-di-*tert*-butyl-1-methylimidazol-2-ylphosphine)Pt(H)}$^+$[CF_3COO]$^-$ (22a). NMR (CD_2Cl_2) ^1H:

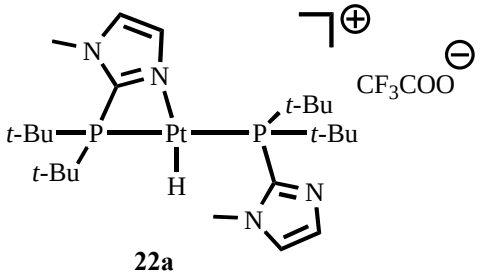

22a

7.47 (s, 1H), 7.31 (s, 1H), 7.15 (s, 1H), 6.42 (s, 1H), 4.03 (s, 3H), 4.00 (s, 3H), 1.46-1.49 (m, 18H), 1.42-1.45 (m, 18H), -20.31 (d, J_{P-H} = 19.0, J_{Pt-H} = 1287.8); ^{13}C $\{^1H\}$: 160.0, 151.9, 139.3. 138.7, 131.0 (d, 9.2), 129.3 (d, 12.9), 125.6, 125.1, 39.1, 38.9, 36.9, 36.6, 35.3 (d, 15.5), 30.2; ^{31}P $\{^1H\}$: 52.7 (d, $J_{P-P-trans}$ = 321.8, J_{Pt-P} = 2352.1), 41.82 (d, $J_{P-P-trans}$ = 322.8, J_{Pt-P} = 2985.9). Anal. Calcd. For $C_{26}H_{47}F_3N_4O_2P_2Pt$ (761.71): C, 41.00; H, 6.22; N, 7.36. Found: C, 44.80; H, 6.83; N, 8.66. IR (CD_2Cl_2): 2965 (m), 1687 (s) cm^{-1}.

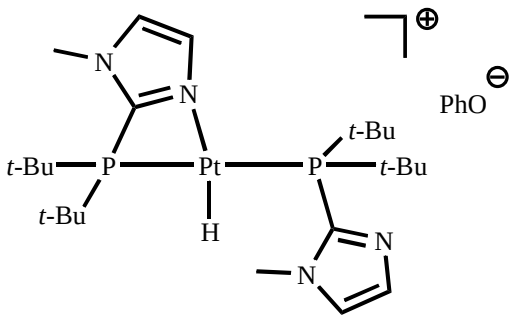

23a

{(η^2-P,N-di-*tert*-butyl-1-methylimidazol-2-ylphosphine)(η^1-P-di-tert-butyl-1-methylimidazol-2-ylphosphine)Pt(H)}$^+$[PhO]$^-$ (23a). NMR(C_6D_6) ^{1}H: 7.22 (s, 2H), 6.97-7.16 (m, 4H), 6.90 (s, 1H), 6.74 (t, 7.0, 1H), 5.95 (s, 1H), 3.51 (s, 3H), 3.45 (s, 3H), 1.24 (d, 15.0, 18H), 0.91 (d, 16.0, 18H), -20.38 (d, $J_{P\text{-}H}$ = 19.0, $J_{Pt\text{-}H}$ = 1273.0, 1H); ^{31}P{^{1}H}: 53.2 (d, $J_{P\text{-}P\text{-}trans}$ = 321.4, $J_{Pt\text{-}P}$ = 2342.7), 43.7 (d, $J_{P\text{-}P\text{-}trans}$ = 320.8, $J_{Pt\text{-}P}$ = 2957.7).

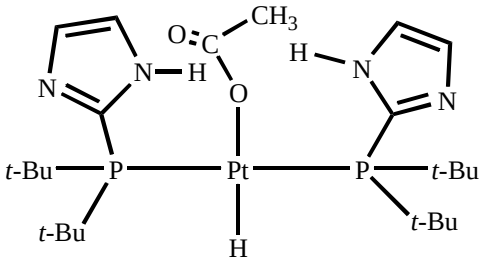

24

Trans-bis(di-*tert*-butyl-imidazol-2-ylphosphine)Pt(H)(CH$_3$COO) (24). NMR(C_6D_6) ^{1}H: 12.91 (br s, 2H), 7.40 (s, 2H), 7.00 (s, 2H), 1.55 (s, 3H), 1.43 (vt, *N* = 15.0, 36H), -22.81 (t, $J_{P\text{-}H}$ = 16.5, $J_{Pt\text{-}H}$ = 1094.8, 1H); ^{31}P{^{1}H}: 50.5 (s, $J_{Pt\text{-}P}$ = 2939.3).

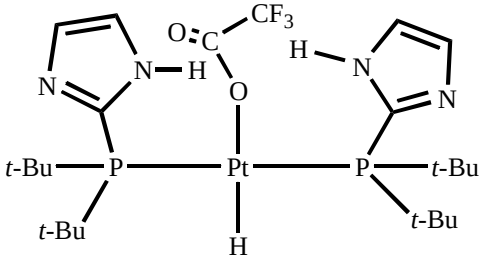

25

Trans-bis(di-*tert*-butyl-imidazol-2-ylphosphine)Pt(H)(CF$_3$COO) (25). NMR(C_6D_6) ^{1}H: 12.21 (br s, 2H), 7.28 (s, 2H), 7.04 (s, 2H), 1.46 (vt, *N* = 15.2, 36H), -23.30 (t, $J_{P\text{-}H}$ = 15.0, $J_{Pt\text{-}H}$ = 1209.8, 1H); ^{31}P{^{1}H}: 51.5 (s, $J_{Pt\text{-}P}$ = 2892.7).

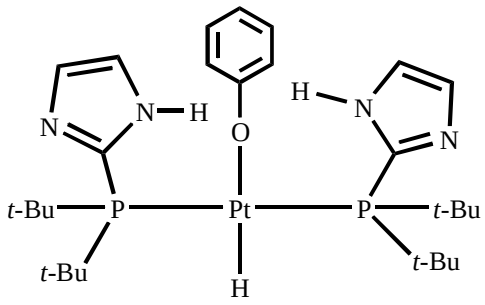

27

Trans-bis(di-*tert*-butyl-imidazol-2-ylphosphine)Pt(H)(PhO) (27). NMR(C_6D_6) ^{1}H: 10.27 (br s, 2H), 7.44 (s, 2H), 6.84 (s, 2H), 6.63-7.23 (m, 5H), 1.42 (vt, *N* = 15.0, 36H), -22.71 (t, $J_{P\text{-}H}$ = 16.5, $J_{Pt\text{-}H}$ = 1104.4, 1H); ^{31}P{^{1}H}: 49.4 (s, $J_{Pt\text{-}P}$ = 2896.6).

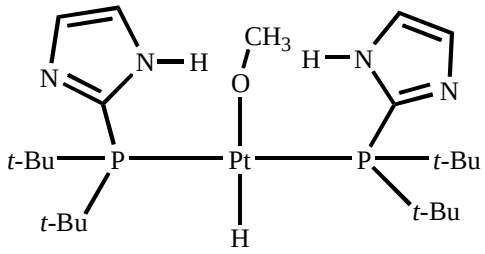

28

Trans-bis(di-*tert*-butyl-imidazol-2-ylphosphine)Pt(H)(CH$_3$O) (28). NMR(C_6D_6) ^{1}H: 10.45 (br s, 2H), 7.48 (s, 2H), 7.03 (s, 2H), 3.43 (s, $J_{Pt\text{-}H}$ = 25.6, 3H), 1.42 (vt, *N* = 14.5, 36H), -22.10 (t, $J_{P\text{-}H}$ = 16.4, $J_{Pt\text{-}H}$ = 1035.2, 1H); ^{31}P{^{1}H}: 48.0 (s, $J_{Pt\text{-}P}$ = 2875.3).

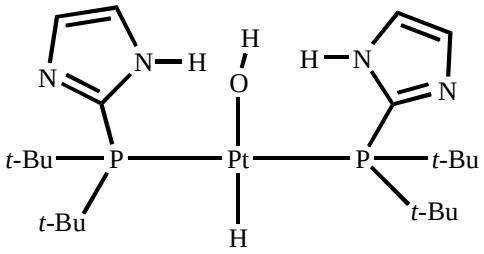

29

Trans-bis(di-*tert*-butyl-imidazol-2-ylphosphine)Pt(H)(OH) (29). NMR(C_6D_6) ^{1}H: 10.51 (br s, 2H), 7.42 (s, 2H), 7.00 (s, 2H), 1.41 (vt, *N* = 15.0, 36H), -21.08 (t, $J_{P\text{-}H}$ = 15.5, $J_{Pt\text{-}H}$ = 1031.9, 1H); ^{31}P{^{1}H}: 48.3 (s, $J_{Pt\text{-}P}$ = 2865.9).

C. Results and Discussion

Reaction between ligands 2a, 2b and $Pt(cod)_2$. The phosphine ligands, 2a and 2b, when treated with platinum(0) complexes such as bis(1,5-cyclooctadiene)platinum [$Pt(cod)_2$] or tris(2-norbornene)platinum complex [$Pt(C_7H_{10})_3$] resulted in products with similar structures. As shown in Figure 3.01, ligand exchange reactions took place at room temperature and a new Pt(0) complex 12a and 12b with two bulky imidazolyl phosphine ligands were made in a moderate yield [66% for complex 12a when $Pt(cod)_2$ was used as Pt(0) precursor] in 1 d. Although the efforts to isolate complex 12b in crystalline form were not successful due to its solubility in a variety of solvents, monitoring the reaction by ^{1}H and $^{31}P\{^{1}H\}$ NMR suggested that the complex 12b was the only product which was made by this reaction and all the NMR data were comparable to those of complex 12a which was successfully isolated and fully characterized by NMR and X-ray crystallography. Reactions using tris(2-norbornene)platinum complex as Pt(0) precursor gave comparable results.

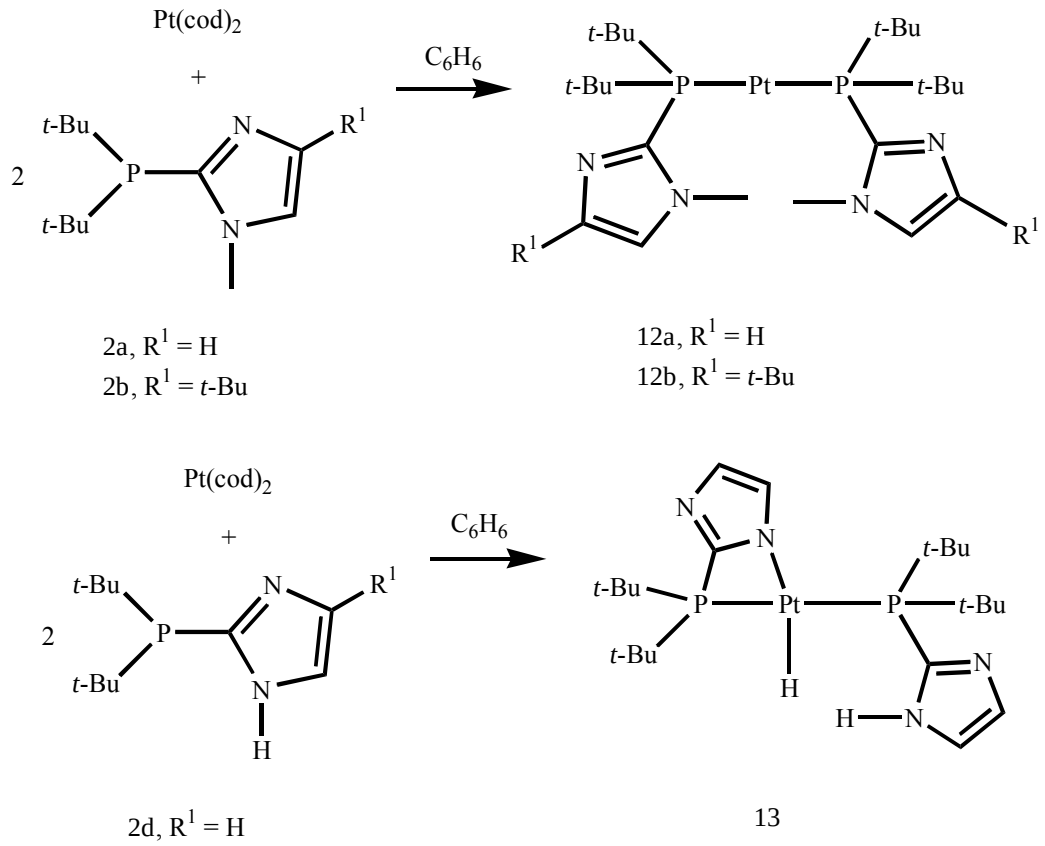

Figure 3.01. Reactions between 2 and $Pt(cod)_2$.

Elemental analysis for complex 12a was consistent with a species of formula PtL_2. NMR and IR spectroscopic data for 12a were similar to those of Pd analog 3a in Chapter 2 but the differences were that $^{31}P\{^1H\}$ NMR spectra exhibited a more downfield sharp singlet (δ 55.7 ppm for 12a vs 32.4 ppm for 3a) with Pt satellites ($J_{Pt\text{-}P}$ = 4247.1 Hz). As in the Pd case, the protons of the N-methyl groups resonated as sharp singlets about 1.2 ppm downfield of those in the free ligand 2a.

Although elemental analysis for 12a along with the NMR spectroscopic data were consistent with PtL_2 species, further characterization such as X-ray diffraction was required to confirm the exact structure. The X-ray crystal structure of 12a (shown in Figure 3.02) is similar to that of Pd analog 3a. Complex 12a also adopted a nearly linear configuration (P-Pt-P angle, 174.7^o), and no agostic interaction was observed either. In general, a hydrogen involved in an agostic interaction shows some spectral data resembling those of a metal hydride.[51-53] Evidence against agostic interactions includes (1) the 1.2 ppm downfield ^{1}H NMR chemical shift of the N-methyl protons on complexation of the ligand, (2) the fact that the resonance appeared as a singlet without satellites indicating there was no Pt-H coupling between the Pt atom and the N-methyl protons, and (3) in the infrared, normal C-H stretching absorptions, between 2865 to 2942 cm^{-1}. Again, the orientations seen for the imidazole rings may be a way for the system to avoid steric interactions between the two bulky tert-butyl groups on the phosphorus atom and the N-methyl group on the imidazole. A similar orientation was seen by Otsuka et al in their crystal structure of Pt[PPh(*t*-Bu)$_2$]$_2$.[54] As a result, there was no chance for the unsubstituted N atom to approach or even coordinate to the center Pt atom. The metal-P distances in 12a and 3a are the same within 0.03 Å and the P-M-P angles are differentiated only by 0.6 degree.[55]

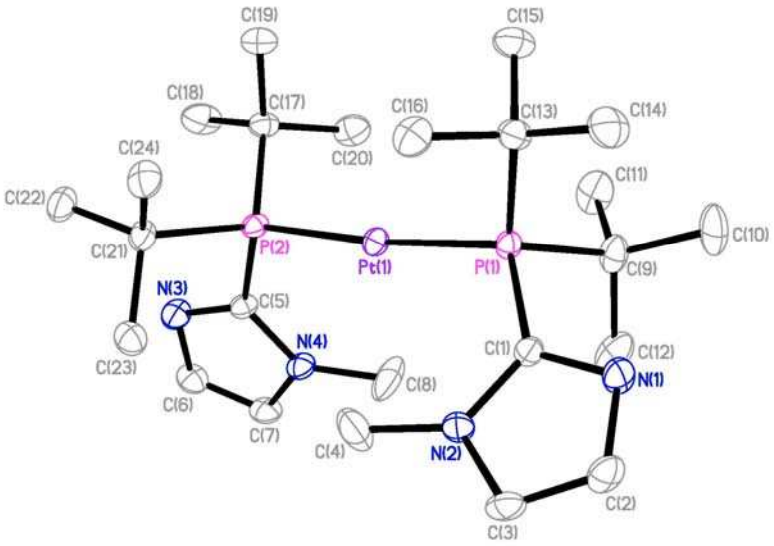

Figure 3.02. X-ray crystal structure of 12a.

Table 3.01. Selected bond lengths (Å) and angles (deg) for complex 12a.

	Bond Lengths (Å)		Bond Angles (deg)
Pt(1)-P(1)	2.2543(6)	P(1)-Pt-P(2)	174.69(2)
Pt(1)-P(2)	2.2468(6)	C(1)-P(1)-Pt(1)	117.59(8)
P(1)-C(1)	1.820(2)	C(5)-P(2)-Pt(1)	116.54(8)
P(2)-C(5)	1.833(2)		

Reaction between ligand 2d and $Pt(cod)_2$. Unlike the above reactions, when the ligand 2d, bearing a hydrogen at N-1 of the imidazole ring instead of a methyl group, was treated with $Pt(cod)_2$, a hydrido-Pt(II) complex 13 was generated as the result of *N-H activation* (yield 71%) (Figure 3.01). Reaction using tris(2-norbornene)platinum complex as Pt(0) precursor gave comparable results.

The NMR spectroscopic data for 13 were remarkably different from that for complex 12a. The fact that there were two doublets with Pt satellites ($J_{Pt\text{-}P}$ = 2940.3 and 2341.2 Hz) on the $^{31}P\{^{1}H\}$ NMR spectra suggested that the two phosphine ligands coordinated to the Pt atom in different modes and coupled to each other ($J_{P\text{-}P\text{-}trans}$ = 327.8 Hz). Interestingly, although the ^{1}H resonance for the atoms of the alkyl substituents on phosphorus appeared as virtual triplets, $^{13}C\{^{1}H\}$ resonances for the same group were doublets, one of the carbon resonances for C-2 of the imidazol-2-yl groups appeared as a doublet at δ 155.8 ppm with J = 75.4 Hz, the other one appeared as a doublet of doublets at δ 139.7 ppm with J = 63.4 and 3.9 Hz. There are two sets of resonances with similar chemical shifts for the corresponding protons and carbons on the two phosphine ligands except that there was only one resonance at δ 10.57 ppm which integrated as one proton (N-H). Most importantly, a resonance appeared as a doublet (J = 20.5 Hz) far upfield at δ -19.17 ppm with satellites ($J_{Pt\text{-}H}$ = 1169.3 Hz). This doublet was most likely arising from a Pt-hydride.

The X-ray data of the complex 13 (Figure 3.03) showed that this product is indeed different from complex 12a, although the only difference between the two

ligands 2a and 2d is whether the N atom is substituted with a methyl group. The three angles around Pt center added up to 353.5^{o}, indicating a square planar geometry with distortion. The two phosphine ligands are located trans to each other, with one phosphine ligand chelating to the Pt center with an anionic imidazole N atom. The angle N-Pt-P(1) is small (68.18^{o}) because of the four-membered chelate ring. The Pt-P bond lengths are significantly longer (about 0.04 Å) than those of complex 12a, consistent with increased steric demand about the metal center and reduced back-bonding to the phosphines. The hydride was not located but the N-H group of the uncoordinated imidazole ring was pointed towards the vacant site of the Pt atom. According to the ^{1}H NMR spectrum, a metal-hydride exists and it is not surprising that the small hydride ligand next to the metal center was not detected. The square-planar geometry around the Pt atom indicates a Pt(II) center. Based on all these data along with elemental analysis results, a hydrido-Pt(II) complex is most likely to be the actual structure of the complex 13.

There are two other possible structures for 13, shown below. The two phosphine ligands could be both neutral (13') or one phosphine ligand could be anionic and the other cationic (13"), but in both cases, no hydride is on Pt.

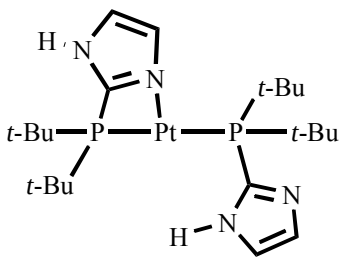

13'

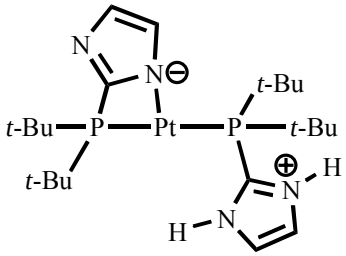

13''

DFT calculations showed that complex 13 has the lowest ground state energy among three structures, which lends additional support to the assignment of hydrido-Pt(II) structure 13 to the product.

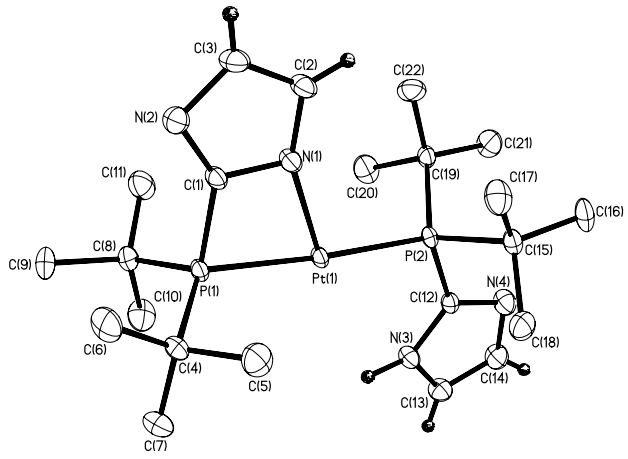

Figure 3.03. X-ray crystal structure of 13.

Table 3.02. Selected bond lengths (Å) and angles (deg) for complex 13.

	Bond Lengths (Å)		Bond Angles (deg)
Pt(1)-P(1)	2.2930(9)	P(1)-Pt-P(2)	176.05(3)
Pt(1)-P(2)	2.2838(8)	N(1)-Pt-P(1)	68.18(8)
Pt(1)-N(1)	2.158(3)	N(1)-Pt-P(2)	109.27(8)
P(1)-C(1)	1.784(4)	C(1)-P(1)-Pt(1)	84.84(12)
P(2)-C(12)	1.811(4)	C(12)-P(2)-Pt(1)	113.63(13)

Alternative routes of making Pt complexes.

Route 1. Reduction of Pt(II) complexes.

Synthesis of $Cl_2Pt(L)_2$. Although synthesis of $Pt(cod)_2$ is well-described,[48] the yields are not always high and certain reagents used are expensive. Therefore alternative routes were sought to make the Pt complexes described above. One route would be to first prepare a Pt(II) complex $Cl_2Pt(L)_2$, which bears two phosphine ligands and then reduce it to a Pt(0) complex using reducing reagents such as sodium amalgam.

The first Pt(II) precursor used was common and readily available $Cl_2Pt(cod)$ which was treated with two equivalents of phosphine ligands 2a, 2b and 2d in benzene. Reactions were monitored by ^{1}H and $^{31}P\{^{1}H\}$ NMR. It seemed that the ligand exchange reaction took place at a relatively slow rate, for example, for ligand 2b, reaction required higher temperature (80 ^{o}C) and 7 days to completely convert the

starting Pt complex to the desired product $Cl_2Pt(L)_2$, although for ligand 2a, no reaction was detected by NMR even the reaction temperature was raised to 100 ^oC. For ligand 2d, after being heated at 85 ^oC for 14 days, reaction made one major product with symmetrical structure along with unreacted ligand and minor products. Therefore, it seems that $Cl_2Pt(cod)$ is an unsuitable precursor to make $Cl_2Pt(L)_2$ when L is as bulky as the ligands used here.

Instead, another common Pt(II) precursor K_2PtCl_4 was considered. According to the literature procedure used for other phosphines,[56] ligands 2a, 2b, 2d and 2e were treated with potassium tetrachloroplatinate in a mixture of alcohol and water (Figure 3.04). With stirring, the red color of potassium tetrachloroplatinate faded and a white precipitate started to form. The white precipitatate was then isolated by filtration and identitified by NMR to be the desired product. The lower temperature (room temperature), shorter reaction period (1-2 d) and moderate yield (60-72%) made this route of making Pt(II) complex with two phosphine ligands valuable and K_2PtCl_4 a better precursor compared with $Cl_2Pt(cod)$.

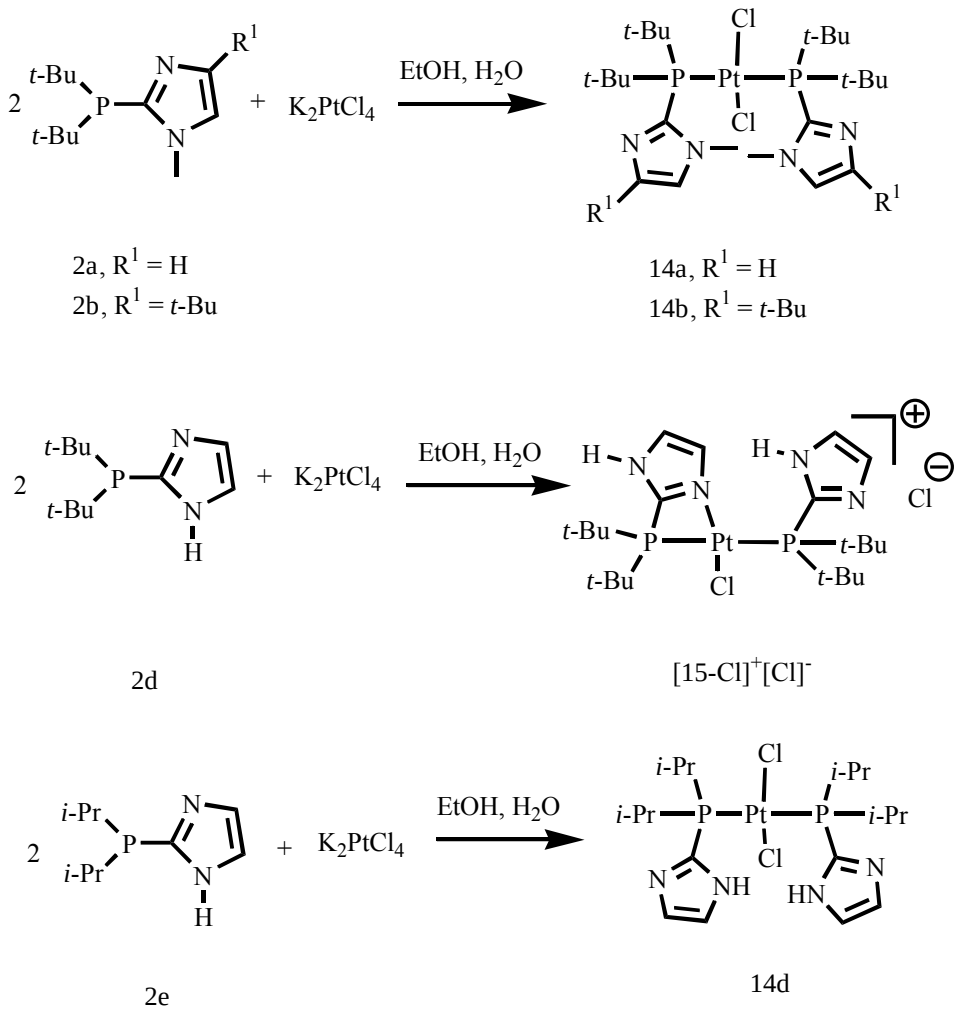

Figure 3.04. Reaction between 2 and K_2PtCl_4 in EtOH and water.

Comparison and characterization of products from K_2PtCl_4 in methanol and water. The white product 14a isolated from reaction of ligand 2a with K_2PtCl_4 in methanol and water has very limited solubility in benzene, but is quite soluble in chloroform. This is expected because of the presence of the chloride ligands in the complex. In the ^1H NMR spectrum, the resonance for *tert*-butyl group on the

phosphine ligand appeared at δ 1.90 ppm as a virtual triplet (N = 13.8 Hz). This fact along with the fact that only sharp singlets were found in the $^{31}P\{^{1}H\}$ NMR spectrum indicates that the two phosphine ligands are chemically equivalent and located trans to each other. It is noteworthy to point out that in ^{1}H NMR spectra, there were two sets of resonances for each proton such as the protons on the imidazole ring and the protons on the N-methyl group of the imidazole, and two singlets with exactly the same Pt-P coupling constants (J_{Pt-P} = 2401.2 Hz) were also found in $^{31}P\{^{1}H\}$ NMR spectrum. It is not hard to interpret these unusual NMR data if the size of the phosphine ligands are considered. The environment around Pt atom is crowded because of the two bulky *tert*-butyl groups on the phosphine ligand along with two chloride ligands and the free rotation along the P-Pt-P axis is limited, hence interconversion of two rotamers is slow on the NMR time scale. This phenomenon was also reported by others too.[57]

The structure of the product 14b from reaction of ligand 2b is similar to that of complex 14a described above, conclusions supported by the similar ^{1}H NMR, $^{31}P\{^{1}H\}$ NMR spectral data, including similar coupling constants.

Unlike complexes 14a and 14b, the product (complex $[15\text{-Cl}]^{+}[Cl]^{-}$) from the reaction of 2d was neither soluble in benzene nor chloroform, whereas it was only soluble in a protic polar solvent such as methanol. In this solvent, the two doublets appeared in the $^{31}P\{^{1}H\}$ NMR spectrum suggested that there were two different phosphine ligands trans to each other ($J_{P-P-trans}$ = 375.8 Hz) on the Pt atom. In the ^{1}H NMR spectrum, three resonances appeared at δ 7.37 ppm (d, 0.8, 2H), 7.16 ppm (d, 1.6, 1H), 5.02 ppm (t, 3.8, J_{Pt-H} = 14.8 Hz, 1H) were found, these resonances were

assigned to the four protons in the imidazole ring in both of the ligands, which also indicated that the two phosphine ligands are not equivalent and the unusual chemical shift (δ 5.02 ppm) and coupling to Pt (J_{Pt-H} = 14.8 Hz) suggested a closer position of this proton to the Pt atom. Based on the different solubility of $[15\text{-Cl}]^+[Cl]^-$ from that of complexes 14a, 14b, the spectral data showing two different phosphorus and our previous experience,[55] an ionic complex with unsymmetrical structure was proposed (Figure 3.04), in which one phosphine ligand is chelating through a N atom since the N atom in the imidazole ring is a readily available ligand and chloride anion leaves the Pt to become the counterion.

In order to confirm the structure, an X-ray diffaraction study was done. An ion exchange reaction took place when $[15\text{-Cl}]^+[Cl]^-$ was treated with KPF_6 in methanol and resulted in the formation of another ionic complex $[15\text{-Cl}]^+[PF_6]^-$. The crystals of $[15\text{-Cl}]^+[PF_6]^-$ were grown in diethyl ether/dichloromethane and the ORTEP diagram of the structure is shown in Figure 3.05.

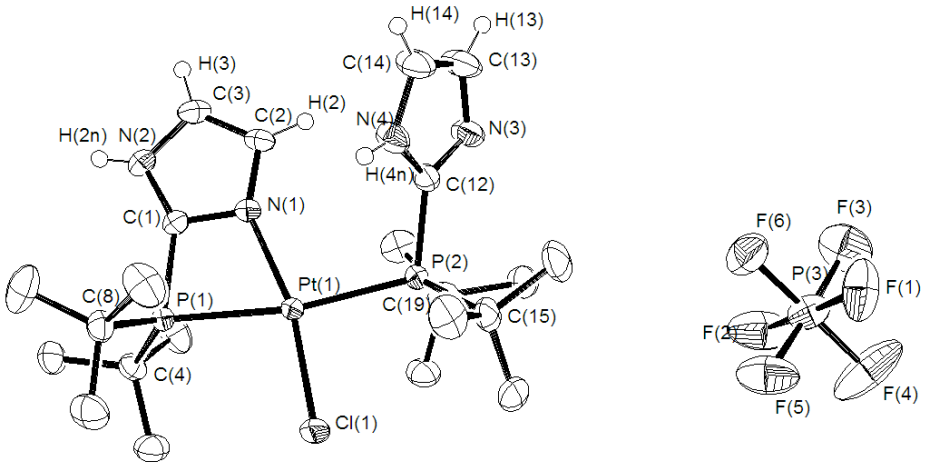

Figure 3.05. Molecular structure of $[15\text{-Cl}]^{+}[PF_6]^{-}$.

Table 3.03. Selected bond lengths (Å) and angles (deg) for complex $[15\text{-Cl}]^{+}[PF_6]^{-}$.

	Bond Lengths (Å)		Bond Angles (deg)
Pt(1)-P(1)	2.335	P(1)-Pt(1)-Cl(1)	96.98
Pt(1)-P(2)	2.312	Cl(1)-Pt(1)-P(2)	94.67
Pt(1)-N(1)	2.041	P(2)-Pt(1)-N(1)	98.64
Pt(1)-Cl(1)	2.291	N(1)-Pt(1)-P(1)	69.71
P(1)-C(1)	1.806	P(1)-Pt(1)-P(2)	167.45
P(2)-C(12)	1.807	N(1)-Pt(1)-Cl(1)	166.67

As shown in Figure 3.05, the Pt(II) center adopts square planar geometry, with the four angles around Pt center adding up to 359.8°. The strained four-member

chelating ring was the reason for the significantly smaller N-Pt-P angle (69.7°). The bond length between Pt and the chelating N atom is 2.041 Å, which is 0.117 Å shorter than that in the hydrido-Pt(II) complex 13, a difference which could be due to the different trans ligand (chloride vs. hydride) and formal charge on the chelating N atom (negative vs. neutral). Given results elsewhere in this thesis, for example the structure of 13, it is rather surprising that the non-chelating imidazole ring is not involved in making hydrogen bond to the chloride ligand.

It is worthy to study the product from the reaction with ligand 2e since it has the same imidazolyl substituent as 2d does but the alkyl substituent on phosphine is the smaller isopropyl group. The white product 14e was very soluble in acetone which is different from the solubility of complex $[15\text{-Cl}]^+[\text{Cl}]^-$ and the NMR showed the structure of 14e was symmetrical. The singlet in the $^{31}\text{P}\{^1\text{H}\}$ NMR with $J_{\text{Pt-P}} = 2487.0$ Hz indicates the symmetric structure (Figure 3.04) similar to that of complex 14a and 14b, but it is also interesting to see that there is only one singlet instead of two singlets when compared to the spectra of complex 14a and 14b. This might be due to the smaller isopropyl substituent which makes enough room for the free rotation of the phosphine ligand along P-Pd-P axis. The difference in reactivity between ligand 2d and ligand 2e is significant but not surprising. In our previous study on Pd chemistry (Chapter 2 and ref. [55]), we found that a phosphine ligand tended to chelate (with loss of an anionic ligand) and produce a cationic metal fragment with strained four-membered chelate when the alkyl substituents are large *tert*-butyl groups, whereas the

phosphine ligand stayed nonchelating when the alkyl substituents are smaller isopropyl groups.

Reduction by Na/Hg. Pt(0) complexes 12a and 12b can be obtained by simply treating Pt(II) complexes 14a and 14b with reducing 1% sodium amalgam in THF. 14a and 14b can be used as they were obtained after filtration: no purification was needed and the yield for this reaction was promising (64-66%) (Figure 3.06). Therefore, this route is reliable for making Pt(0) complexes 12a and 12b compared to that using less readily available $Pt(cod)_2$.

When complex $[15\text{-}Cl]^+[Cl]^-$ was treated with 1% Na/Hg, the reaction was more complicated and several products were produced but no hydride signal was found in the ^1H NMR spectrum. No further purification was carried out to separate these products.

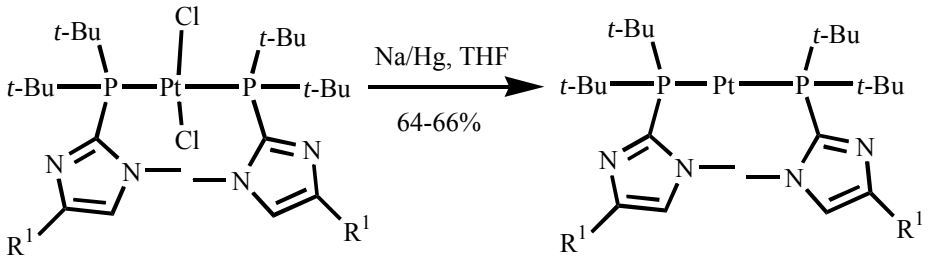

14a, R^1 = H
14b, R^1 = *t*-Bu

12a, R^1 = H
12b, R^1 = t-Bu

Figure 3.06. Formation of 12a, 12b from reduction of 14a and 14b.

For our surprise, the reaction of complex 14e with sodium amalgam was not as straight forward and clean as that of structurally similar complexes 14a and 14b. Rather, several products with symmetrical structure were made and judging from the Pt-P coupling constant, none of these complexes is the analogous Pt(0) complex with two phosphine ligands 2e. Most likely, they were partially reduced products of 14e. No further study was done to identify these compounds.

Route 2. Reaction of K_2PtCl_4 with ligand in the presence of base and alcohol at higher temperature. Following a literature procedure used to make reduced complexes,[58] another potential route was tried to make Pt(0) complexes 12 (Figure 3.07). In this route, only one reaction was involved and using sodium hydroxide as base. Protic solvent ethanol and higher reaction temperature (70 ^{o}C) was required. To our surprise, the structurally similar ligand 2a and 2b gave different results (Figure 3.07).

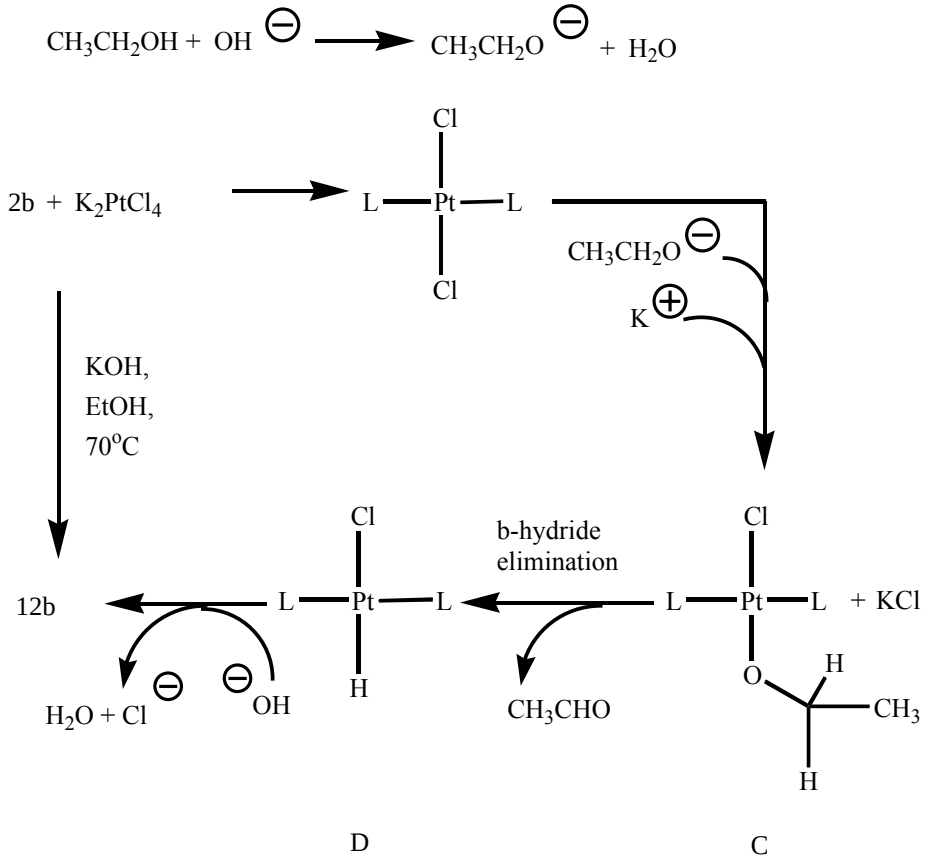

Figure 3.07. Reaction pathway of formation of 12b under basic conditions.

For ligand 2a, after 10 d, there was no reaction at all and no desired product was detected, and the ligand stayed in the solution unchanged even with heating. On the other hand, under exactly the same conditions, ligand 2b did react with base and alcohol and complex 12b was found by NMR in a yield of 36% after 2 d. However, with further heating, a new complex was found in the reaction aliquot along with complex 12b. Judging from the singlet at δ 46.1 ppm (J_{Pt-P} = 2827.3 Hz) in ^{31}P {^{1}H} NMR spectrum and triplet at δ -17.19 ppm in the ^{1}H NMR spectrum, the new complex

was assigned to be complex D (Figure 3.07). As shown in the suggested reaction pathway, the strong base extracts the proton from ethanol and the resulted ethoxide anion then displaces chloride from the Pt to result the intermediate complex C. Complex D is then produced from β-hydride elimination of ethoxide ligand in the intermediate complex C. Although the pure Pt(0) complex 12b was never isolated from complex D due to the similar amount of these two complexes in the reaction mixture, the big difference on the reactivities of ligand 2a and 2b suggested that the steric effect from the *tert*-butyl substitutent on the heterocycle imidazole ring is somehow important in this reaction.

It is not surprising that under same conditions the reaction with ligand 2d was not as predictable because of the N-H group on the imidazole ring. Several products were detected and no further characterizations were done due to the complexity of the reaction.

Because of the lack of preparative utility and generality, this synthetic route was abandoned.

In summary, the promising alternative route of making Pt(0) complexes 12a and 12b involves two steps, first reaction of the ligand with K_2PtCl_4 in H_2O and ethanol followed by reduction using Na/Hg. These two-step reactions are simple and easy to handle. Even though the yields of the reactions are moderate, relatively large amounts of Pt(0) complexes are easily made.

Route 3. Other Pt(0) precursors. A variety of reducing agents were tried besides sodium amalgam to reduce complex $[15\text{-Cl}]^+[Cl]^-$ in order to produce complex 13. However, none of the reducing agents, including formate ($K^+HCO_2^-$), hydrazine (H_2NNH_2), lithium aluminum hydride ($LiAlH_4$), triethylsilane ($HSiEt_3$) and super hydride (Et_3BHLi) gave the expected complex 13, instead, the reactions either gave many species or in some cases such as with formate or lithium aluminum hydride one of the imidazole rings in complex $[15\text{-Cl}]^+[Cl]^-$ was deprotonated and the counterion

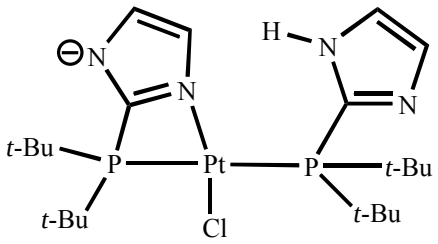

Cl^- was removed so that a neutral complex 16 was obtained. NMR data were consistent with the structure: doublets in $^{31}P\{^1H\}$ NMR showed two inequivalents phosphine ligands and they coupled to each other, four resonances in ^1H NMR for all of the four protons on imidazole ring and each integrated for one proton but only one resonance for N-H which was integrated also for one proton. The solubility of complex 16 is very different from that of complex $[15\text{-Cl}]^+[Cl]^-$, for example, complex 16 is readily soluble in nonpolar solvent such as benzene while $[15\text{-Cl}]^+[Cl]^-$ is only soluble in methanol. This suggests that complex 16 is not ionic but neutral. For characterization purposes, complex 16 was better obtained by reacting complex $[15\text{-Cl}]^+[Cl]^-$ with triethylamine.

In the case of triethylsilane ($HSiEt_3$) as reducing agent, a different product 17 was generated (Figure 3.08) and the structure was determined by X-ray diffraction study (Figure 3.09). Yield was not calculated.

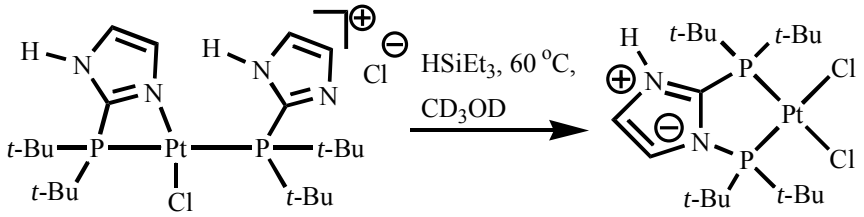

Figure 3.08. Formation of complex 17 from complex $[15\text{-Cl}]^+[Cl]^-$.

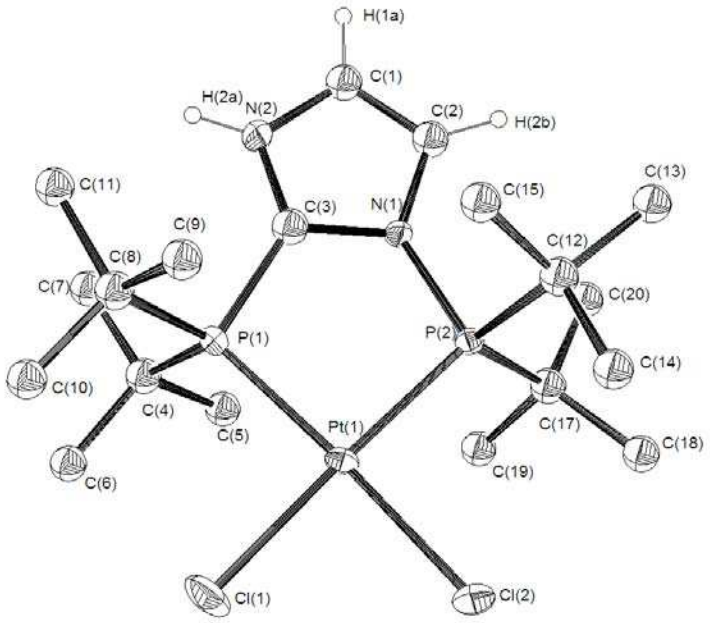

Figure 3.09. Molecular structure of complex 17.

Table 3.04. Selected bond lengths (Å) and angles (deg) for complex 17.

	Bond Lengths (Å)		Bond Angles (deg)
Pt(1)-P(1)	2.252	P(1)-Pt(1)-P(2)	90.62
Pt(1)-P(2)	2.245	P(1)-Pt(1)-Cl(1)	90.83
Pt(1)-Cl(1)	2.338	Cl(1)-Pt(1)-Cl(2)	85.93
Pt(1)-Cl(2)	2.361	Cl(2)-Pt(1)-P(2)	92.83
P(1)-C(3)	1.810	C(3)-P(1)-Pt(1)	103.40
P(2)-N(1)	1.745	N(1)-P(2)-Pt(1)	104.51

Because of the difficulty in the reduction of complex $[15\text{-Cl}]^{+}[Cl]^{-}$, we turned to other available Pt(0) precursors hoping the reactivity of ligand 2d towards the new Pt(0) precursors would be comparable to that of 2d towards $Pt(cod)_2$. At first, tris(norbornene)Pt(0) complex was prepared according to the literature procedure[50] and the reactivity of the ligands towards tris(norbornene)Pt(0) complex was comparable to that towards $Pt(cod)_2$. In another words, complex 12a, 12b and 13 were made with $Pt(C_3H_7)_3$.

Although $Pt(C_3H_7)_3$ seemed to be the right alternative Pt(0) precursor, the preparation always suffered from a poor yield which is opposite to what had been claimed in the literature.[50] After a few trials, we then turned to another Pt(0) precursor, Pt(0)-1,3-divinyl-1,1,3,3-tetramethyldisiloxane, which though expensive is commercially available as a solution in xylenes. As shown in Figure 3.10, the reaction took place as expected and the desired products were made. When the reaction was

monitored by NMR, intermediate complex E was the only product detected at the beginning of the reaction, whereas as the reaction proceeded, more of product 13 formed. For E, based on the facts that the resonance in the $^{31}P\{^{1}H\}$ NMR spectrum is one singlet at δ 47.94 ppm with coupling constant $J_{Pt\text{-}P}$ = 3516.1 Hz and the resonance for *tert*-butyl substituent is one doublet instead of virtual triplet, complex E was thought to be a monophosphine species, and this conclusion was confirmed by the correct integrals of each proton resonance in the ^{1}H NMR spectrum. NMR data are consistent with the presence of one diene ligand in E. A Pt(0) complex with similar structure has been made with ligand $P(C_6H_4Me\text{-}p)_3$.[59] As for reaction rates, the first substitution forming E was fast (requiring only minutes) whereas the second forming 13 was slow (requiring hours). Therefore, an excess of ligand (about 3 moles per mole of Pt) was used and the reaction was allowed to stir at room temperature for 24 h to ensure the complete transformation of the intermediate complex E to product 13. This reaction was quite easy to handle and the yield was moderate (60%), hence a relatively large amount of complex 13 could be prepared for the first time and the exploration of its intriguing chemistry became feasible.

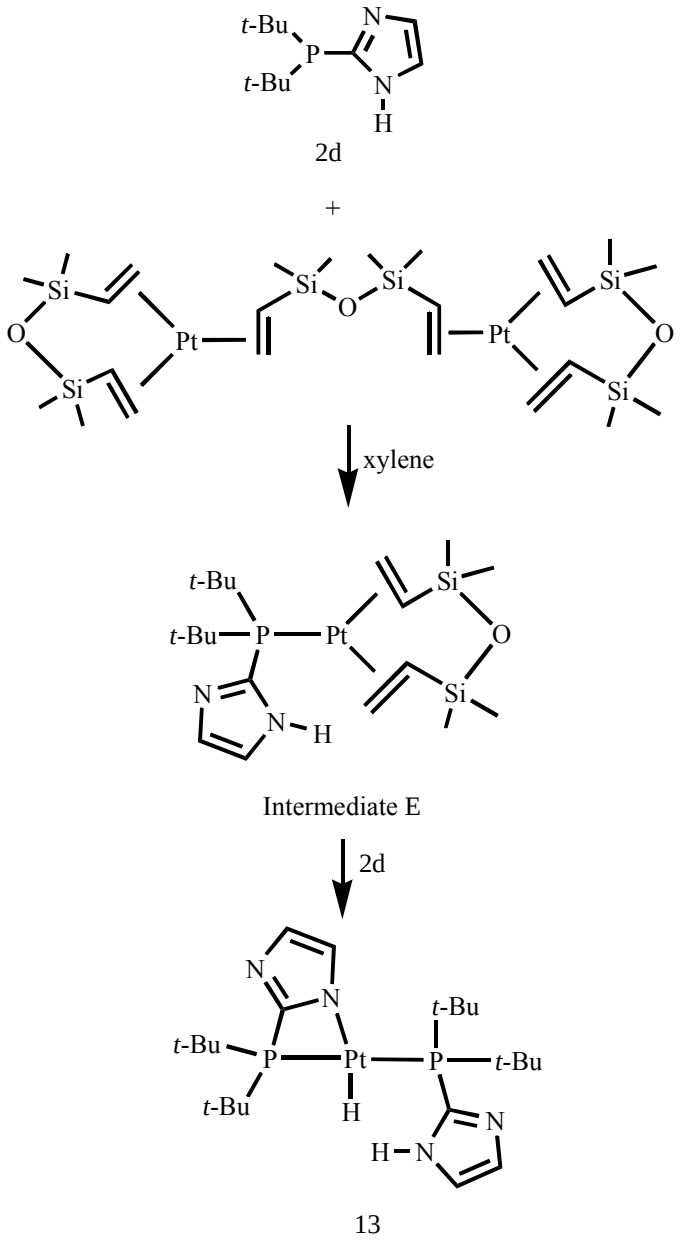

Figure 3.10. Preparation of 13 using Pt(0) precursor $Pt\{(CH_2{=}CHSiMe_2)_2O\}_3$.

Although Pt(0) complex 12a and 12b can be made in a big scale from the reaction of making trans-$Cl_2Pt(L)_2$ followed by the reduction by Na/Hg, it is

interesting to compare the reactivity of the ligand 2a towards this Pt(0) precursor with that of ligand 2d. It turned out that the reaction with 2a was slower: after 24 h, the only product seen was the monosubstituted phosphine-Pt complex with similar structure to complex E.

Reactivities of Pt(0) complexes 12a and 12b. As detailed above, the structures of complex 12a, 12b and 13 are very different: Pt(0) complexes 12a and 12b are two-coordinate, unsaturated 14-electron species which could readily undergo oxidative addition of small molecules, and moreover, the large phosphine ligand could be easily lost from the metal to produce a catalytically active monophosphine intermediate allowing another mode for the binding of other small molecules. On the other hand, complex 13 is a Pt(II) complex with four ligands, however the chelating ring is strained and could potentially be opened upon the addition of other molecules to the metal. Platinum hydride complexes have been recognized to be important intermediates in the homogenation and polymerization reactions of unsaturated organic substrates catalyzed by platinum complexes.[60-64] Therefore, the study of the reactivities of these complexes towards a variety of small molecules would not only provide the fundamental information about the feasibility of O-H and N-H activation steps of relevance to interesting metal-catalyzed organic reactions but the comparison of the reactivities would also be useful to tell how significant the alkyl substituents on phosphine or on the imidazole ring influences the reaction involved in the catalytic cycles.

The small molecules studied have a formula ROH or RNH_2, in which R is H or an alkyl group or an acyl group. All the experiments were done starting with the same initial concentration (0.05 *M* in C_6D_6). Among some of the reactions, O-H activation was found. The reactivities of Pt complexes 12 and 13 towards some other molecules such as olefins and dihydrogen were also studied.

With Acid. When the benzene solution of complex 12a was treated with one equivalent of acetic acid, one new complex was made according to the NMR spectra. In the ^1H NMR spectrum, a new resonance appeared at δ –22.60 ppm as a triplet ($J_{P\text{-}H}$ = 14.6 Hz) with satellites ($J_{Pt\text{-}H}$ = 1077.4 Hz), and meanwhile, in the $^{31}P\{^1H\}$ NMR spectrum, a new singlet showed up with a smaller Pt-P coupling constant (2949.7 Hz for product vs. 4247.1 Hz for 12a). The possible structure of this new complex 19a suggested by the NMR data was a symmetrical hydrido-platinum complex with two phosphine ligands located trans to each other, and an anionic carboxylate group occupying the fourth coordination site around the Pt atom (Figure 3.11). This Pt(II) complex 19a was the only product detected by NMR when one equivalent of acid was added, although starting complex 12a was still present (about 38%) in the reaction solution, in another words, the reaction did not go to completion. When another equivalent of acid was added, a new product 20a was made. As shown in Figure 3.11, the proposed structure of hydrido-Pt(II) complex 20a is unsymmetrical, with one phosphine ligand chelating to the Pt through N atom while the other one located trans is not. The two neutral phosphine ligands and one hydride ligand leave the Pt(II)

complex cationic with a carboxylate anion as a counterion. There was still 17% starting complex 12a left unreacted, 62% of 19a and 21% of 20a. When more acid was added, the amount of complex 20a in the products increased. This can be explained by viewing their structures. The ionic complex 20a can be stabilized by the delocalization of negative charge on the counterion through hydrogen bonding to the excess acid, consistent with the observation that adding more acid generated more of the ionic complex 20a. The reaction went to completion and made pure complex 20a when acetic acid was in large excess, for example, when 12a was dissolved in pure acetic acid, which in addition to giving a large excess of reagent has a high dielectric constant, which would also favor formation of an ionic species from a neutral precursor.

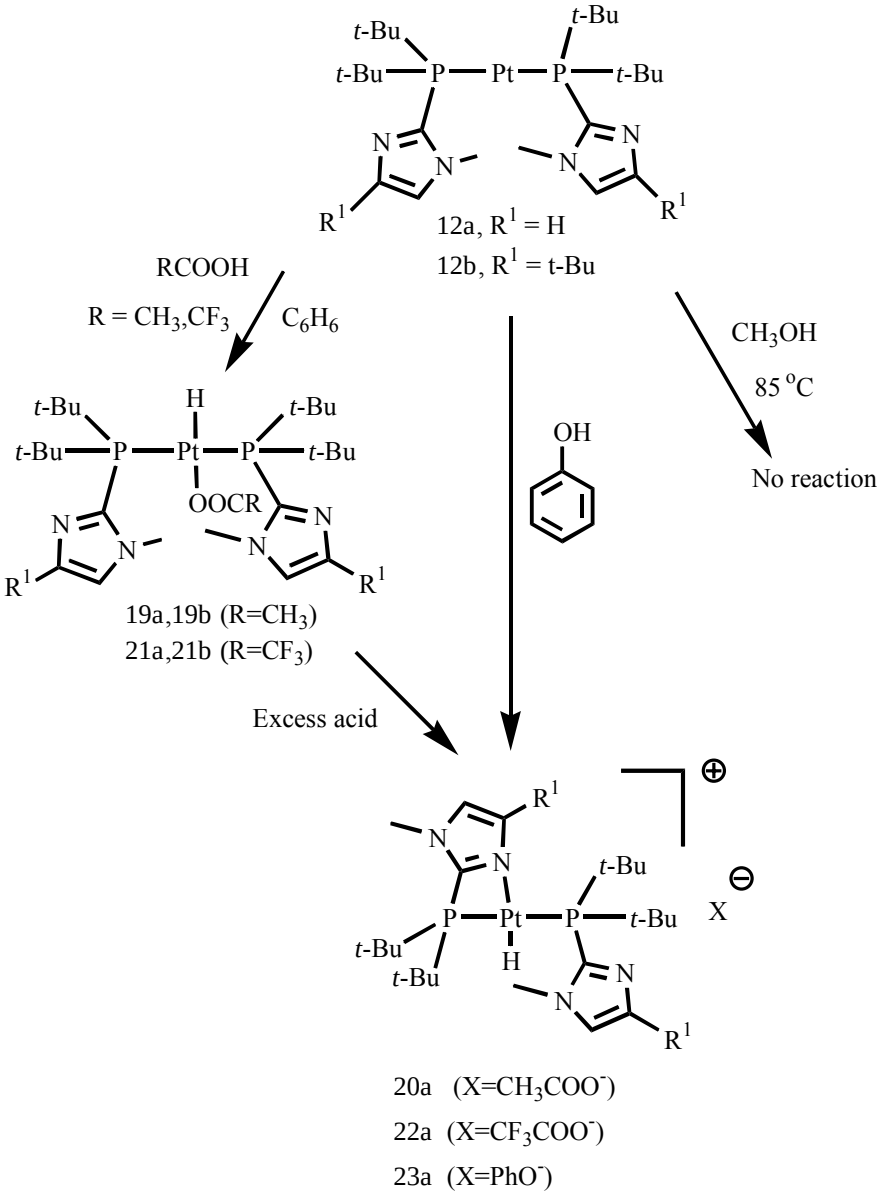

Figure 3.11. Reactivity of Pt(0) complex 12 with ROH.

Metallation of the ligand. The reaction of complex 12b with one equivalent of acetic acid produced 64% of 19b with 36% of 12b stayed unreacted, a product ratio

similar to that seen starting with 12a, however, when another one equivalent of acetic acid was added, complex 19b was still the only product found in a yield of 92%. An unsymmetrical complex similar to 20a did not form with two equivalents of acid, unlike the reaction of complex 12a. When the reaction was carried out in pure deuterated acetic acid, the reaction first made two products, one symmetric, one unsymmetric, and as time went by, the reaction went to completion and the only product was the unsymmetric one. By comparing the NMR data of this unsymmetric product with that of complex 20a from the reaction between pure acetic acid and complex 12a, it was found that the structure of this product was not similar to that of complex 20a, rather, it was the an unsymmetrical complex 18 with methyl group on the 1 position of the imidazole ring metallated, as in the structure proposed below.

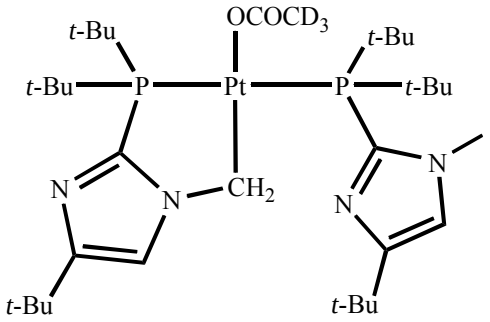

18

The NMR data and behavior of the reaction supported the proposed structure: first of all, doublets at δ 88.5 and 42.6 ppm ($J_{P\text{-}P}$ = 346.2 Hz, $J_{Pt\text{-}P}$ = 2799.9 and 2875.8 Hz) in the $^{31}P\{^{1}H\}$ NMR spectrum and two sets of resonances for the *t*-Bu and aromatic ring proton on the phosphine ligands in the ^{1}H NMR indicated an unsymmetric structure. So far, these data would also be consistent with an

unsymmetrical structure like that of 20a, in which one ligand simply chelates through P and N. The key piece of data pointing toward chelation through P and the former N-methyl *carbon* is in the ^{1}H NMR spectrum, where one of the resonances integrated for 2H rather than 3H and appeared as a singlet with Pt satellites, consistent with coordination of the carbon of the methylene group to Pt atom.

Moreover, as the reaction proceeded for two days, the resonances for the protons on both the Pt-CH_2-N unit and the N-CH_3 group of the second, monodentate phosphine disappeared while the reaction proceeded which would be consistent with the reversible formation of complex 18 from 12b and a mechanism whereby there is H-D exchange of the Pt-CH_2-N and the N-CH_3 protons with the deuterium from the solvent.

The reactivity of complexes 12a and 12b towards the stronger acid trifluoroacetic acid in benzene was studied as well. With one equivalent of CF_3COOH, for complex 12a, reaction went to completion with two products: symmetrical neutral complex 21a (major, 80%) and unsymmetrical ionic complex 22a (minor, 20%). For complex 12b, reaction was complete with 100% symmetric neutral product 21b. Note that these reactions went further to completion than the corresponding ones with acetic acid. Complex 21a was isolated in pure form and the NMR data were consistent with the proposed structure. For example, in ^{1}H NMR spectrum, the resonance at δ -23.22 ppm (triplet, $J_{P\text{-}H}$ = 14.5 Hz, $J_{Pt\text{-}H}$ = 1176.8 Hz) was assigned for the Pt-hydride and resonances at δ 128.7 and 160.0 ppm in the $^{13}C\{^{1}H\}$ NMR spectrum were due to the coordinated trifluoroacetate anion, whereas in the $^{31}P\{^{1}H\}$ NMR spectrum, there was

one singlet (δ 45.3 ppm, J_{Pt-P} = 2884.7 Hz) which suggested that symmetrical structure of complex 21a.

Crystals of 21a were grown for X-ray diffraction study, the results of which are shown in Figure 3.12. As expected, complex 21a features a square-planar Pt center (the sum of the L-Pt-L angles is 359°), on which both of the phosphine ligands are located trans to each other whereas the hydride and trifluoroacetate anion occupy the other two coordination sites. Distortion in this symmetrical but crowded complex include a P-Pt-P angle of 165.78(3)°, which may be described to interactions between the anionic trifluoroacetate ligand and imidazole ring on the phosphine ligands and the small non-located hydride opposite the trifluoroacetate ligand.

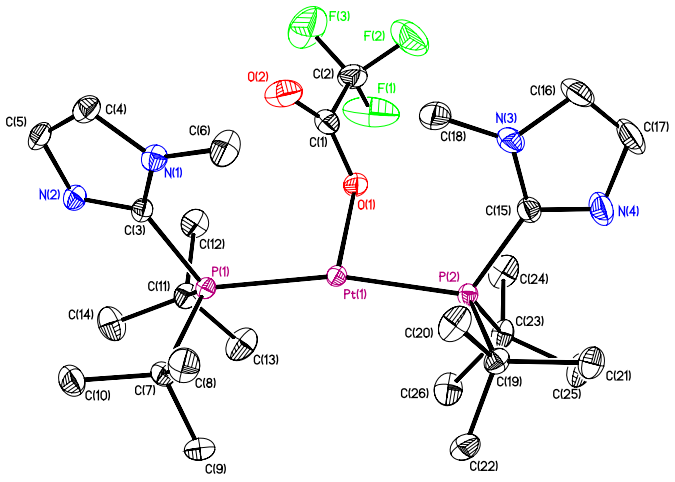

Figure 3.12. Molecular structure of 21a.

Table 3.05. Selected bond lengths (Å) and angles (deg) for complex 21a.

	Bond Lengths (Å)		Bond Angles (deg)
Pt(1)-O(1)	2.145(3)	O(1)-Pt(1)-P(1)	101.25(8)
Pt(1)-P(1)	2.3200(9)	O(1)-Pt(1)-P(2)	92.04(8)
Pt(1)-P(2)	2.3172(9)	P(1)-Pt(1)-P(2)	165.78(3)
O(1)-C(1)	1.263(5)	C(3)-P(1)-Pt(1)	118.63(13)
O(2)-C(1)	1.210(5)	C(15)-P(1)-Pt(1)	117.79(14)

Solvent used in the reaction also determined which product was dominant, for example, when complex 12a was treated with one equivalent of trifluoroacetic acid in dichloromethane which is more polar than benzene, the reaction went to completion and complex 12a converted to two products, 87% of ionic complex 22a and 13% of neutral complex 21a. It was also found that when the pure complex 21a which was isolated from the reaction in benzene was dissolved in dichloromethane, 90% of the complex 21a has converted to complex 22a. This transformation was not only seen in the NMR spectra including the new doublet resonance for hydride in the ^{1}H NMR spectrum and new doublet resonances in the $^{31}P\{^{1}H\}$ NMR spectrum but also was demonstrated by the appearance of another new strong IR absorption at 1687 cm^{-1} in addition to an existing absorption at 1712 cm^{-1}. These data can be explained by noting that the C=O bond in a coordinated trifluoroacetate ligand has more double bond character when compared to the C=O bond in free carboxylic anion, hence, absorption

for C=O stretching in the IR spectrum of ionic complex 22a shows up at higher frequency than that of neutral complex 21a. As for the solvent effect, we note that the dielectric constant of benzene (1.0) is smaller than that of dichloromethane (9.1),[65] therefore the ionic product 22a is more stabilized in solvent dichloromethane than in solvent benzene.

With Phenol. When the complex 12a was treated with phenol, which is less acidic than acetic acid, the reaction did not go to completion (55% conversion) even though phenol was in a large excess (5 equivalents). Surpisingly, the only product seen was the unsymmetric ionic complex 23a (Figure 3.11). The structure of 23a was demonstrated by the fact that the hydride was a doublet instead of a triplet seen also in spectra of ionic complexes 20a and 22a, and the phosphorus resonances were two doublets rather than one singlet. The comparable coupling constants ($J_{Pt\text{-}H}$ = 1273.0 Hz, $J_{P\text{-}H}$ = 19.0 Hz, $J_{Pt\text{-}P}$ = 2342.7 and 2957.7 Hz) to that of the similar complex 22a also suggested the proposed structure.

Unlike complex 12a, the analogous Pt(0) complex 12b did not react with phenol at all, which was quite surprising. When looking at the reaction with acid, complex 12b tends to form a neutral complex only and no ionic complex was formed while complex 12a can form both of the neutral and ionic complexes. The difference in the reactivity between these two complexes is probably due to the increasing steric hindrance at the chelating imidazole nitrogen which would reduce the ability of imidazole to chelate and hence disfavors forming the ionic product.

With Methanol. Complex 12a does not react with methanol (5 equivalents) at all, even at elevated temperature (85 ^{o}C), over a prolonged period (6 d). Complex 12a remained unreacted also when methanol was used as solvent for the reaction (Figure 3.11). Complex 12b also showed no reactivity towards methanol either at room temperature or at higher temperature (85 ^{o}C), either with 5 equivalents of methanol or in neat methanol.

With water. Complex 12a was completely unreactive with 5 equivalents of water in benzene at room temperature. Even though when heated at 85 ^{o}C, no reaction was detected by NMR after 5 d. It seemed that complex 12a was inert to water as it was to methanol. Complex 12b was also completely unreactive with 5 equivalents of water in benzene either at room temperature or at 85 ^{o}C.

With amine or dihydrogen. When a solution of complex 12a in benzene was treated with a primary amine such as benzylamine, or dihydrogen gas, no evidence of coordination of amine or formation of hydride was found in the NMR spectra. The same situation happened to the reactions with complex 12b.

With alkenes and alkene isomerization. Complex 12a did not react with ethylene gas or acrylonitrile in benzene, even at higher temperature (60 ^{o}C). However, things changed when the 1-octene was used as the alkene substrate and methanol was used as solvent. At the beginning, there was no reaction between complex 12a and 5

equivalents of 1-octene at room temperature. Then the temperature was raised to 90 ^{o}C, and after 1 d, the ^{1}H NMR spectra of the reaction solution showed new resonances at δ 5.30-5.51 ppm (m) and 1.58-1.64 ppm (m), whereas the resonances for 1-octene at δ 5.71-5.91 ppm and δ 4.90-5.02 ppm (assigned to the protons on the terminal double bond between C-2 and C-1) appeared less intense. It seemed that the starting alkene, in this case, 1-octene was converting to another alkene compound. By looking at the spectra, it was not hard to find out that the new alkene compound was one of the isomer of 1-octene (Figure 3.13). At 90 ^{o}C, all of the 5 equivalents of 1-octene converted to the new isomer after 3 d. In addition, the ^{31}P{^{1}H} NMR spectrum stayed unchanged throughout the reaction, that is, only the resonance for the complex 12a at δ 55.7 (s, J_{Pt-P} = 4247.1) was detected. Therefore, based on this reaction, the isomerization of 1-octene can be achieved by 20 mol% of Pt(0) complex 12a. The possible pathway was proposed in the Figure 3.13. In the proposed mechanism, deuteration of isomerized alkene would take place but it was possible to tell how much deuteration had occurred. This finding made Pt(0) complex 12a a potential catalyst for alkene isomerization. In the future, more alkene substrate will be tested and the reaction mechanism will be studied.

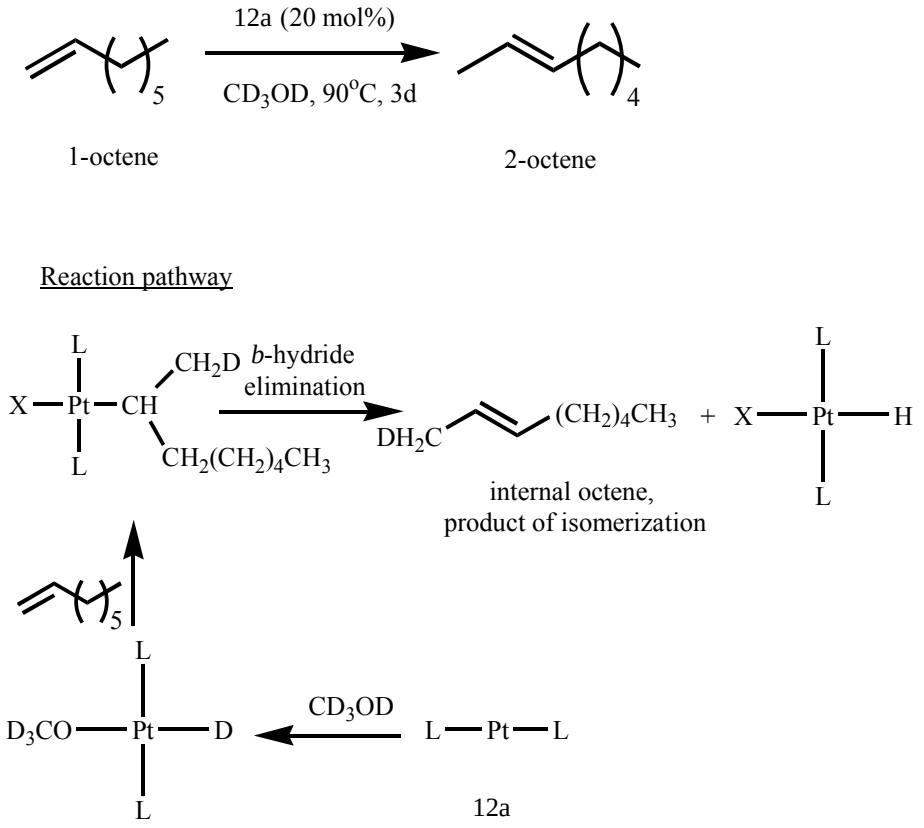

Figure 3.13. Isomerization of 1-octene by 12a.

Reactivities of Pt(H)(II) complex 13.

With acid. The reaction between complex 13 and acetic acid was rapid and clean, making one symmetric neutral complex 24 in less than five minutes (Figure 3.14). The NMR data of 24 are comparable to that of the neutral complex 19a, for example, the similar chemical shift of the hydride resonance (δ –22.81 ppm vs. –22.60 ppm), the similar Pt-H coupling constant (1117.4 Hz vs. 1077.4 Hz), the similar Pt-P coupling canstant (2939.3 Hz vs. 2949.7 Hz) all suggest that the environment around the Pt atom and hydride for these two complexes are similar. The reaction may

proceed by the opening of the chelate ring in the starting complex 13 as a result of protonation of the heterocycle followed by the coordination of the carboxylic anion to the open site of the Pt atom (Figure 3.14).

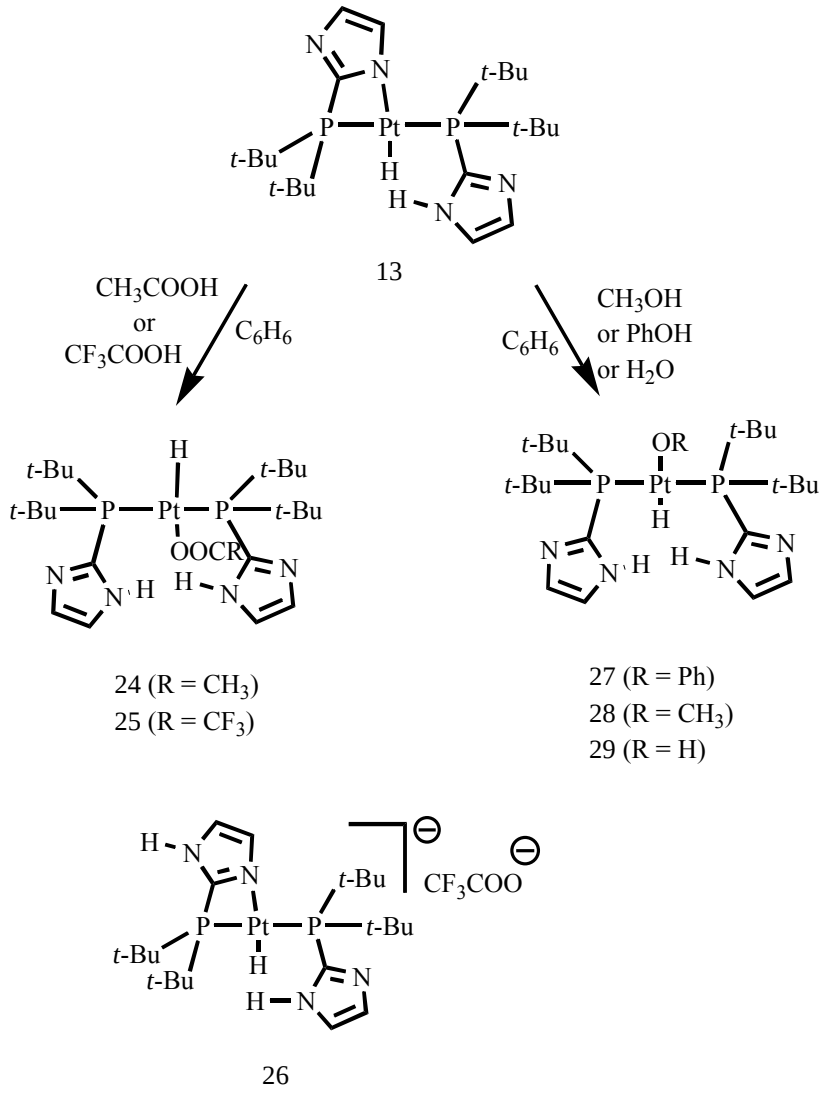

Figure 3.14. Reactivity of Pt(II) complex 13 with ROH.

Similarly, the reaction between complex 13 and trifluoroacetic acid in benzene was done in less than five minutes and only one symmetric product, neutral complex 25 was detected by NMR. The reaction solution was concentrated under vacuum and the residue was redissolved in toluene, then hexane was allowed to diffuse into the toluene solution slowly, to give colorless crystals for X-ray diffraction study. The results are shown in Figure 3.15. To our surprise, the structure thus revealed was not the one we proposed for complex 25, but in contrast, the crystallized material has a similar structure to that of unsymmetrical ionic complex 22a. In short, the solid state structure of the pure crystal was not consistent with the solution NMR data of the reaction. Since the reaction went to completion with solely formation of complex 25 when monitored by NMR, the second complex 26 could form either during the process of the recrystallization because of the change of the solvent or it could form during the reaction but the equilibrium between complex 25 and 26 was so fast that it was not detected by NMR. There were no obvious changes in the ^{1}H and $^{31}P\{^{1}H\}$ NMR spectra of 25 in d_8-toluene while cooling the sample to -60 ^{o}C, but not all material dissolved even at 30 ^{o}C, so we cannot make a conclusion about potential fluxionality of 26 (which was undetected) in solution.

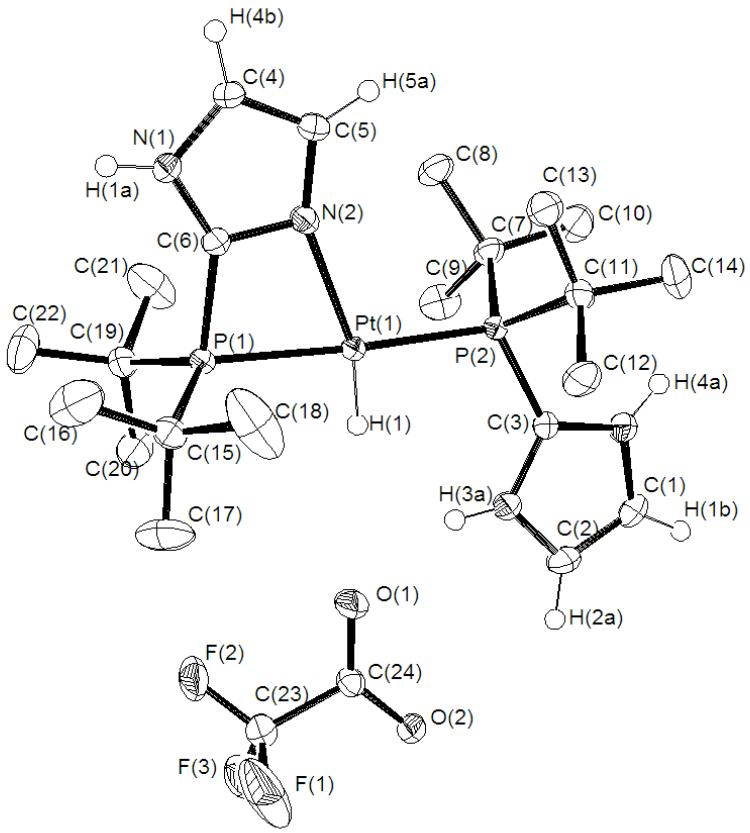

Figure 3.15. Molecular structure of complex 26.

Table 3.06. Selected bond lengths (Å) and bond angles (deg) for complex 26.

	Bond Lengths (Å)		Bond Angles (deg)
Pt(1)-P(1)	2.303	P(1)-Pt(1)-P(2)	175.86
Pt(1)-P(2)	2.282	P(1)-Pt(1)-N(2)	68.74
Pt(1)-N(2)	2.202	P(2)-Pt(1)-N(2)	108.82
P(1)-C(6)	1.816	C(3)-P(2)-Pt(1)	114.66
P(2)-C(3)	1.824	C(6)-P(1)-Pt(1)	83.88

With Phenol. The reaction of complex 13 and 2 equivalents of phenol did not go to completion (61% conversion) and neutral complex 27 which has the similar structure to that of complex 24 was the only product (Figure 3.14).

With Methanol. Unlike complex 12a and 12b, complex 13 did react with methanol with O-H activation, forming product 28 which is similar to 27 from reaction with phenol (Figure 3.14). Although attempts at obtaining the X-ray structure of complex 28 were not successful, the NMR data provided enough information. In the ^{1}H NMR spectrum, the resonance for the methyl group on methanol appeared as a singlet with Pt satellites whereas the methyl group on the free methanol appeared as a sharp singlet. This finding demonstrates that the methoxide anion is indeed coordinated to the Pt atom. The structure of the complex 28 was confirmed by other NMR data such as the hydride resonance, the phosphorus resonance and the coupling constant. With 5 equivalents of methanol, 50% of complex 13 has converted to product 28. It is worthy to note that the reaction did not go completion when methanol was used as the only solvent for the reaction.

With alkenes. Complex 13 showed no reactivity towards either ethylene or the more reactive acrylonitrile in benzene at room temperature in a period of 7 d, in that there was no evidence of the coordination of the double bond to Pt center and complex 13 stayed as it was at the beginning of the reaction.

With amine. The reaction between complex 13 and primary benzylamine was slow. At room temperature, when monitored by NMR, a new singlet at δ 47.8 ppm (J_{Pt-P} = 2863.4 Hz) and the resonance for free ligand were seen in the $^{31}P\{^{1}H\}$ NMR spectrum. In the ^{1}H NMR spectrum, no new hydride signal was found other than the doublet from complex 13. With heating at 70 and 100 ^{o}C, the reaction did not go any further, and it seemed the reaction had reached an equilibrium. NMR data suggested that one phosphine ligand was lost from the Pt center and another symmetric product formed as a result, but not enough information about this symmetric product could be told by NMR and it was also hard to tell if the amine was involved in this reaction.

With water. In contrast to complex 12a and 12b, complex 13 reacted with H_2O in benzene in a similar way as it reacted with methanol or phenol and made one product, neutral complex 29 (Figure 3.14). At room temperature, with 5 equivalents of water added to the benzene solution, the reaction reached equilibrium after 15 min. A new resonance at δ -21.08 ppm (t, J_{P-H} = 1031.9 Hz) in the ^{1}H NMR spectrum was assigned for the hydride of the symmetric complex 29. The new singlet (δ 48.3 ppm, J_{Pt-P} = 2865.9 Hz) in the $^{31}P\{^{1}H\}$ NMR spectrum suggested the symmetric structure of 29. With 5 equivalents of water, 67% of complex 13 had converted to complex 29, however, the equilibrium could be pushed further if the amount of the water was increased. If 20 equivalents of water was added to benzene solution, even though water has limited solubility in benzene, with the help of shaking and mixing, after 20 min, 86% of complex 13 has converted to complex 29. It would be significant to

isolate pure 29 in an effort to see how the two N-H bonds in the imidazole ring are involved in hydrogen bonding.

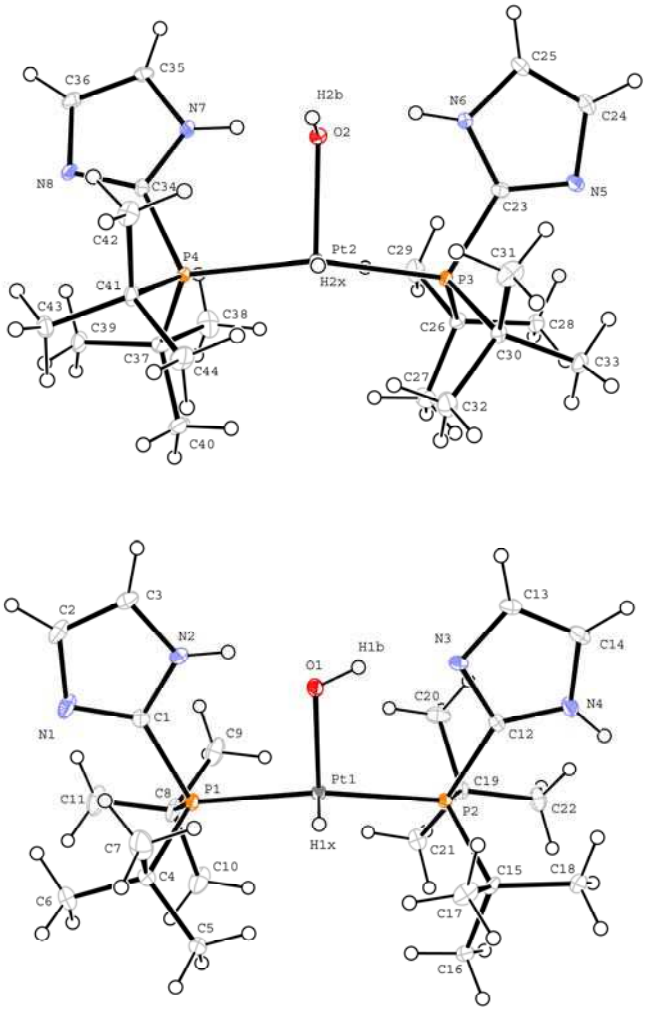

Figure 3.16. Molecular structure of complex 29. Conformer F (top) and G (bottom).

Table 3.07. Selected bond lengths (Å) and bond angles (deg) for complex 29.

	Bond Lengths (Å)		Bond Angles (deg)
O(1)-Pt(1)	2.159(3)	O(1)-Pt(1)-P(2)	98.21(8)
O(1)-H(1B)	0.8400	O(1)-Pt(1)-P(1)	95.21(8)
O(2)-Pt(2)	2.152(3)	P(2)-Pt(1)-P(1)	165.06(4)
O(2)-H(2B)	0.8400	O(2)-Pt(2)-P(3)	96.49(8)
P(1)-Pt(1)	2.3209(11)	O(2)-Pt(2)-P(4)	97.30(8)
P(2)-Pt(1)	2.3197(10)	P(3)-Pt(2)-P(4)	164.14(4)
P(3)-Pt(2)	2.3078(10)		
P(4)-Pt(2)	2.3087(10)		

Table 3.08. Hydrogen bonds for complex 29.

D-H…A	d(D-H)	d(H…A)	d(D…A)	<(DHA)
N(2)-(2A)…O(1)	0.85(5)	1.73(5)	2.555(5)	161(4)
O(1)-H(1B)…N(3)	0.84	1.78	2.567(5)	154.3
N(6)-H(6)…O(2)	0.83(4)	1.80(4)	2.596(5)	160(4)
N(7)-H(7)…O(2)	0.82(4)	1.74(4)	2.545(4)	166(5)

Hence, crystals of 29 were grown for analysis by X-ray diffraction. With an excess of water added to the reaction solution, the diffusion of less polar hexane allowed the growth of fine crystals suitable for X-ray diffraction. As shown in Figure 3.16, two distinct conformers of the product, F and G, were found in the unit cell of complex 29, each with a different hydrogen bonding network. In solid structure G, the hydride ligand acts as both hydrogen bond donor and acceptor to form two hydrogen bonds with the N-H and N in the imidazole ring. The distance between hydroxide hydrogen and the interacting nitrogen on the imidazole ring was 1.78 Å and the distance between N-H and oxygen of the hydoxide ligand was 1.73(5)Å, both of which

fall in the range of N-H distance and O-H distance involved in hydrogen bonding.[66] The imidazole rings on the two phosphine ligands are positioned in a different way in order to form the hydrogen bond with hydroxide ligand, therefore, structure G is unsymmetrical. On the other hand, in structure F, O-H bond of hydroxide ligand are pointing outward the plane so that the oxygen can form two hydrogen bonds with N-H in both of the imidazole ring on the phosphine ligands, in this case, the hydroxide ligand only acts as hydrogen bond acceptor. Obviously, structure F is closer to being symmetric. The distance between N-H and oxygen were 1.80(4) and 1.74(4)Å which were also in the range of N-H distance involved in hydrogen bonding.

The comparisons of the reactivities of the Pt complexes 12a, 12b and 13 towards compound ROH were summarized in Table 3.09.

Table 3.09. Comparisons of Reactivities of Pt (0) complexes 12a, 12b and Pt(II) complex 13 towards compound ROH.[a]

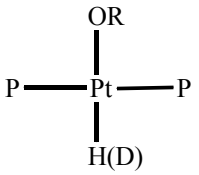

H

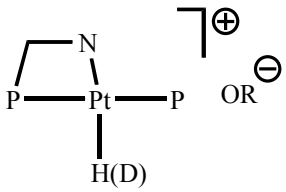

I

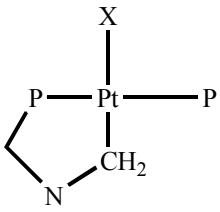

J

Pt complex	CF_3COOH	CH_3COOH	PhOH	CH_3OH	H_2O	CD_3COOD[b]	CD_3OD[b]
12a	1 equiv. 80% H 20% I	1 equiv. 62% H 38% 12a. 2 equiv. 62% H 21% I 17% 12a	5 equiv. 55% I 45% 12a	5 equiv. 85 °C no rxn	5 equiv. 85 °C no rxn	Complete Rxn 100% I	No rxn
12b	1 equiv. 100% H	1 equiv. 64% H 36% 12b. 2 equiv. 92% H 8% 12b	5 equiv. No rxn	5 equiv. No rxn	5 equiv. 85 °C no rxn	Intial: 80% H, 20% I. After 1 d: complete rxn 100% J	No rxn
13	1 equiv. 100% H	1 equiv. 100% H	2 equiv. 61% H 39% 13	5 equiv. 50% H 50% 13	5 equiv. 67% H 33% 13	90% H 10% 13 or I	Rxn not complete H[c]

[a]Reaction was carried out (0.05 *M* complex in C_6D_6) at room temperature, unless otherwise stated.
[b]Pure solvent.
[c]Ratio was not obtained due to the overlap of the resonances in the NMR spectrum.

D. Conclusion

In summary, Pt complexes with a series of structurally similar bifunctional imidazolyl phosphine ligands 2a, 2b, 2d, and 2e were synthesized, and their Pt complexes 12a, 12b and 13 were studied and compared.

Some of the results obtained are comparable to the results in chapter 2, for example, in the reaction with $Pt(cod)_2$, both of the ligands 2a and 2b made Pt(0) complexes 12a and 12b, similar to 3a and 3b. When reacted with Pt(II) complex K_2PtCl_4 in the presence of water and ethanol, 2a and 2b both gave the symmetric trans-L_2PtCl_2 complex 14a and 14b. In addition, the effect of phosphine alkyl groups (*i*-Pr versus *t*-Bu) can be seen in the isolation of neutral, symmetrical trans-L_2PtCl_2 complex 14e and ionic, unsymmetrical $[15\text{-Cl}]^+Cl^-$.

When the reactivities of the structurally similar Pt(0) complexes 12a and 12b were compared, 12b was less reactive towards O-H compounds than 12a. In addition, complex 12b tends to give symmetrical neutral products and not chelated ionic ones, which shows the steric effect of the bulky *tert*-butyl group on the C-4 position.

Important new information comes from comparisons between ligand 2a and 2d, having an N-H group or an N-CH_3 group on the imidazole ring. The N-H group has dramatic influence on the reactivity, for example, N-H activation took place and hydrido Pt(II) complex 13 was made in the reaction of 2d with Pt (0) precursor such as $Pt(cod)_2$ when a N-H group was available. When reacted with Pt(II) complex K_2PtCl_4

in the presence of water and ethanol, 2d gave the unsymmetrical ionic complex [15-Cl]$^{+}$[Cl]$^{-}$

Under identical conditions, the reactivities of 12a and 13 with O-H compounds of acidity ranging from that of trifluoroacetic acid to water were quite different also. Complex 12a reacted significantly only with more acidic species, whereas 13 reacted with all O-H compounds tested, resulting in O-H activation. Moreover, complex 13 always gave symmetrical trans-L_2Pt(H)(OR) complex, depending on conditions, 12a could also give unsymmetrical species formed by dissociation of the anionic ligand OR.

Chapter 6 outlines future work, which will explore the ability of NH containing ligands to activate other small molecules and various substrates.

E. References

(1) Shilov, A. E.; Shul'pin, G. B. Activation and Catalytic Reactions of Saturated Hydrocarbons in the Presence of Metal Complexes; Kluwer: Boston, 2000.

(2) Stahl, S. S.; Labinger, J. A.; Bercawm J. E. *Angew. Chem., Int. Ed.* Engl. 1998, *37*, 2181.

(3) Lin, M.; Shen, C.; Garcia-Zayas, E. A.; Sen, A. *J. Am. Chem. Soc.* 2001, *123*, 1000.

(4) Periana, R. A.; Taube, D. J.; Gamble, S.; Taube, H.; Satoh, T.; Fuji, H. *Science* 1998, *280*, 560.

(5) Shilov, A. E.; Shul'pin, G.B. *Chem. Rev.* 1997, *97*, 2879.

(6) Zhong, H. A.; Labinger, J. A.; Bercaw, J. E. *J. Am. Chem. Soc*. 2002, *124*, 1378.

(7) Johanasson, L.; Ryan, O. B.; Romming, C.; Tilset, M. *J. Am. Chem. Soc.* 2001, *123*, 6579.

(8) Thomas, J. C.; Peters, J. C. *J. Am. Chem. Soc.* 2001, *123*, 5100.

(9) Wick, D. D.; Goldberg, K. I. *J. Am. Chem. Soc.* 1997, *119*, 10235.

(10) Puddephatt, R. J. *Coord. Chem. Rev.* 2001, *219*, 157.

(11) Hofmann, K. A.; von Narbutt, *J. Ber.* 1908, *41*, 1625.

(12) Liu, C.; Han, X.; Wang, X.; Widenhoefer, R. A. *J. Am. Chem. Soc.* 2004, *126*, 3700.

(13) Wang, X.; Widenhoefer, R. A. *Organometallics* 2004, *23*, 1649.

(14) Bender, C. F.; Widenhoefer, R. A. *J. Am. Chem. Soc.* 2005, *127*, 1070.

(15) Qian, H.; Han, X.; Widenhoefer, R. A. *J. Am. Chem. Soc.* 2004, *126*, 9536.

(16) P. Wiseman, *An ntroduction to Industrial Organic Chemistry* (Applied Science, London, 1979).

(17) Atkins, K. E.; Walker, W. E.; Manyik, R. M. *J. Chem. Soc. Chem. Commun.* 1971, 330.

(18) Zakharkin, L. I.; Babich, S. A.; Pisareva, I. V.; *Izv. Akad. Nauk SSSR Ser. Khim.* 1976, 1616.

(19) Biachini, J. P.; *J. mol. Catal.* 1981, *10*, 247.

(20) Inoue, Y.; et al. Bull. Chem. Soc. Jpn. 1983, 56, 637.

(21) Dzhemilev, U. M.; Sidorova, V. V.; Kunakova, R. V. *Izv. Akad. Nauk SSSR Ser. Khim.* 1983, 584.

(22) Inoue, Y.; Otsuka, Y.; Hashimoto, H. *Bull. Chem. Soc. Jpn.* 1984, *57*, 3345.

(23) Jensen, C. M.; Trogler, W. C. *Science* 1986, *233*, 1069-1071.

(24) Ramprasad, D.; Yue, H.; Marsella, J. A. *Inorg. Chem.* 1988, *27*, 3151-3155.

(25) Crabtree, R. H. *J. Chem. Soc., Dalton Trans.* 2001, 2437-2450.

(26) Ritleng, V.; Sirlin, C.; Pfeffer, M. *Chem. Rev.* 2002, *102*, 1731-1770.

(27) Handbook of C-H Transformations; Dyker, G.; Wiley-VCH: Weinheim, Germany, 2005.

(28) Hackett, M.; Ibers, J. A.; Jernakoff, P.; Whitesides, G. M.; *J. Am. Chem. Soc.* 1986, *108*, 8094-8095.

(29) Hackett, M.; Whitesides, G. M. *J. Am. Chem. Soc.* 1988, *110*, 1449-1462.

(30) Kanzelberger, M.; Zhang, X.; Emge, T. J.; Goldman, A. S.; Zhao, J.; Incarvito, C.; Hartwig, J. F. *J. Am. Chem. Soc.* 2003, *125*, 13644-13645.

(31) Chantson, J. T.; Lots, S. *J. Organomet. Chem.* 2004, *689*, 1315-1324.

(32) Fornies, J.; Green, M.; Spencer, J. L.; Stone, F. G. A. *J. Chem. Soc. Dalton Trans.* 1977, 1006-1009.

(33) Hedden, D.; Roundhill, D. M.; Fults, W. C.; Rheingold, A. L. *J. Am. Chem. Soc.* 1984, *106*, 5014-5016.

(34) Park, S.; Johnson, M. P.; Roundhill, D. M. *Organometallics* 1989, *8*, 1700-1707.

(35) Farnetti, E.; Nardin, G.; Graziani, M. *J. Organomet. Chem.* 1991, *417*, 163-172.

(36) Driver, M. S.; Hartwig, J. F. *J. Am. Chem. Soc.* 1996, *118*, 4206-4207.

(37) Driver, M. S.; Hartwig, J. F. *Organometallics* 1997, *16*, 5706-5715.

(38) Garcia, J. J.; Casado, A. L.; Iretskii, A.; Adams, H.; Maitlis, P. M.; *J. Organomet. Chem.* 1998, *558*, 189-192.

(39) Hirano, M.; Onuki, K.; Kimura, Y.; Komiya, S. *Inorg. Chim. Acta.* 2003, *352*, 160-170.

(40) Jimenez-Tenorio, M.; Puerta, M. C. Valerga, P. *Eur. J. Inorg. Chem.* 2005, 2631-2640.

(41) Pittard, K. A.; Cundari, T. R.; Gunnoe, T. B.; Day, C. S.; Peterson, J. L. *Organometallics* 2005, *24*, 5015-5024.

(42) Zhang, J.; Gandelman, M.; Shimon, L. J. M.; Rozenberg, H.; Milstein, D. *Organometallics* 2004, *23*, 4026-4033.

(43) Ziegler, T.; Li, J. *Organometallics* 1995, *14*, 214-223.

(44) Chen. Y.; Clemmer, D. E.; Armerntrout, P. B. *J. Am. Chem. Soc.* 1994, *116*, 7815-7826.

(45) Shoner, S. C.; Humphreys, K. J.; Barnhart, D.; Kovacs, J. A. *Inorg. Chem.* 1995, *34*, 5933-5934.

(46) Haak, S.; Neela, A.; Stoeckli-Evans, H.; Suss-Fink, G.; Thomas, C. M.; *Chem. Commun. (Cambridge)* 1999, *19*, 1959-1960.

(47) Su, M.; Chu, S.; *Chemical Physics Letters* 1998, *282*, 25-28.

(48) Green, M.; Howard, J. A. K.; Spencer, J. L.; Stone, F. G. A. *J. Chem. Soc. Dalton Trans.* 1997, 271.

(49) J. Am. Chem. Soc. 1986, 108, 1180.

(50) Ogoshi, S.; Morita, M.; *J. Organomet. Chem.* 2004, *689*, 662-665.

(51) Brookhart, M.; Green, M. L. *J. Organomet. Chem.* 1983, *250*, 395-408.

(52) Brookhart, M.; Green, M. L. Wonk, L.-L. *Prog. Inorg. Chem.* 1988, *36*, 1-124.

(53) Elschenbroich, C.; Salzer, A. *Organometallics: A Concise Introduction*; 2nd ed.; VCH: Weinheim, 1992.

(54) Otsuka, S.; Yoshida, T.; Matsumoto, M.; Nakatsu, S.; *J. Am. Chem. Soc.* 1976, *98*, 5850-5858.

(55) Grotjahn, D. B.; Gong, Y.; Zakharov, L. N.; Golen, J. A.; Rheingold, A. L. *J. Am. Chem. Soc.* 2006, *128*, 438-453.

(56) Inorg. Synth. 1979, 19, 100.

(57) Cheney, A. J.; Shaw, B. L.; *J. Chem. Soc. Dalton Trans.* 1972, 754.

(58) Goel, R. G.; Ogini, W. O.; Srivastava, R. C. *J. Organomet. Chem.* 1981, *214*, 405-417.

(59) Hitchcock, P. B.; Lappert, M. F.; MacBeath, C.; Scott, F. P. E.; Warhurst, N. J. W. *J. Organomet. Chem.* 1997, *528*, 185-190.

(60) Hsu, C. Y.; Orchin, M. *J. Am. Chem. Soc.* 1975, *97*, 3553.

(61) Cheng, C. H.; Kuritzkes, L.; Eisenberg, R. *J. Organometal. Chem.* 1980, *190*, C21.

(62) Attig, T. G.; Clark, H. C.; Wong, C. S. *Can. J. Chem.* 1977, *55*, 189.

(63) Thorn, D. L.; Hoffman, R. *J. Am. Chem. Soc.* 1978, *100*, 2079.

(64) Venanzi, L. M. *Coord. Chem.* 1980, *20*, 99.

(65) Brown, W. H.; Foote, C. S. *Organic Chemistry*, 2nd Ed, p 276; Sanders College Publishing: 1998.

(66) Jeffery, G. A. *An Introduction to hydrogen Bonding*; Oxford: New York, 1997.

CHAPTER 4

Study of Bidentate Imidazolylphosphine Ligands with Different Bite Angles on Palladium and Platinum

A. Introduction

Generation of aromatic amines from the reaction of aryl halides or aryl triflates and amines catalyzed by palladium catalysts is synthetically important because aromatic amines are fundamental building blocks in natural products and organic materials.[1-3] Classical methods to prepare mixed alkylaryl amines can be tedious and problematic.[4,5] The use of chelating phosphine ligands has been reported to greatly improve the palladium-catalyzed chemistry that forms arylamines from aryl halides or aryl triflates.[6-8]

Palladium complexes containing the labile, sterically hindered, monodentate triarylphosphine ligands such as P(*o*-tolyl)$_3$ were originally the only catalysts for the intermolecular amination reaction involving amines in the presence of tin amides.[9-12] Kinetic studies, along with investigations of the ligand steric effects on selectivity, showed that the unusual effectiveness of P(*o*-tolyl)$_3$ was due to the fact that each intermediate in the catalytic cycle was a highly unsaturated, monophosphine complex and the selectivity for amination over reduction was enhanced by steric bulk.[11,13] Therefore, it was remarkable when a very different class of phosphine ligand, tightly bound chelating phosphines such as DPPF (1,1'-bis(diphenylphosphino)-ferrocene and BINAP (2,2'-bis(diphenylphosphino)1,1'-binaphthyl) (Figure 4.01), were found to be

more effective than P(*o*-tolyl)$_3$ in the amination chemistry for many amine and aromatic substrates.[7.8]

A chelating ligand possesses three major characteristics: electron-donating ability, steric properties, and P-M-P angle which is often called "bite angle". The effect of these three properties on the selectivity in hydroformylations,[14-16] carbon dioxide hydrogenation,[17] and alkyne hydrosilylation[18,19] has been investigated over the years. However, chelating phosphines are often used in cross coupling chemistry, and few systematic studies have been conducted to reveal how all three factors affect this palladium- and nickel-catalyzed chemistry. Most of the focus has been placed upon the effect of bite angle,[20] or on electronic and steric properties of monodentate phosphines.[21]

In rough terms, chelation inhibits β-hydrogen elimination of alkyl groups,[22,23] and a similar effect appears to control the selectivity of amido complexes that are intermediates in the amination chemistry. It was shown that β-hydrogen elimination from amido complexes occurs from a 14-electron, three-coordinate intermediate.[24] In contrast, C-N bond-forming reductive elimination of amines from square planar Pd(II) complexes can occur from either a four- or three-coordinate intermediate.[25]

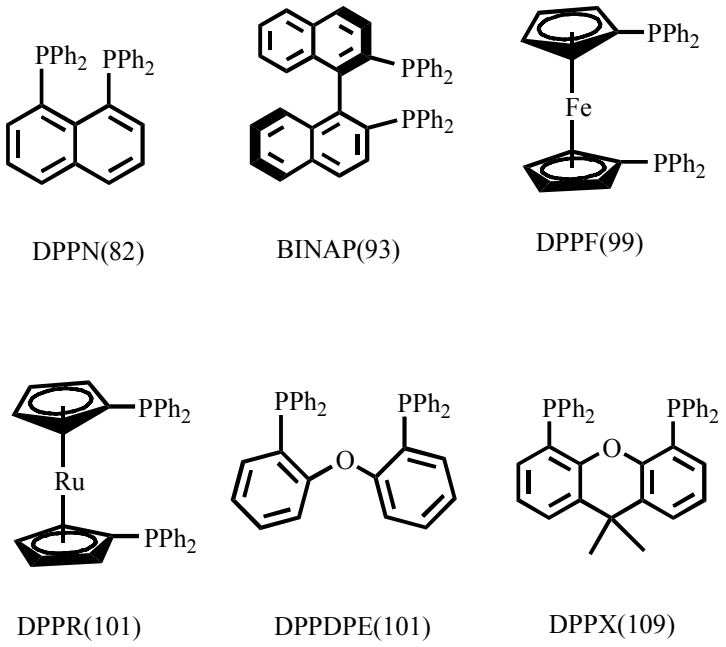

Figure 4.01. Bidentate ligands and their bite angles (deg).

More hindered chelating ligands are expected to combine the benefits of hindered P(*o*-tolyl)$_3$ with the benefits of chelation. Electron poor ligands are expected to enhance the formation of amination products since reductive elimination is accelerated by reducing the electron density at the metal center.[26] Finally, increasing the size of bite angle created by the chelating phosphine is expected to increase the yields of amination product, since reductive elimination is typically faster for complexes with chelating ligands containing large bite angles than it is for complexes with small bite angles.[20] However, the study of amination of aryl bromides showed that the increased steric bulk in the ligand caused an increase in the amount of reduction product, not the amination product, and also electronic properties of

bidentate ligands had little effect on the selectivity of the amination reactions, and finally increasing ligand bite angles from 82° to 109° (Figure 4.01) gave decreased ratios of amine to arene products (the latter are the result of β-hydrogen elimination).[27] The results from these studies showed that the rate for reductive elimination should not be the dominant consideration when ligands for the next generation amination catalysts are designed.

The themes of platinum and bidentate ligand bite angle also appear in a reaction which is important on an industrial scale, the hydroformylation of alkenes.[29,30] Most often cobalt and rhodium catalysts are applied, but Pt-Sn systems with phosphorus ligands are also known.[31] Especially in the asymmetric hydroformylation of styrene, platinum-based catalysts have been extensively studied.[32-35] For the platinum-catalyzed hydroformylation of terminal alkenes, most often (di)phosphine ligands are employed.[36-39] Rigid xanthene-based diphosphine have been shown to give active and selective platinum catalysts for the hydroformylation of 1-octene.[40]

An early study of effect of diphosphine chelate ring size on catalytic performance by Hayashi et al. described that in the case of diphosphine ligands steric rather than electronic factors determine the reaction rate and regioselectivity.[41,42] The addition of 1,2-bis(diphenylphosphino)ethane (dppe) decreased the reaction rate. The catalytic activity increased dramatically when a four-carbon-bridged diphosphine such as dppb was used. The calculated natural bite angle of this ligand is around 98°, whereas that of dppe is 90°.[43]

In order to begin studying the combined effects of bidentate diphosphine bite angle and imidazole substituents on phosphorus, thus far three kinds of bidentate phosphine ligands bearing heterocyclic imidazole rings (shown in Figure 4.02) have synthesized in the Grotjahn lab.[44] The synthesis of these new ligands is outside the scope of this thesis, however, here we report some preliminary studies of the behavior of these imidazolylphosphine ligands on Pd and Pt.

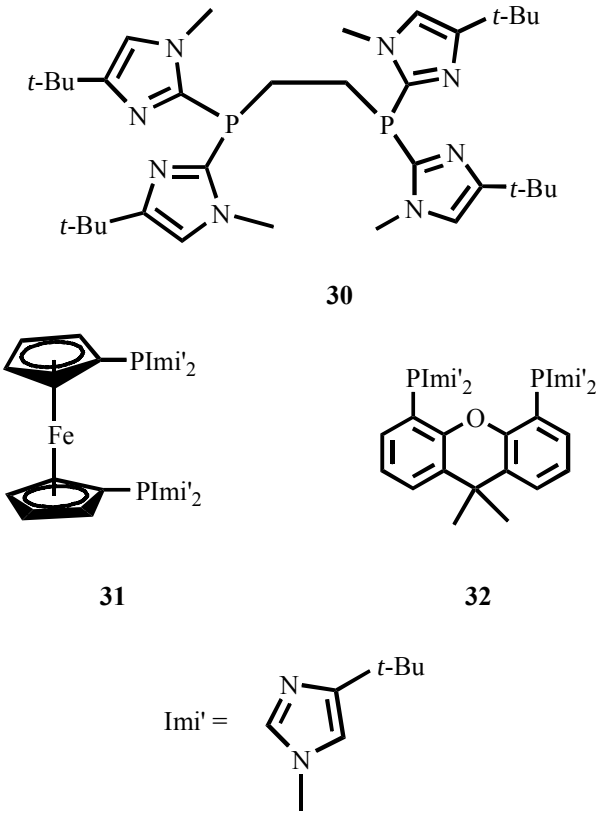

30 **31** **32**

Figure 4.02. Structure of bidentate imidazolylphosphine ligands **30**, **31** and **32**.

B. Experimental Section

Ligands **30**, **31** and **32** and complex **36** were new and prepared by other group members.[44]

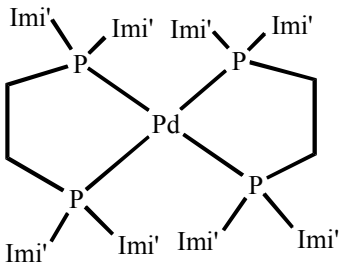

33

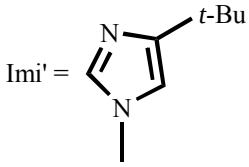

Preparation of bis(η^2-Imi'$_2$PCH$_2$CH$_2$Pimi'$_2$)Pd(0) complex (33). In the glove box, ligand **30** (188 mg, 0.29 mmol) was weighed in a clean vial containing a stir bar and Cp(allyl)Pd (29.6 mg, 0.14 mmol) was weighed into the same vial. Dry and deoxygenated benzene (5 mL) was then added to the mixture to afford a dark red solution. The reaction mixture was then allowed to stir at room temperature. After 1 d, the reaction mixture turned to pale yellow from dark red, the reaction was stopped and solvent was removed on the vacuum line. The resulting solid was recrystallized by first dissolving in hexane/dichloromethane (3 mL) then chilling to –50 ^{o}C. The pure product **33** (163 mg, yield 80%) was obtained as white flaky crystals after removing the mother liquor and washing with cold hexane and drying under vacuum. NMR (C_6D_6) ^{1}H: 6.30 (s, 8H), 3.19 (t, 10.5, 8H), 3.05 (s, 24H), 1.27 (s, 72H); ^{31}P{^{1}H}: -3.6 (s). Anal. Calcd. For $C_{68}H_{112}N_{16}P_4Pd$ (1382.72): C, 59.01; H, 8.16; N, 16.19. Found: C, 56.77; H, 7.69; N, 15.48.

Preparation of (η^2-Imi'$_2$PCH$_2$CH$_2$PImi'$_2$)Pd(Ph) complex (34). In the glove box, ligand **30** (124 mg, 0.19 mmol) was weighed in a clean vial containing a magnetic stir bar, Cp(allyl)Pd (42.3 mg, 0.20 mmol) was transferred to the same vial, then iodobenzene (47.4 mg, 0.23 mmol) was added to the vial via syringe. Dry and deoxygenated benzene (4 mL) was added to give red solution and the solution was allowed to stir at room temperature. After 2 d, the solvent was removed under vacuum. The resulting residue was recrystallized by slowly diffusing hexane into a THF solution to afford yellow crystals. Pure complex **34** was obtained after the crystals were washed and dried (88 mg, yield 43%). NMR (CD_2Cl_2) ^{1}H: 6.90 (d, 2.0, 2H), 6.81-6.88 (m, 5H), 6.74 (d, 2.0, 2H), 3.99 (s, 6H), 3.15 (s, 6H), 2.93-3.00 (m, 2H), 2.71-2.79 (m, 2H), 1.32 (s, 18H), 1.28 (s, 18H); ^{13}C {^{1}H}: 155.2 (d, 13.3), 154.8 (d, 10.0), 153.6, 152.5, 149.3, 138.7, 127.1 (d, 9.4), 123.9, 121.4, 121.1, 38.0, 34.8, 32.7, 32.5, 32.3, 30.6, 30.4, 26.2; ^{31}P{^{1}H}: 19.7 (d, 20.4), 10.0 (d, 20.3). Anal. Calcd. For $C_{40}H_{61}IN_8P_2Pd$ (929.24): C, 50.61; H, 6.48; N, 11.80. Found: C, 51.82; H, 7.44; N, 10.84.

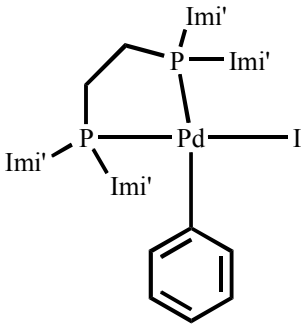

34

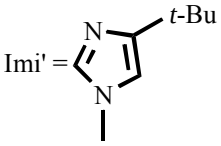

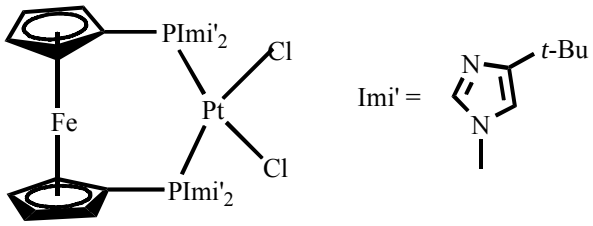

36

NMR data of complex 36. NMR ($CDCl_3$, 200 MHz) ^{1}H: 6.73 (s, 4H), 4.80 (s, 4H), 4.31 (s, 4H), 4.08 (s, 12H), 1.27 (s, 36H); $^{31}P\{^1H\}$: -27.0 (s, J_{Pt-P} = 3787.3 Hz).

Reaction of complex 36 with hydrazine. In a J-Young tube, complex **36** (10.2 mg, 0.01 mmol) was weighed and $CDCl_3$ (0.7 mL) was added to the NMR tube to give an orange-colored solution. After initial NMR spectra were observed, hydrazine (5.2 mg, 0.10 mmol) was added to the NMR tube, the color of the NMR solution turned from orange to yellow. NMR spectra were observed and one major complex, tentatively identified as **37**, was detected. NMR ($CDCl_3$, 200 MHz) ^{1}H: 6.59 (s, 4H), 5.88 (s, 4H), 4.64 (s, 4H), 3.51 (s, 12H), 1.23 (s, 36H); $^{31}P\{^1H\}$: -36.6 (s, J_{Pt-P} = 3389.6 Hz).

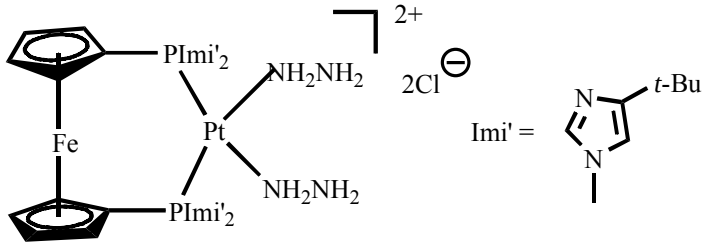

37

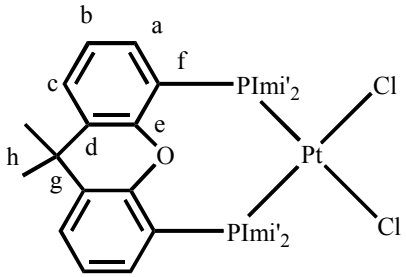

38

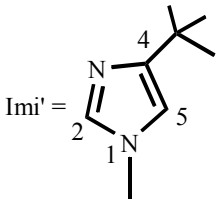

Preparation of cis-(η^2-L)$PtCl_2$ (38). Ligand **32** (651.7 mg, 0.796 mmol) and $(cod)PtCl_2$ (303 mg, 0.810 mmol) were weighed in a clean vial, then dry and deoxygenated dichloromethane (10 mL) was added to afford a clear solution. The reaction mixture was allowed to stir at room temperature inside the glovebox. After 2 h, the reaction was stopped and reaction mixture was concentrated to dryness. The solid residue was dissoloved in a 1:1 mixture of dichloromethane and diethyl ether (5 mL) and then chilled to –50 ^{o}C. The crystalline solid formed was isolated by removing the supernatant with a pipet and washing with cold diethyl ether then drying under vacuum to give colorless crystals (848.6 mg, 98%). NMR ^{1}H ($CDCl_3$, 200 MHz): 8.36 (br s, 2H, a-H), 7.62 (d, 7.6, 2H, c-H), 7.28 (t, 7.2, 2H, b-H), 6.42 (br s, 4H, Imi-5-H), 3.81 (br, 12H, Imi'-N-CH_3), 1.77 (s, 6H, h-H), 1.12 (s, 36H, Imi-4-C$(CH_3)_3$); $^{31}P\{^{1}H\}$ ($CDCl_3$, 80.9 MHz): –34.7 (s, $J_{Pt\text{-}P}$ = 3709.4 Hz). Anal. Calcd. For $C_{47}H_{64}Cl_2N_8OP_2Pt$ (1085.00): C, 52.03; H, 5.95; N, 10.33. Found: C, 51.73; H, 6.20; N, 10.32.

Reaction of complex 38 with AgOTf and benzylamine and NMR data of complex 39. In a J-Young tube, complex **38** (68.0 mg, 0.063 mmol) was weighed and CD_2Cl_2 (0.7 mL) was added to the NMR tube to give a clear solution. After initial NMR spetra were observed, silver triflate (33.1 mg, 0.13 mmol) was added to the NMR solution and a white precipitate formed right away. The white precipitate was removed by filtration and benzylamine (3.9 mg, 0.073 mmol) was added to the filtrate via syringe. One new complex **39** was detected by NMR. The NMR solution was transferred to a clean vial and concentrated to dryness, and the resulting solid was recrystallized from diethyl ether/dichloromethane to give white crystals (24.4 mg, yield was not calculated due to the uncertain structure of complex **39)**. NMR (CD_2Cl_2) ^{1}H: 10.63 (br s, 1H), 10.06 (br s, 1H), 8.06 (t, 8.5, 2H), 7.56-7.62 (m, 2H), 7.20-7.24 (m, 1H), 7.07 (s, 2H), 7.04 (t, 7.5, 2H), 6.96 (t, 8.0, 4H), 6.56 (s, 1H), 6.55 (s, 1H), 6.49 (d, 1.0, 1H), 6.46 (d, 2.5, 1H), 5.85 (br s, 1H), 5.64 (br s, 1H), 3.47 (s, 3H), 3.18 (s, 3H), 2.95 (s, 3H), 2.70 (s, 3H), 2.18 (s, 3H), 1.73 (s, 3H), 1.56 (s, 9H), 1.45 (s, 18H), 1.07 (s, 9H); ^{31}P{^{1}H}: -43.9 (d, $J_{P\text{-}P}$ = 18.6 Hz, $J_{Pt\text{-}P}$ = 3327.1 Hz), -44.9 (d, $J_{P\text{-}P}$ = 18.6 Hz, $J_{Pt\text{-}P}$ = 3459.0 Hz).

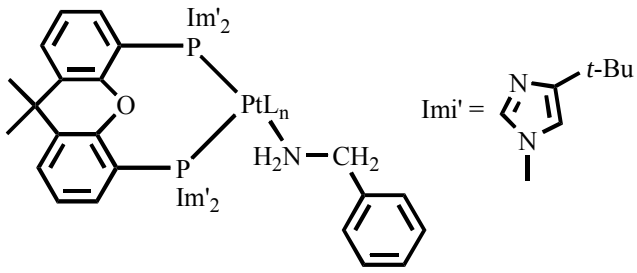

39

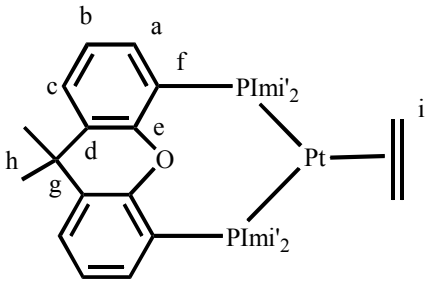

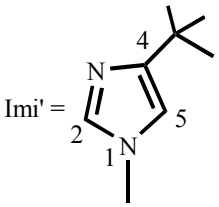

40

Preparation of (η^2-L)Pt($H_2C=CH_2$) complex (40). A 50 mL round-bottom Schlenk flask containing 1% sodium amalgam (Na/Hg) was filled with nitrogen. Dry and deoxygenated THF (25 mL) was then added followed by the addition of complex **38** (147.9 mg, 0.136 mmol) in THF (5 mL). Ethylene gas was bubbled through the top solution while the reaction mixture was stirring. After 15 min, ethylene was removed when the solution was saturated, and the reaction was allowed to stir at room temperature overnight. The upper grey suspension was separated from the sodium amalgam and the sodium amalgam was washed with THF a few times. The grey suspension and the washes were combined and filtered through cotton and Celite. The filtrate was concentrated to dryness to give a grey solid. The crude product was then recrystallized by slowly diffusing hexane into a benzene solution to afford colorless crystals (110 mg, 78%). ^{1}H NMR (C_6D_6, 200 MHz): 7.13 (d, 1.2, 2H, c-H), 6.91-6.95 (m, 2H, a-H), 6.81 (t, 7.4 Hz, 2H, b-H), 6.33 (s, 4H, Imi-5-H), 3.35 (s, 12H, Imi-N-CH_3), 2.47 (s, $J_{Pt\text{-}H}$ = 64.2 Hz, 4H, i-H), 1.51 (s, 6H, h-H), 1.31 (s, 36H, Imi-4-C(CH_3)$_3$); ^{13}C{^{1}H}(C_6D_6, 125.7 MHz): 158.3 (e-C), 152.9 (vt, N = 10.8 Hz, Imi-4-C), 143.3 (Imi-2-C), 135.7 (d-C), 131.6 (a-C), 126.0 (c-C), 123.9 (b-C), 121.8 (f-C), 118.2 (Imi-5-C), 38.3 (s, $J_{Pt\text{-}C}$ = 25.9 Hz, i-C), 37.0 (g-C), 34.2 (Imi-N-CH_3), 32.5 and 30.9 (Imi-4-C(CH_3)$_3$), 27.1 (h-C); ^{31}P{^{1}H} (C_6D_6, 80.9 MHz): –10.6 (s, $J_{Pt\text{-}P}$ = 3566.2 Hz).

Anal. Calcd. For $C_{49}H_{68}N_8OP_2Pt$ (1042.14): C, 56.47; H, 6.58; N, 10.75. Found: C, 56.86; H, 6.44; N, 10.37.

Reaction of complex 40 with trifluoacetic acid. In a J-Young NMR tube, complex **40** (16.6 mg, 0.016 mmol) was weighed and C_6D_6 was added to the NMR tube to give a colorless solution. After initial NMR spectra were observed, trifluoroacetic acid (3.0 mg, 0.026 mmol) was added to the NMR solution via syringe. The NMR spectra were observed and a new complex **41** was proposed on the basis of the changes in chemical shifts and also the Pt-P coupling constant. No further purification was done. NMR (C_6D_6, 200 MHz) ^{1}H: 7.16-7.23 (m, 2H), 6.87 (s, 2H), 6.76 (s, 2H), 3.28 (s, 12H), 2.28 (s, J_{Pt-H} = 65.8 Hz, 4H), 1.50 (s, 6H), 1.30 (s, 36H); ^{31}P{^{1}H}: -16.4 (br s, J_{Pt-P} = 3731.3 Hz).

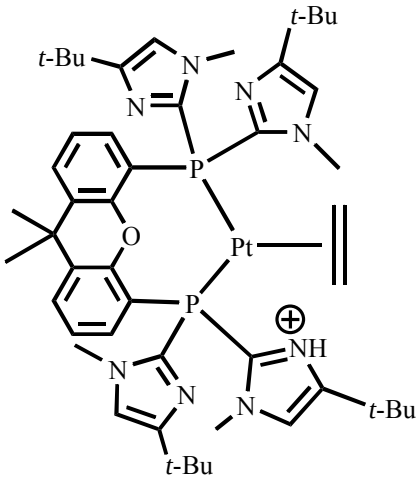

41

C. Results and Discussion

Chapters 2 and 3 have focused on monophosphine ligands with one imidazolyl substituent and two alkyl substituents on phosphorus, and their palladium and platinum complexes. In this chapter, as a start to studying the chemistry of bidentate analogs, we synthesized various bidentate imidazolylphosphine ligands, **30, 31** and **32** (Figure 4.02), which are expected to have different bite angles. The two phosphorus atoms each bearing two imidazolyl substituents in ligand **30** were connected by an ethylene group and the bite angle is expected to be slightly smaller than 90°. Ligand **31** has a similar structure to DPPF therefore its bite angle is expected to be about 99°. Similarly, the bite angle of ligand **32** is expected to be around 109° because of the structural similarity between ligand **32** and DPPX.

Synthesis, characterization of Pd(0) complex of ligand 30. Following the same procedure for preparing the two-coordinate monophosphine Pd(0) complexes described in previous work,[45] a Pd(0) complex with two bidentate ligands **30** was prepared (Figure 4.03). Slightly more than two equivalents of ligand **30** was mixed with one equivalent of Cp(allyl)Pd and stirred at room temperature. After 1 d, the NMR data of the aliquot showed that the reaction was clean with only a small amount of excess unreacted ligand as the other identifiable product in the $^{31}P\{^{1}H\}$ NMR spectrum besides the desired product, Pd(0) complex **33**. After the isolation of the pure

product as a white solid, ^{1}H, $^{13}C\{^{1}H\}$ and $^{31}P\{^{1}H\}$ NMR spectra were taken to confirm the structure.

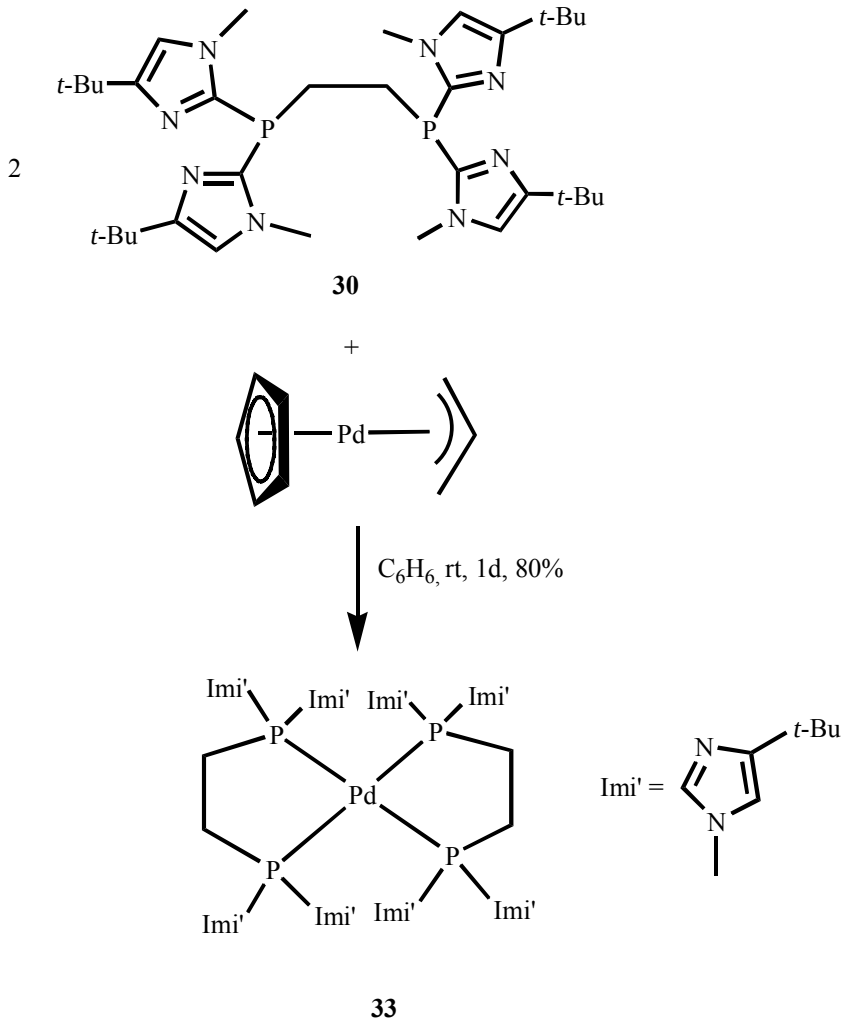

Figure 4.03. Formation of complex **33** from reaction of **30** with Pd(II) precursor.

The ^{1}H NMR spectrum of complex **33** showed resonances that are consistent with the highly symmetrical proposed structure. When compared to the spectrum of starting ligand **30**, all the signals were present but the resonance for N-methyl protons on imidazole ring shifted about 0.1 ppm upfield, whereas the resonance for aromatic

protons on imidazole ring shifted 0.15 ppm downfield, and the resonance for ethylene proton shifted downfield even more, about 0.3 ppm. In the ^{31}P NMR spectrum, there was only one singlet that appeared at δ 3.6 ppm which was also consistent with the highly symmetrical proposed structure, which means all the phosphorus atoms are chemically and magnetically equivalent. When compared to the ligand **30**, the phosphorus resonance for the product was shifted 49 ppm downfield, indicating the coordination of the phosphine ligand to the metal. The same conclusion can be drawn from the ^{13}C NMR spectrum also. Elemental analysis was also consistent with the formula.

Reactivity of complex 33 with aryl halides. Complex **33** did not react with iodobenzene at room temperature, but did so after heating (90 ^{o}C) and a rather long reaction period (4 d) (Figure 4.04). Although complex **34**, which was the oxidative addition product of iodobenzene, was made and was the major product, it was not the only product according to $^{31}P\{^{1}H\}$ NMR spectrum. The slow rate of oxidative-addition is not surprising since complex **33** is saturated, and oxidative-addition would require loss of one chelating ligand, moreover the small bite angle of the remaining ligand would make the Pd(0) complex less reactive to oxidative-addition.

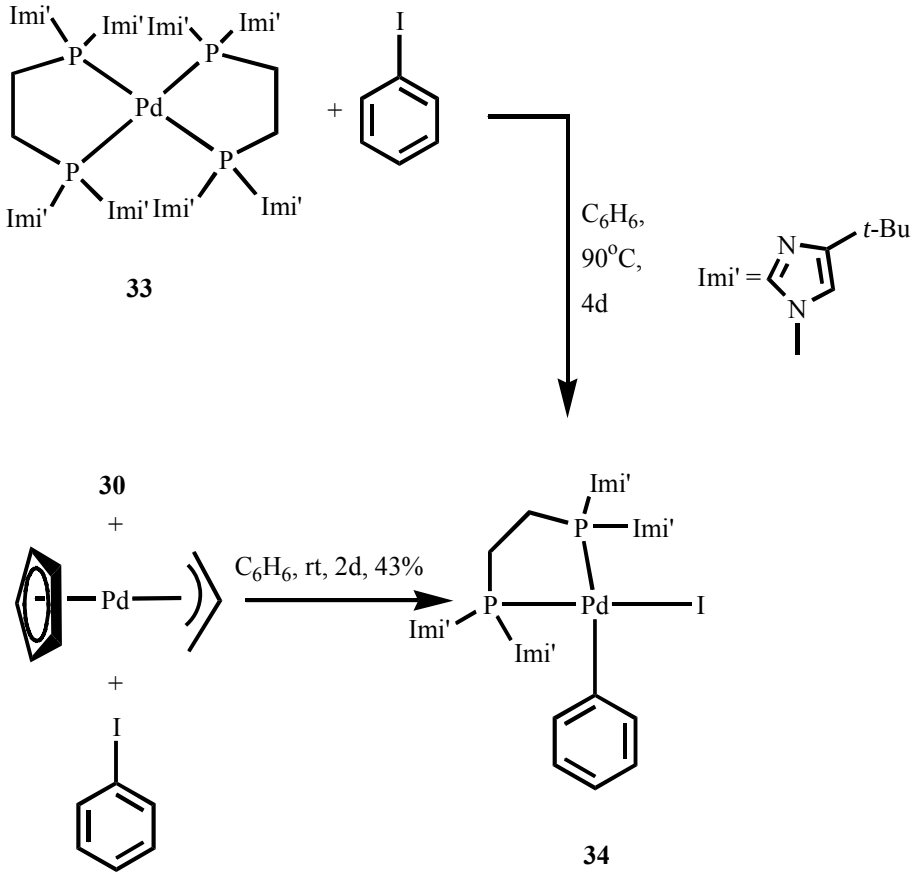

Figure 4.04. Formation of complex **34** by two different routes.

Reactivity of ligand 30 with mixture of aryl halides and Cp(allyl)Pd. In order to avoid formation of **33**, only one equivalent of ligand **30** was mixed with one equivalent of Cp(allyl)Pd quickly followed by one equivalent of iodobenzene. At room temperature, a yellow solid was generated and isolated. The yellow solid was recrystallized from hexane/THF and NMR data showed that it was complex **34** (Figure

4.04). NMR data for a sample prepared in CD_2Cl_2 showed a structure which was not symmetrical. In the $^{31}P\{^1H\}$ NMR spectrum, there were two doublets which were 10 ppm apart (δ 19.7 ppm and 10.0 ppm), which is considered reasonable because their chemical shifts were influenced by the trans iodide and phenyl ligands which were electronically different, and the coupling constant $J_{P\text{-}P}$ = 20 Hz is in the expected range for cis P-P coupling. In the ^1H NMR spectrum, the protons on two imidazolyl substituents were differentiated, along with the protons on the two carbons in the ethylene group.

The reactivity was different when bromobenzene was used instead of iodobenzene in the similar reaction (Figure 4.05). At room temperature, when equimolar amounts of all the reactants were mixed, a product was made right away and the comparable NMR data of the product suggested the exactly same structure to that of Pd(0) complex **33**. Further reaction did not proceed until heating at 60 ^oC, then a new product started to show up slowly. In the $^{31}P\{^1H\}$ NMR spectrum, the resonances of this new complex **35** appeared as two doublets with the chemical shift similar to that of complex **34** and with a P-P coupling constant of 44 Hz, larger than the value seen in spectra of **34**. We were not able to isolate complex **35** due to the decomposition of this product upon further heating.

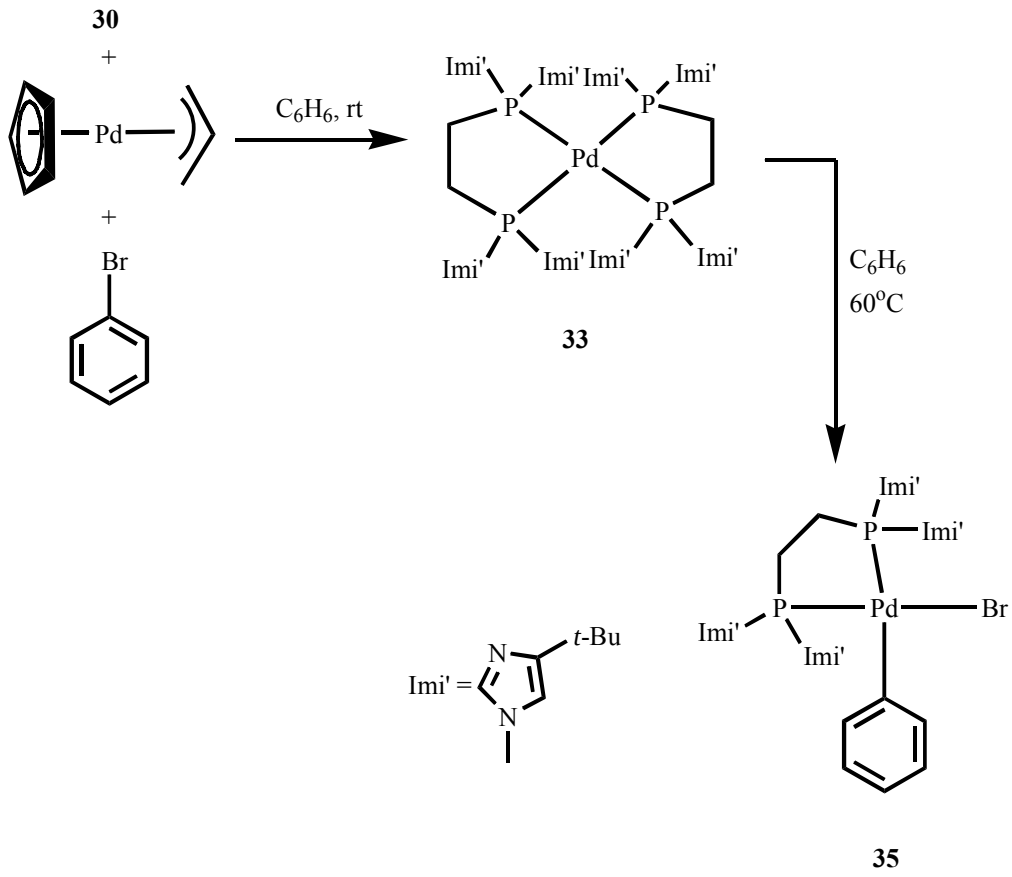

Figure.4.05. Reaction of **30** with bromobenzene and Cp(allyl)Pd.

Reactivity of complex 34 with amine. The complex **34** was allowed to react with benzylamine either directly or by first removing iodide ligand with ionizing reagent such as silver triflate then followed by the addition of amine. In either case, the reaction was not clean and many intermediate species were generated.

The preceding experiments with Pd and ligand **30** were done relatively early in our studies. The following experiments focus on Pt, which as a third-row transition metal tends to have stronger metal-ligand bonds, which could be expected to allow us to more easily isolate stable products. In addition, the coupling between ^{195}Pt and other nuclei yields valuable information on metal-ligand bonding. Finally, because of synthetic advances in the lab, the bidentate phosphines **31** and **32** had become available, and their expected large bite angles made these attractive candidates for study.

Reaction of complex 36 with hydrazine. Orange-colored platinum complex **36** bearing bidentate ligand **31** and two chloride ligands which locate cis to each other were synthesized. Complex **36** is symmetric as demonstrated by the only singlet at δ –27.0 ppm (J_{Pt-P} = 3787.3 Hz) in $^{31}P\{^{1}H\}$ NMR spectrum. When complex **36** was treated with 10 equivalents of hydrazine, a clean reaction took place and a new complex **37** was detected by NMR (Figure 4.06). In $^{31}P\{^{1}H\}$ NMR spectrum, the singlet shifted 9.6 ppm upfiled (δ –36.6 ppm, J_{Pt-P} = 3389.6 Hz). In the ^{1}H NMR spectrum, there was no hydride resonance found. Most likely, complex **37** is an ionic Pt(II) complex with two neutral hydrazine ligands, and two chloride ions are the couterions. The Pt-P coupling constant for **37** is 400 Hz smaller, perhaps because of the influence of hydrazine ligands and the charge on the complex, or both. Further work will be needed to verify the tentative structural assignment and the significance of the spectral changes.

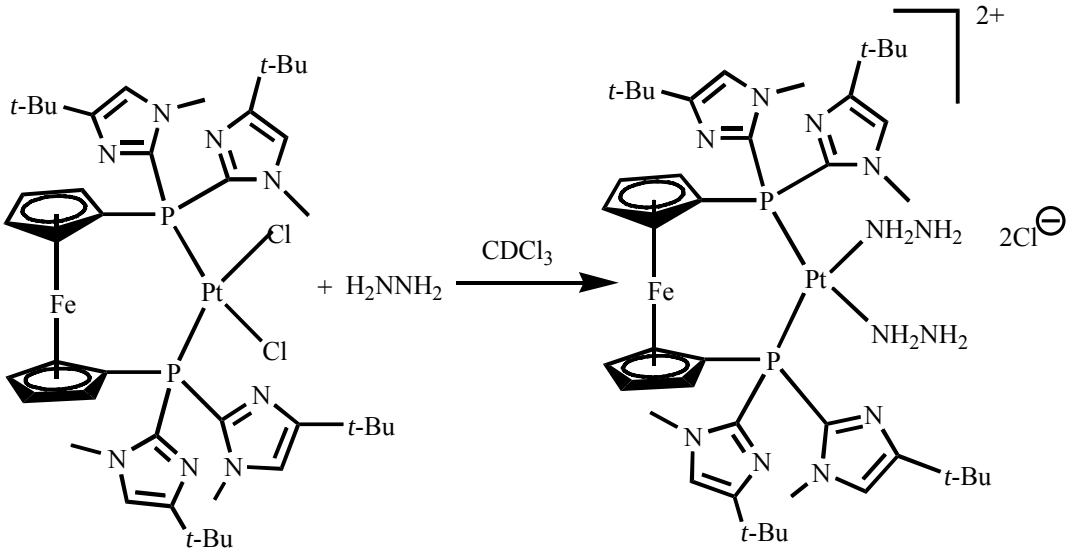

36 **37**

Figure 4.06. Reactivity of complex **36** with hydrazine.

Synthesis of cis-(L)$PtCl_2$ complex 38. The reaction of ligand **32** and (cod)$PtCl_2$ was carried out in dichloromethane at room temperature. The reaction was rapid and after only 1 h the cod ligand was substituted completely by ligand **32**, and a new complex **38** was obtained in a good yield (98%) (Figure 4.07). The NMR data of the pure complex in $CDCl_3$ were consistent with the structure. A singlet at δ –35.0 ppm with Pt satellites ($J_{Pt\text{-}P}$ = 3709.4 Hz) in its $^{31}P\{^1H\}$ NMR spectrum suggested coordination of the ligand **32** to Pt and the symmetrical structure of product **38**. Complex **38** was more soluble in chloroform than in benzene. All the resonances and integrals of the resonances in ^1H NMR spectrum matched with the structure as well.

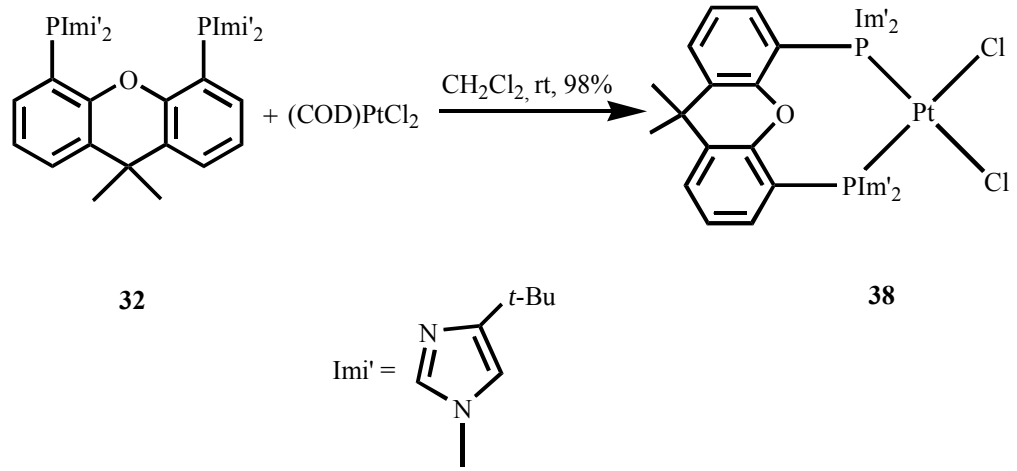

Figure 4.07. Synthesis of complex **38** from complexation of ligand **32** to Pt.

Complex **38** was recrystallized by slowly diffusing diethyl ether into dichloromethane solution of crude product to give X-ray diffraction suitable crystals. The solid state structure of complex **38** is shown in Figure 4.08 and selected bond lengths and bond angles are shown in Table 4.01.

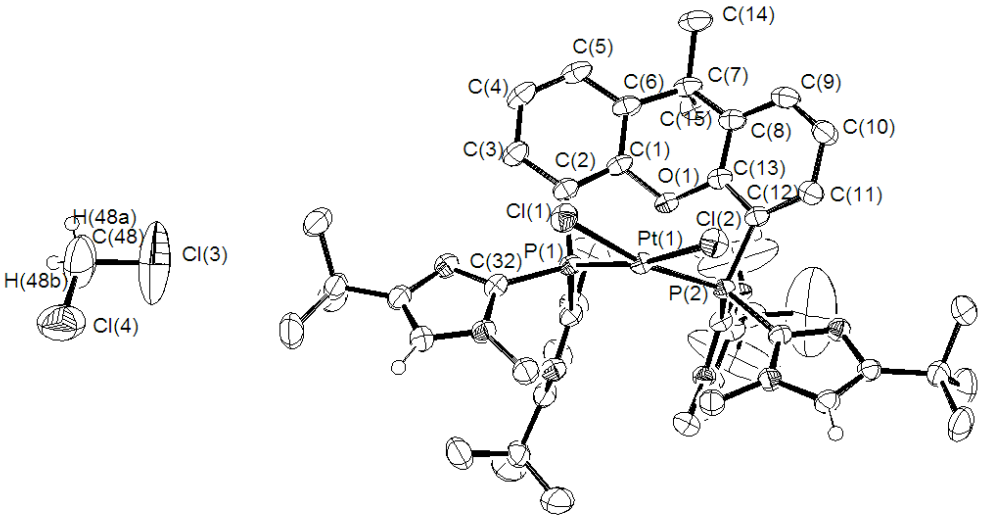

Figure 4.08. Molecular structure of complex **38**.

Table 4.01. Selected bond lengths (Å) and bond angles (deg) for complex **38**.

	Bond Lengths (Å)		Bond Angles (deg)
Pt(1)-P(1)	2.243	P(1)-Pt(1)-P(2)	101.64
Pt(1)-P(2)	2.254	P(1)-Pt(1)-Cl(1)	84.24
Pt(1)-Cl(1)	2.342	Cl(1)-Pt(1)-Cl(2)	88.75
Pt(1)-Cl(2)	2.341	Cl(2)-Pt(1)-P(2)	84.21

As shown in Figure 4.08 and Table 4.01, the Pt center adopts a slightly distorted square planar geometry (four angles around Pt center added up to 358.8^{o}) and The bite angle P-Pt-P is 101.64^{o}.

Reactivity of complex 38 with amine. Complex **38** reacts with ionizing reagent silver triflate and the primary amine benzylamine to generate a new complex **39** (Figure 4.09). One equivalent of complex **38** was dissolved in dichloromethane then 2 equivalents of silver triflate was added, whereupon a white precipitate, presumably silver chloride formed. After the precipitate was removed, the NMR spectrum showed that there was only one singlet at δ –45.0 ppm with Pt satellites (J_{Pt-P} = 3928.2 Hz) in the $^{31}P\{^{1}H\}$ NMR spectrum which meant only one major product was present in the filtrate, and the absorption at 1237 cm^{-1} in the IR spectrum of the filtrate suggested ionic triflate.[46] When benzylamine was added to the filtrate, another complex **39** was made and isolated by recrystallization. The NMR data of the isolated crystals suggested the very unsymmetrical structure of complex **39**, since there were two doublets at δ –43.9 ppm and –44.9 ppm (J_{P-P} = 18.6 Hz, J_{Pt-P} = 3327.1 Hz and 3459.0 Hz) in $^{31}P\{^{1}H\}$ NMR spectrum. In the ^{1}H NMR spectrum, there were four sharp singlets assigned for N-CH_3 which suggested that the four imidazole rings are in four different environments. Resonances for the protons in benzylamine were found also in the ^{1}H NMR spectrum, although no information about other ligands was

obtained. Since complex **39** is highly unsymmetric, the other ligands could be anything except for another benzylamine molecule.

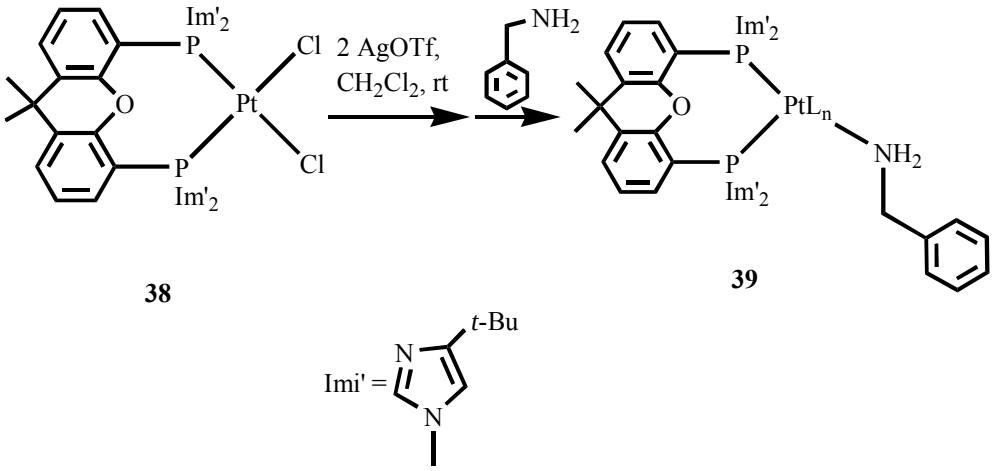

Figure 4.09. Reaction of **38** with AgOTf and amine.

Synthesis and structure of (L)Pt(ethylene)(0) complex 40. Pt (II) Complex **38** can be reduced to Pt(0) complex **40** by Na/Hg in the presence of ethylene gas (Figure 4.10). After being stirred at room temperature for 2 h, the crude product was obtained by removing the solvent and it was pure by NMR. In the ^{1}H NMR spectrum, the singlet appeared at δ 2.47 ppm with Pt satellites ($J_{Pt\text{-}H}$ = 64.2 Hz) which integrated for four protons demonstrated the coordination of the ethylene molecule to Pt. The singlet for complex **40** shifted 24 ppm downfield in ^{31}P{^{1}H} NMR compared to that of complex **38**.

The crude product could be purified further by recrystallizing it from hexane/benzene to give colorless crystals in excellent yield (78%). X-ray diffraction analysis of complex **40** was done and the solid state structure is shown in Figure 4.11, whereas selected bond lengths and bond angles are listed in Table 4.02. The bite angle P(1)-Pt(1)-P(2) is 107.89^{o} and the sum of the four angles around Pt center is 359^{o} which indicates trigonal planar geometry. The ethylene moiety bound to Pt in η^2 fashion since the bond lengths between Pt and two carbons are similar. The bond length between two sp^2 carbon in the coordinated ethylene is 1.408 Å which is longer than that in free ethylene (1.34 Å) because of the backbonding of Pt to the double bond.

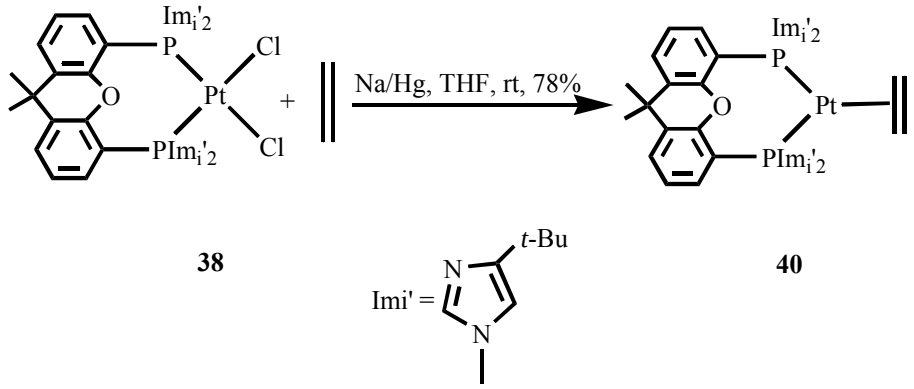

Figure 4.10. Synthesis of complex **40** from complex **38.**

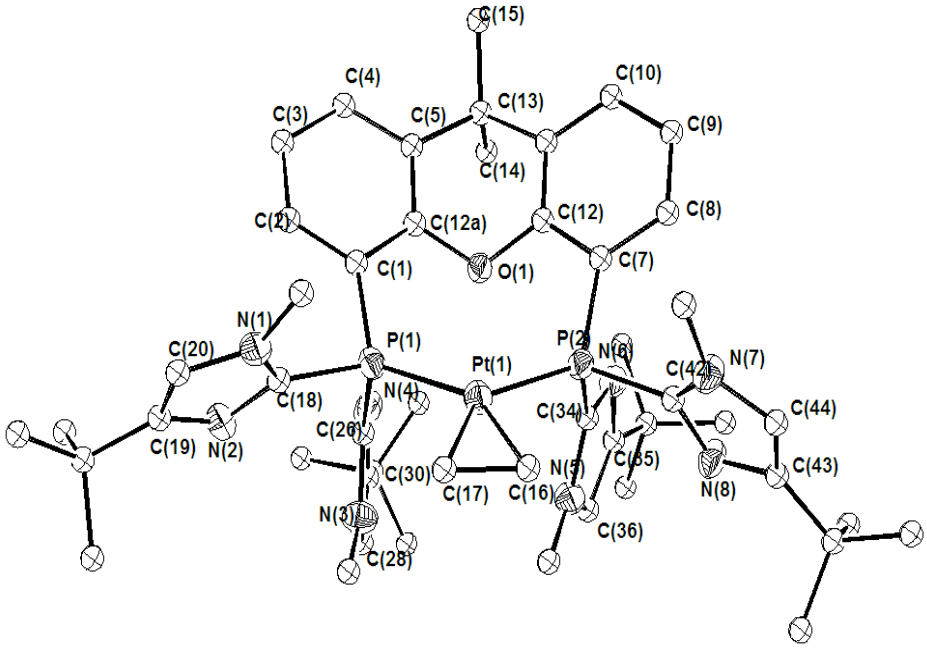

Figure 4.11. Molecular structure of complex **40**.

Table 4.02. Selected bond lengths (Å) and bond angles (deg) for complex **40**.

	Bond Lengths (Å)		Bond Angles (deg)
Pt(1)-P(1)	2.293	P(1)-Pt(1)-P(2)	107.89
Pt(1)-P(2)	2.272	P(1)-Pt(1)-C(17)	109.49
Pt(1)-C(16)	2.100	C(17)-Pt(1)-C(16)	38.97
Pt(1)-C(17)	2.121	C(16)-Pt(1)-P(2)	102.81
C(16)-C(17)	1.408	C(1)-P(1)-Pt(1)	124.61
P(1)-C(1)	1.806	C(7)-P(2)-Pt(1)	122.95
P(2)-C(7)	1.815		

Reactivity of complex 40 with acid. It was known that $Pt(C_2H_4)(0)$ complex with P-P bidentate phosphine ligands can react with acid and either $[Pt(C_2H_5)]^+$ or $[Pt(H)(C_2H_4)]^+$ could be the product depending on the angle subtended at platinum by two phosphorus atoms.[47] When dbpp ($^tBu_2P(CH_2)_3P^tBu_2$, bite angle 100°) or dbpx (*o*-($^tBu_2PCH_2)_2C_6H_4$, bite angle 105°) is the bidentate ligand, the product is $[Pt(C_2H_5)(dbpp)]^+$ or $[Pt(C_2H_5)(dbpx)]^+$ and $[Pt(H)(C_2H_4)(dbpe)]^+$ is the product in the case of dbpe($^tBu_2P(CH_2)_2P^tBu_2$, bite angle 90°) (Figure 4.12). Therefore, in case of complex **40** which has a bite angle similar to dbpx reacting with trifluoroacetic acid, a product $[Pt(C_2H_5)(L)]^+$ would be expected. In fact, a complex **41** with symmetric structure (Figure 4.13) was detected but no hydride signal was seen in the ^1H NMR spectrum. In the $^{31}P\{^1H\}$ NMR spectrum, a broad singlet (δ –16.4 ppm, $J_{Pt\text{-}P}$ = 3731.3 Hz) instead of two doublets with Pt satellites suggested the symmetrical structure of complex **41**, or a rapid equilibrium between unsymmetrical structures at ambient NMR probe temperature. While it is possible that that one of the imidazole rings is protonated by the acid and the interexchange between the protonated imidazole ring and other imidazole rings is fast and causes the broadening of the phosphorus resonance, further work will be needed to verify this hypothesis.

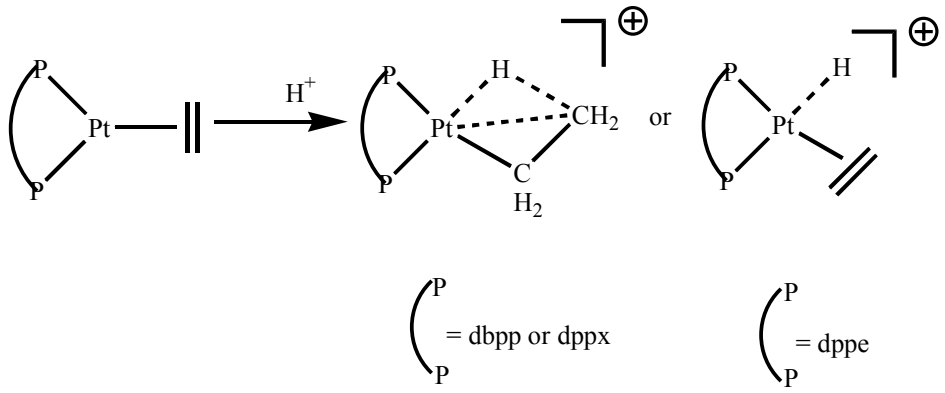

Figure 4.12. Reaction between Pt(ethylene)(0) complexes with P,P-bidenate ligand and acid.

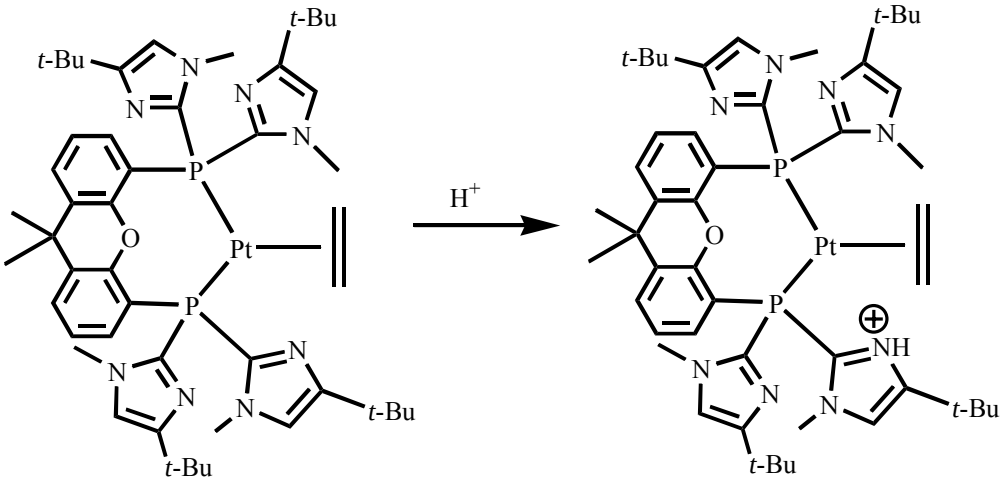

40 **41**

Figure 4.13. Reaction of complex **40** with acid.

D. Conclusion

Bidentate phosphine ligands containing imidazolyl substituents were synthesised, their bite angles varies from 90 to 109°. Preliminary study of these ligands on Pd and Pt has been done and results showed that in some cases the imidazole rings were involved in reactivity, but clearly more detailed studies need to be done to investigate the bifunctionality of the chelating imidazolylphosphine ligands.

The bite angle in square-planar Pt(II) complex **38** is 101.6° and bite angle in trigonal planar Pt(0) complex **40** is 107.9°. The difference in these bite angles is thought to be due to the different oxidation state of Pt center. These results are consistent with the literature examples.[48,49]

E. References

(1) Buckingham, J. *Dictionary of Natural Products*, 1st ed.; University Press: Cambridge, MA, 1994.

(2) Negwer, M. *Organic –Chemical Drugs and Their Synonyms (an international survey*), 7th ed.; Akademie Verlag GmbH: Berlin, 1995.

(3) MacDiarmid, A. G.; Epstein, A. J. In *Science and Applications of Conducting Polymers*; Salaneck, W. R., Clark, D. T., Samuelsen, E. J., Eds.; Adams Hilger: New York, 1991; p 117.

(4) Lindley, J. *Tetrahedron* **1984**, *40*, 1433-1456.

(5) Paine, A. *J. Am. Chem. Soc.* **1987**, *109*, 1496-1502.

(6) Hartwig, J. F. *Synlett* **1997**, 329-340.

(7) Driver, M. S.; Hartwig, J. F. *J. Am. Chem. Soc.* **1996**, *118*, 7217-1718.

(8) Wolfe, J. P.; Wagaw, S.; Buchwald, S. L. *J. Am. Chem. Soc.* **1996**, *118*, 7215-7216.

(9) Kosugi, M.; Kameyama, M.; Migita, T. *Chem. Lett.* **1983**, 927-928.

(10) Kosugi, M.; Kameyama, M.; Migita, T. *Nippon Kagaku Kaishi* **1985**, *3*, 547-551.

(11) Louie, J.; Paul, F.; Hartwig, J. F. *Organometallics* **1996**, *15*, 2794-2805.

(12) Guram, A. S.; Buchwald, S. L. *J. Am. Chem. Soc.* **1994**, *116*, 7901-7902.

(13) Hartwig, J. F.; Paul, F. *J. Am. Chem. Soc.* **1995**, *117*, 5373-5374.

(14) Unruh, J. D.; Christenson, J. R. *J. Mol. Catal.* **1982**, *14*, 19-34.

(15) Kranenburg, M.; Kamer, P. C. J.; van Leeuwen, P. W. N. M.; Vogt, D.; Keim, W. *J. Chem. Soc., Chem. Commun.* **1995**, 2177-2178.

(16) Casey, C. P.; Whiteker, G. T.; Melville, M. G.; Petrovich, L. M.; Gavey, J. J., J. A.; Powell, D. R. *J. Am. Chem. Soc.* **1992**, *114*, 5535-5543.

(17) Angermund, K.; Baumann, E. D.; Fornika, R.; Gorls, H.; Kessler, M.; Leitner, W.; Luts, F. *Chem. Eur. J.* **1997**, *3*, 755-764.

(18) Hofmann, P.; Meier, C.; Englert, U.; Schmidt, M. U. *Chem. Ber.* **1992**, *125*, 353-365.

(19) Hofmann, P.; Meier, C.; Hiller, W.; Heckel, M.; Riede, J.; Schmidt, M. U. *J. Organomet. Chem.* **1995**, 51-70.

(20) Brown, J. M.; Guiry, P. J. *Inorg. Chim. Acta.* **1994**, *220*, 249-259.

(21) Farina, V.; Krishman, B. *J. Am. Chem. Soc.* **1991**, *113*, 99585-9595.

(22) Hayashi, T. Konishi, M.; Kobori, Y.; Kumada, M.; Higuchi, T.; Hirotsu, K. *J. Am. Chem .Soc.* **1984**, *106*, 158-163.

(23) Whitesides, G. M.; Gaasch, J. F.; Stedronsky, E. R. *J. Am. Chem. Soc.* **1972**, *94*, 5258-5270.

(24) Hartwig, J. F. *J. Am. Chem. Soc. 1996*, *118*, 7010-7011.

(25) Driver, M. S.; Hartwig, J. F. *J. Am. Chem. Soc.* **1997**, *119*, 8232.

(26) Collman, J. P.; Hegedus, L. S.; Norton, J. R.; Finke, R. G.; *Principles and Applications of Organotransition Metal Chemistry*; University Science Books: Mill Valley, CA, 1987; pp 324-329.

(27) Hamann, B. C.; Hartwig, J. F. *J. Am. Chem. Soc.* **1998**, *120*, 3694-3703.

(28) Frohning, C. D.; Kohlpainter, C. W.; Bohnen, H. W. In *Applied Homogeneous Catalysis with Organometallic Compounds*, 2nd ed.; Cornils, B., Herrmann, W. A., Eds.; VCH: Weinheim, Germany, 2002; Vol. 1, p 31.

(29) Bohnen, H. W.; Cornils, B. *Adv. Catal.* **2002**, *47*, 1.

(30) Arnoldy, P. In *Rhodium Catalyzed Hydroformylation*; Van Leeuwen, P. W. N. M., Claver, C., Eds.; Kluwer: Dordrecht, The Netherlands, 2001; p 203.

(31) Hsu, C. Y.; Orchin, M. *J. Am. Chem. Soc.* **1975**, *97*, 3553.

(32) Petöcz, G.; Berente, Z.; Kégl, T.; Kollár, L. *J. Organomet. Chem.* **2004**, *689*, 1188.

(33) Stille, J. K.; Su, H.; Brechot, P.; Parinello, G.; Hegedus, L. S. *Organometallics* **1991**, *10*, 1183.

(34) Consiglio, G.; Nefkens, S. C A.; Borer, A. *Organometallics* **1991**, *10*, 2046.

(35) Parinello, G.; Stille, J. K. *J. Am. Chem. Soc.* **1987**, *109*, 7122.

(36) Wesemann, L.; Hagen, S.; Marx, T.; Pantenburg, I.; Nobis, M.; Driessen-Hölscher, B. *Eur. J. Inorg. Chem*. **2002**, 2261.

(37) Sturm, T.; Weissensteiner, W.; Mereiter, K.; Kégl, T.; Jeges, G.; Petölz, G.; Kollár, L. *J. Organomet. Chem.* **2000**, *595*, 93.

(38) Ancollotti, F.; Lami, M.; Marchionna, M. *J. Mol. Catal.* **1991**, *66*, 37.

(39) Kollar, L.; Bakos, J.; Heil, B.; Sandor, P.; Azalontai, G. *J. Organomet. Chem.* **1990**, *385*, 147.

(40) Van der Veen, L. A.; Keeven, P. K.; Kamer, P. C. J.; Van Leeuwen, P. W. N. M. *Dalton Trans***. 2000**, 2105.

(41) Hayashi, T.; Kawabata, Y.; Isoyama, T.; Ogata, I. *Bull. Chem. Soc. Jpn.* **1981**, *54*, 3438.

(42) Kawabata, Y.; Hayashi, T.; Ogata, I. *J. Chem. Soc., Chem. Commun*. **1979**, 462.

(43) Van Leeuwen, P. W. N. M.; Kamer, P. C. J.; Reek, J. N. H.; Dierkes, P. *Chem.* Rev. **2000**, *100*, 2741.

(44) Grotjahn, D. B, et al. unpublished results.

(45) Grotjahn, D. B.; Gong, Y.; Zakharov, L. N.; Golen, J. A.; Rheingold, A. L. *J. Am. Chem. Soc.* 2006, *128*, 438.

(46) Stang, P. J.; Huang, Y. H.; Arif, A. M. *Organometallics* **1992**, *11*, 231-237.

(47) Mole, L.; Spencer, J. L.; Carr, N.; Orpen, A. G. *Organometallics* **1991**, *10*, 49-52.

(48) Miedaner, A.; Raebiger, J. W.; Curtis, C. J.; Miller, S. M.; DuBois, D. L. *Organometallics* **2004**, *23*, 3670-2679.

(49) Freixa, Z.; van Leeuwen, P. W. N. M. *Dalton Trans.* **2003**, 1890-1901.

CHAPTER 5

Catalysis of C-N Bond Formation

A. Introduction

The catalytic amination of aryl halides represents a mild alternative to classical methods of aryl C-N bond formation.[1-5] The palladium-catalyzed amination of aryl halides has become an important method for the synthesis of arylamines found in pharmaceuticals,[6,7] materials with important electronic properties,[8-10] and ligands for early metal catalysts.[11] Ligands such as P^{t}Bu$_3$,[12-14] biphenylP^{t}Bu$_2$,[15] and heterocyclic carbenes[16,17] create catalysts with increased activity and allow milder conditions to be used. For example, reactions can be run at room temperature, with low catalyst loading, and with inactive substrates, such as aryl chlorides.[12-16, 18]

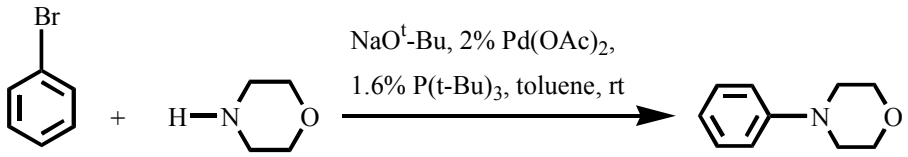

Figure 5.01. Pd-catalyzed coupling reaction between aryl bromide and secondary amine.

A mechanistically different reaction which could be used to make amines is the hydroamination of unactivated olefins with alkyl- or arylamines. However it remains

problematic. Although the attack of nucleophile on olefins in the Pt(II) has been known for almost a century,[19-22] it is not until recently that the effective Pt(II)-catalyzed protocols for the addition of carbon,[23,24] nitrogen[25], and oxygen[26] nucleophiles to unactivated olefins.[27,28] Recently, Pt(II)-catalyzed intramolecular hydroamination of γ- and δ-amino olefins to form nitrogen heterocycles has been reported (Figure 5.02).[29]

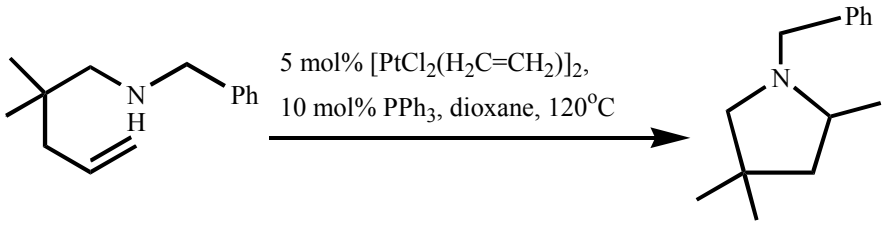

Figure 5.02. Pt-catalyzed intramolecular hydroamination of unactivated olefin with secondary amine.

In both transformations, proton transfer was proposed to be involved in the catalytic cycle. A heterocycle on a phosphine ligand could be expected either to help the proton transfer step as an internal base or act as a hydrogen bond acceptor or donor (in a protonated form) to promote the binding of the substrate. The heterocycle could be imidazole or pyridine. Therefore, a series of phosphine ligands analogous to that used in the literature but containing imidazole or pyridine substituents were synthesized and tested in the catalytic reactions mentioned above.

B. Experimental Section

Synthesis of N-phenylmorpholine. The procedure used to synthesize N-phenylmorpholine is similar to that used in literature.[30] In a glove box, tri-*tert*-butylphosphine (3.5 mg, 0.017 mmol) and palladium acetate (5.1 mg, 0.022 mmol) were weighed in a reaction flask. Sodium *t*-butoxide (158.6 mg, 1.65 mmol) was transferred to the same flask followed by the addition of bromobenzene (342.9 mg, 2.18 mmol) and morpholine (189.8 mg, 2.18 mmol) via syringe. After dry and degassed toluene (3 mL) was added to afford orange-colored mixture, the reaction was allowed to stir at room temperature and monitored by TLC. After 1 d, when TLC showed there was no bromobenzene left, the reaction was stopped and filtered through cotton to give yellow solution. The yellow filtrate was then loaded on a Chromatatron and 20:1 hexane:ethylacetate was used as developing solvent. The third fraction was collected and solvent was removed by rotary evaporation to give white crystals (200 mg, yield 56%).

General procedure for study of the palladium-catalyzed coupling reaction between bromobenzene and morpholine. In a glove box, ligand P(*t*-Bu)$_3$, 2b, 2c, 2d or 30 (0.8 mol% or 1.6 mol%) and palladium acetate (1 or 2 mol%) were weighed in a reaction vial, sodium *t*-butoxide (150 mol%) was transferred to the same vial followed by the addition of bromobenzene (100 mol%) and morpholine (100 mol%) via syringe. Dry and degassed toluene (about 2 mL) was added to afford orange-colored mixture and hexadecane (100 μL) was added also as internal standard, and the reaction mixture

was then stirred at room temperature. 10 μL of the reaction mixture was taken after 6 h, 1 d, 5 d and 7 d and was diluted in 100 μL of toluene and 1 μL of the diluted reaction aliquot was injected into a HP-6890 gas chromatograph. The yield of the product N-phenylmorpholine was then determined by the peak area of the product relative to that of internal standard with known amount.

Determination of the response factor of N-phenylmorpholine. A solution was prepared by dissolving N-phenylmorpholine (16.0 mg, 0.098 mmol) and hexadecane (22.4 mg, 0.099 mmol) in dry toluene (10 mL), 1 μL of the solution was injected into GC spectrometer. Then the peak areas for both N-phenylmorpholine and hexadecane was compared and the ratio obtained was the response factor for N-phenylmorpholine.

Synthesis of ligand 42, 43 and 44 and substrate benzyl(2,2-dimethyl-4-pentenyl)amine (45). Ligand 42, 43 and 44 were prepared by other group members.[32] Substrate benzyl(2,2-dimethyl-4-pentenyl)amine 45 was prepared by another group member using the literature procedure.[29]

General procedure for study of the platinum-catalyzed intramolecular hydroamination of unactivated olefins with secondary alkylamine. In a J-Young NMR tube, phosphine ligand PPh_3, 42, 43 or 44 (10 mol%) and di-μ-dichloro-bis(ethylene)diplatinum complex (5 mol%) were weighed, dry and deoxygenated dioxane-d_8 (1 mL) was added. The mixture was sonicated and an initial NMR spectrum was observed. Substrate 45 (100 mol%) was added to the NMR tube, NMR spectra were observed and then the tube was heated in an oil bath at 120 ^{o}C or 100 ^{o}C.

After 16 h, 1 d, 2d, the NMR tube was removed from the heating source and the NMR spectra were acquired. The conversion of the substrate 45 was calculated based on the integrals in the ^{1}H NMR spectrum.

C. Results and Discussion

Palladium-catalyzed amination of aryl halides. As shown in Figure 5.03, the proposed mechanism for the catalytic cycle of amination of an aryl halide begins with the loss of one ligand followed by oxidative additon of aryl halide to the palladium center, resulting in the formation of complex K. The binding of amine to K would generate a four-coordinate square-planar Pd(II) complex L. Then base could enter the cycle to help the deprotonation of amine and removal of the halide from the palladium center, which would result in formation of complex M. Finally, reductive elimination of the cis aryl and amine ligands in complex M would release arylamine product and regenerated the catalyst.

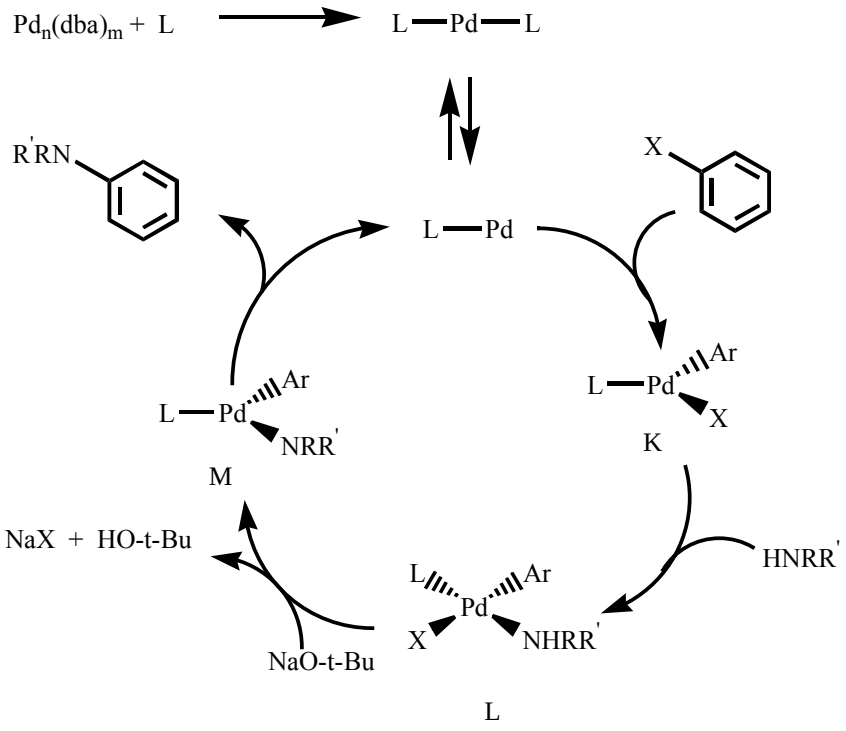

Figure 5.03. Proposed catalytic cycle for amination reaction.

Table 5.01. Comparison of different catalyst systems for amination reaction.

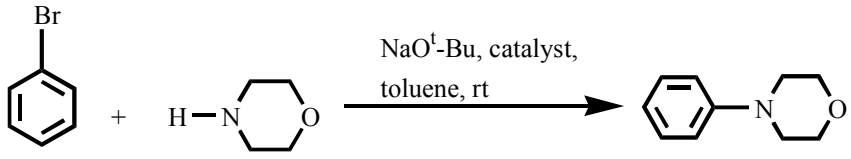

Catalyst used	Reaction period (d)	Yield (%)
2% $Pd(OAc)_2$, 1.6% P(*t*-Bu)$_3$	0.25, 1, 2, 7	40.4, 59.6, -----, -----
2% $Pd(OAc)_2$, 1.6% 2b	0.25, 1, 2, 7	1.42, -----, 14.7, 49.6
1% $Pd(OAc)_2$, 0.8% 2b	0.25, 1, 2, 7	0.83, 1.31, 1.77, -----
1% $Pd(OAc)_2$, 0.8% 2c	0.25, 1, 2, 7	-----, -----, -----, 0.39
2% $Pd(OAc)_2$, 1.6% 2d	0.25, 1, 2, 7	no product
2% $Pd(OAc)_2$, 1.6% 30	0.25, 1, 2, 7	no product

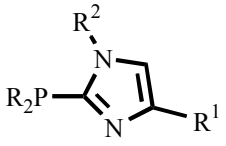

2b, R = *t*-Bu, R^1 = *t*-Bu, R^2 = Me
2c, R = *i*-Pr, R^1 = *t*-Bu, R^2 = Me
2d, R = *t*-Bu, R^1 = H, R^2 = H

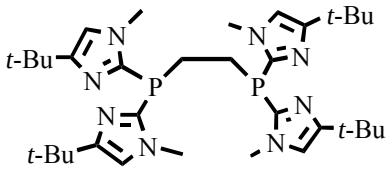

30

As shown in Table 5.01, under identical conditions to those used in the literature for P(*t*-Bu)$_3$,[30] the catalyst system of 1.6 % ligand 2b with 2% $Pd(OAc)_2$ gave the best result among the imidazolylphosphine ligands tried, although it gave slower reaction than the combination of 1.6% P(*t*-Bu)$_3$ and 2% $Pd(OAc)_2$. The amount

of the catalyst loading had effect on the formation of the product dramatically. It was surprising that the analogous ligands 2c and 2d did not generate a good catalyst and it was perhaps even more surprising that the bidentate ligand 30 did not catalyze the reaction to give any product.

According to our previous study,[31] the first step of the catalytic cycle, the oxidative-addition of aryl halide to Pd center, was fast for ligands 2b and 2c. The second step, the coordination of amine, was possible to the oxidative-addition product in both cases and the binding of amine was stabilized through hydrogen bonding in the case of 2c, though stoichiometric amine binding as studied in Chapter 2 occurred in systems lacking a halide ligand or ion. Therefore, in future work, either aryl triflates may be substrates of choice, or the important step in this reaction using ligand 2b and 2c is either the proton transfer step or the last step, reductive-elimination, which might be influenced by using bidentate ligands with large bite angles.

Our previous study also showed that the oxidative-addition of aryl halide to Pd center for bidentate ligand 30 was relatively slow, which perhaps explains why no product was detected using ligand 30. In addition, the bite angle of ligand 30 is around 90^{o} which was already demonstrated to decrease the rate of the reductive-elimination step.

The results reported here are preliminary, and more studies need to be done in order to improve this reaction, for example, new bidentate imidazolylphosphine ligands with bigger bite angles.

Intramolecular hydroamination of unactivated olefin with secondary amine. As shown in Figure 5.04, platinum-catalyzed hydroamination may be initiated by formation of platinum amine complex N, C-N bond formation presumably occurs via intramolecular ligand exchange resulting the formation of complex O, followed by outer-sphere attack of the pendant amine on the olefin to give complex P. Deprotonation/chloride displacement then could take place to generate complex Q followed by intermolecular protonlysis of the Pt-C bond, presumably via a Pt(IV) hydride intermediate to give complex R. Finally, ligand exchange from Pt-amine complex S would release product and regenerate the catalyst.

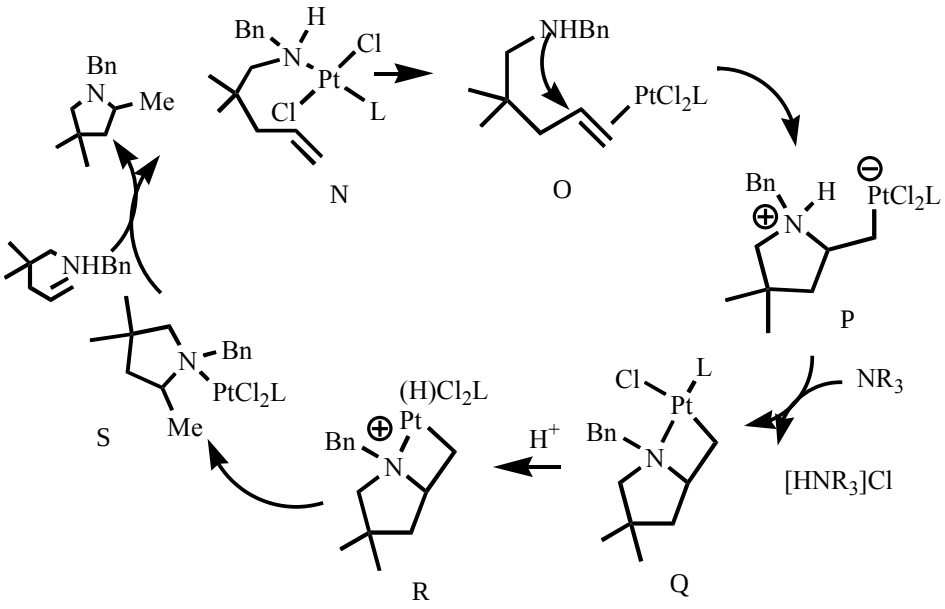

Figure 5.04. Proposed mechnism for intramolecular hydroamination.

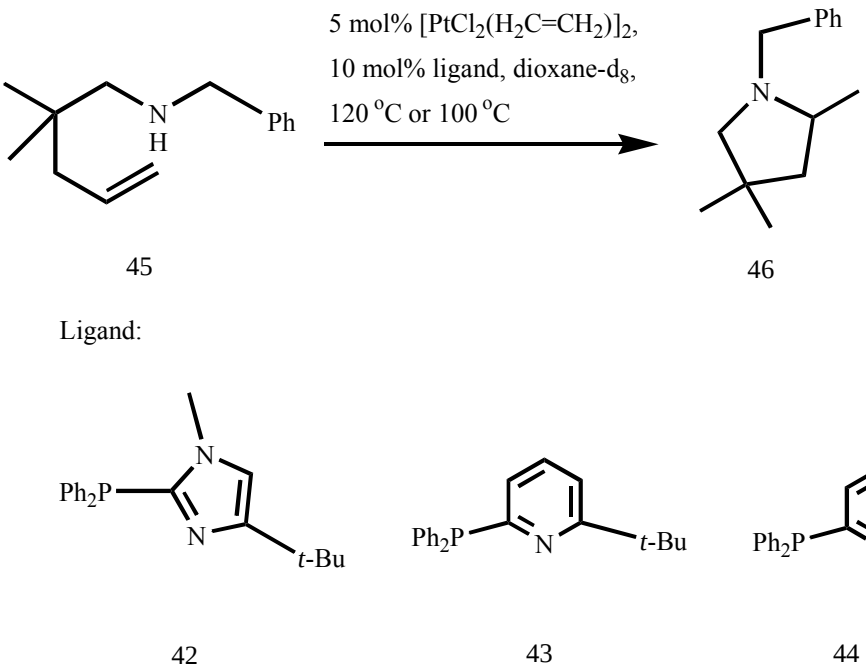

Figure 5.05. Bifunctional imidazolyl- or pyridyl-phosphine ligands.

Three bifunctional imidazolyl- or pyridyl-phosphine ligands (shown in Figure 5.05) with $[PtCl_2(H_2C=CH_2)]_2$ (II) complex were tried on the intramolecular hydroamination of substrate benzyl(2,2-dimethyl-4-pentenyl)amine. The reaction condition used was identical to that was used in the literature[29] and reaction was monitored by NMR. After the reactions in the NMR tube have been heated for 16 h at 120 ^oC, NMR spectra were taken. For the reaction using ligand 43, ^1H NMR spectrum showed that all of the substrate 45 has converted to the cyclized product 46, while for the reactions using ligand 42, only 42% of substrate converted, for the reaction using ligand 44, only 40% of substrate converted. Further heating (2 d at 120 ^oC) did not

help the complete conversion of the substrate 45 to 46. At 100 ^{o}C, the use of ligand 43 also resulted in the complete conversion of 45 to 46 within 1 d, the other two reactions using ligand 42 and 44 did not give and product 46. Therefore, among these three ligands, ligand 43 was the most effective one for this particular reaction.

Although more careful and detailed studies, such as monitoring the reaction using GC or GC-MS, are necessary to draw any conclusion, on the basis of these preliminary results, we can presume that the basicity of the heterocycle in the ligand is important (comparison between 42 and 43) as well as the size of the *ortho*- substituent to the *N* atom in the heterocycle (comparison between 43 and 44). Our goal is to find a general efficient catalyst for the hydroamination reactions and learn about the role that heterocycle plays in the catalytic pathway. Therefore, more ligands with different structures and substrates with different functionalities will be tried, and once improved catalysts are found, mechanistic studies will be done as well.

D. Conclusion

Our imidazolylphosphine ligands were tried on the Pd-catalyzed coupling reaction of bromobenzene and morpholine, and the results showed that the combination of our ligands and Pd(0) precursor generated a catalyst for this reaction at room temperature, although the catalyst was not as active as the literature examples. Although the bidentate imidazolylphosphine ligands 30 was tried as well, this example does not have an exceptionally large bite angle, and therefore other bidentate imidazolylphosphine ligands need to be tested.

Some of our imidazolylphosphine and pyridylphosphine ligands were tried on the Pt-catalyzed intromolecular hydroamination of unactivated olefins and secondary alkylamines. The preliminary results showed that the ligand 44, di-phenyl-2-*tert*-butyl-pyridylphosphine ligand and Pt(II) precursor can generate a better catalyst for the intromolecular hydroamination of substrate 45, for example, reaction can take place at lower temperature, which is an exciting indication that the heterocycle indeed can help in this case. However, these results are preliminary and further and detailed study will be done.

E. References

(1) Hartwig, J. F. *Angew. Chem., Int. Ed*. 1998, *37*, 2046.

(2) Hartwig, J. F. *Acc. Chem. Res.* 1998, *31*, 852.

(3) Wolfe, J. P.; Wagaw, S.; Marcoux, J.-F.; Buchwald, S. L. *Acc. Chem. Res.* 1998, *31*, 805.

(4) Yang, B. H.; Buchwald, S. L. *J. Organomet. Chem.* 1999, *576*, 125.

(5) Hartwig, J. F. In *Modern Amination Methods*; Ricci, A.; Ed.; Wiley-VCH: Weinheim, Germany, 2000.

(6) Hong, Y.; Senanayake, C. H.; Xiang, T.; Vandenbossche, C. P.; Tanoury, G. J.; Bakale, R. P.; Wald, S. A. *Tetrahedron Lett*. 1998, *39*, 3121-3124.

(7) Hong, Y. P.; Tanoury, G. J.; Wilkinson, H. S.; Bakale, R. P.; Wald, S. A.; Senanayake, C. H. *Tetrahedron Lett*. 1997, *38*, 5663-5666.

(8) Goodson, F. E.; Hartwig, J. F. *Macromolecules* 1998, *31*, 1700-1703.

(9) Singer, R. A.; Sadighi, J. P.; Buchwald, S. L. *J. Am. Chem. Soc*. 1998, *120*, 213-214.

(10) Spetseris, N.; Ward, R. E.; Meyer, T. Y. *Macromolecules* 1998, *31*, 3158-3161.

(11) Greco, G. E.; Popa, A. I.; Schrock, R. R. *Organometallics* 1998, *17*, 5591.

(12) Yamamoto, T.; Nishiyama, M.; Koie, Y. *Tetrahedron Lett*. 1998, *39*, 2367.

(13) Nishiyama, M.; Yamamoto, T.; Koie, Y.; *Tetrahedron Lett*. 1998, *39*, 617.

(14) Hartwig, J. F.; Kawatsura, M.; Hauk, S. I.; Shaughnessy, K. H.; Alcazar-Roman, L. M. *J. Org. Chem.* 1999, *64*, 5575.

(15) Wolfe, J. P.; Tomori, H.; Sadighi, J. P.; Yin, H.; Buchwald, S. L. *J. Org. Chem.* 2000, *65*, 1158.

(16) Stauffer, S. R.; Lee, S.; Stambuli, J. P.; Hauck, S. I.; Hartwig, J. F. *Org. Lett.* 2000, *2*, 1423.

(17) Grasa, G. A.; Viciu, M. S.; Huang, J. K.; Nolan, S. P. *J. Org. Chem.* 2001, *66*, 7729.

(18) Hamann, B. C.; Hartwig, J. F. *J. Am. Chem. Soc.* 1998, *120*, 7369.

(19) Hofmann, K. A.; von Narbutt, J. *Ber*. 1908, *41*, 1625.

(20) Chatt, J.; Vallarino, L. M.; Venanzi, L. M. *J. Chem. Soc.* 1957, 2496.

(21) Palumbo, R.; De Renzi, A.; Panunzi, A.; Paiaro, G. *J. Am. Chem. Soc*. 1969, 91, 3874.

(22) Fanizzi, F. P.; Intini, F. P.; Maresca, L.; Natile, G. *J. Chem. Soc., Dalton Trans.* 1992, 309.

(23) Liu, C.; Han, X.; Wang, X.; Widenhoefer, R. A. *J. Am. Chem. Soc.* 2004, *126*, 3700.

(24) Wang, X.; Widenhoefer, R. A. *Chem. Commun.* 2004, 660.

(25) Wang, X.; Widenhoefer, R. A. *Organometallics* 2004, *23*, 1649.

(26) Qian, H.; Han, X.; Widenhoefer, R. A. *J. Am. Chem. Soc.* 2004, *126*, 9536.

(27) Hahn, C.; Cucciolito, M. E.; Vitagliano, A. *J. Am. Chem. Soc.* 2002, *124*, 9038.

(28) Kerber, W. D.; Koh, J. H.; Gagne, M. R. *Org. Lett.* 2004, *6*, 3013.

(29) Bender, C. F.; Widenhoefer, R. A. *J. Am. Chem. Soc.* 2005, *127*, 1070-1071.

(30) Hartwig, J. F. *J. Org. Chem.* 2002, *67*, 5553-5566.

(31) Grotjahn, D. B.; Gong, Y.; Zakharov, L. N.; Golen, J. A. Rheingold, A. L. *J. Am. Chem. Soc*. 2006, 128, 438-453.

(32) Grotjahn, D. B, et al. Unpublished results.

CHAPTER 6

Future Work

A. Continuing on studying of Pt complexes with bifunctional imidazolylphosphine ligands.

We have demonstrated the activation of O-H bond in compound ROH is possible, most notably using water itself. With hydrido Pt complex 13 we have also demonstrated the stabilization of H-Pt-OR units by hydrogen bonding interactions with the oxygen atom of the attached ligand. Further exploration and utilization of these intriguing effects need to be investigated.

B. Study the effects of bidentate bifunctional imidazolylphosphine ligands on palladium-catalyzed C-N bond formation.

Our preliminary trials of using bifunctional imidazolylphosphine ligands on Pd-catalyzed C-N bond formation was done and the results was not the best compared to the reported literature examples. There is substantial room for improvement. Our thorough study on sterically demanding hybrid imidazolylphosphine ligands on Pd(0) and Pd(II) provide the facts that the amine binding is possible at least in the absence of halide and the heterocyclic ring helped to stabilize the binding of amine through secondary hydrogen bonding interactions. However, the reductive elimination of the product may be problematic. Therefore, in the future, we would like to try aryl triflate

substrates and / or some bidentate ligands which have both larger bite angles and at the same time the heterocyclic substituents on the phosphorus which could help with either proton transfer or hydrogen bonding and hopefully to improve the catalyst system.

C. Study the effects of bifunctional heterocyclic phosphine ligands on platinum-catalyzed intramolecular hydroamination and hydration of olefins.

The intramolecular hydroamination of unactivated olefins with secondary alkylamines, which could be very useful in synthesizing cyclic amines, was reported by the Widenhoefer group to be catalyzed by Pt(II) complex $[PtCl_2(H_2C=CH_2)]_2$ and phosphine ligand PPh_3 at 120 ^oC. Our preliminary results from running the reaction under the same condition except for using a pyridylphosphine as the ligand instead of PPh_3 showed that reaction was done at lower temperature (100 ^oC). In the future, we could look this reaction into much details and try pyridinylphosphine ligands with different substituents on the pyridine or even different substituents on phosphorus and can try imidazolylphosphine ligands as well. Other alkene additions will also be tried.

D. Search for catalyst for hydroamination or hydration of unsaturated bond using combinatorial technology.

Our ultimate goal is finding the catalyst for the challenging hydration and hydroamination of unsaturated bonds. With the knowledge we have on the ligands and on the metals from thousands of experiments, we can selectively do screening experiments using combinatorial technology. With a hit found, we can then optimize it and study it. The GC or GC-MS will be used to monitor these reactions, which will speed catalyst discovery.